Holocene hydroclimate reconstruction in East Africa, based on multi-proxy analysis of lake sediments

-

Reconstructie van hydroklimaatverandering in Oost-Afrika doorheen het Holoceen, gebaseerd op multi-proxy analyse van meersedimenten

Gijs De Cort

2016

Ghent University, Faculty of Sciences, Department of Biology, Limnology Unit
Royal Museum for Central Africa, Department of Earth Sciences

Thesis submitted in partial fulfilment of the requirements for the degree of Doctor in Science: Geology

Promoters:

Prof. Dr. Dirk Verschuren
Dr. Florias Mees

Members of the examination committee:

- Prof. Dr. Stephen Louwye, Ghent University (chairman)
- Prof. Dr. Marc De Batist, Ghent University (secretary)
- Prof. Dr. Sébastien Bertrand, Ghent University
- Dr. Hilde Eggermont, Royal Belgian Institute of Natural Sciences
- Prof. Dr. Daniel Olago, University of Nairobi
- Prof. Dr. Blas Valero-Garcés, Instituto Pirenaico de Ecología

Public thesis defence: Friday June 17th, 2016. Ghent University, Ghent, Belgium.

The work presented in this thesis was funded by the Belspo BRAIN-be project 'PAMEXEA - Patterns and mechanisms of climate extremes in East Africa', the U.S. National Geographic Society and the FWO Flanders research project 'Community dynamics of water fleas in East African mountain lakes: integration of (palaeo-)limnology and (palaeo-)genetics'. In addition, I acknowledge funding for fieldwork and work visits abroad provided by FWO Flanders and the Faculty of Sciences of Ghent University.

The fieldwork on Mt. Kenya and Lake Bogoria was conducted with permission from the National Council for Science and Technology of Kenya (NCST/5/002/R/441 and NCST/RRI/12/1/BS011/44), the Kenya Wildlife Service (KWS/CL&P/029), and the National Environmental Monitoring Authority (NEMA Access Permit AGR/7/2010 registrations 0021 and 0029). The research materials were exported under Material Transfer Agreement A11/TT/1040 between the Kenya Wildlife Service, the University of Nairobi, and Ghent University.

Please refer to this work as: De Cort G. (2016) Holocene hydroclimate reconstruction in East Africa, based on multi-proxy analysis of lake sediments. PhD thesis, Ghent University, Ghent, Belgium.

Cover: Nasikie Engida as seen from the northern shore. Photo by Gijs De Cort.

DANKWOORD - *ACKNOWLEDGEMENTS*

Allereerst ben ik heel veel dank verschuldigd aan mijn promoter Dirk. Enkele uren van jouw vak 'Paleoklimatologie' waren genoeg om mij te laten begeesteren door het onderwerp waarop ik de laatste vier jaar heb gewerkt. Ik heb nog maar weinig mensen ontmoet die zo gepassioneerd zijn door hun vak, en die ook nog eens de gave bezitten om die passie over te brengen op anderen. Je deur stond steeds open wanneer ik (weer eens) het noorden kwijt was, en even binnenspringen volstond dan voor een hoop nieuwe inspiratie en motivatie. De weg van deze thesis was er een van vallen en opstaan, maar je hebt me steeds alle vertrouwen gegeven. Daar ben ik enorm dankbaar voor. Daarnaast wil ik ook mijn co-promoter Florias bedanken. Ondanks mijn beperkte mineralogische voorkennis kon ik steeds bij jou terecht voor raad en vragen, en ik heb sinds het begin van het PAMEXEA-project erg veel van jou geleerd.

I also want to thank the members of the examination committee for their willingness to review this work and to improve it through their remarks and suggestions. Dan, I especially want to thank you for your help and advice over the past years. It meant a lot to know that your door was always open to me when I was in Nairobi. Hilde, ook jij verdient een speciale vermelding. Niet alleen voor de moeite om mijn werk zo zorgvuldig te beoordelen nu je al even de wereld van de harde wetenschap achter je hebt gelaten, maar ook voor je raad en steun bij het begin van mijn doctoraat en voor je fijne gezelschap tijdens de campagne op Mount Kenya.

Vier jaar geleden begon ik als enige doctoraatsstudent in wat een van de kleinste onderzoeksgroepen van onze universiteit moet zijn geweest. Yoeri, de onmisbare schakel die onverstoorbaar alles draaiende houdt, moet ik niet alleen bedanken voor de steeds verzorgde sfeer en gezelligheid, maar ook voor zijn meer dan welkome hulp in het labo. Els, ook jou wil ik bedanken voor de fijne collega die je was en voor de erg gewaardeerde hulp, zeker tijdens het naderen van mijn deadline. Ook mijn allereerste bureaugenote, Dorien, mag ik niet vergeten. Spijtig genoeg vertrok jij al snel naar andere oorden, maar ik denk nog vaak terug aan de leuke tijd in ons lokaal op het vijfde.

Het doet me plezier dat de 'Limno', vier jaar en twee verhuizingen later, is uitgegroeid tot een gezellige en energieke bende. Wannes, zelfs na twee jaar van elkaar aanstaren boven onze computerschermen, ben je nog steeds mijn favoriete bureau-eilandgenoot. Dank je voor de leuke momenten, en de onuitputtelijke voorraad onnozelheden die mij meermaals tot tranen toe hebben doen schaterlachen. Mike, bedankt voor de leuke tijden en voor het delen van je passie over alles wat met voedsel te maken heeft, je hebt me meermaals aan het nadenken gezet. *Aynalem, the pleasure of working together was all mine, and I have learned a great deal from you. We went from being colleagues to being friends, and I wish you and your family the best of luck.* Geert, ook jou wil ik bedanken. Ik ben blij dat ik jou en Stef heb leren kennen, en ik hoop dat we onze film- en spelletjesavonden zullen blijven onderhouden. Jorunn, bedankt om steeds je opgewekte zelf te zijn. Je weet het, ik sta altijd klaar om samen eens lekkere sappige ribbe… *EUHM* ik bedoel een slaatje te gaan eten! Thijs, niet alleen had ik het plezier om samen met jou een uitdagend nieuw meer te gaan verkennen, je stond ook steeds klaar met raad en daad of gewoon voor een goeie babbel. Weet dat ik enorm veel aan jou gehad heb het voorbije jaar, en dat ik je daar erg dankbaar voor ben. Verder wil ik ook alle collega's van de TEREC bedanken voor de leuke sfeer op en naast het werk.

Over the past years, I was lucky enough to be able to pay multiple visits to faraway Kenya, a fascinating and captivating country. These were all priceless experiences, which I got to share with my colleagues. I've had more unforgettable encounters than I can name here, but it has to be emphasized that my work would have been impossible without the great help that I got during these trips. Abi, I want to thank you and your family for taking good care of me during my first visit to Nairobi, and for teaching me my first words in Kiswahili. I am grateful that I got to know you, and I wish you the best of luck for the future. Caxton, thanks for taking good care of the Lake Bogoria sediment traps and hydrolab measurements. Where would the Limnology Unit be without you?! I want to thank everyone involved in the HSPDP project for the wonderful week I got to spend at the Lake Magadi drill site in the summer of 2014. Robin and Bernie, many thanks for involving me in the exciting work on Nasikie Engida. I also want to thank you explicitly for our interesting discussions and the extensive advice you were always willing to give me, they have been of great help in writing this thesis. I am also grateful to Raphael Kimosop and the team of Lake Bogoria National Reserve, and Anthony Mbuthia for taking care of everything to enable the field work at Nasikie Engida. Many thanks also to Ursi Brupbacher for her kind help during my visits at ETH Zürich.

Natuurlijk was het niet al wetenschap wat de klok sloeg de voorbije jaren. Joost en Katrijn, Pieter-Jan en Helena, Koen en Lies, Ruben en Emily, Sietse, het doet deugd te weten dat ik steeds op zulke goeie vrienden kan rekenen. Ook mijn ploegmaats van BBC Olympia Denderleeuw wil ik bedanken voor de jarenlange vriendschap, evenals het UGent basketbalteam. Bedankt aan mijn fantastische reismaatjes Laurence en Arne, en aan 'de biologen' Vyshal, Joost, Lander, Lynn, Yannick, Lien, Eva en Kenny. *Fellow PhD climbers Phil, Jesper and Stan, thanks for getting me off my lazy bum these past months.* Aan alle andere oude of nieuwe vrienden, de economie-crew / Chinese poepers (Klaas, Daan, Angelos, Renaat, Benne), Gert en Peter, Ángel en Alexander, Team Komen Eten (Marianne en Bastiaan, Evelyne en Steven, Jef, Glynn en Sander), Bart en Nele, Sien en Cham, Lara en Stijn, Marieke en Ernest, Andy en Jens, Simon a.k.a. Saimn-I, en alle anderen: bedankt!

Al heel mijn leven ben ik gezegend met de beste zus en broer ter wereld. Goele, als kind schreven we op onze slaapkamer samen natuurkrantjes om aan onze ouders te verkopen. Eigenlijk doen we allebei nog steeds hetzelfde, op onze eigen manier. Bedankt voor alles! Wout, dank je om steeds mijn grote broer en (hier ga ik spijt van krijgen...) grote voorbeeld te zijn. De kleine spruit die Marie en jij verwachten, krijgt fantastische ouders! Moe en Va, het is onbegonnen werk om jullie te bedanken voor alles wat jullie de voorbije 29 jaar voor mij hebben gedaan. Ik heb steeds jullie onvoorwaardelijke steun gekregen, en dat is meer dan een zoon zich wensen kan.

Zo'n drie jaar geleden heb ik het geluk gehad de (buur)vrouw van mijn leven tegen het lijf te lopen. Sarah, jij bent het beste dat me ooit is overkomen, en ik ben je meer verschuldigd dan je ooit zult weten. Dank je voor de liefde, steun en inspiratie die je me elke dag geeft. Ik ben benieuwd naar wat de toekomst ons brengen zal, maar ik heb het gevoel dat we samen alles aankunnen.

TABLE OF CONTENTS

The regional climate of East Africa

The hydroclimatic setting of East Africa is unique when compared to other low-latitude regions of the world. In general, the seasonality of rainfall in the tropics is linked to the intertropical convergence zone (ITCZ), the band of deep convection associated with the convergence of the northern and southern hemisphere trade winds (Waliser and Gautier, 1993). While much of the tropics are hence characterized by the high amounts of rainfall generated by the atmospheric convection associated with intense surface heating, large parts of East Africa seem to be anomalously dry (Fig. 1). Several factors are thought to be responsible for this (Nicholson, 1996), one of which is the region's complex topography (Sepulchre et al., 2006; Fig. 2). To the East, a coastal plain borders the Indian Ocean, while westward the interior highlands rise, dominated by the East African Rift System (EARS), formed by slow tectonic separation of the Nubian and Somali plates. The rain shadow created by this high terrain, especially the Kenya and Ethiopia Domes, prevents moist air from the Congo Basin to completely cross East Africa. The Congo Air Boundary (CAB), the atmospheric convergence zone where tropical Atlantic and Indian Ocean-derived air flows meet (Nicholson, 1996), is largely situated along the mountainous western shoulder of the East African Rift System. This allows moisture originating from the Atlantic to contribute a significant amount of rainfall to Ethiopia and the western part of the East African plateau (Levin et al., 2009; Mapande and Reason, 2005), whereas easternmost equatorial East Africa and the Horn of Africa receive virtually all of their precipitation from the Indian Ocean. Unlike the Congo air flow sourced from the Atlantic Ocean, the northeast and southeast monsoons that originate over the Indian Ocean are associated with subsiding air and are therefore relatively dry (Nicholson, 1996). Complex air-flow patterns associated with mountain relief and coast-line orientation further contribute to low and unevenly distributed rainfall (Kinuthia, 1992; Nicholson, 1996; Viste and Sorteberg, 2013, Yang et al., 2015). In addition also a number of rift lakes in the region are of such large dimension that they substantially influence local climate dynamics (e.g. Anyah and Semazzi, 2009). All these factors have produced extremely complex meteorological patterns, with stunning differences in hydrological regime occurring over distances on the order of only tens of kilometres (Nicholson, 1996).

The ITCZ shifts latitudinally throughout the year between the northern and southern hemisphere, trailing the band of seasonally maximum solar insolation (Philander et al., 1996). Over East Africa, ITCZ migration spans the widest latitudinal range in the world (Fig. 3), from ca. 15°N in boreal summer to 15°S in boreal winter. Around the East African equator, this results in a bimodal yearly rainfall pattern (Fig. 4). Monthly rainfall variation in Nairobi (Kenya, 1°17' S) clearly demonstrates this, with the twice-yearly passage of the ITCZ creating two rain seasons from March to May (MAM, 'long rains') and from October to December (OND, 'short rains'), alternated by the two dry seasons of January-February (JF) and June-July-August-September (JJAS). Toward the northern and southern subtropics, the two wet seasons merge into one, coinciding with boreal or austral summer, respectively, as illustrated by the climatograms of Addis Ababa (Ethiopia, 9°02' N) and Lilongwe (Malawi, 13°59' S). A recent study highlighted the importance of the yearly cycle of monsoonal winds and Indian Ocean sea surface temperatures (SSTs) in the origin of the bimodal rainfall pattern in equatorial East Africa (Yang et al., 2015). SSTs in the western Indian Ocean are higher in the rainy

seasons and highest during the long rains of MAM, providing the main explanation for the difference in magnitude between the long and the short rain seasons. The JF season is more or less uniformly dry because of advection of dry, stable air from the cold northern Indian Ocean. During the JJAS dry season, easterly-sourced precipitation is similarly suppressed because of a cool western Indian Ocean (resulting from seasonally enforced coastal upwelling), but the easternmost reach of the West African monsoon creates a northwest to southeast pattern of diminishing rainfall. This means that during the JJAS season, Atlantic-sourced moisture is able to reach the central Kenya Rift Valley (including Lake Bogoria, Fig. 4) and Mount Kenya, important locations discussed in this thesis (see below).

On seasonal and longer time scales, SST variations in the world's tropical oceans often translate into consistent patterns of East African rainfall. In particular, the amount and intensity of short (OND) rains show strong tele-connection to the El Niño Southern Oscillation (ENSO), with El Niño conditions and associated warming in the western Indian Ocean causing higher rainfall over equatorial East Africa (Goddard and Graham, 1999), while increasing the incidence of drought over northern (Ethiopia and the Sudano-Sahelian belt) and southern parts of the (East) African tropics (Camberlin et al., 2001). Additionally, an Indian Ocean Dipole pattern has been reported as a distinct and important mode of variability impacting the short rains (Saji et al., 1999), while some studies also indicate an influence of Atlantic Ocean SSTs on precipitation over the western parts of East Africa (Nicholson, 1996; Camberlin et al., 2001; Anyah and Semazzi, 2006). The long (MAM) rains are much less correlated to ENSO or any other large SST anomaly (Ogallo et al., 1988), and the amount of short rains in any given year yields little or no predictive power regarding the following long rains (Lyon, 2014).

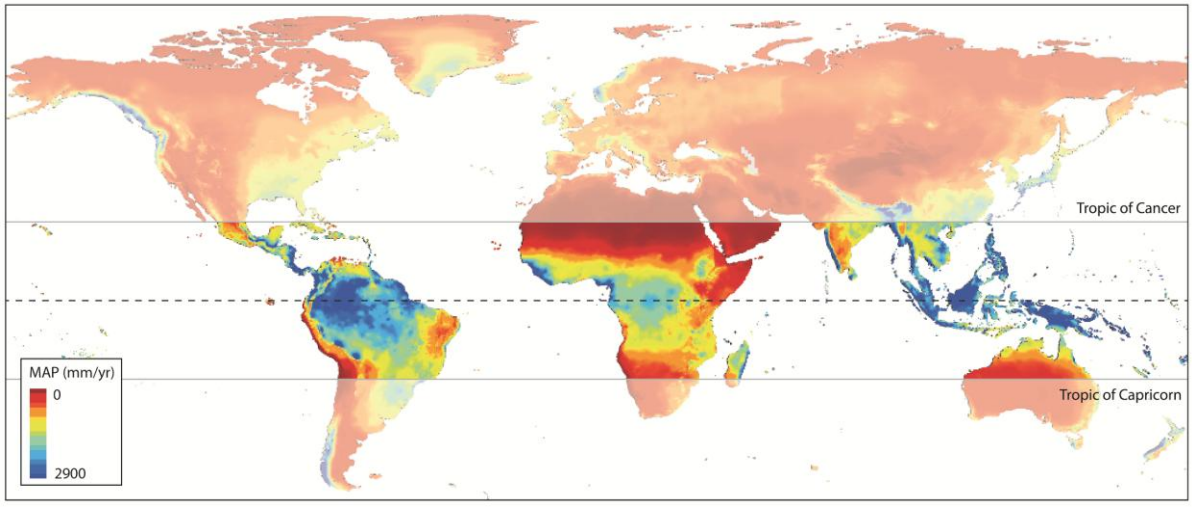

Fig. 1 Mean annual precipitation in the global tropical belt for the period 1950-2000, with East Africa standing out as an anomalously dry region. Figure generated using the WorldClim global precipitation dataset (Hijmans et al., 2005).

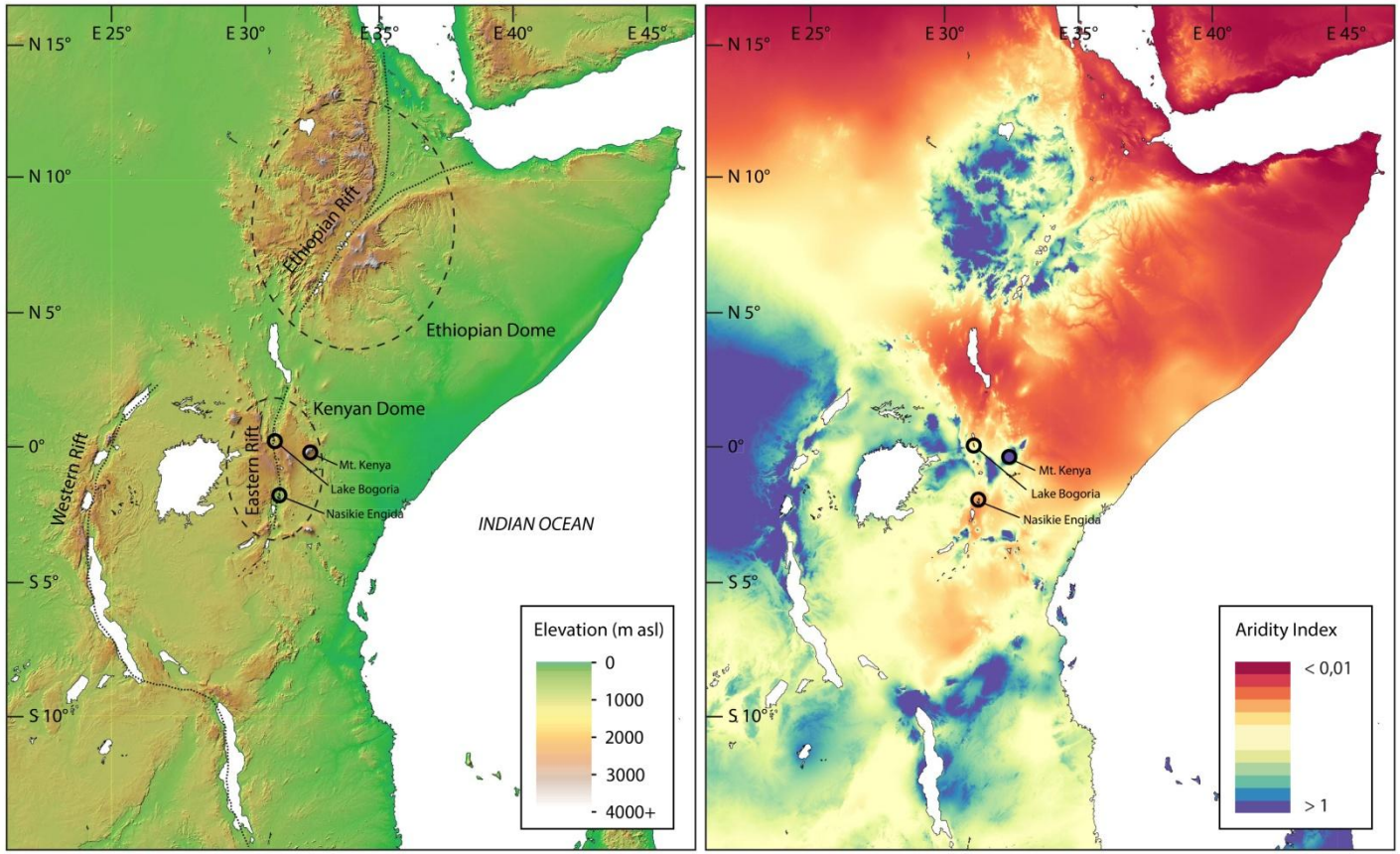

Fig. 2 Left: Topography of East Africa, dominated by the EARS. GMTED2010 digital elevation dataset obtained from US Geological Survey, http://earthexplorer.usgs.gov. Right: CGIAR-CSI Global Aridity Index (Trabucco and Zomer, 2009), defined as

$$aridity\ index = \frac{mean\ annual\ precipitation}{mean\ annual\ potential\ evapotranspiration}$$

illustrating the spatially complex patterns of hydrological regimes, influenced mostly by topography, the position of large lakes, and the barrier to westerly flow created by the western shoulder of the East African plateau. Note that in this formulation, aridity index values increase for more humid conditions. Mount Kenya, Lake Bogoria and Nasikie Engida, three important sites in this thesis, are also depicted.

Societal relevance of climate research in East Africa

The combination of relatively low total annual rainfall and great inter-annual variability (Fig. 5) has created a semi-arid or even arid tropical climate regime over much of East Africa, with humid and sub-humid conditions mostly restricted to the interior highlands. Consequently, the ecosystems and societies of equatorial East Africa have traditionally been subject to low and irregular water-resource availability. Over the past decades, a series of droughts has highlighted the endemic vulnerability of the vast drylands of northern Kenya, eastern Uganda, southern Ethiopia and Somalia to failing rains, with dramatic outcomes for the pastoralists and subsistence farmers inhabiting the area. This was demonstrated recently in 2011 by a severe famine in the Horn of Africa, affecting more than 13 million people in the region, with more than 250,000 fatal casualties in Somalia alone (Hillier and Dempsey, 2012; Checchi and Robinson, 2013). The currently ongoing drought in central and eastern Ethiopia, directly related to the strong El Niño conditions of 2015, has required significant humanitarian assistance to prevent widespread loss of life, with ca. 10 million people in need of emergency food supply in early 2016 (FEWS Net, 2016). The history of East African countries has been punctuated by drought-related related famine for as long as historical sources are available, often with huge tolls on livestock and human life. Recorded crises are obviously biased toward the last century, but a number of events has been traced back from written sources, most extensively for Ethiopia where limited evidence goes back to around the start of the Common Era (Webb and von Braun, 1994; Wolde-Georgis, 1997). Despite food-relief systems in some involved countries being improved since the end of the 20th century (Graham et al. 2012), the enormous challenge remains to develop a sustainable agricultural economy in a future of climate change, growing demographic pressure and naturally scarce land and water resources. Ca. 75% of the total labour force in East Africa is associated to smallholder, rain-fed agriculture (Salami et al., 2010). However, in areas where crop cultivation is hydrologically sustainable, available farmland is under severe pressure from population growth, land degradation and deforestation. This has driven expansion of farming to the vast (semi-)arid drylands of the region (which, for example, make up 80% of Kenya's total land surface), where crop cultivation is not possible without unsustainable irrigation from deep aquifers or endorheic lakes. In these regions, pastoralism has traditionally formed the dominant mode of living, but is now falling under increasing pressure by land conflicts, government policies and overgrazing (Schmidt and Pearson, 2016). These societal transformations have only further established severe, recurrent drought as one of the principal hazards in the region.

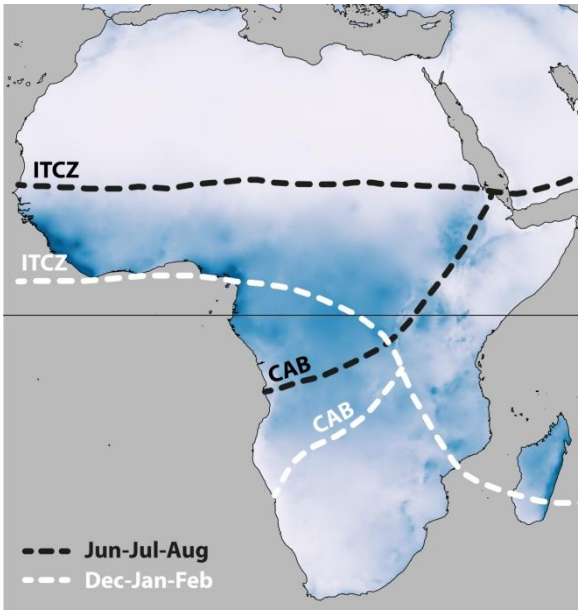

Fig. 3 Simplified representation of the mean seasonal positions of the ITCZ and CAB over Africa during NH summer (JJA) and winter (DJF).

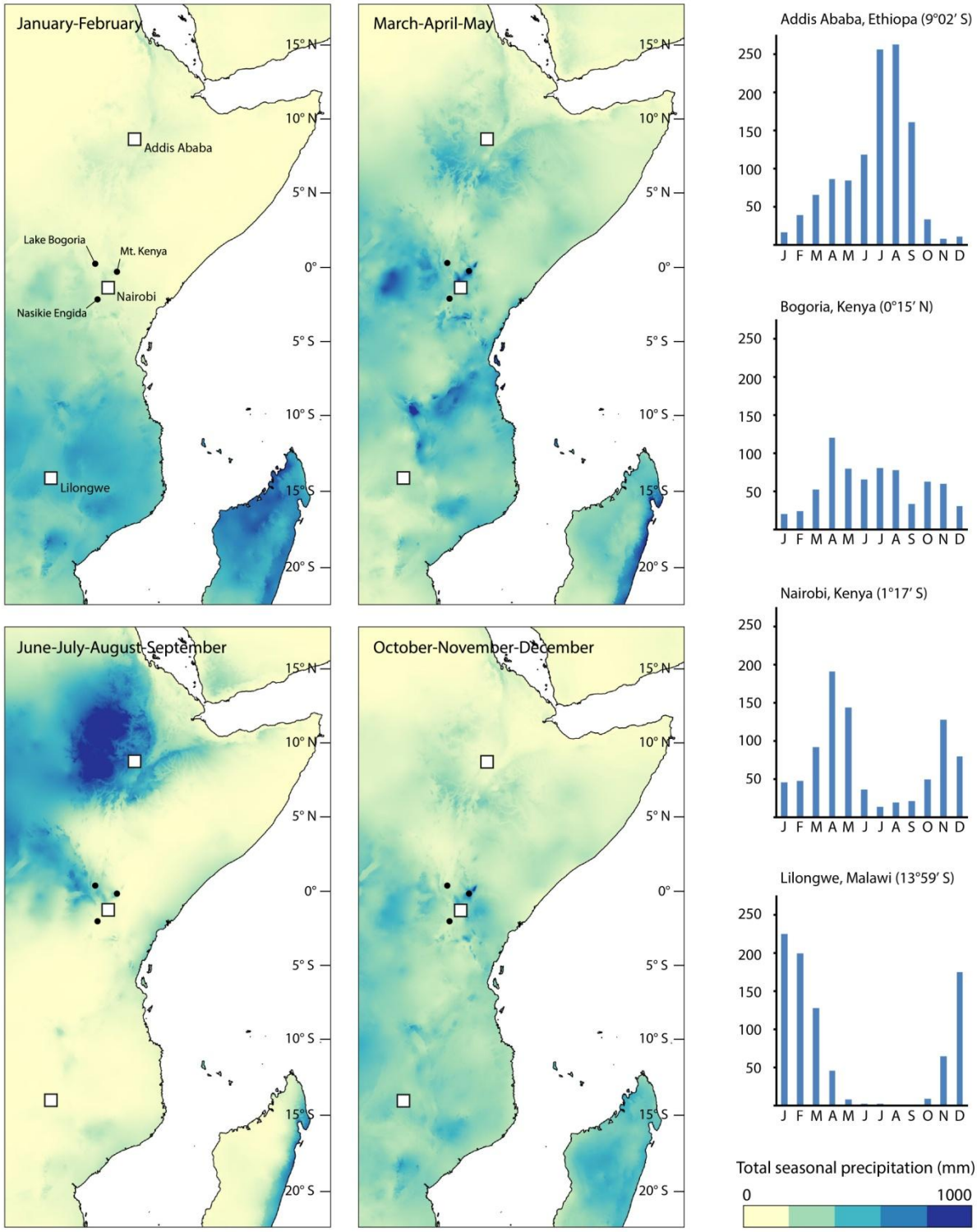

Fig. 4 Seasonal precipitation averages for December-January-February, March-April-May, June-July-August and September-October-November over the 1950-2000 period. Climatograms (late-20th century to present) of Addis Ababa, Nairobi, Lake Bogoria and Lilongwe illustrate the different seasonal rainfall regimes. Figure generated using the WorldClim global precipitation dataset (Hijmans et al., 2005). Mount Kenya and Nasikie Engida, two other important sites in this thesis, are also depicted.

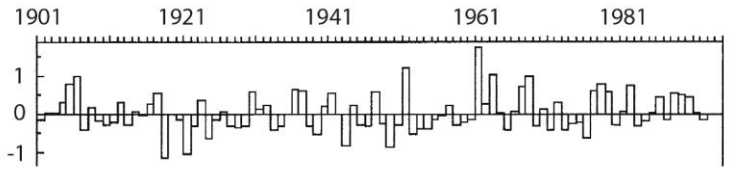

Fig. 5 Rainfall fluctuations in East Africa from 1901 to 1994, expressed as regionally averaged standardized departure from the long-term mean (Nicholson, 2000).

The quality of long-term weather and climate predictions is a major bottleneck hampering successful drought mitigation and adaptation. Precipitation projections are inherently more uncertain than temperature projections (Rowell, 2012), with higher spatial and seasonal dependence (Orlowsky and Seneviratne, 2012). In East Africa in particular, the naturally large temporal variability in rainfall at all time scales hampers identification of a uniquely anthropogenic signature in the trends observed during recent decades. General circulation model (GCM) studies, playing an important role in the assessment of future scenarios by the Intergovernmental Panel on Climate Change (IPCC), foresee likely increases in precipitation rates and intensity of high rainfall events during the OND and MAM wet seasons with indications for less severe droughts from the early 21st century onward (Shongwe et al., 2011) due to a generally more "El Niño-like" climate (Vecchi and Soden, 2007). However, this would require a reversal of the current trend of decreasing MAM (the main agricultural growing season) precipitation observed over the past three decades (Funk et al., 2008). This drying trend is explained by the authors by the disproportionately rapid anthropogenic warming of the Indian Ocean leading to a westward extension of the ascending branch of the tropical atmospheric Walker circulation into the eastern Indian Ocean, increasing convection and rainfall over the tropical Indian Ocean instead of over East Africa (Williams and Funk, 2011). The authors of this study expect this pattern of decreasing wet-season precipitation to continue into the century ahead, opposing IPCC predictions. Another study linked the decline in the East African long rains to a shift to warmer SSTs over the western tropical Pacific and cooler SSTs over the central and eastern tropical Pacific (Lyon and DeWitt, 2012), as part of natural multidecadal variability (Lyon et al., 2014; Yang et al., 2014). The mutually incompatible conclusions of these recent studies, and the absence of a consensus on even the sign of probable future rainfall trends, illustrate the limited understanding of the dynamics that drive East African rainfall.

This situation is extremely problematic for accurately predicting 21st century hydroclimate change. At the moment, robust climate forecasting at spatial and temporal scales relevant to human societies is far from evident in East Africa. Crucially, if local governments and economies are to strategically prepare for the future, the gap between current prediction capability and user needs has to be narrowed (WCRP-ICPO 2011). However, while GCMs are mostly incapable of incorporating important local mechanisms of rainfall distribution, especially over the complex terrain of East Africa, regional studies highlight the importance of resolving both regional-scale atmospheric processes and local effects like land surface on rainfall simulation (Niang et al., 2014). Indeed, some studies using high-resolution regional climate models forced by GCM-projections on the lateral and ocean boundaries suggest a future reduction in the long rains (Vizy and Cook, 2012; Cook and Vizy, 2013), contradicting overall GCM results. A recent study applied a logical framework to explore the possible causes for this East African climate paradox (an observed drying over the past decades

versus a GCM-projected wettening), such as model shortcomings, variable balances between forcings, land-use changes and anthropogenic aerosol injection into the atmosphere (Rowell et al., 2015). In their conclusions, the authors underline the need for a better understanding of the natural background of long-term climate variability in the region.

Paleoclimatology, the study of past climate change

The discipline of paleoclimatology encompasses all research fields occupied with the study of climate or climate-related phenomena in Earth's recent or distant past. Knowing how climate has naturally varied over the course of history has become invaluable for our understanding of climate dynamics all over the world. Furthermore, reconstructions of past climatic conditions can serve as a baseline against which to compare modern-day anthropogenic climate change, which is essential to correctly evaluate present observations and reliably predict future trends (Masson-Delmotte et al. 2013). In this regard, paleoclimate records can even serve as a tool used by climate modelers to calibrate and test their models, validating their ability to project future scenarios (Schneider and Mastrandrea, 2007). For example, the technique of paleoclimate data assimilation constrains models to follow paleoclimate observations within their uncertainty limits, providing an estimate of the full climate state that is most suitable with known proxy data (e.g. Widmann et al., 2010; Goosse et al., 2012).

A variety of natural archives has been used to infer past climate change. In the Northern Hemisphere, tree-ring records and ice cores have traditionally dominated paleoclimate research covering the period since the last Ice Age (e.g. Mann et al., 2008; Fig. 6). However, in tropical Africa, tree species suitable for dendroclimatological reconstructions are scarce, because local climate fails to drive the seasonal variation in wood growth required to produce reliable annual growth rings, and trees that do contain demonstrably annual rings have little potential to be preserved intact long after death (Dunbar & Cole, 1999). With the rapidly shrinking ice cap of Mount Kilimanjaro (Tanzania), and the small and unstable valley glaciers on Mount Kenya (Kenya) and the Rwenzori range (DR Congo, Uganda) being the only centres of glaciation, the possibility of recovering continuous and reliably dated ice-core records is also limited (Verschuren, 2004); even the ice-core record from Mount Kilimanjaro (Thompson et al., 2002) is essentially undated, and its very age and integrity are subjects of continued debate (e.g. Kaser et al., 2010). However, across East Africa, large-scale continental rifting and the resulting EARS have provided excellent conditions for the formation of numerous sedimentary basins (Wescott et al., 1996). While the western 'Albertine' branch of the EARS mainly contains large, deep lakes, the eastern 'Gregory' branch harbours a string of mostly smaller, shallow lakes. In addition to tectonic forces, a large number of lakes have also been created through volcanic activity (e.g. Melack, 1978) or (to a more localized extent) past glacial action in the formerly glaciated mountain ranges of Ethiopia, Uganda and Kenya (e.g. Eggermont et al., 2009). Paleolimnology, the interpretation of past conditions and processes in lake basins mainly through study of lake sediments, is a multidisciplinary science that has played a pivotal role in paleoclimatic research for decades (Last and Smol, 2001). This is because lakes, given that a number of requirements are met, have the ability to focus a diverse range of environmental indicators from the water column or catchment, and preserve them in their relatively undisturbed and continuously deposited sediments. Because of the many climate-sensitive lakes scattered across East Africa, their sedimentary archives have formed the single-most dominant source of paleoclimate information that has been collected for the region (Verschuren, 2004). A number of factors inherent to tropical African lacustrine systems complicate a straightforward conversion of recovered sediment records

to robust reconstructions of past environmental variability, such as frequent and widespread desiccation events partly destroying older deposits and ambiguous controls of certain climate variables on the proxies under study (Verschuren, 2003). However, recent advances have shown the value of high-quality sediment archives of African lakes in tackling longstanding research questions on historical climate change and its interaction with humans and natural ecosystems (Verschuren and Russell, 2009). Without a doubt, African paleolimnology will continue to prove crucial in resolving the current unknowns of past tropical climate dynamics.

Objectives and structure of this thesis

The work presented in this thesis was undertaken with the ultimate aim of improving the understanding of past, natural hydroclimate variability that has taken place in equatorial East Africa. Sediments collected from a diverse set of Kenyan lakes (Fig. 7), situated around the area of the furthest eastward reach of Atlantic-Ocean derived precipitation (i.e. close to the CAB), provide the basis for describing important historical events and patterns in moisture balance change, and their effects on regional ecosystems on various time scales. For each site a range of both long-established and novel analytical techniques is deployed, focusing mainly on the sedimentological, and mineralogical characteristics of the records. The choice for a multi-proxy approach was made deliberately, since a comprehensive understanding of each system was strived for. Especially when intending hydroclimate reconstruction, targeting multiple proxies contained within the sediments is often necessary, since few proxies exhibit a simple, one-to-one relationship to rainfall or other moisture-balance related variables. Furthermore, internal dynamics of different lakes may respond to climate change very distinctly from each other, and climate-to-proxy controls within a given lake system may even change over time, further justifying the broad, integrative paleolimnological approach followed throughout this thesis. Hydroclimate variability at time scales of decades to millennia is discussed, as the entire late- and post-glacial record since the peak of the last Ice Age (19,000 years ago) is treated before zooming in on the last 2,000 years. The insights obtained from the newly generated data are placed within a state-of-the-art context of current East African paleoclimatology. This way, this thesis will contribute to the delineation of past hydroclimate variability, and allow better differentiation between region-wide events and smaller-scale patterns.

Chapter 1 reports the study of a new sediment record of Lake Rutundu, a small crater lake on the eastern flank of Mount Kenya (Fig. 8). The results provide a detailed overview of moisture balance change over the past ca. 19,000 years since the Last Glacial Maximum, i.e. covering the entire late-Glacial period and the current interglacial period of the Holocene. New insights regarding the occurrence of abrupt, severe century-scale drought spells over the course of the Holocene and their impact on ecosystems throughout the continent are discussed.

My personal contribution to this chapter includes: all laboratory analyses (with the exception of radiometric dating analyses, charcoal counting and LOI), all data analysis, age model construction and all writing.

In **chapter 2**, focus is shifted to the most recent 2,000 years in history. As part of the International Geosphere-Biosphere Programme (IGBP) PAGES-2k Consortium's initiative to update and publish the next-generation database of climate datasets of the last two millennia, an extensive compilation and evaluation of available moisture balance records of the entire African continent is presented.

My personal contribution to this chapter includes: writing of abstract, 'Introduction' (ca. 80 %), 'Regional climate dynamics of the African continent' (ca. 50%), 'The Holocene context' (ca. 50%), 'African hydroclimate variability during the last two millennia' (ca. 40%), 'Discussion' (ca. 90%).

Chapter 3 discusses sedimentological and mineralogical evidence from sediment cores collected earlier in lakes Bogoria (Fig. 9), Nakuru and Elementeita to ascertain the regional impact of a number of drought episodes on the saline lakes of the Kenya Rift Valley. This chapter consists of a peer-reviewed research paper published in Palaeogeography, Palaeoclimatology, Palaeoecology and is (provisionally) presented in its original form. For a large part, it involves a revisit and extended discussion of previously obtained results, as the data on Lake Bogoria were collected by Ilse Bessems in the context of her PhD (submitted in 2007).

My personal contribution to this chapter includes: data analysis, age model construction, writing (75%).

In **chapter 4**, the sediment archive of Lake Bogoria is further explored. Multi-proxy analysis on a new set of sediment cores collected in 2014 provides the basis for a first continuous, high-resolution record of hydrological and ecological change covering the past ca. 1,300 years at this hypersaline rift lake.

My personal contribution to this chapter includes: field work, all laboratory analyses (with the exception of radiometric dating analyses and charcoal counting), data analysis, age model construction and all writing.

In search of new lake sediment records to improve the spatial coverage of East African high-quality paleoclimate archives, **chapter 5** deals with the exploration and evaluation of Nasikie Engida (Fig. 10) as an archive for reconstructing past moisture balance variability. A newly acquired sediment sequence from this previously uncored hypersaline lake reveals the site's potential to produce a first paleoclimate reconstruction of the southernmost Kenya Rift Valley covering at least the late Holocene with high resolution.

My personal contribution to this chapter includes: field work, all laboratory analyses, data analysis, all writing.

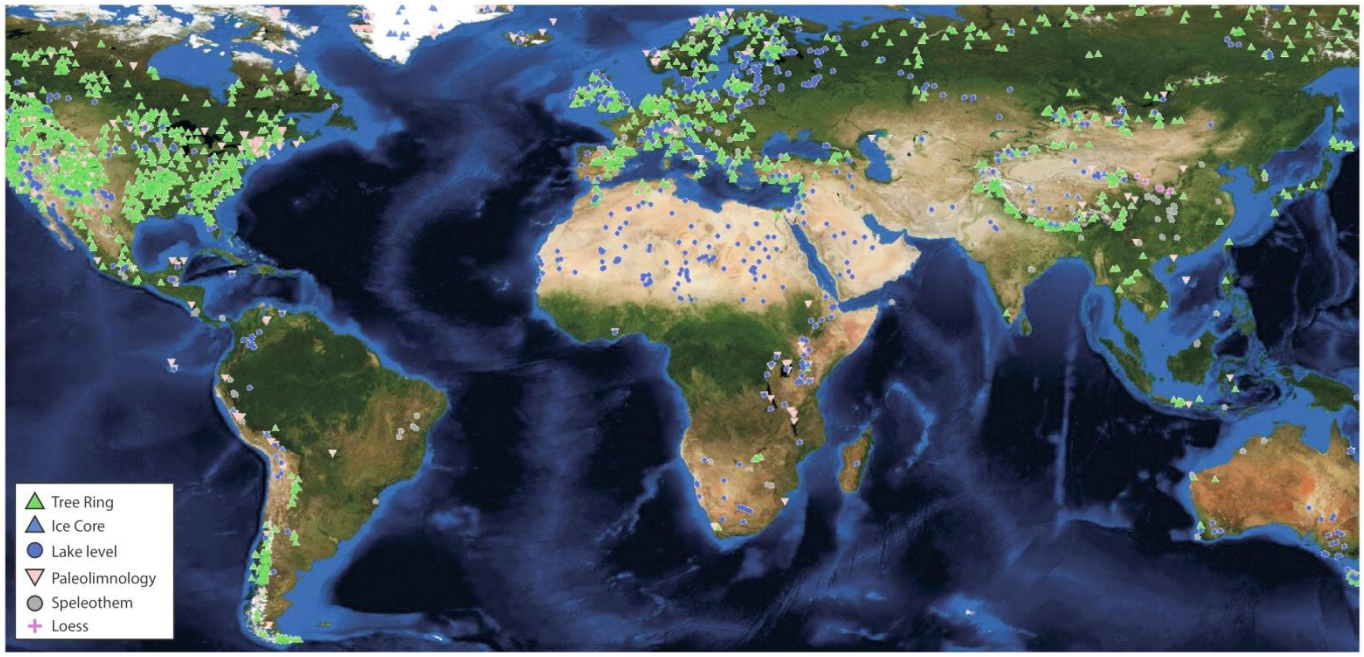

Fig. 6 Visualization of the geographical coverage of continental paleoclimate records included in the US National Oceanic and Atmospheric Administration (NOAA) online paleoclimate database (NOAA, 2016). High northern hemisphere latitudes harbour a variety of record types dominated by tree-ring records, while in Africa, (ancient) lakes provide the dominant source of data. The blue 'lake level' sites across northern Africa mostly represent discontinuous and low-resolution lake-level position records from now-desiccated lakes. The limited number of 'paleolimnology' sites represent the more continuous, higher-resolution lake records. In Africa these are much less common than in temperate and high northern latitudes, and mostly restricted to eastern Africa.

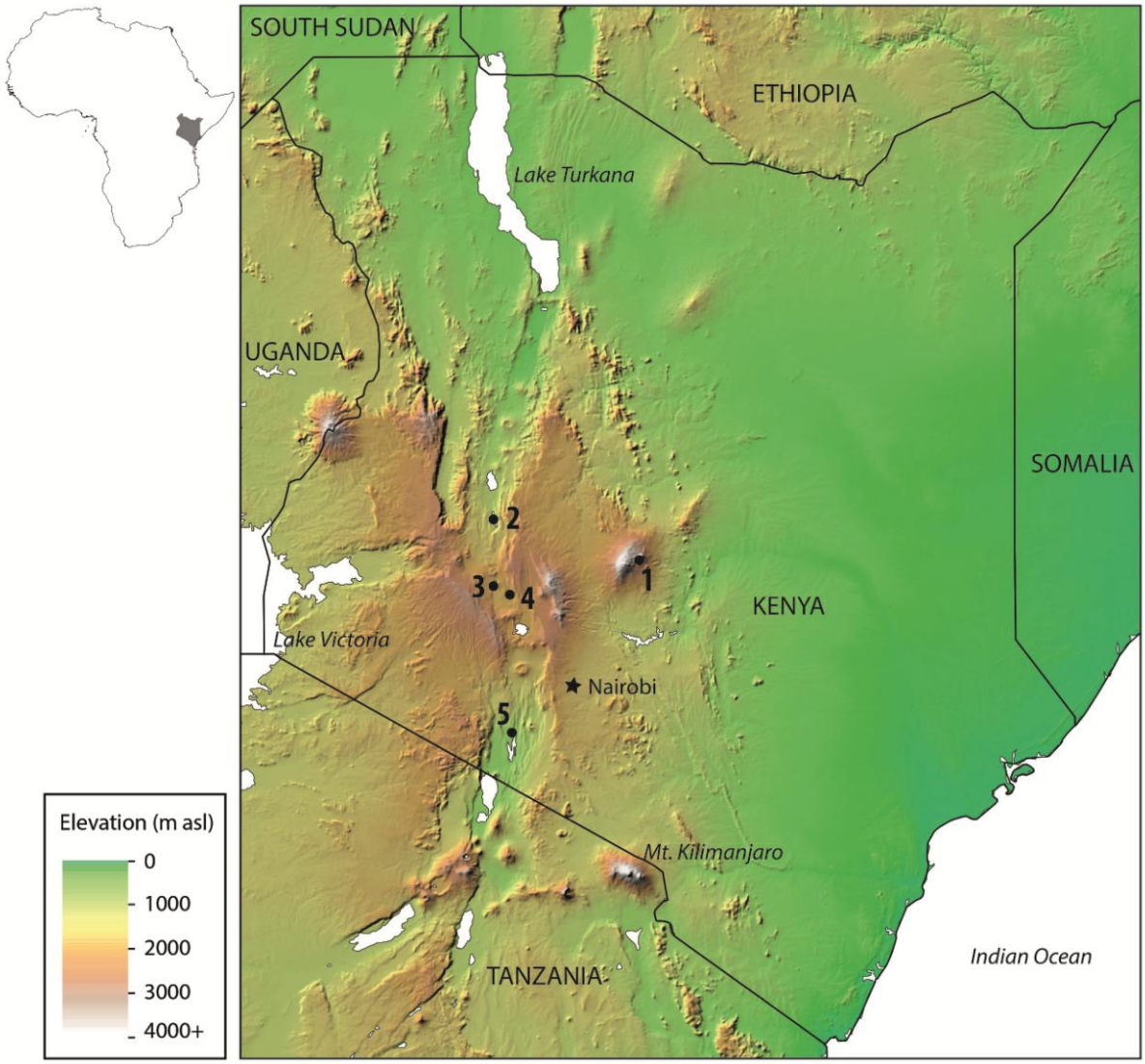

Fig. 7 Location of study sites discussed in this thesis. 1: Lake Rutundu, Mount Kenya, 2: Lake Bogoria, 3: Lake Nakuru, 4: Lake Elementeita, 5: Nasikie Engida.

Fig. 8 Lake Rutundu, a crater lake at 3080 m above sea level on the eastern flank of Mount Kenya. Photo by Hilde Eggermont.

Fig. 9 The central basin of Lake Bogoria, a tectonic hypersaline alkaline lake in the central Kenya Rift Valley, as seen from the west. Photo by Gijs De Cort.

Fig. 10 Nasikie Engida, a tectonic hypersaline alkaline lake in the dry southern Kenya Rift Valley, as seen from the northeastern river mouth. Photo by Gijs De Cort.

References

Anyah RO, Semazzi FHM. (2009) Idealized simulation of hydrodynamic characteristics of Lake Victoria that potentially modulate regional climate. International Journal of Climatology 29:971-981.

Anyah RO, Semazzi FHM. (2006) Climate variability over the Greater Horn of Africa based on NCAR AGCM ensemble. Theoretical and Applied Climatology 86:39-62.

Camberlin P, Janicot S, Poccard I. (2001) Seasonality and atmospheric dynamics of the teleconnection between African rainfall and tropical sea-surface temperature: Atlantic vs. ENSO. International Journal of Climatology 21:973-1005.

Checchi F, Robinson W. (2013) Mortality among populations of southern and central Somalia affected by severe food insecurity and famine during 2010-2012. FAO/FSNAU and FEWS NET.

Cook KH, Vizy EK. (2013) Projected Changes in East African Rainy Seasons. Journal of Climate 26:5931-5948.

Costa K, Russell J, Konecky B, Lamb H. (2014) Isotopic reconstruction of the African Humid Period and Congo Air Boundary migration at Lake Tana, Ethiopia. Quaternary Science Reviews 83:58-67.

Hillier D, Dempsey B. (2012) A dangerous delay: the cost of late response to early warnings in the 2011 drought in the Horn of Africa. Oxfam and Save the Children policy paper. Oxfam International and Save the Children, Oxford, UK.

Dunbar R, Cole J. (1999) ARTS—Annual records of tropical systems, (ARTS), recommendations for research: Summary of scientific priorities and implementation strategies, PAGES Workshop Report Series 99-1 Past Global Change, Bern., PAGES workshop report series 99-1. PAGES/CLIVAR, Bern.

Eggermont H, Van Damme K, Russell J. (2009) Rwenzori Mountains (Mountains of the Moon): headwaters of the White Nile. In: Dumont H (ed), The Nile: origin, environments, limnology and human use. Springer Science, pp. 243-261.

Funk C, Dettinger MD, Michaelsen JC, Verdin JP, Brown ME, Barlow M, Hoell A. (2008) Warming of the Indian Ocean threatens eastern and southern African food security but could be mitigated by agricultural development. Proceedings of the National Academy of Sciences of the United States of America 105:11081-11086.

Goddard L, Graham NE. (1999) Importance of the Indian Ocean for simulating rainfall anomalies over eastern and southern Africa. Journal of Geophysical Research-Atmospheres 104:19099-19116.

Goosse H, Guiot J, Mann ME, Dubinkina S, Sallaz-Damaz Y. (2012) The medieval climate anomaly in Europe: Comparison of the summer and annual mean signals in two reconstructions and in simulations with data assimilation. Global and Planetary Change 84-85:35-47.

Graham J, Rashid S, Malek M. (2012) Disaster response and emergency risk management in Ethiopia. In: Dorosh P, Rashid S (eds), Food and agriculture in Ethiopia: progress and policy challenges. University of Pennsylvania Press, Philadelphia, USA, pp. 256-279.

Hijmans RJ, Cameron SE, Parra JL, Jones PG, Jarvis A. (2005) Very high resolution interpolated climate surfaces for global land areas. International Journal of Climatology 25:1965-1978.

Kaser G, Mölg T, Cullen NJ, Hardy DR, Winkler M. (2010) Is the decline of ice on Kilimanjaro unprecedented in the Holocene? The Holocene, 20(7):1079-1091.

Kinuthia JH. (1992) Horizontal and vertical structure of the Lake Turkana jet. Journal of Applied Meteorology 31:1248-1274.

Last W, Smol J. (2001) An introduction to basin analysis, coring, and chronological techniques used in paleolimnology. In: Last W, Smol J (eds), Basin analysis, coring and chronological techniques. Kluwer Academic Publishers, Dordrecht, The Netherlands, pp. 1-5.

Levin NE, Zipser EJ, Cerling TE. (2009) Isotopic composition of waters from Ethiopia and Kenya: Insights into moisture sources for eastern Africa. Journal of Geophysical Research-Atmospheres 114, DOI: 10.1029/2009JD012166.

Lyon B. (2014) Seasonal Drought in the Greater Horn of Africa and Its Recent Increase during the March May Long Rains. Journal of Climate 27:7953-7975.

Lyon B, Barnston AG, DeWitt DG. (2014) Tropical pacific forcing of a 1998-1999 climate shift: observational analysis and climate model results for the boreal spring season. Climate Dynamics 43:893-909.

Lyon B, DeWitt DG. (2012) A recent and abrupt decline in the East African long rains. Geophysical Research Letters 39. DOI: 10.1029/2011GL050337.

Mann ME, Zhang Z, Hughes MK, Bradley RS, Miller SK, Rutherford S, Ni F. (2008) Proxy-based reconstructions of hemispheric and global surface temperature variations over the past two millennia. Proceedings of the National Academy of Sciences of the United States of America 105:13252–13257.

Mapande AT, Reason CJC. (2005) Links between rainfall variability on intraseasonal and interannual scales over western Tanzania and regional circulation and SST patterns. Meteorology and Atmospheric Physics 89:215-234.

Masson-Delmotte V, Schulz M, Abe-Ouchi A, Beer J, Ganopolski A, González Rouco J, Jansen E, Lambeck K, Luterbacher J, Naish T, Osborn T, Otto-Bliesner B, Quinn T, Ramesh R, Rojas M, Shao X, Timmermann A. (2013) Information from paleoclimate archives. In: Stocker T, Qin D, Plattner G, Tignor M, Allen S, Boschung J, Nauels A, Xia Y, Bex V, Midgley P (eds), Climate Change 2013: the physical science basis Contribution of Working Group I to the Fifth Assessment Report of the Intergovernmental Panel on Climate Change, Cambridge, UK and New York, USA.

Melack JM. (1978) Morphometric, physical and chemical features of the volcanic crater lakes of western Uganda. Archiv Fur Hydrobiologie 84:430-453.

Famine Early Warning Systems Network FEWS NET. (2016) www.fews.net.

National Oceanic and Atmospheric Administration NOAA. (2016) Paleoclimatology Data. https://www.ncdc.noaa.gov/data-access/paleoclimatology-data.

Niang I, Ruppel O, Abdrabo M, Essel A, Lennard C, Padgham J, Urquhart P. (2014) Africa. In: Barros V, Field C, Dokken D, Mastrandrea M, Mach K, Bilir T, Chattarjee M, Ebi K, Estrada Y, Genova R, Girma B, Kissel E, Levy A, MacCracken S, Mastrandrea P, White L (eds), Climate Change 2014: impacts, adaptation, and vulnerability Part B: Regional aspects Contribution of Working Group II to the Fifth Assessment Report of the Intergovernmental Panel on Climate Change, Cambridge, UK and New York, USA.

Nicholson S. (1996) A review of climate dynamics and climate variability in Eastern Africa. In: Johnson T, Odada E (eds), The limnology, climatology and paleoclimatology of the East African lakes. Gordon and Breach, pp. 25-56.

Nicholson, S. (2000) The nature of rainfall variability over Africa on time scales of decades to millennia. Global and Planetary Change 26:137-158.

Ogallo LJ, Janowiak JE, Halpert MS. (1988) Teleconnection between seasonal rainfall over East-Africa and global sea-surface temperature anomalies. Journal of the Meteorological Society of Japan 66:807-822.

Orlowsky B, Seneviratne SI. (2012) Global changes in extreme events: regional and seasonal dimension. Climatic Change 110:669-696.

Philander S, Gu D, Halpern D, Lambert G, Lau NC, Li T, Pacanowski RC. (1996) Why the ITCZ is mostly north of the equator. Journal of Climate 9:2958-2972.

Rowell DP. (2012) Sources of uncertainty in future changes in local precipitation. Climate Dynamics 39:1929-1950.

Rowell DP, Booth BBB, Nicholson SE, Good P. (2015) Reconciling Past and Future Rainfall Trends over East Africa. Journal of Climate 28:9768-9788.

Saji NH, Goswami BN, Vinayachandran PN, Yamagata T. (1999) A dipole mode in the tropical Indian Ocean. Nature 401:360-363.

Salami A, Kamara A, Brixiova Z. (2010) Smallholder agriculture in East Africa: trends, constraints and opportunities. Working Papers Series N° 105. African Development Bank, Tunis, Tunisia.

Schmidt M, Pearson O. (2016) Pastoral livelihoods under pressure: Ecological, political and socioeconomic transitions in Afar (Ethiopia). Journal of Arid Environments 124:22-30.

Schneider S, Mastrandrea M. (2007) Paleoclimate relevance to global warming. In: Elias S (ed), Encyclopedia of Quaternary Science. Elsevier, pp. 2010-2020.

Sepulchre P, Ramstein G, Fluteau F, Schuster M, Tiercelin JJ, Brunet M. (2006) Tectonic uplift and Eastern Africa aridification. Science 313:1419-1423.

Thompson LG, Mosley-Thompson E, Davis ME, Henderson KA, Brecher HH, Zagorodnov VS, Mashiotta TA, Lin PN, Mikhalenko VN, Hardy DR, Beer J. (2002) Kilimanjaro ice core records: Evidence of Holocene climate change in tropical Africa. Science 298:589-593.

Trabucco A, Zomer R. 2009. Global Aridity Index (Global-Aridity) and Global Potential Evapo-Transpiration (Global-PET) geospatial database. CGIAR Consortium for Spatial Information. Published online, available from the CGIAR-CSI GeoPortal at http://www.csi.cgiar.org.

Vecchi GA, Soden BJ. (2007) Global warming and the weakening of the tropical circulation. Journal of Climate 20:4316-4340.

Verschuren D. (2003) Lake-based climate reconstruction in Africa: progress and challenges. Hydrobiologia 500:315-330.

Verschuren D. (2004) Decadal to century-scale climate variability in tropical Africa during the past 2000 years. In: Battarbee R, Gasse F, Stickley C (eds), Past climate variability through Europe and Africa. Kluwer, Dordrecht, The Netherlands, pp. 139-158.

Verschuren D, Russell JM. (2009) Paleolimnology of African lakes: beyond the exploration phase. PAGES news 17:112-114.

Viste E, Sorteberg A. (2013) Moisture transport into the Ethiopian highlands. International Journal of Climatology 33:249-263.

Vizy EK, Cook KH. (2012) Mid-Twenty-First-Century Changes in Extreme Events over Northern and Tropical Africa. Journal of Climate 25:5748-5767.

Waliser DE, Gautier C. (1993) A satellite-derived climatology of the ITCZ. Journal of Climate 6:2162-2174.

Webb P, von Braun J. (1994) Famine and food security in Ethiopia: lessons for Africa. John Wiley and Sons, Canada.

Wescott W, Morley C, Karanja, F.M. (1996) Tectonic controls on the development of rift-basin lakes and their sedimentary character: examples from the East African Rift System. In: Johnson TC, Odada EO (eds), The limnology, climatology and paleoclimatology of the East African lakes. Gordon and Breach Publishers, pp. 3-21.

Widmann M, Goosse H, van der Schrier G, Schnur R, Barkmeijer J. (2010) Using data assimilation to study extratropical Northern Hemisphere climate over the last millennium. Climate of the Past 6:627-644.

Williams AP, Funk C. (2011) A westward extension of the warm pool leads to a westward extension of the Walker circulation, drying eastern Africa. Climate Dynamics 37:2417-2435.

Wolde-Georgis T. (1997) El Niño and Drought Early Warning in Ethiopia. Internet Journal of African Studies 2.

World Climate Research Programme (WCRP) WCRP, International CLIVAR Project Office ICP. (2011) Drought predictability and prediction in a changing climate. WCRP informal report no. 21/2011. ICPO publication series no 162.

Yang WC, Seager R, Cane MA, Lyon B. (2014) The East African Long Rains in Observations and Models. Journal of Climate 27:7185-7202.

Yang WC, Seager R, Cane MA, Lyon B. (2015) The Annual Cycle of East African Precipitation. Journal of Climate 28:2385-2404.

1 FIVE HOLOCENE DROUGHT PULSES RECORDED IN A POSTGLACIAL MOISTURE-BALANCE RECORD FROM MT. KENYA

De Cort, Gijs[1,2]; Verschuren, Dirk[1]; Eggermont, Hilde[3]; Barao, Lucia[4]; Daniel Conley[5]; Blaauw, Maarten[6]; Engstrom, Daniel R.[7]; Haug, Gerald H.[8]; Omuombo, Christine[9]; Olago, Daniel[9]

[1]*Limnology Unit, Department of Biology, Ghent University. K.L. Ledeganckstraat 35, 9000 Ghent, Belgium.*
[2]*Department of Earth Sciences, Royal Museum for Central Africa. Leuvensesteenweg 13, 3080 Tervuren, Belgium.*
[3]*Royal Belgian Institute for Natural Sciences, Belgian Biodiversity Platform, Vautierstraat 29, 1000 Brussels, Belgium.*
[4]*Ecosystem Management Research Group, Department of Biology, University of Antwerp. Universiteitsplein 1C, 2610 Wilrijk, Belgium.*
[5]*Department of Geology, Lund University. Sölvegatan 12, 22362 Lund, Sweden.*
[6]*School of Geography, Archaeology and Palaeoecology, Queen's University Belfast. BT7 1NN Belfast, United Kingdom.*
[7]*St. Croix Watershed Research Station, Science Museum of Minnesota. Marine on St. Croix, MN 55047, USA.*
[8]*Geological Institute, Department of Earth Sciences, ETH Zürich. Sonneggstrasse 5, 8092 Zürich, Switzerland.*
[9]*Department of Geology, University of Nairobi. Chiromo Campus, PO Box 30197 - 00100, Nairobi, Kenya.*

This chapter is in preparation for submission to *Nature Geoscience* or equivalent. The author list and sequence may still change.

The large majority of continental moisture-balance records from tropical and northern sub-tropical Africa appear to infer a more or less abrupt transition between a wet early- to mid-Holocene and drier late-Holocene climate. This contrasts with deep-sea sediment records, in which Holocene climate variability is manifested as a sequence of climate cycles, and with continuous speleothem records, in which it is manifested as pulses of drought (i.e., temporary weakened monsoon dynamics) super-imposed on a long-term trend of gradual drying. This chapter presents a high-resolution continental moisture-balance record from Mt Kenya spanning the past 19,000 years, which reveals all known major Holocene drought episodes, centered on 8200, 6500, 5300, 4200 and 2900 years ago, in a temporally well-constrained framework of the post-glacial climate history of equatorial East Africa. In conjunction with the speleothem data, this Mt Kenya record indicates that the commonly reported evidence for abrupt mid-Holocene African drying more likely reflects non-linear and site-specific feedbacks between actual regional climate history and the proxy assumed to represent it; and that a relatively short-lived episode of climatic drought pushed the system governing that proxy beyond the threshold of recovery to its previous state. These results imply that if the chronology of a sufficiently large fraction of African continental moisture-balance records could be improved, the now diverse timing of the end of the African Humid Period recorded in them would cluster around the ages of these major droughts.

INTRODUCTION

Following the arid conditions of the Last Glacial Maximum (LGM), a large part of the African continent experienced the Early to Mid-Holocene as a period much more humid than today (Gasse, 2000). During this so-called African Humid Period (AHP, ca. 15-5 ka BP; deMenocal et al., 2000), the Sahara desert was a green savannah with annual grasses and shrubs and large lakes (Jolly et al., 1998; Leblanc et al., 2006; Lézine et al., 2011) and in East Africa, the present-day shallow and often saline lakes of the Ethiopian and Kenyan Rift systems were fresh and stood much higher than today

(Barker et al. 2004). While the timing and abruptness of the onset and ending of the AHP in the different affected regions has been the subject of major discussion (e.g. deMenocal et al., 2000; Kröpelin et al., 2008; Tierney and deMenocal, 2013; McGee et al., 2013; Junginger et al., 2014; Weldeab et al., 2014), shorter-lived climate fluctuations within the AHP have received much less attention, mostly because of the scarcity of well-dated, high-resolution proxy time series with adequate climate sensitivity both in the early and late Holocene (Verschuren, 2003). The postglacial sediment record of Lake Rutundu, a small crater lake on Mt. Kenya in equatorial East Africa, is used to document century-scale climate variability embedded within the multi-millennial AHP climate trend. This multi-proxy reconstruction of lake evolution over the past 19,000 years, based on 324-cm sediment core sequence RUT09 (see supplementary information), provides detailed information on the region's moisture-balance history. Firmly anchored in time by a robust age model, it reveals five major episodes of Holocene drought. The apparently sudden ending of the AHP suggested by diverse individual records from sites throughout northern and equatorial Africa often coincides with the timing of one of the drought events recorded at Lake Rutundu. In this chapter, it is argued that site-specific hydrological or ecosystem recovery following these events has influenced the perceived timing and spatial complexity of the AHP termination.

STUDY SITE

Lake Rutundu (0° 02' 30" N, 37° 27' 50" E) is a small (ca. 0.1 km²), shallow (11 m) lake occupying a single-event eruption crater on the eastern flank of Mount Kenya, 3080 m above sea level (a.s.l.). The lake has no above-ground outflow, but subsurface outflow has allowed lake waters to remain fresh and oligotrophic, with a conductivity of 35 µS/cm and a pH of 7.6. The catchment is small, consisting only of the crater rim, made up of relatively unconsolidated trachytic tuffs (Baker, 1967). The lake is situated in the ericaceous vegetation belt, ca. 90 m above the present tree line (Wooller et al., 2003). Situated in Equatorial East Africa, Mount Kenya's climate is dominated by a bimodal seasonal rainfall pattern caused by the twice-yearly passage of the intertropical convergence zone (ITCZ), with long (March-May) and short (October-November) rainy seasons alternated by drier periods. Rainfall on the mountain is highest in the forest belt and decreases with altitude. Micro-orographic effects cause the southeast flanks to receive the highest amount of precipitation (Hastenrath, 1995).

CORING

In August 2009, four overlapping sections of ca. 1 m in length where collected from the deepest part of the lake with a single-drive square-rod Livingstone coring device. The most recently deposited surface sediments were recovered using a Uwitec gravity core device, and were extruded in the field at 1-cm intervals. The overlapping sections were combined to form the continuous 324-cm composite sequence RUT09.

ANALYSES

Porosity and water, organic matter and carbonate content were determined at 1-cm intervals by the Loss-On-Ignition (LOI) method, which measures the weight loss after drying 1 cc of sediment overnight at 105 °C, burning for 4 hours at 550 °C and ashing for 2 hours at 1000 °C (Dean, 1974). Volume-specific magnetic susceptibility was measured at 2-mm intervals using a Bartington point sensor MS2E mounted on a Multisensor Core Logger (Geotek Ltd, Daventry, Northants, UK), after which the specific dry sediment weight was used to obtain mass-specific magnetic susceptibility

values (χ). Samples at 4- to 8-cm intervals were measured for grain size by laser diffraction using a Malvern Mastersizer S, after sample pretreatment with 10% HCl, 30% H_2O_2 and 10% KOH for the removal of carbonates, organic matter and biogenic silica respectively (Vaasma, 2008). Non-destructive X-ray fluorescence (XRF) analysis was conducted on split core halves using an AVAATECH X-Ray Fluorescence Core Scanner at a 1-mm interval. Elemental counts were taken as ratios to eliminate matrix effects. Si/Al ratio was used as an indicator of biogenic silica content, with Al a correction for catchment-derived mineral Si (Brown 2015). Additionally, biogenic silica content was determined every 4 to 8 cm using a continuous analysis technique tracing the dissolution of Si and Al in 0.5 M NaOH in real-time (Koning et al., 2002, Barão et al., 2014). It has been shown that, in settings rich in readily dissolvable non-biogenic Si such as volcanic glass, this technique has the advantage of distinguishing between biogenic and minerogenic reactive phases (Appendix 1; Barão et al., 2015), despite being very time-consuming. Linear regression with measurements of BSi determined for identical core depths following standard procedure, i.e. a time-step analysis of Si extracted over a 3-h period using 1% Na_2CO_3 as solvent (Conley and Schelke, 2001), allowed to calculate a conversion factor to correct higher-resolution (2- to 4-cm intervals) standard BSi measurements for reactive non-biogenic Si. BSi flux levels were calculated using the sediment accumulation rates produced by the age model. Charcoal particles were counted at 1-cm intervals under a binocular microscope following sieving at 100µm. after which charcoal flux rates were calculated.

AGE MODEL

Age-depth relationship is based on 33 bulk sediment or charcoal samples (Table 1) analyzed for ^{14}C by accelerator mass spectrometry (AMS). ^{210}Pb dating constrained the most recently deposited sediments (Table 2), with sediment age at depth and accumulation rates being calculated based on the constant rate of supply (CRS) model. However, incompatibility with lower radiocarbon dates and unrealistic sedimentation rates of the ^{210}Pb-dated core segment suggest a serious underestimation of the lower ^{210}Pb ages. This problem has recently been the subject of a dedicated study which highlighted the danger of ^{210}Pb-chronologies, when unconstrained by independent sources of age information, yielding unrealistically young ages for the lower parts of the studied sediment profile (Tylmann et al., 2016). Probable causes for these discrepancies are violations of the assumptions made by the most common models for age calculation, i.e. significant variability in atmospheric or sedimentary ^{210}Pb flux through time. It seems likely, given the available age information below the ^{210}Pb-dated section, that such a scenario might be the case for RUT09 as well. Without ^{137}Cs or other chronostratigraphic markers to calibrate the ^{210}Pb dating results, the decision was made to omit pre-1960 ^{210}Pb ages. An age model (Fig. 1) was constructed using the CLAM software package for R (Blaauw, 2010), applying a smooth spline function (smoothing factor 0.65) and 10,000 model iterations, calibrating ^{14}C ages with the Northern-Hemisphere terrestrial radiocarbon calibration curve (Reimer et al. 2013). Three event deposits were excluded from the final model: a tephra layer at 249-251 cm and two turbidites at 254-256.5 and 312-314 cm sediment depth. Three radiocarbon dates in the lowermost part of the core were refuted in the final model. One bulk sample at 323-324 cm and two charcoal samples at 313-317 and 317-321 resulted in an age model with too many reversals and were excluded. The amount of measurable carbon was very low in these samples, so contamination by modern material during sample treatment cannot be excluded. The age model results in a best-fit basal age of 18,700 cal yr BP within a 2σ probability range of 18,600-19,100 cal yr BP. Bulk sediment mass accumulation rates (in $g.cm^{-2}.yr^{-1}$, Fig. 1) are highest during the Late-Glacial

part of the core, gradually decreasing into the Holocene with a slight rebound during the Younger Dryas epoch. Minimum levels are reached at ca. 10 kyr BP. Afterwards, accumulation rates rise during the mid-Holocene with maxima at 6,500, 5,500 and 3,000 cal yr BP, to decrease again during the past two millennia.

code	depth	material	^{14}C age	max cal age (2σ, cal yr BP)	min cal age (2σ, cal yr BP)	probability
	cm		*^{14}C yr*	*cal yr BP*	*cal yr BP*	
SacA34960	39.5-40.5	bulk OM	1650 ± 30	1461	1418	0.085
				1485	1485	0.001
				1619	1518	0.853
				1686	1677	0.011
Poz-79687	67-68	bulk OM	2720 ± 30	2865	2761	0.95
UBA-26039	70-71	bulk OM	2655 ± 29	2797	2742	0.885
				2843	2820	0.065
SacA34961	70-71	bulk OM	2825 ± 30	3005	2851	0.948
				3016	3015	0.002
Poz-79688	73-74	bulk OM	2735 ± 30	2880	2764	0.942
				2916	2913	0.007
Poz-79689	84-85	bulk OM	3090 ± 30	3374	3227	0.095
UBA-26040	100-101	bulk OM	3332 ± 34	3640	3476	0,937
				3678	3670	0,013
SacA34962	104.5-105.5	bulk OM	3530 ± 30	3891	3715	0.95
OS-90777	124-125	bulk OM	4410 ± 30	5054	4867	0.903
				5214	5190	0.041
				5230	5228	0.002
				5256	5251	0.004
SacA34963	125.5-126.5	bulk OM	4170 ± 30	4597	4586	0.02
				4767	4611	0.73
				4830	4783	0.199
UBA-24285	134-135	bulk OM	4635 ± 32	5333	5305	0.194
				5354	5347	0.016
				5367	5357	0.021
				5464	5371	0.719
UBA-24286	143-144	bulk OM	5034 ± 50	5899	5661	0.95
UBA-24287	154-155	bulk OM	5517 ± 41	6232	6220	0.028
				6402	6275	0.922
UBA-24288	161-162	bulk OM	5778 ± 33	6657	6496	0.95
UBA-24289	169-170	bulk OM	5770 ± 52	6676	6441	0.949
				6710	6710	0.001
UBA-24290	181-182	bulk OM	6287 ± 34	7272	7162	0.95
UBA-24291	192-193	bulk OM	7593 ± 37	8443	8349	0.95
UBA-24296	192-193	charcoal	7295 ± 37	8175	8023	0.95
OS-108571	204-205	bulk OM	8330 ± 35	9458	9266	0.95
UBA-24292	205-206	bulk OM	8341 ± 45	9161	9155	0.005
				9474	9252	0.945
UBA-24293	219-220	bulk OM	10134 ± 42	11522	11504	0.012
				12017	11607	0.938
UBA-24294	227-228	bulk OM	10508 ± 44	12274	12239	0.025
				12324	12308	0.007
				12627	12381	0.918
UBA-24295	233-234	bulk OM	11003 ± 44	12996	12738	0.95
UBA-24297	233-234	charcoal	10951 ± 49	12956	12713	0.95
OS-108572	248-249	bulk OM	12200 ± 75	14389	13809	0.95
UBA-26041	264-268	charcoal	12946 ± 70	15733	15240	0.95
OS-108573	278-279	bulk OM	13950 ± 65	17160	16630	0.95
UBA-26042	296-302	charcoal	14377 ± 69	17757	17274	0.95
UBA-27242	302-310	charcoal	15177 ± 129	18719	18110	0.95
UBA-26043*	313-317	charcoal	14611 ± 72	17987	17589	0.95
OS-108574	318-319	bulk OM	15150 ± 50	18582	18261	0.95
UBA-26044*	317-321	charcoal	14177 ± 113	17584	16921	0.95
OS-90868*	323-324	bulk OM	12300 ± 50	14587	14053	0.95

Table 1 Radiocarbon dating results for core RUT09. Asterisks indicate dates that were not incorporated in the age model.

depth	^{210}Pb age	^{210}Pb age error
cm	*yr AD*	*yr AD*
0-1	2008.1	4.9
1-2	2005.6	5.1
2-3	2002.6	5.4
4-5	1995.6	6.2
8-9	1975.7	9.9
12-13*	1951.3	10.7
13-14*	1946.9	12.1
16-17*	1936.5	15.9
20-21*	1917.2	28.4
24-25*	1894.7	55.6

Table 2 ^{210}Pb-dating results for core RUT09. Asterisks indicate samples that are potentially dated as too young and were consequently omitted from the age model.

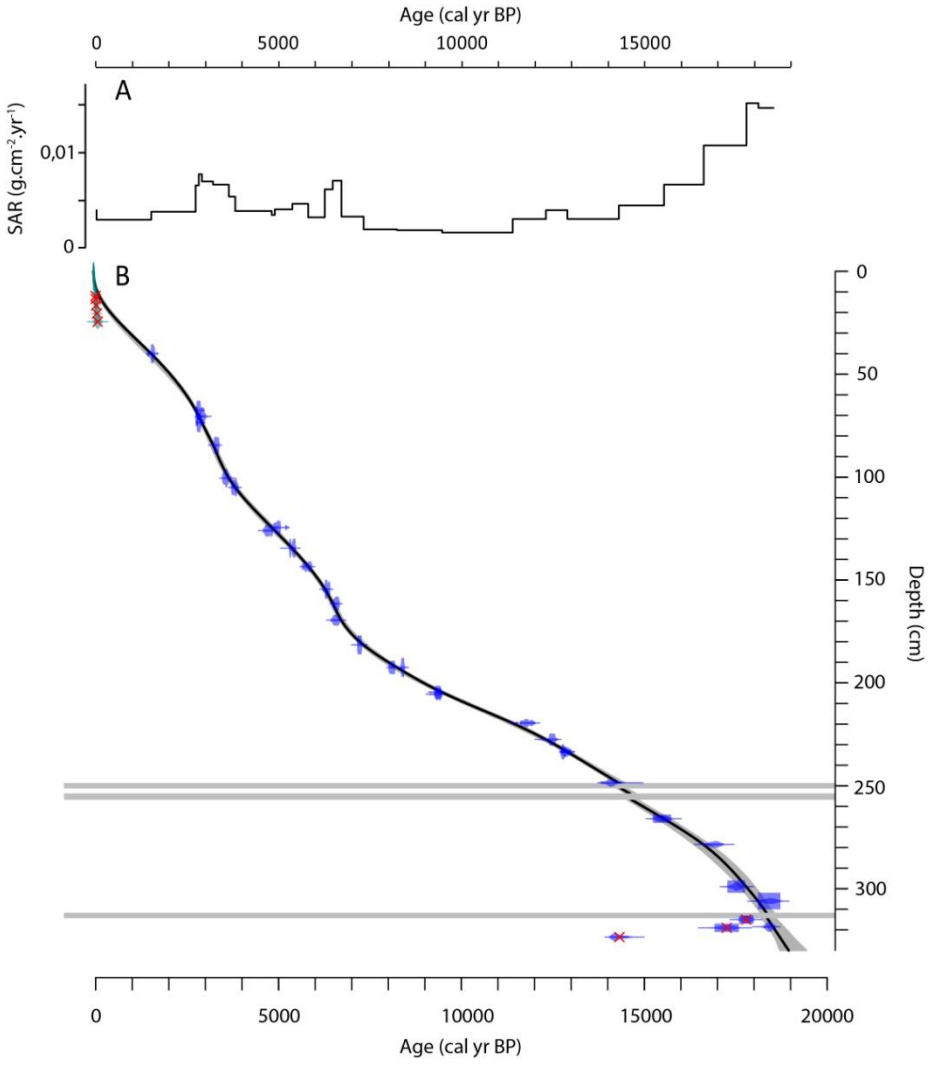

Fig. 1 a: Sediment mass accumulation rate (SAR) in g dry mass per cm² per year, calculated for intervals constrained by directly dated depths. b: Age-depth model for core RUT09, with ^{210}Pb-derived ages in green and ^{14}C ages in blue. Full black line shows best-fit age, grey shading represents 95% confidence interval. Grey bars depict event deposits that were omitted from the model.

INTERPRETING THE MULTI-PROXY LAKE RUTUNDU RECORD

Because of its small and topographically closed catchment, the water level of Lake Rutundu reacts in a fast and straightforward way to changes in local climatic moisture balance. During former highstands a large part of the crater was filled with water, preventing clastic mineral material from the inner slopes reaching the middle of the lake. Sedimentation was dominated by in-lake productivity, resulting in high organic-matter content (%OM) and low rates of sediment accumulation. During lowstands, a larger part of the crater catchment was exposed to sheet erosion. With the lakeshore much closer to the depositional center of the lake, clastics mobilized during rains could more easily reach the core site and organic matter from settling phytoplankton became diluted during sedimentation, resulting in lower %OM values. Following this reasoning, variation in %OM and tracers of clastic input (mass-specific magnetic susceptibility [χ]) primarily reflect fluctuations in lake level and thus climatic moisture balance (Fig. 2a-b). These proxies are also influenced by secondary drivers. χ is accentuated during glacial and late-glacial periods by the enhanced soil mobility when vegetation cover was incomplete. Equilibrium-line altitude (ELA) was depressed by more than 1000 m during the Last Glacial Maximum (LGM; Loomis, 2013), which means that conditions at Lake Rutundu were probably similar to the modern afroalpine belt (Wooller et al., 2003). This is also suggested by very low charcoal flux rates (Fig. 2d), which indicate an environment that was not favorable for wildfires (i.e. low temperatures, sparse local vegetation; van der Werf et al., 2008). Sedimentary OM content is also determined by variability in phytoplankton production, which in this tropical mountain lake is expected to be influenced by temperature (Michelutti et al., 2015).

LATE-PLEISTOCENE CLIMATE EVENTS

Dry conditions have frequently been inferred for East Africa during and immediately after the LGM (Gasse et al., 2000). This Late-Pleistocene aridity peaked during Heinrich Event 1 (H1, ca. 16-17 kyr BP, Stager et al., 2011). Accordingly, low %OM and peak χ values in the Rutundu record indicate very low lake levels from 19 to 16 kyr BP (Fig. 2a-b). High ratios of coarse to fine silt indicate a catchment not stabilized by vegetation. After H1, monsoonal moisture delivery to Mount Kenya started picking up, at first slowly from 16 kyr BP and faster from 14.5 kyr BP onwards. The largely synergistic positive effects of northern hemisphere summer insolation and the post-glacial rise in atmospheric CO_2 have been identified as the principal causes for the invigoration of monsoon rainfall over equatorial East Africa at this time (Otto-Bliesner et al., 2014). Lake Rutundu's late-glacial %OM record is consistent with the global record of Late-Pleistocene climate change: a bimodal wetter phase during the warm Bølling-Allerød interstadial (BA, 14.5-12.8 kyr BP) including a short interruption sometimes referred to as the Older Dryas (ca. 13.5-13.2 kyr BP), and a return to drier conditions during the Younger Dryas cold reversal (YD, 12.8-11.5 kyr BP). The timing of these events at Lake Rutundu matches their occurrences in other parts of the world where they have been extensively documented (Rosen et al., 2014; Ehlers et al., 2015; Clark et al., 2012), strongly supporting not only the sediment chronology, but also the interpretation of %OM as principally a humidity indicator.

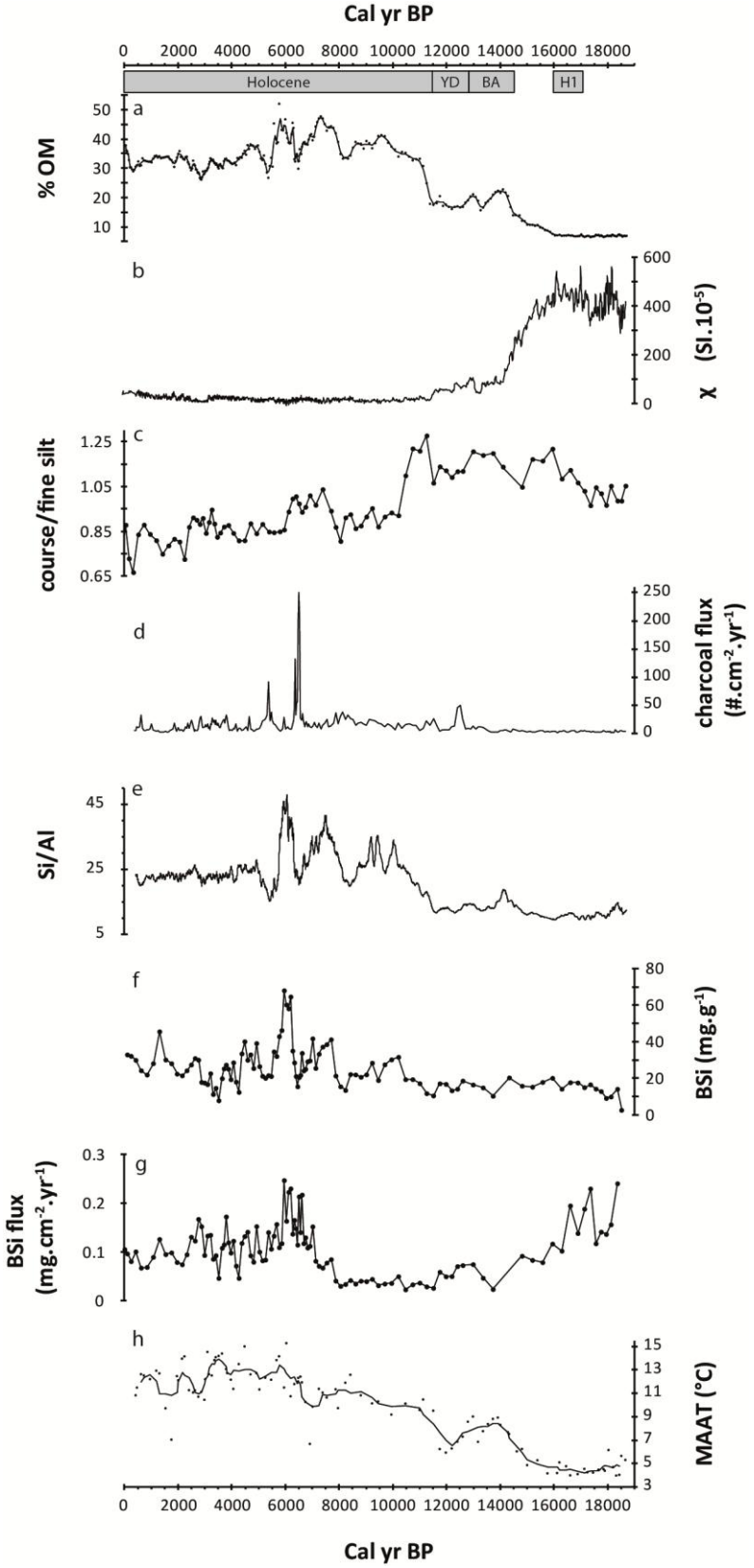

Fig. 2 Moisture balance proxies for Lake Rutundu core RUT09. a: %OM (solid black line depicts three-point running average), b: magnetic susceptibility corrected for dry weight (χ), c: coarse/fine silt as derived from grain-size analysis, d: charcoal flux rates, e: Si/Al ratio, f: BSi content, g: BSi flux rates, h: mean annual air temperature (MAAT, solid line depicts five-point running average) from molecular biomarkers (Loomis, 2013).

EARLY-HOLOCENE HUMIDITY

Following the YD, Lake Rutundu water level sharply rose at ca. 11.5 kyr BP, reflecting the abrupt resumption of strong monsoon rainfall at the onset of the Holocene (Talbot et al., 2007). Values of χ drop to near-zero at this point, suggesting that the exposed portion of the crater basin was reduced to the upper crater slopes. Shortly after a full vegetation cover was restored (Wooller et al., 2003), allowing higher amounts of charcoal to be generated than during preceding late-glacial conditions while strongly limiting erosion as indicated by an abrupt shift to smaller grain sizes (Fig. 2c). Previous studies have shown that the Holocene moisture balance history of East Africa (at least the part which receives a significant share of Atlantic-derived moisture) at and even south of the equator (to ca. 10° S) follows the pattern dictated by northern hemisphere orbital forcing, with very humid conditions during the early- to mid-Holocene coincident with maximum northern hemisphere summer insolation (e.g. Gasse, 2000; Barker et al., 2002; Vincens et al., 2005; Tierney et al., 2008; Tierney & DeMenocal 2013). This peak insolation displaced the meteorological equator further northward into the NH, advecting more moisture deeper into the continent across northern Africa (Kutzbach and Otto-Bliesner, 1982). In East Africa, wet conditions were promoted by the associated increase in dry-season (June-August) precipitation and a subsequent reduction of rainfall seasonality (Tierney et al., 2011a). Reasons for this were an increased influx of moisture from Atlantic sources because of a weakening of the easterly trade winds, and higher precipitation over easternmost East Africa because of increased SSTs in the western Indian Ocean. In the Rutundu record, peak %OM levels (>40% of bulk dry mass) are reached by ca. 9.7 kyr BP, showing show that also on Mt. Kenya humidity peaked during the early Holocene. The water level probably reached as high as the porous upper crater rim allowed without significantly increasing sub-surface outflow.

SEQUENCE OF CENTURY-SCALE DROUGHTS SUPER-IMPOSED ON GRADUAL HOLOCENE DRYING

Five important sections with low %OM values can be identified in the Holocene portion of core RUT09, signifying century-scale events of anomalous climatic drought (Fig. 3a). The first of these (R1) is dated to have occurred between 8,400 and 8,000 years ago. Most probably it is the regional expression of the widespread 8.2-kyr event (Alley et al., 1997), an abrupt shift to colder, drier conditions recorded from different parts of the world. Though initially reported from northern high-latitude than low-latitude areas, there is ample evidence that this was in fact a global-scale event (Morrill and Jacobsen, 2005; Cheng et al., 2009). Two more abrupt, century-scale shifts to arid conditions interrupt the high organic matter levels of the early- to mid-Holocene Rutundu record, dated to 6.7-6.3 ka (R2) and 5.5-5.2 ka BP (R3), both characterized by peaks in charcoal flux signifying significant increases in drought-triggered wildfires. The fourth episode of prominent drying, dated to 4.3-3.9 ka (R4), appears to mark the definitive ending of early/mid-Holocene humid conditions on Mt Kenya. After this event, %OM never again surmounted 35%. During the late-Holocene, the regionally most arid conditions are registered around 2.9 ka (R5), when %OM levels were the lowest of the past 11,000 years.

The very high %OM values (>45 % of bulk dry mass) centered on 7.3 and 6 ka BP do not necessarily reflect the highest water levels of Lake Rutundu during the mid-Holocene. Higher in-lake productivity may have overprinted the lake-level proxy at this time, with intensive diatom production as evident from high amounts and flux rates of biogenic silica (BSi) and high levels of Si/Al (Fig. 2e-g). Diatoms often make up a major component of phytoplankton communities of oligotrophic alpine lakes

(Battarbee et al., 2002). Probably, this peak productivity was stimulated by the regional mid-Holocene temperature optimum (Loomis, 2013; Fig. 2h). In Lake Rutundu's high-mountain setting, this temperature rise was probably accentuated relative to the surrounding lowlands. Situated near modern-day tree-line, maximum temperature might have provided favorable conditions for algal growth. A study of three tropical alpine lakes in Ecuador documented no or even slightly negative trends in algal production associated with recent warming temperatures, attributed to increased thermal stability of lake waters (Michelutti et al., 2015). At Lake Rutundu, increased diatom productivity suggests that the water column remained well-mixed even during the warm mid-Holocene, so that increased temperatures translated in higher growth rates rather than nutrient limitation. This overprint of high mid-Holocene algal productivity complicates a quantitative water-level reconstruction throughout the Holocene based on %OM, however it does not compromise the Rutundu %OM record as tracer of severe intermittent drought episodes, from which the Lake Rutundu ecosystem was able to recover.

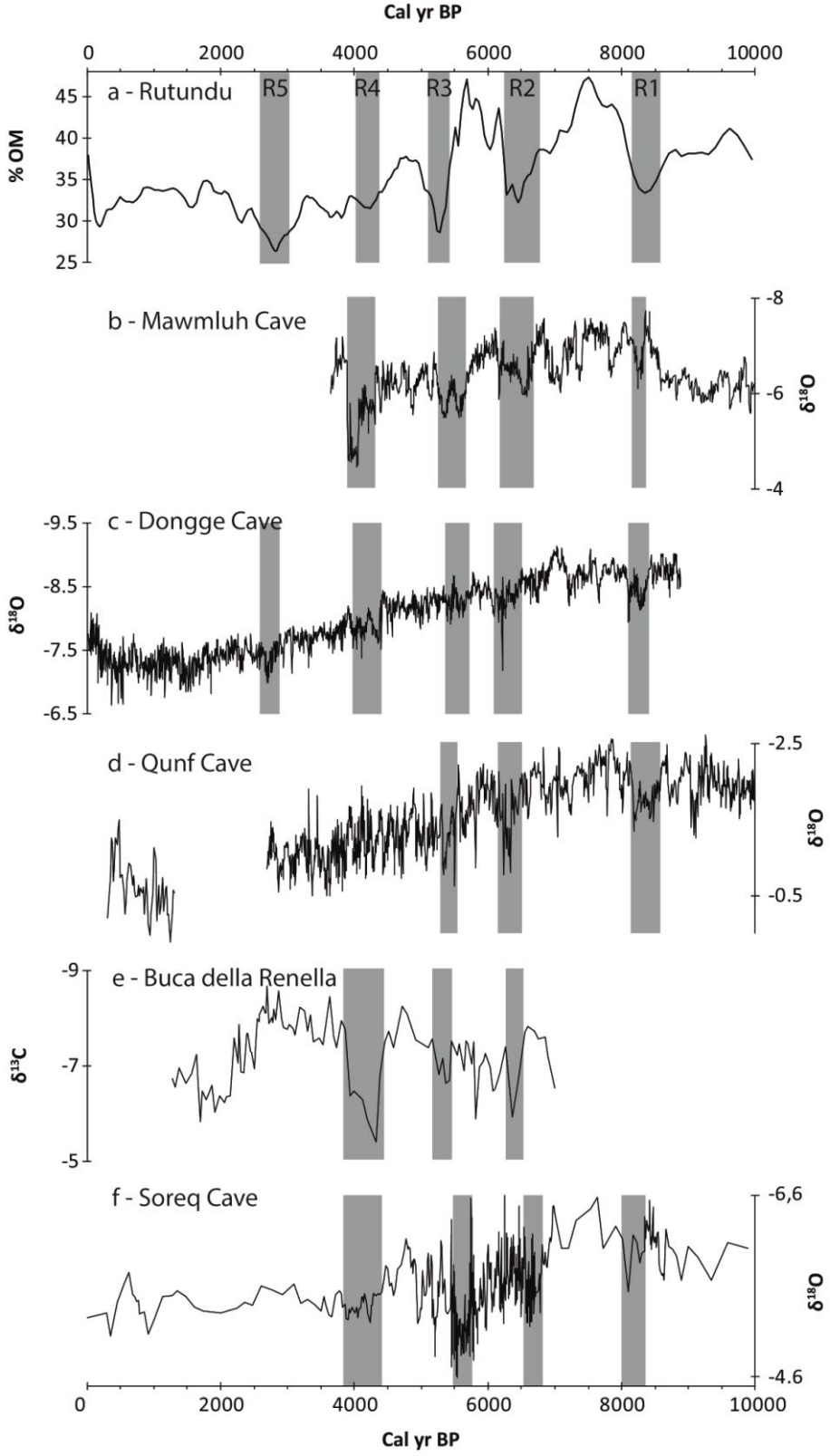

Fig. 3 a: Lake Rutundu Holocene %OM record demonstrating century-scale episodic drought throughout the Holocene, b: Mawmluh Cave (NE India) $\delta^{18}O$ in ‰ VPDB (Berkelhammer et al., 2012), c: Dongge Cave (SE China) DA $\delta^{18}O$ in ‰ VPDB (Wang et al., 2005), d: Qunf Cave (S Oman) Q5 $\delta^{18}O$ in ‰ VPDB (Fleitmann et al., 2007), e: Buca della Renella (N Italy) $\delta^{13}C$ in ‰ VPDB (Drysdale et al., 2006), f: Soreq Cave (Israel) $\delta^{18}O$ in ‰ VPDB (Bar-Matthews et al., 2003; Bar-Matthews and Ayalon, 2011).

GLOBAL CLIMATE TELECONNECTIONS

The continuous, high-resolution nature and robust chronology of Lake Rutundu's sediment record have produced a reliable and unique history of century-scale East African drought throughout the Holocene. It testifies of at least five events that show a remarkable similarity to episodes of decreased Indian Ocean monsoon activity as evident from high-resolution, well-dated speleothem records from the northern subtropics (Fig. 3b-f). R1, or the 8.2-kyr event, clearly disrupted maximum early-Holocene humidity levels in northeast India (Mawmluh Cave, Fig. 3b; Berkelhammer et al., 2012), southern China (Dongge Cave, Fig. 3c; Wang et al., 2005) and Oman (Qunf Cave, Fig. 3d; Fleitmann et al., 2007). These three archives also attest to temporarily weakened Indian monsoon dynamics in the northern hemisphere subtropics coinciding with mid-Holocene events R2-4. Furthermore, these events also occurred in the Mediterranean-Atlantic realm. In the Judean Mountains of Israel, R1-4 can be discerned in a stalagmite record from Soreq Cave (Bar-Matthews et al., 2003, Fig. 3f; Bar-Matthews and Ayalon, 2011), while droughts recorded in an Italian flowstone spanning the past seven millennia (Buca della Renella, Fig. 3e; Drysdale et al., 2006) can be correlated to events R2-4. Event R5 can be linked to a drought pulse at Dongge Cave. It also occurs more or less synchronous with a prolonged cessation of stalagmite growth at Qunf Cave attributed to marked aridity. On the other hand, the Late-Holocene precipitation minimum at Mawmluh Cave and Buca della Renella seems to have occurred ca. 800 years later. Periodic cooling and/or increased freshwater release into the North Atlantic (Bond et al., 2001) seems to play a role in at least some of these episodes (Barber et al., 1999; Wagner et al., 2013), with a reduction of warm water flow northward from the equator reducing the ocean-land temperature contrast resulting in reduced rainfall in areas under Atlantic monsoon influence (Street-Perrott and Perrott, 1990). However, periodic cooling of the North Atlantic was also linked to episodes of a weakened Indian Ocean monsoon system throughout the Holocene (e.g. Gupta et al., 2003) through atmospheric teleconnections (Zhang et al., 2015). In an extensive review paper, Wang et al. (2014) also noted this global coherence of the dominant sub-orbital monsoon variability patterns. Beside changes in thermohaline circulation driven by the North Atlantic, low solar activity and explosive volcanic eruptions have also been named as possible forcings of century-scale Holocene climate variability (Mayewski et al., 2004; Wanner et al., 2011). Whatever the cause, the global nature of these events suggests that, at Lake Rutundu, they have probably been brought about by a simultaneous reduction of both western and eastern moisture sources. The detailed capturing of the complete sequence of century-scale drought anomalies, and the strong temporal and mechanistic link with a band of well-dated extratropical speleothems spanning a longitudinal distribution from Italy to eastern China, shows that the Lake Rutundu drought sequence reflects the true climate history of East Africa.

RELEVANCE TO THE TIMING OF AFRICAN HUMID PERIOD (AHP) TERMINATION

Most continental hydroclimate records from (sub-)tropical Africa spanning the entire Holocene, of which the majority is based on lake-sediment archives, are subject to several complexities such as ambiguous proxy controls or proxy sensitivity to system-specific and regionally variable hydrological or ecological thresholds. Most of these records provide little evidence for periodic weakening of monsoon rainfall. Instead their Holocene history is dominated by a single, and often abrupt, local moisture-balance shift which is assumed to reflect a similarly abrupt shift in regional climate. Importantly, the inferred timing of these permanent shifts is often coincident with one of the five century-scale arid events recorded at Lake Rutundu (Fig. 4, 5). For example, in the δD_{wax} record of

Lake Tana (northwest Ethiopia), the single-most important hydroclimatic shift of the Holocene is dated to the 8.2 ka R1 event (fig. 4b; Costa et al., 2014). While Ti levels as a runoff proxy suggest partial recovery in rainfall (Marshall et al., 2011), Lake Tana suddenly and permanently suffered a severe decrease in moisture advection from the Atlantic Ocean. A diatom record of Lake Victoria suggests that the early Holocene humidity maximum ended abruptly between 8.3 and 7.8 ka BP leaving rainfall more seasonally restricted (fig. 4e; Stager et al., 2003), with a coincident increase in seasonally dry forest plant species (fig. 4d; Kendall, 1969). Paleo-Lake Suguta in the northern Kenya Rift valley abruptly dried out shortly after 8.5 ka BP (fig. 4c; Garcin et al., 2009). In Niger, the early-Holocene occupants of Gobero abandoned this site because of severe aridification setting in at 8.2 cal yr BP (Sereno et al. 2008). Palynological and sedimentological evidence from Lake Edward (DR Congo-Uganda) situates the abrupt ending of conditions wetter than present at shortly after ca. 6.7 ka BP (Beuning and Russell, 2004), coinciding with event R2. An abrupt and permanent drop in $CaCO_3$ accumulation rate and a sharp increase in $\delta^{18}O$ in Lake Tilo (Ethiopian Rift Valley), interpreted as a sudden decline in hydrothermal inflow, is dated to 6.4-6.2 cal yr BP (Lamb et al., 2000), i.e. overlapping with the peak of R2 at Lake Rutundu. The timing of event R3 coincides with the sudden increase in aeolian dust flux from the western Sahara to the Atlantic Ocean (fig. 4f; deMenocal et al., 2000) at ca. 5.5 kyr BP, often cited as the abrupt ending of the AHP and the 'Green Sahara' due to nonlinear threshold responses in dust-source hydrology (Holmes et al., 2008) and/or vegetation (Liu et al., 2006). A rapid, permanent decline in local moisture balance at this time is also evident for ethiopian lakes Abiyata (fig. 4g; Chalié and Gasse, 2002), Ashenge (fig. 4i; Marshall et al., 2009) and Chew Bahir (fig. 4h; Foerster et al., 2012). Despite caveats linked to dating of paleo-shorelines, an abrupt and permanent lake level decrease of ca. 50 m at Lake Turkana was dated to 5270 ± 300 cal yr BP, within error range of R3 (Garcin et al., 2012). A recent study integrating all previously published results on Turkana lake level change showed that the early- to mid-Holocene history of this lake was complex, with a number of arid events superimposed on a longer-term drying trend starting at ca. 8 kyr BP, i.e. similar to what is observed at Lake Rutundu (Bloszies et al., 2015). This work highlights the importance of such an integrated approach, since separate paleo-shoreline records from different locations within the same catchment yielded discontinuous and incomplete results (Butzer et al., 1980; Owen et al., 1982; Brown and Fuller 2008; Garcin et al., 2012; Forman et al., 2014). Lake Tanganyika's supply of western moisture started its permanent decline, with a first δD_{wax} shift at 5.5-5 kyr BP and culminating in maximum (least depleted) values at ca. 4.2 kyr BP (fig. 4k; Tierney et al., 2008). A similar pattern is observed in δD_{wax} records extracted from Lake Challa (fig. 4l; Tierney et al., 2011b), near Mt. Kilimanjaro and in marine sediments from the Gulf of Aden (fig. 4j; see below, Tierney and deMenocal, 2013). While these three δD_{wax} records were combined to derive an interpreted single wet-to-dry transition centered on 4.9 kyr BP (Tierney and deMenocal, 2013), they all hint at shorter-term variability around this center age. However, all three lack the proxy data resolution to reliably distinguish between separate events within the 6-4 kyr BP time frame, and the chronology of the Tanganyika and Aden records is further complicated by large carbon reservoir effects. The Lake Yoa region of northern Chad can be treated as a good illustration of stepwise ecosystem response to a sequence of drought pulses superimposed on a gradual aridification trend. The transition of early-Holocene 'Green Sahara' savannah to the present-day hyper-arid desert saw a first strong reduction of truly tropical plant taxa ca. 5.5 kyr BP (R3),

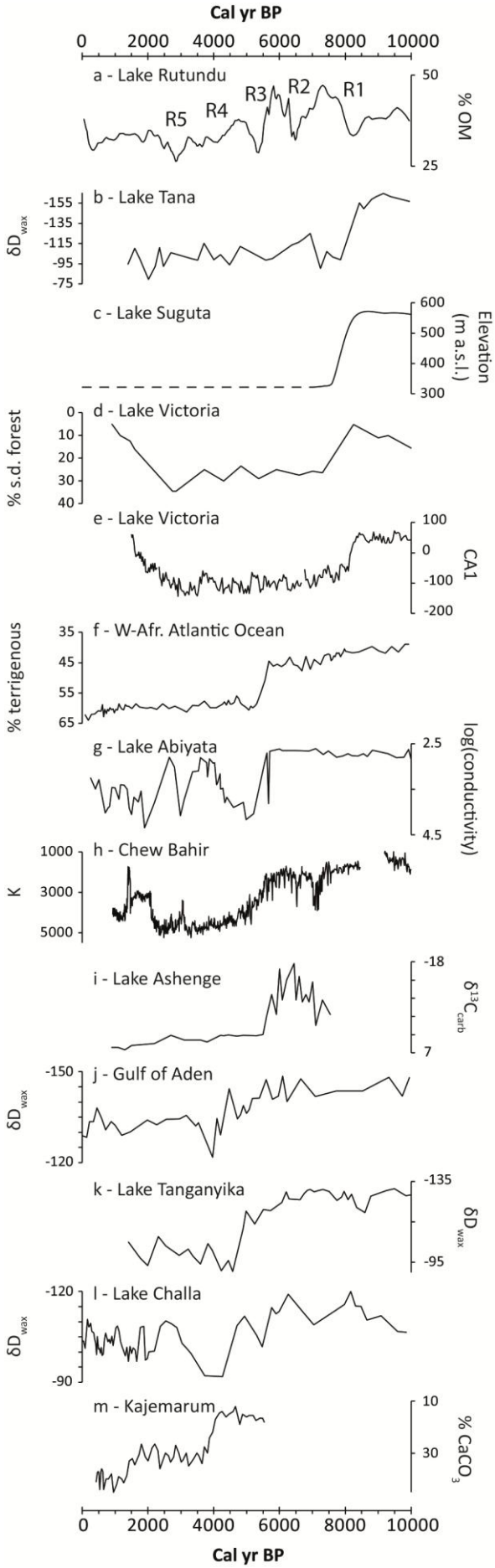
Cal yr BP
0
2000
4000
6000
8000
10000
a - Lake Rutundu
R5
R4
R3
R2
R1
50
25
% OM
b - Lake Tana
-155
-135
-115
-95
-75
δD wax
c - Lake Suguta
600
500
400
300
Elevation (m a.s.l.)
d - Lake Victoria
0
10
20
30
40
% s.d. forest
e - Lake Victoria
100
0
-100
-200
CA1
f - W-Afr. Atlantic Ocean
35
45
55
65
% terrigenous
g - Lake Abiyata
2.5
4.5
log(conductivity)
h - Chew Bahir
1000
3000
5000
K
i - Lake Ashenge
-18
7
δ13Ccarb
j - Gulf of Aden
-150
-120
δD wax
k - Lake Tanganyika
-135
-95
δD wax
l - Lake Challa
-120
-90
δD wax
m - Kajemarum
10
30
% CaCO3
0
2000
4000
6000
8000
10000
Cal yr BP

Fig. 4 (previous page) Inferred abrupt terminations of the African Humid Period throughout Africa coincided with century-scale dry spells R1-4 identified in the Lake Rutundu record.

a: RUT09 %OM 3-point running average
b: Lake Tana δD_{wax} in ‰ vs VSMOW (Costa et al., 2014)
c: paleo-Lake Suguta water level (Garcin et al., 2009)
d: Lake Victoria seasonally dry forest pollen (Kendall, 1969)
e: Lake Victoria core Ibis-1 diatoms CA1 (Stager et al., 2003)
f: Atlantic Ocean ODP Site 658C terrigenous sediment (deMenocal et al., 2000)
g: Lake Abiyata diatom-reconstructed conductivity, in log $\mu S.cm^{-1}$ (Chalié and Gasse, 2002)
h: Chew Bahir XRF potassium counts (Foerster et al., 2012)
i: Lake Ashenge $\delta^{13}C$ of carbonate in ‰ vs VPDB (Marshall et al., 2009)
j: Gulf of Aden δD_{wax} in ‰ vs VSMOW (Tierney et al., 2013)
k: Lake Tanganyika δD_{wax} in ‰ vs VSMOW (Tierney et al., 2008)
l: Lake Challa δD_{wax} in ‰ vs VSMOW (Tierney et al., 2011)
m: Kajemarum Oasis % $CaCO_3$ (Street-Perrott et al., 2000)

which were finally eradicated ca. 4.2 kyr BP (R4) together with the plant taxa typical for semi-arid Sahel vegetation, which had initially replaced them (Kröpelin et al., 2008). Meanwhile, sedimentological indicators of the initially fresh Lake Yoa sets the first signs of regional aridity at 5.6 kyr BP (Francus et al., 2013), followed by hydrological closure of the basin and an abrupt increase in lake-water salinity at 4.2 kyr BP (Eggermont et al., 2008). Strikingly, both periods also saw temporary increases of dust mobilization, as evidenced in elevated magnetic susceptibility values (Kröpelin et al., 2008): still modest at 5.6 kyr BP, stronger at 4.2-4.1 kyr BP, and then followed by the continuous increase characteristic for the later stages of desertification under fragmentary vegetation cover. In many northern sub-tropical regions, anomalous drought centered on 4.2 kyr BP appears to have been the most pronounced climatic event of the later Holocene. For example, drought at Lake Tana resulting in reduced Nile flow at this time is thought to have contributed to the demise of the Egyptian Old Kingdom (Bell, 1971; Marshall et al., 2011; Welc & Marks, 2014) while at the same time, the Akkadian empire collapsed as a consequence of an abrupt aridification of Mesopotamia (Weiss et al., 1993; Cullen et al., 2000). Cultural collapse related to severe drought is reported throughout the eastern Mediterranean at 4.3-3.9 kyr BP (Roberts et al., 2011). At Kajemarum Oasis, in semiarid northeastern Nigeria, summer monsoon precipitation declined permanently at 4.1 cal yr BP (fig. 4m; Street-Perrott et al., 2000). In an earlier review of 20th century records, Gasse (2000) identified major drought spells at 8.2 and 6.6 kyr BP (corresponding to R1 and R2), before abrupt and permanent lake-level drops in Ethiopia and the Sahel at 4 kyr BP (corresponding to R4). Despite being grouped with a record from Lake Tanganyika to derive an average wet-to-dry transition age of 4.9 kyr BP (Tierney and deMenocal, 2013), Lake Challa and Gulf of Aden δD_{wax} levels clearly peak at 4.2-4 kyr BP (Tierney et al., 2011b; Tierney and deMenocal, 2013). Northwest India also saw an abrupt reduction of rainfall leading to de-urbanization and cultural transformation of the Indus Civilization (Dixit et al., 2014), suggesting a widespread failure of the Indian Ocean monsoon. Few records provide evidence of an abrupt transition to a more negative hydrological regime at the timing of R5. This is to be expected, since most sites over the continent had already shifted by this time, especially in North and East Africa. In the West African tropics, a major arid event seems to have occurred around this time. The third millennium BP rain forest crisis, evident from pollen records throughout the region (Elenga et al., 1996; Reynaud-Farrera et al., 1996; Maley and Brenac, 1998), situates major disturbance to the

central African rain forest at 3-2 kyr BP (Elenga et al., 2004). The low-resolution nature of most pollen records and high chronological uncertainties due to a plateau in the ^{14}C calibration curve within this time frame have complicated exact description of this event (Ngomanda et al., 2009). In East Africa, a number of lake sediment records indicate severe drought at ca. 2,700 cal yr BP, such as Lake Edward (Russell and Johnson, 2005) and a number of Ugandan crater lakes (Bessems, 2007).

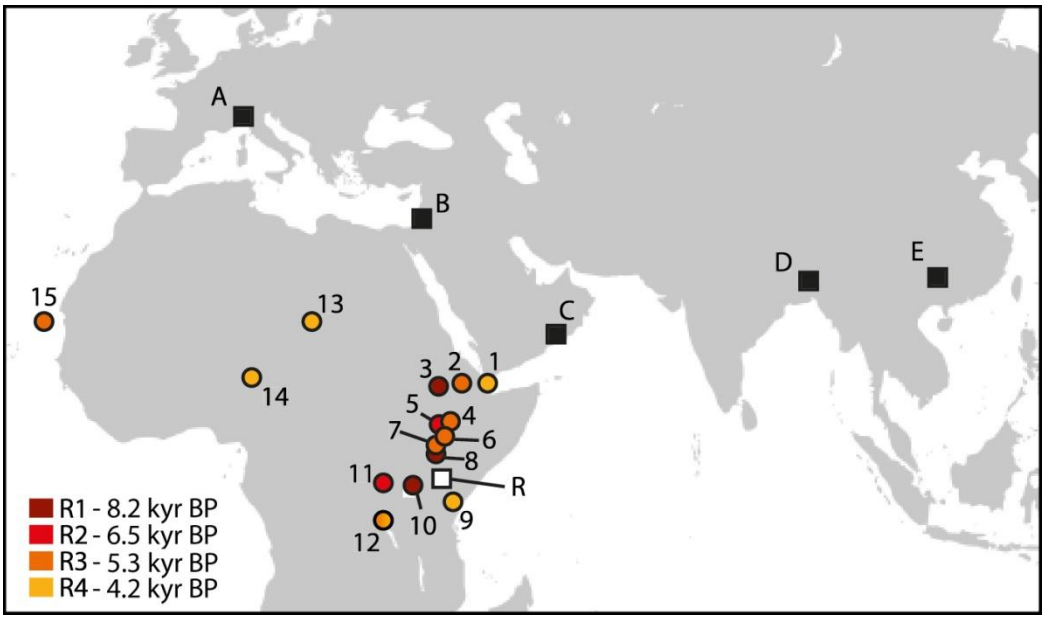

Fig. 5 Locations of records mentioned in discussion. Circles depict African records where abrupt shifts in one or more climate proxies coincide with RUT09 arid events R1-4 as depicted by color coding. White square depicts Lake Rutundu, black squares depict extratropical speleothem records.

A: Buca della Renella, Italy (Drysdale et al., 2006)
B: Soreq Cave, Israel (Bar-Matthews et al., 2003)
C: Qunf Cave, Oman (Fleitmann et al., 2007)
D: Mawmluh Cave, India (Berkelhammer et al., 2012)
E: Dongge Cave, China (Wang et al., 2005)
1: Gulf of Aden core P178-15P (Tierney and deMenocal, 2013)
2: Lake Ashenge, Ethiopia (Marshall et al., 2009)
3: Lake Tana, Ethiopia (Costa et al., 2014)
4: Lake Abiyata, Ethiopia (Chalié and Gasse, 2002)
5: Lake Tilo, Ethiopia (Lamb et al., 2000)
6: Chew Bahir, Ethiopia (Foerster et al., 2012)
7: Lake Turkana, Kenya/Ethiopia (Garcin et al., 2012)
8: Paleo-lake Suguta, Kenya (Garcin et al., 2009)
9: Lake Challa, Kenya/Tanzania (Tierney et al., 2011)
10: Lake Victoria, Uganda/Kenya/Tanzania (Stager et al., 2003)
11: Lake Edward, Uganda/DR Congo (Beuning and Russell, 2004)
12: Lake Tanganyika, Tanzania/Burundi/DR Congo/Zambia (Tierney et al., 2008)
13: Lake Yoa, Chad (Kröpelin et al., 2008)
14: Kajemarum Oasis, Nigeria (Street-Perrott et al., 2000)
15: Atlantic Ocean ODP 658C (deMenocal et al., 2000)

Many efforts have been undertaken to synthesize North African paleohydrological records (e.g. Petit-Maire, 1993; Kuper and Kröpelin, 2006), and a stepwise aridification of Sahara climate toward modern-day hyperarid conditions has been described (Hoelzmann et al., 2004). Recently, a locally abrupt but regionally time-transgressive AHP over northern tropical and subtropical Africal has been proposed, with the principal wet-to-dry transition occurring progressively later at lower latitudes because of the southward shift in mean latitudinal position of the tropical rain belt resulting from decreasing summer insolation (Shanahan et al., 2015). However, this interpretation implies abrupt retreat of the tropical rain belt (i.e., a major and permanent rain failure) from each individual site along the north-to-south transect. Instead, the prominent paleohydrological shift representing AHP termination at most sites probably did not encompass an abrupt decrease in local precipitation (or climatic moisture balance in general) but results from non-linearity in the relationship between the paleoproxy signatures of local hydrological and/or ecosystem response and a mostly gradual long-term decreasing trend in Holocene rainfall. In hydrological time series, common transitions in lake system behaviour are the threshold water depth for bottom oxygenation, which controls nutrient recycling, organic-matter preservation and bioturbation; or the cessation of (sub-) surface outflow, which leads to hydrological closure and evaporative concentration of dissolved salts (e.g. Francus et al., 2013). In time series of terrestrial vegetation dynamics, transitions can be governed by thresholds of fire occurrence, the length/severity of seasonal drought, or the depth of a groundwater aquifer (Williams et al., 2011). The latitudinal time-transgressive pattern of AHP termination arises because more northerly sites farther inland generally exhibit lower P-E levels, and faced with a gradually decreasing moisture balance these systems are thus more likely to be pushed over a 'point of no return' from which the system does not recover, sooner than their equatorial counterparts. Secondly, the century-scale episodes of anomalous drought, described here from Mount Kenya and reminiscent of the weak-monsoon episodes in South and East Asian speleothems, punctuated a gradual Holocene trend of decreasing rainfall throughout northern tropical and subtropical Africa, and significantly increased the likelihood of crossing the threshold moisture balance levels required for an ecosystem shift that is picked up by environmental proxy records. Interestingly, in addition to north-south oriented transgressiveness of mid- to late Holocene drying, an east-west gradient has also been reported for both northern subtropical and tropical Africa (Lézine et al., 2011; Shanahan et al., 2015). The precise cause of this pattern remains unclear, but the overwriting effect of subsequent Holocene drought pulses can be expected to have played an equally significant role as in a north-south oriented climate trend.

To summarize, this study suggests that short-lived, century-scale climate events have had much more far-reaching consequences on the African continent than often assumed. Throughout the Holocene, they promoted ecosystems already subject to a gradual, orbitally-driven rainfall decrease, to shift beyond the limits of subsequent recovery. Because these threshold levels of hydroclimatic conditions are inherently variable across ecosystems, the Holocene sequence of droughts recorded at Lake Rutundu has had a major impact on the spatial and temporal complexity of the AHP termination that is observed in other continental proxy records. Based on these results, it can be hypothesized that if the chronology of a significant fraction of these hydroclimatic records could be improved, the diverse timing of apparently abrupt local AHP termination would cluster around the timing of the five prominent drought episodes recorded at Lake Rutundu.

REFERENCES

Alley RB, Mayewski PA, Sowers T, Stuiver M, Taylor KC, Clark PU. (1997) Holocene climatic instability: A prominent, widespread event 8200 yr ago. Geology 25:483-486.

Baker B. (1967) Geology of the Mount Kenya area. In: Ministry of Natural Resources GSoK (ed), Nairobi, Kenya.

Bar-Matthews M, Ayalon A. (2011) Mid-Holocene climate variations revealed by high-resolution speleothem records from Soreq Cave, Israel and their correlation with cultural changes. Holocene 21:163-171.

Bar-Matthews M, Ayalon A, Gilmour M, Matthews A, Hawkesworth CJ. (2003) Sea-land oxygen isotopic relationships from planktonic foraminifera and speleothems in the Eastern Mediterranean region and their implication for paleorainfall during interglacial intervals. Geochimica Et Cosmochimica Acta 67:3181-3199.

Barao L, Clymans W, Vandevenne F, Meire P, Conley DJ, Struyf E. (2014) Pedogenic and biogenic alkaline-extracted silicon distributions along a temperate land-use gradient. European Journal of Soil Science 65:693-705.

Barao L, De Cort G, Meire P, Verschuren D, Struyf E. (2015) Biogenic Si analysis in volcanically imprinted lacustrine systems: the case of Lake Rutundu (Mt. Kenya). Biogeochemistry 125:243-259.

Barber DC, Dyke A, Hillaire-Marcel C, Jennings AE, Andrews JT, Kerwin MW, Bilodeau G, McNeely R, Southon J, Morehead MD, Gagnon JM. (1999) Forcing of the cold event of 8,200 years ago by catastrophic drainage of Laurentide lakes. Nature 400:344-348.

Barker P, Talbot M, Street-Perrott A, Marret F, Scourse J, Odada E. (2004) Late Quaternary climate variability in intertropical Africa. In: Battarbee R, Gasse F, Stickley C (eds), Past climate variability through Europe and Africa. Kluwer, Dordrecht, The Netherlands, pp. 117-138.

Barker P, Telford R, Gasse F, Thevenon F. (2002) Late Pleistocene and Holocene palaeohydrology of Lake Rukwa, Tanzania, inferred from diatom analysis. Palaeogeography Palaeoclimatology Palaeoecology 187:295-305.

Battarbee RW, Thompson R, Catalan J, Grytnes JA, Birks HJB. (2002) Climate variability and ecosystem dynamics of remote alpine and arctic lakes: the MOLAR project. Journal of Paleolimnology 28:1-6.

Bell B. (1971) Dark ages in ancient history .1. First dark age in Egypt. American Journal of Archaeology 75:1-26.

Berkelhammer M, Sinha A, Stott L, Cheng H, Pausata FSR, Yoshimura K. (2012) An Abrupt Shift in the Indian Monsoon 4000 Years Ago. Climates, Landscapes, and Civilizations 198:75-87.

Bessems I, Verschuren D, Russell JM, Hus J, Mees F, Cumming B. (2008) Palaeolimnological evidence for widespread late 18th century drought across equatorial East Africa. Palaeogeography, Palaeoclimatology, Palaeoecology 259:107-120.

Beuning KRM, Russell JM. (2004) Vegetation and sedimentation in the Lake Edward Basin, Uganda-Congo during the late Pleistocene and early Holocene. Journal of Paleolimnology 32:1-18.

Blaauw M. (2010) Methods and code for 'classical' age-modelling of radiocarbon sequences. Quaternary Geochronology 5:512-518.

Bloszies C, Forman SL, Wright DK. (2015) Water level history for Lake Turkana, Kenya in the past 15,000 years and a variable transition from the African Humid Period to Holocene aridity. Global and Planetary Change 132:64-76.

Bond G, Kromer B, Beer J, Muscheler R, Evans MN, Showers W, Hoffmann S, Lotti-Bond R, Hajdas I, Bonani G. (2001) Persistent solar influence on north Atlantic climate during the Holocene. Science 294:2130-2136.

Brown E. (2015) Estimation of biogenic silica concentrations using scanning XRF: insights from studies of Lake Malawi sediments. In: Croudace I, Rothwell R (eds), Micro-XRF studies of sediment cores. Springer, pp. 267-278.

Brown FH, Fuller CR. (2008) Stratigraphy and tephra of the Kibish Formation, southwestern Ethiopia. Journal of Human Evolution 55:366-403.

Butzer K. (1980) The Holocene lake plain of Lake Rudolph, East Africa. Physical Geography 1:42-58.

Chalié F, Gasse F. (2002) Late Glacial-Holocene diatom record of water chemistry and lake level change from the tropical East African Rift Lake Abiyata (Ethiopia). Palaeogeography Palaeoclimatology Palaeoecology 187:259-283.

Cheng H, Fleitmann D, Edwards RL, Wang XF, Cruz FW, Auler AS, Mangini A, Wang YJ, Kong XG, Burns SJ, Matter A. (2009) Timing and structure of the 8.2 kyr BP event inferred from delta O-18 records of stalagmites from China, Oman, and Brazil. Geology 37:1007-1010.

Clark PU, Shakun JD, Baker PA, Bartlein PJ, Brewer S, Brook E, Carlson AE, Cheng H, Kaufman DS, Liu ZY, Marchitto TM, Mix AC, Morrill C, Otto-Bliesner BL, Pahnke K, Russell JM, Whitlock C, Adkins JF, Blois JL, Clark J, Colman SM, Curry WB, Flower BP, He F, Johnson TC, Lynch-Stieglitz J, Markgraf V, McManus J, Mitrovica JX, Moreno PI, Williams JW. (2012) Global climate evolution during the last deglaciation. Proceedings of the National Academy of Sciences of the United States of America 109:E1134-E1142.

Costa K, Russell J, Konecky B, Lamb H. (2014) Isotopic reconstruction of the African Humid Period and Congo Air Boundary migration at Lake Tana, Ethiopia. Quaternary Science Reviews 83:58-67.

Cullen HM, deMenocal PB, Hemming S, Hemming G, Brown FH, Guilderson T, Sirocko F. (2000) Climate change and the collapse of the Akkadian empire: Evidence from the deep sea. Geology 28:379-382.

Dean WE. (1974) determination of carbonate and organic-matter in calcareous sediments and sedimentary-rocks by loss on ignition - comparison with other methods. Journal of Sedimentary Petrology 44:242-248.

deMenocal P, Ortiz J, Guilderson T, Adkins J, Sarnthein M, Baker L, Yarusinsky M. (2000) Abrupt onset and termination of the African Humid Period: rapid climate responses to gradual insolation forcing. Quaternary Science Reviews 19:347-361.

Dixit Y, Hodell DA, Petrie CA. (2014) Abrupt weakening of the summer monsoon in northwest India similar to 4100 yr ago. Geology 42:339-342.

Conley DJ, Schelke CL. (2001) Biogenic silica. In: Smol J, Birks H, Last W (eds), Tracking environmental change using lake sediments vol. 3: Terrestrial, algal and siliceous indicators. Kluwer Academic Publishers, pp. 281-294.

Drysdale R, Zanchetta G, Hellstrom J, Maas R, Fallick A, Pickett M, Cartwright I, Piccini L. (2006) Late Holocene drought responsible for the collapse of Old World civilizations is recorded in an Italian cave flowstone. Geology 34:101-104.

Eggermont H, Verschuren D, Fagot M, Rumes B, Van Bocxlaer B, Kropelin S. (2008) Aquatic community response in a groundwater-fed desert lake to Holocene desiccation of the Sahara. Quaternary Science Reviews 27:2411-2425.

Ehlers J, Hughes P, Gibbard P. (2015) The Ice Age. John Wiley and Sons, Hoboken, New Jersey, US.

Elenga H, Maley J, Vincens A, Farrera I. (2004) Palaeoenvironments, palaeoclimates and landscape development in Atlantic equatorial Africa: a review of key sites covering the last 25 kyrs. In: Battarbee W, Gasse F, Stickley C (eds), Past climate variability through Europe and Africa. Kluwer, Dordrecht, The Netherlands, pp. 181-198.

Elenga H, Schwartz D, Vincens A, Bertaux J, de Namur C, Martin L, Wirrmann D, Servant M. (1996) Diagramme pollinique holocène du lac Kitina (Congo): mise en évidence de changements paléobotaniques et paléoclimatiques dans le massif forestier du Mayombe. Comptes Rendus de l'Académie des Sciences Paris 232:403-410.

Fleitmann D, Burns SJ, Mangini A, Mudelsee M, Kramers J, Villa I, Neff U, Al-Subbary AA, Buettner A, Hippler D, Matter A. (2007) Holocene ITCZ and Indian monsoon dynamics recorded in stalagmites from Oman and Yemen (Socotra). Quaternary Science Reviews 26:170-188.

Foerster V, Junginger A, Langkamp O, Gebru T, Asrat A, Umer M, Lamb HF, Wennrich V, Rethemeyer J, Nowaczyk N, Trauth MH, Schaebitz F. (2012) Climatic change recorded in the sediments of the Chew Bahir basin, southern Ethiopia, during the last 45,000 years. Quaternary International 274:25-37.

Forman SL, Wright DK, Bloszies C. (2014) Variations in water level for Lake Turkana in the past 8500 years near Mt. Porr, Kenya and the transition from the African Humid Period to Holocene aridity. Quaternary Science Reviews 97:84-101.

Francus P, Von Suchodoletz H, Dietze M, Donner RV, Bouchard F, Roy AJ, Fagot M, Verschuren D, Kropelin S. (2013) Varved sediments of Lake Yoa (Ounianga Kebir, Chad) reveal progressive drying of the Sahara during the last 6100 years. Sedimentology 60:911-934.

Garcin Y, Junginger A, Melnick D, Olago DO, Strecker MR, Trauth MH. (2009) Late Pleistocene-Holocene rise and collapse of Lake Suguta, northern Kenya Rift. Quaternary Science Reviews 28:911-925.

Garcin Y, Melnick D, Strecker MR, Olago D, Tiercelin JJ. (2012) East African mid-Holocene wet-dry transition recorded in palaeo-shorelines of Lake Turkana, northern Kenya Rift. Earth and Planetary Science Letters 331:322-334.

Gasse F. (2000) Hydrological changes in the African tropics since the Last Glacial Maximum. Quaternary Science Reviews 19:189-211.

Gupta AK, Anderson DM, Overpeck JT. (2003) Abrupt changes in the Asian southwest monsoon during the Holocene and their links to the North Atlantic Ocean. Nature 421:354-357.

Hastenrath S. (1995) Glacier recession on Mount kenya in the context of the global tropics. Bulletin de l'Institution Français d'Etudes Andines 24:633-638.

Hoelzmann P, Gasse F, Dupont LM, Salzmann U, Staubwasser M, Leuschner DC, Sirocko F. (2004) Palaeoenvironmental changes in the arid and subarid belt (Sahara-Sahel-Arabian peninsula) from 150 kyr to present. Past Climate Variability through Europe and Africa 6:219-256.

Holmes JA. (2008) Ecology - How the Sahara became dry. Science 320:752-753.

Jolly D, Prentice IC, Bonnefille R, Ballouche A, Bengo M, Brenac P, Buchet G, Burney D, Cazet JP, Cheddadi R, Edorh T, Elenga H, Elmoutaki S, Guiot J, Laarif F, Lamb H, Lezine AM, Maley J, Mbenza M, Peyron O, Reille M, Reynaud-Farrera I, Riollet G, Ritchie JC, Roche E, Scott L, Ssemmanda I, Straka H, Umer M, Van Campo E, Vilimumbalo S, Vincens A, Waller M. (1998) Biome reconstruction from pollen and plant macrofossil data for Africa and the Arabian peninsula at 0 and 6000 years. Journal of Biogeography 25:1007-1027.

Junginger A, Roller S, Olaka LA, Trauth MH. (2014) The effects of solar irradiation changes on the migration of the Congo Air Boundary and water levels of paleo-Lake Suguta, Northern Kenya

Rift, during the African Humid Period (15-5 ka BP). Palaeogeography Palaeoclimatology Palaeoecology 396:1-16.

Kendall R. (1969) An ecological history of the Lake Victoria basin. Ecological Monographs 39:121-176.

Koning E, Epping E, Van Raaphorst W. (2002) Determining biogenic silica in marine samples by tracking silicate and aluminium concentrations in alkaline leaching solutions. Aquatic Geochemistry 8:37-67.

Kröpelin S, Verschuren D, Lezine AM, Eggermont H, Cocquyt C, Francus P, Cazet JP, Fagot M, Rumes B, Russell JM, Darius F, Conley DJ, Schuster M, von Suchodoletz H, Engstrom DR. (2008) Climate-driven ecosystem succession in the Sahara: The past 6000 years. Science 320:765-768.

Kuper R, Kröpelin S. (2006) Climate-controlled Holocene occupation in the Sahara: Motor of Africa's evolution. Science 313:803-807.

Kutzbach JE, Otto-Bliesner BL. (1982) The sensitivity of the African-Asian monsoonal climate to orbital parameter changes for 9000 years BP in a low-resolution general-circulation model. Journal of the Atmospheric Sciences 39:1177-1188.

Lamb AL, Leng MJ, Lamb HF, Mohammed MU. (2000) A 9000-year oxygen and carbon isotope record of hydrological change in a small Ethiopian crater lake. Holocene 10:167-177.

Leblanc M, Favreau G, Maley J, Nazoumou Y, Leduc C, Stagnitti F, van Oevelen PJ, Delclaux F, Lemoalle J. (2006) Reconstruction of Megalake Chad using Shuttle Radar Topographic Mission data. Palaeogeography Palaeoclimatology Palaeoecology 239:16-27.

Lézine AM, Hely C, Grenier C, Braconnot P, Krinner G. (2011) Sahara and Sahel vulnerability to climate changes, lessons from Holocene hydrological data. Quaternary Science Reviews 30:3001-3012.

Liu ZY, Wang Y, Gallimore R, Notaro M, Prentice IC. (2006) On the cause of abrupt vegetation collapse in North Africa during the Holocene: Climate variability vs. vegetation feedback. Geophysical Research Letters 33.

Maley J, Brenac P. (1998) Vegetation dynamics, palaeoenvironments and climatic changes in the forests of western Cameroon during the last 28,000 years BP. Review of Palaeobotany and Palynology 99:157-187.

Marshall MH, Lamb HF, Davies SJ, Leng MJ, Kubsa Z, Umer M, Bryant C. (2009) Climatic change in northern Ethiopia during the past 17,000 years: A diatom and stable isotope record from Lake Ashenge. Palaeogeography Palaeoclimatology Palaeoecology 279:114-127.

Marshall MH, Lamb HF, Huws D, Davies SJ, Bates R, Bloemendal J, Boyle J, Leng MJ, Umer M, Bryant C. (2011) Late Pleistocene and Holocene drought events at Lake Tana, the source of the Blue Nile. Global and Planetary Change 78:147-161.

Mayewski PA, Rohling EE, Stager JC, Karlen W, Maasch KA, Meeker LD, Meyerson EA, Gasse F, van Kreveld S, Holmgren K, Lee-Thorp J, Rosqvist G, Rack F, Staubwasser M, Schneider RR, Steig EJ. (2004) Holocene climate variability. Quaternary Research 62:243-255.

McGee D, deMenocal PB, Winckler G, Stuut JBW, Bradtmiller LI. (2013) The magnitude, timing and abruptness of changes in North African dust deposition over the last 20,000 yr. Earth and Planetary Science Letters 371:163-176.

Michelutti N, Wolfe AP, Cooke CA, Hobbs WO, Vuille M, Smol JP. (2015) Climate Change Forces New Ecological States in Tropical Andean Lakes. Plos One 10.

Morrill C, Jacobsen RM. (2005) How widespread were climate anomalies 8200 years ago? Geophysical Research Letters 32.

Ngomanda A, Neumann K, Schweizer A, Maley J. (2009) Seasonality change and the third millennium BP rainforest crisis in southern Cameroon (Central Africa). Quaternary Research 71:307-318.

Loomis SE. (2013) On branched glycerol dialkyl glycerol tetraethers: Development of a paleotemperature proxy. Unpublished PhD thesis. Brown University, Providence, USA.

Otto-Bliesner BL, Russell JM, Clark PU, Liu ZY, Overpeck JT, Konecky B, deMenocal P, Nicholson SE, He F, Lu ZY. (2014) Coherent changes of southeastern equatorial and northern African rainfall during the last deglaciation. Science 346:1223-1227.

Owen RB, Barthelme JW, Renaut RW, Vincens A. (1982) Paleolimnology and archaeology of Holocene deposits northeast of Lake Turkana, Kenya. Nature 298:523-529.

Petit-Maire N. (1993) Past global climatic changes and the tropical arid/semi-arid belt in the North of Africa. In: Thorweihe U, Schandelmeier H (eds), Geoscientific research in Northeast Africa. Balkema, Rotterdam, The Netherlands, pp. 551-560.

Reimer PJ, Bard E, Bayliss A, Beck JW, Blackwell PG, Ramsey CB, Buck CE, Cheng H, Edwards RL, Friedrich M, Grootes PM, Guilderson TP, Haflidason H, Hajdas I, Hatte C, Heaton TJ, Hoffmann DL, Hogg AG, Hughen KA, Kaiser KF, Kromer B, Manning SW, Niu M, Reimer RW, Richards DA, Scott EM, Southon JR, Staff RA, Turney CSM, van der Plicht J. (2013) INTCAL13 and MARINE13 radiocarbon age calibration curves 0-50,000 years cal bp. Radiocarbon 55:1869-1887.

Reynaud-Farrera I, Maley J, Wirrmann D. (1996) Végétation et climat dans les forets du sud-ouest Cameroun depuis 4770 ans BP. Analyse pollinique des sédiments du lac Ossa. Comptes Rendus de l'Académie des Sciences Paris 322:749-755.

Roberts N, Eastwood WJ, Kuzucuoglu C, Fiorentino G, Caracuta V. (2011) Climatic, vegetation and cultural change in the eastern Mediterranean during the mid-Holocene environmental transition. Holocene 21:147-162.

Rosen JL, Brook EJ, Severinghaus JP, Blunier T, Mitchell LE, Lee JE, Edwards JS, Gkinis V. (2014) An ice core record of near-synchronous global climate changes at the Bolling transition. Nature Geoscience 7:459-463.

Russell JM and Jonhson TC. (2005) A high-resolution geochemical record from Lake Edward, Uganda Congo and the timing and causes of tropical African drought during the late Holocene. Quaternary Science Reviews 24:1375-1389.

Sereno PC, Garcea EAA, Jousse H, Stojanowski CM, Saliege JF, Maga A, Ide OA, Knudson KJ, Mercuri AM, Stafford TW, Kaye TG, Giraudi C, N'Siala IM, Cocca E, Moots HM, Dutheil DB, Stivers JP. (2008) Lakeside Cemeteries in the Sahara: 5000 Years of Holocene Population and Environmental Change. Plos One 3.

Shanahan TM, McKay NP, Hughen KA, Overpeck JT, Otto-Bliesner B, Heil CW, King J, Scholz CA, Peck J. (2015) The time-transgressive termination of the African Humid Period. Nature Geoscience 8:140-144.

Stager JC, Cumming BF, Meeker LD. (2003) A 10,000-year high-resolution diatom record from Pilkington Bay, Lake Victoria, East Africa. Quaternary Research 59:172-181.

Stager JC, Ryves DB, Chase BM, Pausata FSR. (2011) Catastrophic Drought in the Afro-Asian Monsoon Region During Heinrich Event 1. Science 331:1299-1302.

Street-Perrott FA, Holmes JA, Waller MP, Allen MJ, Barber NGH, Fothergill PA, Harkness DD, Ivanovich M, Kroon D, Perrott RA. (2000) Drought and dust deposition in the West African Sahel: A 5500-year record from Kajemarum Oasis, northeastern Nigeria. Holocene 10:293-302.

Street-Perrott FA, Perrott RA. (1990) Abrupt climate fluctuations in the tropics - the influence of Atlantic-Ocean circulation. Nature 343:607-612.

Talbot MR, Filippi ML, Jensen NB, Tiercelin JJ. (2007) An abrupt change in the African monsoon at the end of the Younger Dryas. Geochemistry Geophysics Geosystems 8.

Tierney JE, deMenocal PB. (2013) Abrupt Shifts in Horn of Africa Hydroclimate Since the Last Glacial Maximum. Science 342:843-846.

Tierney JE, Lewis SC, Cook BI, LeGrande AN, Schmidt GA. (2011a) Model, proxy and isotopic perspectives on the East African Humid Period. Earth and Planetary Science Letters 307:103-112.

Tierney JE, Russell JM, Damste JSS, Huang YS, Verschuren D. (2011b) Late Quaternary behavior of the East African monsoon and the importance of the Congo Air Boundary. Quaternary Science Reviews 30:798-807.

Tierney JE, Russell JM, Huang YS, Damste JSS, Hopmans EC, Cohen AS. (2008) Northern hemisphere controls on tropical southeast African climate during the past 60,000 years. Science 322:252-255.

Tylmann W, Bonk A, Goslar T, Wulf S, Grosjean M. (2016) Calibrating 210Pb dating results with varve chronology and independent chronostratigraphic markers: problems and implications. Quaternary Geochronology 32:1-10.

Vaasma T. (2008) Grain-size analysis of lacustrine sediments: a comparison of pre-treatment methods. Estonian Journal of Ecology 57:231-243.

van der Werf GR, Randerson JT, Giglio L, Gobron N, Dolman AJ. (2008) Climate controls on the variability of fires in the tropics and subtropics. Global Biogeochemical Cycles 22:1-13.

Verschuren D. (2003) Lake-based climate reconstruction in Africa: progress and challenges. Hydrobiologia 500:315-330.

Vincens A, Buchet G, Williamson D, Taieb M. (2005) A 23,000 yr pollen record from Lake Rukwa (8 degrees S, SW Tanzania): New data on vegetation dynamics and climate in Central Eastern Africa. Review of Palaeobotany and Palynology 137:147-162.

Wagner AJ, Morrill C, Otto-Bliesner BL, Rosenbloom N, Watkins KR. (2013) Model support for forcing of the 8.2 ka event by meltwater from the Hudson Bay ice dome. Climate Dynamics 41:2855-2873.

Wang PX, Wang B, Cheng H, Fasullo J, Guo ZT, Kiefer T, Liu ZY. (2014) The global monsoon across timescales: coherent variability of regional monsoons. Climate of the Past 10:2007-2052.

Wang YJ, Cheng H, Edwards RL, He YQ, Kong XG, An ZS, Wu JY, Kelly MJ, Dykoski CA, Li XD. (2005) The Holocene Asian monsoon: Links to solar changes and North Atlantic climate. Science 308:854-857.

Wanner H, Solomina O, Grosjean M, Ritz SP, Jetel M. (2011) Structure and origin of Holocene cold events. Quaternary Science Reviews 30:3109-3123.

Weiss H, Courty MA, Wetterstrom W, Guichard F, Senior L, Meadow R, Curnow A. (1993) The genesis and collapse of 3rd millennium North Mesopotamian civilization. Science 261:995-1004.

Welc F, Marks L. (2014) Climate change at the end of the Old Kingdom in Egypt around 4200 BP: New geoarchaeological evidence. Quaternary International 324:124-133.

Weldeab S, Menke V, Schmiedl G. (2014) The pace of East African monsoon evolution during the Holocene. Geophysical Research Letters 41:1724-1731.

Williams JW, Blois JL, Shuman BN. (2011) Extrinsic and intrinsic forcing of abrupt ecological change: case studies from the late Quaternary. Journal of Ecology 99:664-677.

Wooller MJ, Swain DL, Ficken KJ, Agnew ADQ, Street-Perrott FA, Eglinton G. (2003) Late Quaternary vegetation changes around Lake Rutundu, Mount Kenya, East Africa: evidence from grass cuticles, pollen and stable carbon isotopes. Journal of Quaternary Science 18:3-15.

Zhang X, Jin L, Jia W. (2015) Centennial-scale teleconection between North-Atlantic sea surface temperatures and the Indian summer monsoon during the Holocene. Climate Dynamics.

2 AFRICAN HYDROCLIMATIC VARIABILITY DURING THE LAST 2,000 YEARS

De Cort, Gijs[1,2]; Nash, David[3]; Chase, Brian[4]; Verschuren, Dirk[1]; Shanahan, Tim[5]; Nicholson, Sharon[6]; Lézine, Anne-Marie[7]; Asrat, Asfawossen[8];

[1]*Limnology Unit, Department of Biology, Ghent University. K.L. Ledeganckstraat 35, 9000 Ghent, Belgium*
[2]*Department of Earth Sciences, Royal Museum for Central Africa. Leuvensesteenweg 13, 3080 Tervuren, Belgium*
[3]*School of Environment and Technology, University of Brighton. Lewes Road, BN2 4GJ Brighton, UK*
[4]*Institut des Sciences de l'Evolution de Montpellier, UMR 5554, Centre National de Recherche Scientifique/Université Montpellier 2, Bat. 22, CC061, Place Eugène Bataillon, 34095 Montpellier Cedex 5, France*
[5]*Department of Geological Sciences, The University of Texas at Austin. 1 University Station, C9000, Austin, Texas 78712, USA*
[6]*Department of Earth, Ocean and Atmospheric Science, Florida State University. 32306-4520 Tallahassee, Florida, USA*
[7]*Laboratoire des sciences du climat et de l'environnement, UMR 8212 CNRS-CEA-UVSQ, Orme des merisiers, 91191 Gif-sur-Yvette Cedex, France*
[8]*College of Natural Sciences, Addis Ababa University. PO Box 1176, Addis Ababa, Ethiopia*

This chapter is a product of the PAGES Africa-2k Working Group and is in preparation for submission to *Quaternary Science Reviews*. The author sequence may still change, and some parts contributed by myself and Dirk Verschuren may be excised for use in a separate publication focused in greater detail on time-series quality screening and temporal patterns in the proxy records from East Africa.

Africa is a continent vulnerable to climate change, mainly through variability in rainfall with potentially serious societal consequences. A growing number of data sources indicate that this hydrological variability is an intrinsic part of natural African climate. This chapter, co-authored by members of the PAGES Africa2k Working Group, presents an extensive assessment and discussion of proxy, historical and instrumental data on historical hydroclimate change over the past 2000 years. Despite being characterized by mostly spatially disjunctive records with often less-than-optimal chronological control and data resolution, the available data allows the exploration of major patterns in northwestern, eastern and southern Africa throughout five subsequent time windows covering the last two millennia. This results in a continental-scale synthesis of moisture balance trends through history, which is complemented with a discussion of possible driving mechanisms and suggestions for future research.

1 INTRODUCTION

From the humid equatorial Congo Basin to the (hyper-) arid deserts in the northern and southern subtropics, Africa is characterised by a wide range of hydroclimate regimes. In large parts of the continent, human livelihoods are intimately linked to the amount of local rainfall and the occurrence of climate extremes. Determining the full range of natural climate variability on temporal and spatial scales most relevant to ecosystem functioning and human well-being is of utmost importance to anticipate the impact of, and improve the preparedness of communities to, future climate change. Whereas efforts to synthesize continent-specific patterns of temperature change over the past two millennia have made good progress (e.g., PAGES 2k Consortium, 2013), regional to continent-scale patterns of past hydroclimate variability remain less well documented, especially for the tropics and

the Southern Hemisphere (but see Neukom et al., 2010; Lorrey, 2014). Africa is cited by the Intergovernmental Panel on Climate Change (IPCC) as a key continent where proxy-based climate reconstructions are currently too limited to support regional climate-change assessments (Masson-Delmotte et al., 2013). Indeed, African time series of either temperature- or moisture-related climate variables spanning (a significant portion of) the last two millennia with adequate temporal resolution and age control remain relatively sparse (Neukom and Gergis, 2012*;* Nicholson et al., 2013) and display a highly uneven spatial distribution (Verschuren, 2004).

Partly this is because the classic high-resolution archives of tree rings and ice cores are mostly lacking. Tree species suitable for dendroclimatological reconstructions are scarce, because local climates fail to drive the strong seasonal variation in wood growth required to produce reliable annual rings; and trees which do grow demonstrably annual rings often have little potential to be preserved intact long after death (Dunbar and Cole, 1999). The potential of continuous and reliably dated ice core records is also extremely limited, given that the only centres of glaciation are the small and rapidly shrinking glaciers of Mt Kilimanjaro (Tanzania), Mt Kenya (Kenya) and the Rwenzori range (DR Congo, Uganda).

Across much of Africa, lake-sediment records are the most important source of evidence on past climate change (Verschuren, 2004). Yet while lakes and wetlands of various depth and size are numerous in many regions of western, eastern and southern Africa, only a small sub-set of them have been found to combine adequate hydrological sensitivity (and thus robust proxy signatures of past hydroclimatic variability) with demonstrably continuous sediment accumulation over the past 2000 years (Verschuren, 2003). Frequently the timing and duration of successive wet and dry episodes is uncertain because desiccation horizons, cryptic hiatuses and large changes in sedimentation rate modify the depth-time relationship beyond what can be constrained by ^{14}C dating (Verschuren, 1999a; Verschuren and Russell, 2009). In a large swath of western tropical Africa, lake-based climate-proxy records with high temporal resolution are scarce because the shallow ponds and marshes distributed throughout the region dried out during episodes of (relatively modest) drought, while depositional environments along rivers are too dynamic to have preserved datable sediment records. As a result, only a handful of well-dated records spanning the last 2000 years with robust climate signals at inter-annual to decade-scale resolution are currently available.

In regions with little potential for high-quality lake-sediment records, such as southern Africa, a diverse range of other climate archives, including speleothems (e.g. Holmgren et al., 2003) and more recently hyrax middens (Chase et al., 2012) have been explored. Pollen records of past vegetation change extracted from lake and swamp sediments are often poorly dated with poor temporal resolution, and the complex nature of the region's flora can create fossil pollen assemblages that are difficult to interpret in terms of past shifts in climate regimes (Meadows et al., 2010; Chase et al., 2015a). As a result, previous reviews of climate change in southern Africa during the last few millennia (Tyson and Lindesay, 1992; Tyson et al., 2000a) have drawn heavily on stable carbon and oxygen ratios ($\delta^{13}C$, $\delta^{18}O$) from speleothems. However, these records have also proven difficult to interpret, and consensus as to exactly which climate variable(s) they reflect remains a matter of debate.

These various continental climate archives are supplemented by a limited number of deep-sea sediment cores, corals and shell middens. All together, the spatial coverage of African paleoclimate records remains at least an order of magnitude less than that in Europe or North America. With instrumental weather data generally covering only part of the 20th century (Nicholson et al., 2012a; Nicholson et al., 2012b), climate-related information gleaned from historical documentary sources covering the last 2-3 centuries constitute a crucial bridge between instrumental and paleo-data on the all-important hydroclimate variability occurring at (multi-) decadal time scales.

This paper represents the joint effort of members of the PAGES (Past Global Changes) Africa2k Working Group to compile and assess the quality of currently available high-resolution datasets on hydroclimatic variability from the African continent spanning the last 2000 years, and to combine them into a provisional pan-African synthesis. Where possible, we mostly direct our attention to reconstructions with the highest degree of continuity, and displaying robust signatures of past hydroclimate change in well-understood climate indicators (proxies). While the currently available data have obvious shortcomings in terms of quality and geographical coverage, they do exhibit sufficient spatial coherence in hydroclimatic signals to justify exploration of the synchrony of temporal patterns between Africa's major climate regions. In the overview below (section 4) we sequentially focus on all the evidence pertaining to each of six major time periods recognised within the last 2000 years: the first millennium AD, the Medieval Climate Anomaly (MCA; AD 900-1250), the Little Ice Age (LIA; AD 1250-1750), the end of the LIA (AD 1750-1850), the Early Modern Period (1850-1950), and the period of recent warming (from 1950 onwards). In the three time periods since the end of the LIA, an increasing proportion of evidence on past hydroclimate variability is derived from historical documents and instrumental time series.

2 REGIONAL CLIMATE DYNAMICS OF THE AFRICAN CONTINENT

With exception of the continent's northern and southern extremes, the amount and seasonal distribution of rainfall over much of Africa is mainly linked to the annual north-south migration of the Intertropical Convergence Zone (ITCZ) and its associated rain belt (e.g. Nicholson, 2008; Nicholson, 2009, 2011). The mean latitudinal position of the ITCZ shifts throughout the year, trailing the zone of maximum solar insolation and simultaneously drawing monsoonal rainfall onto the continent. A second convergence zone, the Congo Air Boundary (CAB), marks the separation between air flows derived from the Atlantic and Indian Oceans. At the warm-temperate northern and southern tips of the continent, rainfall is mainly linked to the frontal systems of the mid-latitude westerlies, bringing wintertime precipitation maxima in both hemispheres. The sub-tropical regions which remain out of the reach of both the tropical rain belt and the temperate weather system are characterised by deserts. In addition to these general climate mechanisms, factors such as topography and year-to-year variability in circulation patterns over the transition zones between summer and winter rainfall regimes add up to complex patterns of regional rainfall, controlled by diverse dynamic causes (Nicholson, 2000).

On the Atlantic side of Africa, the ITCZ migrates seasonally between 2° in boreal winter and 9° N in boreal summer, reflecting combined influence of the latitudinal shift in peak insolation and northward cross-equatorial ocean currents. The eponymic 'African' monsoon of western and northern Africa displays a substantial south-to-north decreasing gradient in mean annual

precipitation, while year-to-year rainfall variability at any location is subject mainly to SST variability in the equatorial and southern Atlantic Ocean (Camberlin et al., 2001; Nicholson and Webster, 2007; Losada et al., 2010). Paleodata and modelling studies have demonstrated the sensitivity of this system to abrupt and sustained shifts in moisture at longer time scales, driven by changes in the latitudinal gradient of Atlantic SSTs (Giannini et al., 2003; Liu et al., 2004; Shanahan et al., 2009) and positive land-surface and vegetation feedbacks on monsoon intensity (Kutzbach and Otto-Bliesner, 1982; Street-Perrott and Perrott, 1990; Claussen et al., 1999; Renssen et al., 2006).

In East Africa, seasonal ITCZ migration spans the widest latitude range in the world. Around the equator this causes a characteristic bimodal pattern of two rainy seasons, often from March to May (MAM, “long rains”) and from October to December (OND, ”short rains”), separated by two dry seasons of variable intensity. Toward the northern and southern subtropics the two wet seasons merge into one, coinciding respectively with boreal and austral summer. Since the CAB is most often situated along the mountainous western shoulder of the East African Rift System, Atlantic-derived moisture contributes a significant amount of rainfall to Ethiopia, the western part of the East African plateau and the Kenya highlands (Mapande and Reason, 2005; Levin et al., 2009), whereas easternmost equatorial East Africa and the Horn of Africa receive virtually all their precipitation from the Indian Ocean. Yang et al. (2015) highlight the importance of the yearly cycle of monsoonal winds and Indian Ocean SSTs in the creation of bimodal rainfall seasonality in East Africa and the difference in magnitude between the two rain seasons. On interannual time scales, the amount and intensity of short (OND) rains display a strong correlation to Indian Ocean SSTs, which themselves are connected to the El Niño Southern Oscillation (ENSO) and the Indian Ocean Dipole (IOD; Saji et al., 1999), with warming in the western Indian Ocean associated with El Niño conditions and a positive state of the IOD causing higher rainfall over equatorial East Africa (Goddard and Graham, 1999), while simultaneously inhibiting summer rainfall over the northern and southern parts of East Africa, the Sudano-Sahelian belt and much of southern Africa apart from its western strip (Camberlin et al., 2001). The long (MAM) rains of equatorial East Africa are much less correlated to ENSO or any other large SST anomaly (Ogallo et al., 1988; Hastenrath et al., 1993; Okoola, 1999; Camberlin and Okoola, 2003; Pohl and Camberlin, 2011) operating at the inter-annual to sub-decadal time scale.

Southern Africa spans the interface between tropical climate systems and the temperate moisture-bearing systems associated with the southern westerlies (Tyson, 1986; Preston-Whyte and Tyson, 1993; Tyson and Preston-Whyte, 2000). As such, regional-scale climate dynamics within the subcontinent are characterised by marked rainfall seasonality and the juxtaposition of distinct austral winter and summer rainfall zones. In the interior and eastern portions of southern Africa, precipitation is rare during winter (JJA), as continental cooling causes a high-pressure cell to develop over the region. Here, most rain falls during the summer months as continental and sea-surface temperatures increase, resulting in the advection of moist air by tropical easterly flow from the southwestern Indian Ocean (Reason and Mulenga, 1999). In contrast, in the temperate southwestern Cape a wintertime shift of the westerly storm track towards the equator results in greater influence of associated frontal systems and consequently a wet winter climate. In the summer, as the westerlies shift poleward, climate of the southwestern Cape is dominated by the South Atlantic Anticyclone, suppressing uplift and creating extended summer drought (Tyson, 1986; Preston-Whyte and Tyson, 1993). While the temperate and tropical systems are often considered as distinct,

Code	Site	Main proxies	Reference
9501	Marine core site GeoB9501	dust	Mulitza et al., 2010
RA	Rao	historical sources	Nicholson, 1979
AD	Awdaghast (Tedgaoust)	historical sources	Nicholson, 1979
TA	Tassili n'Ajjer	tree-ring width	Cremaschi et al., 2006
TI	Tibesti mountain massif	historical sources	Nicholson, 1979
YO	Lake Yoa	magnetic susceptibility, grain size, geochemistry, diatoms, chironomids, pollen	Kröpelin et al., 2008; Eggermont et al., 2008; Francus et al., 2013
DG	Dongola	historical sources	Nicholson, 1979
KM	Kajemarum Oasis	ostracod Sr/Ca and δ18O	Street-Perrott et al., 2000
BD	Bougdouma Oasis	diatom-inferred salinity	Gasse and Van Campo, 1994
CH	Lake Chad	sedimentology, pollen, historical sources	Maley, 1973; Maley, 1981; Maley, 1989; Maley, 1993
BO	Lake Bosumtwi	carbonate δ18O	Shanahan et al., 2009
TZ	Lake Tizong	pollen, diatoms	Nguetsop et al., 2013
MB	Lake Mbalang	pollen, diatoms	Vincens et al., 2010; Nguetsop et al., 2011
BB	Lake Bambili	pollen	Lézine, 2013
OS	Lake Ossa	diatoms	Nguetsop et al., 2010
NG	Lake Nguene	pollen	Ngomanda et al., 2007
KL	Lake Kamelété	pollen	Ngomanda et al., 2007
KT	Lake Kitina	clay mineralogy	Bertaux et al., 2000
SN	Lake Sinnda	clay mineralogy	Bertaux et al., 2000
AS	Lake Ashenge	diatoms	Marshall et al., 2009
AB	Lake Abhé	stratigraphy	Gasse, 1977
HY	Lake Hayq	carbonate δ18O	Lamb et al., 2007
AY	Lake Abiyata	bulk-sediment geochemistry, diatoms, pollen	Legesse et al., 2002
CB	Chew Bahir	K content	Foerster et al., 2012
TK	Lake Turkana	carbonate content	Halfman et al., 1994
AL	Lake Albert	gauge data	Sutcliffe and Parks, 1999
ED	Lake Edward	Mg content of calcite	Russel and Johnson, 2007
UC	West-Uganda crater lakes	stratigraphy, bulk-sediment geochemistry, diatoms	Russell et al., 2007; Bessems et al., 2008; Colombaroli et al., 2014; Van Zinderen Bakker and Coetzee, 1972; Mills et al., 2014
VC	Lake Victoria	diatoms, gauge data	Stager et al., 2005; Sene and Plinston, 1994
BR	Lake Baringo	stratigraphy, bulk-sediment geochemistry, pollen	Bessems et al., 2008; Kiage and Liu, 2009
LS	Loboi Swamp and Kesubo Marsh	stratigraphy, mineralogy, pollen, diatoms	Ashley et al., 2004; Driese et al., 2004
BG	Lake Bogoria	bulk-sediment geochemistry, mineralogy	De Cort et al., 2013
NK	Lake Nakuru	bulk-sediment geochemistry	De Cort et al., 2013
EL	Lake Elementeita	bulk-sediment geochemistry	De Cort et al., 2013
OL	Lake Oloidien	stratigraphy, bulk sediment geochemistry	Verschuren, 1999a; Verschuren, 1999b
SO	Lake Sonachi	stratigraphy, bulk sediment geochemistry	Verschuren, 1999b
NV	Lake Naivasha	stratigraphy, bulk sediment geochemistry, diatoms, chironomids	Verschuren et al., 2000
SL	Sacred Lake	leaf-wax δD	Konecky et al., 2014

CL	Lake Challa	varve thickness, molecular biomarkers (BIT)	Wolff et al., 2011; Buckles et al., 2016
MI	Malindi Reef	coral Ba/Ca	Fleitmann et al., 2007
TY	Lake Tanganyika	stromatolite δ18O, paleoshorelines, ostracods, diatoms, gauge data	Cohen et al., 1997; Alin and Cohen, 2003; Stager et al., 2009; Nicholson, 1999
RU	Lake Rukwa	historical sources	Nicholson, 1999
ML	Lake Malawi	stratigraphy, biogenic silica content	Owen et al., 1990; Johnson et al., 2001
PF	Pafuri	tree-ring δ13C	Woodborne et al., 2015
CAC	Cold Air Cave	speleothem δ13C	Holmgren et al., 2003
LV	Limpopo Valley	pollen	Ekblom et al., 2012
WK	Wonderkrater	pollen	Scott, 1982; Thackeray, 1999; Truc et al., 2013
DC	Dante's Cave	speleothem δ18O	Sletten et al., 2013
SP	Spitzkoppe	hyrax-midden δ15N	Chase et al., 2009
KR	Kuiseb River	pollen	Scott, 1996
1084B	Marine core site ODP 1084B	foram Mg/Ca and species assemblages	Farmer et al., 2005
EB	Elands Bay	mollusc δ18O and mineralogy	Cohen et al., 1992
VV	Verlorenvlei	diatoms	Stager et al., 2012
CC	Cango Cave	speleothem δ18O	Talma and Vogel, 1992
SW	Seweweekspoort	hyrax-midden δ15N	Chase et al., 2013

Table 1 Sites discussed in this thesis. Codes refer to denominations of sites in Fig. 1.

significant interaction does occur between them, particularly during austral spring and autumn when strong frontal systems may combine with tropical circulation to induce substantial meridional flow of moist air across the subcontinent (Tyson, 1986). Transitional between the summer and winter rainfall zones (sensu Chase and Meadows, 2007) is a zone of aseasonal rainfall. The climate of this transition zone varies strongly from hyper-arid along the western Orange River valley to humid along the coast of the southern Cape. Over century to multi-millennial time scales, varying dominance of the tropical and temperate systems causes significant change in the climatic conditions of this region (van Zinderen Bakker, 1976; Cockcroft et al., 1987; Chase and Meadows, 2007).

3 THE HOLOCENE CONTEXT

Hydroclimate variability across Africa during the last 2000 years must be considered within the context of longer-term Holocene trends. Over the last 11,700 years, most regions experienced substantial changes in climatic moisture balance, which at the multi-millennial time scale are believed to have been controlled mostly by changes in local solar insolation associated with the precessional cycle of Earth's orbit around the Sun (Kutzbach, 1981; Kutzbach and Liu, 1997; Joussaume et al., 1999; Braconnot et al., 2000). During the early Holocene, northern hemisphere summertime insolation was at a maximum, resulting in much wetter conditions than today throughout northern subtropical and tropical Africa (Vincens et al., 1999; Gasse, 2000; Hoelzmann et al., 2001; Lézine, 2013; Tierney and deMenocal, 2013). With Earth's perihelion gradually shifting to southern hemisphere summer over the course of the Holocene, proxy records from this region show a time-transgressive deterioration of moisture balance toward a dry late Holocene (Lézine et al., 2011; Shanahan et al., 2015). In East Africa, sites at or even below the equator (as far south as c. 10° S) seem to have followed the pattern of northern hemisphere summer insolation (Gasse, 2000). It is thought that wetter conditions there during the early Holocene were caused by the reduction of rainfall seasonality caused by an increase in dry-season precipitation (Tierney et al., 2011a). Further south in eastern Africa, some records show the expected inverse pattern, i.e. an orbitally-driven early Holocene drought followed by generally wetter late Holocene conditions (Castañeda et al., 2007; Schefuß et al., 2011; Truc et al., 2013; Chevalier and Chase, 2015). However, in southwestern Africa a largely in-phase relationship between the hemispheres has been found (Chase et al., 2009; Chase et al., 2010; Collins et al., 2011), contradicting the prediction of orbitally-driven north-south anti-phasing in Holocene hydroclimate trends. In the temperate mid-latitude region of the southern Cape, a long-term trend toward more humid conditions seems to have been concurrent with generally cooler conditions since the mid-Holocene (Chase and Meadows, 2007; Chase et al., 2013), but more precise higher-resolution records from this region are required before robust conclusions can be drawn. Together, these longer-term climate trends imply that in most, but not all, regions of sub-Saharan Africa, changes in hydroclimate over the last 2000 years are superimposed on a general long-term decline in moisture availability.

Fig. 1 (next page) Location of sites mentioned in this chapter. Modern-day hydrological regime is showed through the CGIAR-CSI Global Aridity Index (Trabucco and Zomer, 2009), defined as

$$aridity\ index = \frac{mean\ annual\ precipitation}{mean\ annual\ potential\ evapotranspiration}$$

Note that in this formulation, aridity index values increase for more humid conditions. The four smaller panes below demonstrate seasonal rainfall variability throughout the African continent.

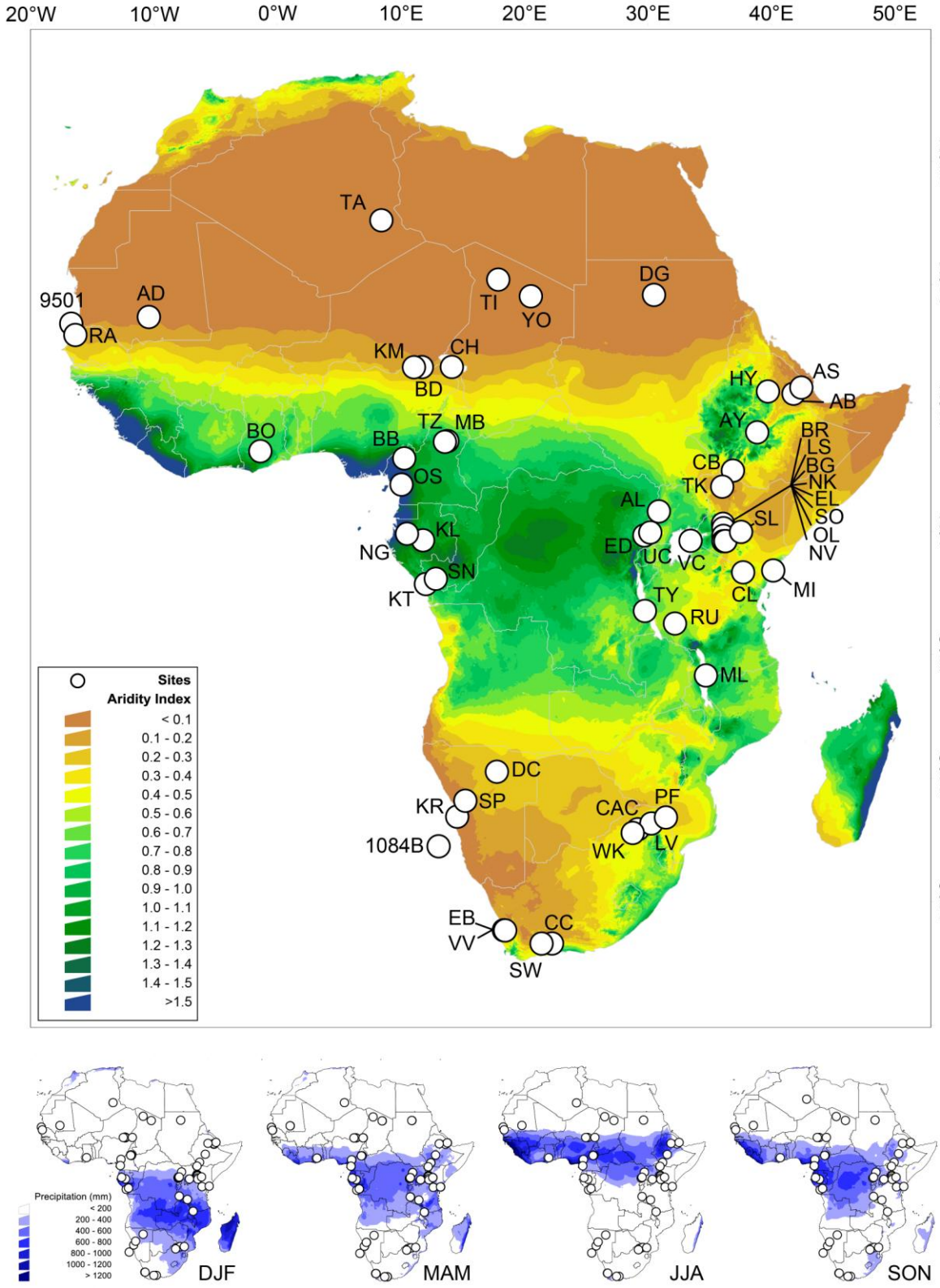
20°W
10°W
0°W
10°E
20°E
30°E
40°E
50°E
30°N
20°N
10°N
0°N
10°S
20°S
30°S
TA
9501
AD
RA
TI
YO
DG
KM
CH
BD
HY
AS
AB
AY
BR
LS
BG
NK
EL
SO
OL
NV
TZ
MB
BB
BO
OS
CB
TK
AL
SL
KL
NG
ED
UC
VC
SN
KT
TY
CL
MI
RU
ML
DC
KR
SP
CAC
PF
1084B
WK
LV
EB
VV
CC
SW
Sites
Aridity Index
< 0.1
0.1 - 0.2
0.2 - 0.3
0.3 - 0.4
0.4 - 0.5
0.5 - 0.6
0.6 - 0.7
0.7 - 0.8
0.8 - 0.9
0.9 - 1.0
1.0 - 1.1
1.1 - 1.2
1.2 - 1.3
1.3 - 1.4
1.4 - 1.5
>1.5
Precipitation (mm)
< 200
200 - 400
400 - 600
600 - 800
800 - 1000
1000 - 1200
> 1200
DJF
MAM
JJA
SON

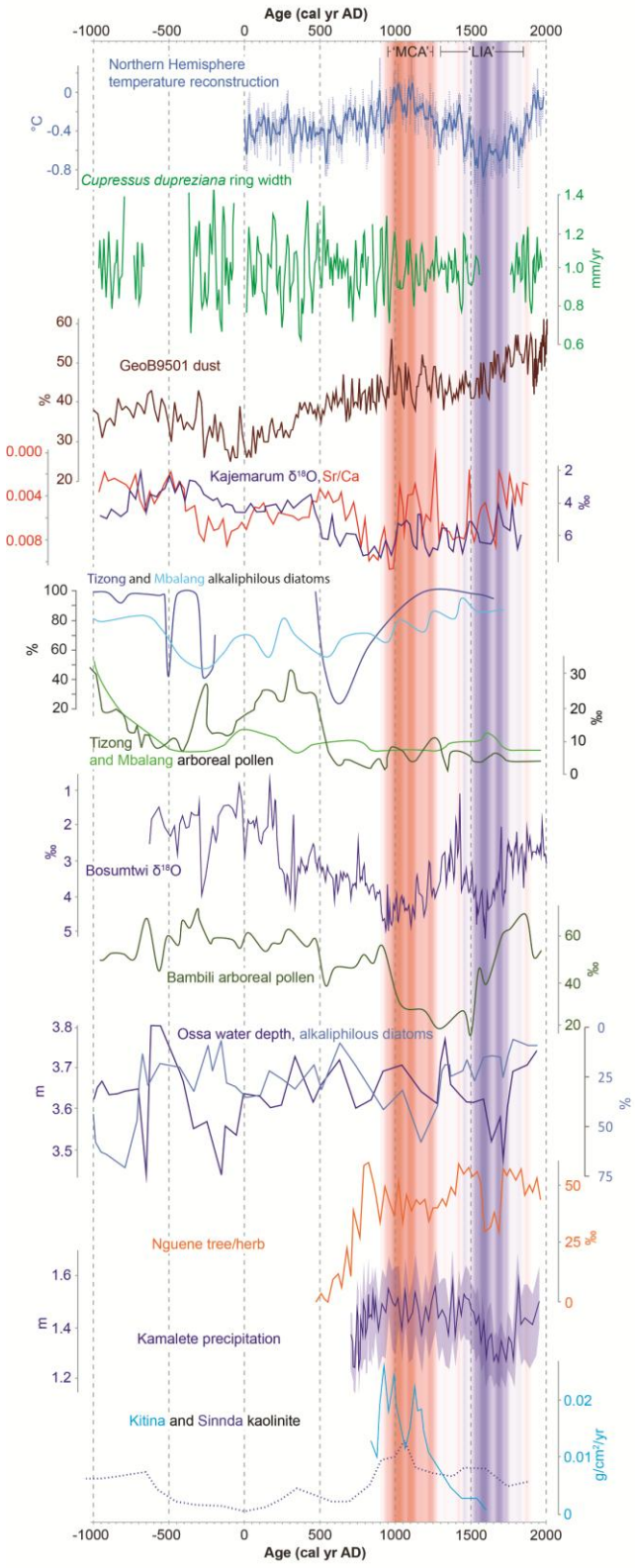

Fig. 2 Compilation of most important hydroclimate-proxy records from West Africa. See Fig. 1 and Table 1 for exact locations and references.

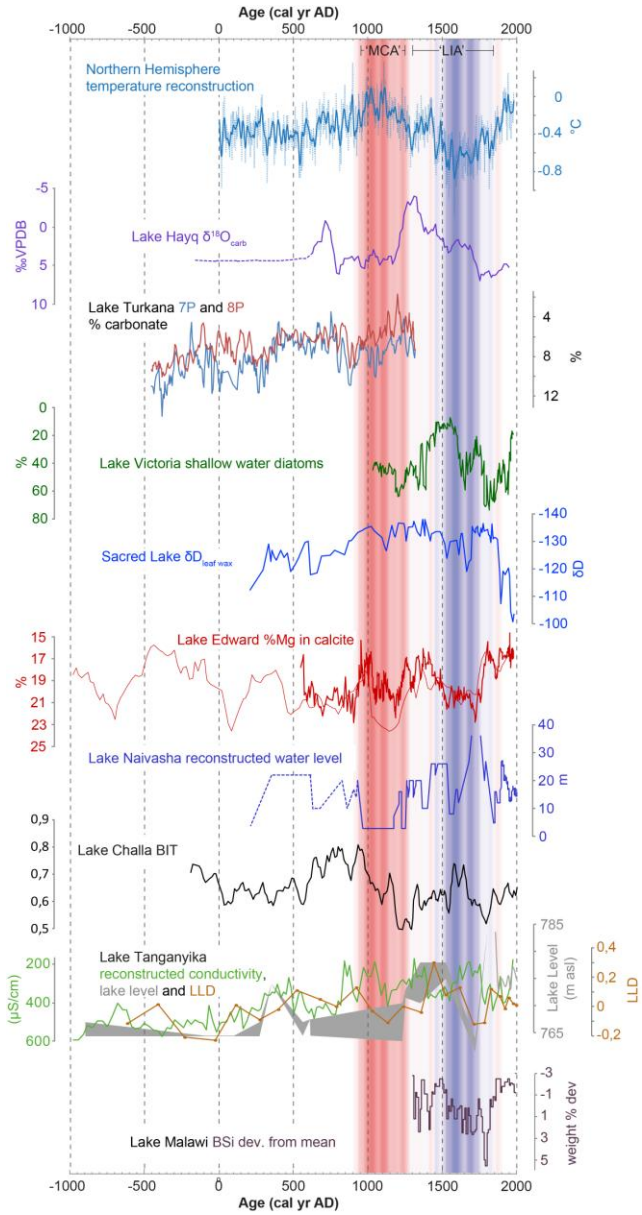

Fig. 3 Compilation of most important hydroclimate-proxy records from East Africa. See Fig. 1 and Table 1 for exact locations and references.

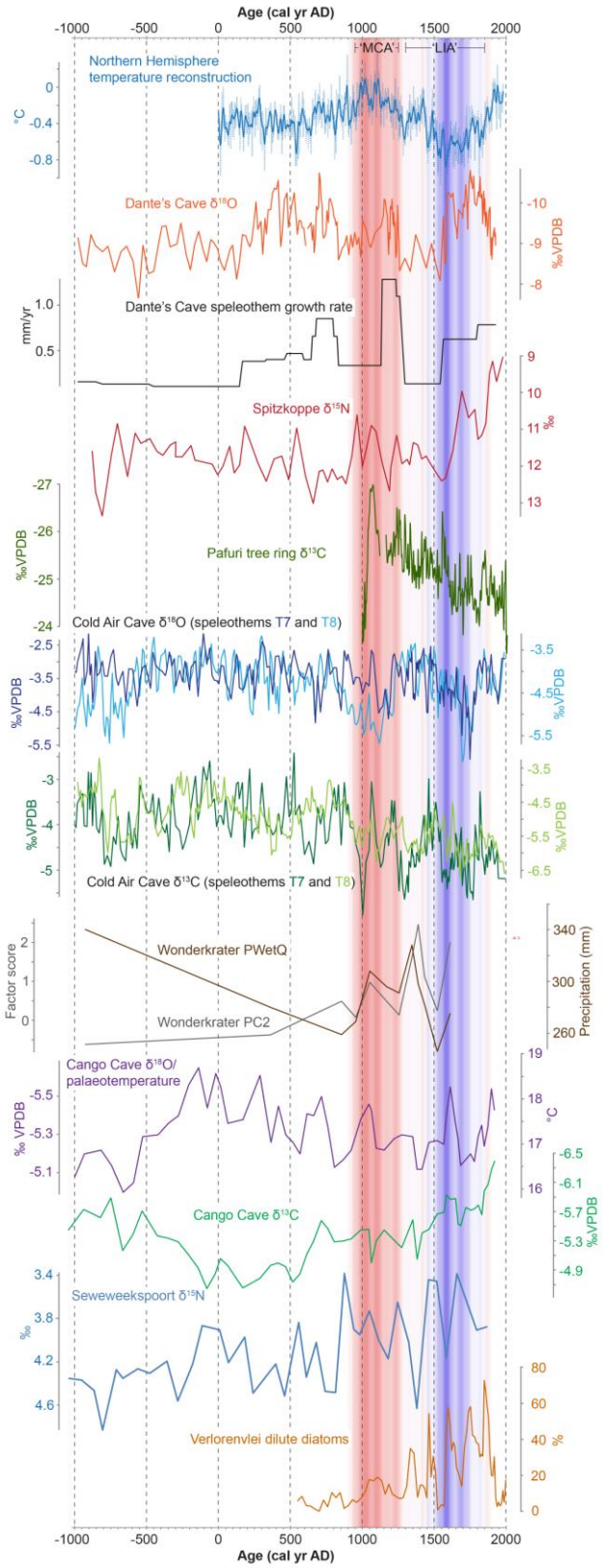

Fig. 4 Compilation of most important hydroclimate-proxy records from South Africa. See Fig. 1 and Table 1 for exact locations and references.

4 AFRICAN HYDROCLIMATE VARIABILITY DURING THE LAST TWO MILLENNIA

4.1 The first millennium AD

We start in the Sahara of North Africa, which 2000 years ago was already an arid desert subject almost year-round to dry north-northeasterly trade winds (Kröpelin et al., 2008). Unfortunately, the sediment record of Lake Yoa in northern Chad (Kröpelin et al., 2008; Eggermont et al., 2008; Francus et al., 2013), the only demonstrably continuous paleohydrological archive from the central Sahara to date, is rather uninformative on the region's hydroclimatic variability within the last two millennia. A rare record from the northwestern Sahara, discontinuous and based on ring-width variations in ^{14}C-dated *Cupressus dupreziana* (cedar) used as construction timber in the Tassili n'Ajjer of southeastern Algeria, shows a reduction in multi-decadal to century-scale rainfall variability coincident with apparent drying from ca. AD 500 to 750 (Cremaschi et al., 2006) but otherwise no clear sustained wetter and drier phases within the last two millennia.

Well-dated and informative climate-proxy records for this period from West Africa are mostly from the humid western and equatorial ('central') parts of the subcontinent near the Atlantic coast (Fig. 1, 2). At Lake Bosumtwi (Ghana), lake-carbonate δ^{18}O variations indicate that, after a ca. 900-year period of relatively moist conditions, an abrupt shift towards greater aridity ca. AD 250 was followed by a sustained gradual trend towards drier conditions continuing until the end of the first millennium (ca. AD 950; Shanahan et al., 2009). The onset of this drying trend is supported by a marine dust record from offshore Senegal (GeoB9501), which indicates that starting c. 100 AD and continuing through the first millennium, the western Sahel region of North Africa experienced gradual drying and loss of vegetation cover (Mulitza et al., 2010). At Kajemarum Oasis in semiarid northeastern Nigeria, variations in ostracod shell Sr/Ca and δ^{18}O indicate a first phase of drying ca. 300-0 BCE and a later phase of more prominent drying starting between ca. AD 500 and 650 (Street-Perrott et al., 2000). The somewhat different timing and rate of change in the Sr/Ca and δ^{18}O records from this site likely reflects differences in how each proxy exactly traces local hydrological change. Nevertheless the most intense drought recorded in the Sr/Ca data, dated to c. AD 750-1000, is also evident in the desiccation of neighbouring lakes (Holmes et al., 1999) and a large salinity increase at Bougdouma Oasis in Niger (Gasse and Van Campo, 1994), suggesting a robust regional phenomenon.

In the transition zone between the northern unimodal and equatorial bimodal rainfall zones, a low-resolution diatom record from Lake Tizong in northern Cameroon documents a significant lowstand between c. 450 and 850 AD (Nguetsop et al., 2013), consistent with fossil pollen data from the same site showing expansion of grassland starting c. AD 500 after a c. 800-year long phase of forest growth. At nearby Lake Mbalang, a corresponding lowstand is centered on c. 550 AD (Nguetsop et al., 2011). The timing of these transitions is more or less synchronous with the drying inferred at Kajemarum Oasis.

Farther south, at Lake Bambili in the mountains of western Cameroon, the % tree pollen indicates stable moist conditions from 250 BCE until AD 500, followed by an abrupt shift to more open vegetation c. AD 500. Recovery of the forest between c. AD 600 and 950 (Lézine, 2013) suggests that the inferred drought was relatively short-lived, and that wetter conditions prevailed again towards the end of the first millennium. A diatom-based lake-level reconstruction from Lake Ossa, near the Atlantic Ocean coast another 250 km further south (Nguetsop et al., 2010), does not show any strong

signal during the first millennium AD, whereas it does provide evidence for a lowstand in the late first millennium BCE, more or less synchronous with inferred drought at Kajemarum Oasis.

Proxy records from Atlantic West Africa around and immediately south of the equator, although incomplete for this period, reveal a distinctly different temporal pattern of hydroclimate change compared to sites further north. Pollen-based moisture-balance reconstructions from Lakes Nguene and Kamelété, Gabon, indicate that the driest conditions of the last 2000 years occurred before AD 500 and 700, respectively (the onset of lacustrine sedimentation at these sites), and that humidity gradually increased to peak around AD 750 (Nguene) or towards the end of the first millennium (Kamelété). The strongest evidence for this wetting trend is an expansion of the tropical rainforest (Ngomanda et al., 2007). Time series of a sedimentary clay-weathering index from Lakes Kitina and Sinnda in southern Congo (Bertaux et al., 2000), though of limited temporal resolution and/or incomplete, similarly suggest a shift to wetter conditions towards the end of the first millennium.

Most lake records from East Africa (Fig. 3) suggest that the region experienced an episode of pronounced aridity shortly before and around the start of the Common Era. Lasting a century or longer, this period may represent the region's driest conditions of the middle to late Holocene (Verschuren and Charman, 2008). Variation in the carbonate content of two sediment cores from the northern part of Lake Turkana, reflecting Omo River inflow and thus precipitation over the Ethiopian plateau, indicates that several arid events occurred between ca. 200 BCE and AD 300 (Halfman et al., 1994). A lake-level reconstruction for Lake Tanganyika based on fossil ostracod assemblages suggests that its lowest level of the past 2500 years was reached between BCE 200 and AD 0 (Alin and Cohen, 2003). This is in accord with stromatolite $\delta^{18}O$, ancient shorelines and diatom-inferred conductivity, which suggest relatively dry conditions from 200 BCE until around AD 200 (Cohen et al., 1997; Stager et al., 2009). Crescent Island Crater, the deepest basin of Lake Naivasha (central Kenya Rift Valley), was completely desiccated until about AD 200 (Verschuren, 2001). In western Uganda, peak %Mg levels of calcite deposited in Lake Edward point to a distinct phase of intense evaporation at this time (Russell and Johnson, 2005), evidence for pronounced regional aridity that has also been recorded at three Ugandan crater lakes nearby (Russell et al., 2007; Colombaroli et al., 2014). At Sacred Lake, a shallow swampy crater lake on the lower slopes of Mt. Kenya, high (less depleted) δD values in plant leaf waxes indicate increased aridity shortly before AD 300 (Konecky et al., 2014). Finally, at Lake Challa near Mt Kilimanjaro in easternmost equatorial Africa, a shift to generally low values of the Branched to Isoprenoid Tetraether (BIT) index from bacterial cell-wall lipids indicate reduced monsoonal rainfall between AD 0 and 200 (Buckles et al. 2016). The exceptionally well-constrained ^{14}C chronology of Lake Challa's sediment archive adds significance to the exact timing of its signature for this episode of widespread aridity. The varve-thickness record from Lake Challa, which is understood to mostly reflect rainfall variability at the inter-annual time scale (Wolff et al., 2011), notably does not show a corresponding signal during this period.

Following this dry episode, much of East Africa appears to have enjoyed a slightly wetter period between ca. AD 200 and 600. In equatorial East Africa it is evidenced by refilling of the previously dry Lake Naivasha, culminating in a relative highstand lasting until ca. AD 600 (Verschuren, 2001). Reduced %Mg values of Lake Edward calcite in the period AD 200-400 (Russell and Johnson, 2005) documents similarly wet conditions on the western shoulder of the East African plateau, while at Lake Tanganyika a contemporaneous humid phase is dated to between ca. AD 250 and 550 (Stager et

al., 2009). Also Lake Kivu immediately north of Lake Tanganyika must have experienced a positive water balance during this period, since its overflow into Lake Tanganyika via the Rusizi River was reactivated ca. AD 550 (Cohen et al., 1997). At the northern extreme of East Africa, a diatom record from Lake Ashenge (northern Ethiopia; Marshall et al., 2009) and a potassium record from Chew Bahir (southern Ethiopia; Foerster et al., 2012) indicate that relatively wet conditions also prevailed on the Ethiopian plateau during the first half of the first millennium AD, although age control during this period (and the last 2000 years in general) is poor in both of these records. Machado et al. (1998) found evidence for this inferred wet period from infilled valley deposits in the northern Ethiopian highlands. The transition to more arid conditions around AD 500 suggested in all these records supports the hypothesis that the rise and fall of the Aksumite Empire was climate-related (Butzer, 1971).

Following this regionally fairly coherent pattern, the available records attest to considerably greater spatial variability during the second half of the first millennium AD. Lake Edward experienced a succession of multi-decadal droughts, superimposed on overall low humidity levels, between AD 400 and 890 (Russell and Johnson, 2005). Lake Tanganyika's level fell after the AD 250-550 high stand, followed by a gradual rebound toward the end of the first millennium AD (Alin and Cohen, 2003; Stager et al., 2009). At Sacred Lake on Mt. Kenya an abrupt drought dated to ca. AD 650 was followed by a gradual recovery of precipitation to reach an inferred maximum ca. AD 1000 (Konecky et al., 2014). In the northern Kenya Rift Valley, Omo River inflow to Lake Turkana was relatively high between c. AD 400 and 800 (Halfman et al., 1994), whereas a number of massive trona (sodium carbonate) deposits in the sediments of hypersaline Lake Bogoria suggests a succession of distinctly negative water-balance anomalies from ca. AD 700 to 1000 (Chapter 4). Further south in the Kenya Rift Valley, Lake Naivasha slipped from high to fluctuating lake levels ca. AD 600 (Verschuren, 2001); in southeastern Kenya by contrast, Lake Challa experienced between ca. AD 600 and 1000 the wettest conditions of the past 2,200 years (Buckles et al., 2016). What many of the East African records do have in common is evidence for a short but distinct period of higher rainfall towards the end of the first millennium AD. Examples include Lake Hayq ca. AD 700 (Lamb et al., 2007), Lake Turkana ca. AD 750 (Halfman et al., 1994), Lake Edward between AD 900 and 1000 (Russell et al., 2007), Lake Tanganyika ca. AD 800-850 (Alin and Cohen, 2003; Stager et al., 2009), Lake Naivasha ca. AD 900 (both peak lake level and low conductivity: Verschuren et al., 2000; Verschuren, 2001) and Lake Challa at AD 950 (Buckles et al., 2016). Taking into account chronological uncertainty on all these lake archives, these signatures may well represent the same region-wide episode of inferred peak rainfall. From its timing in the best-dated records, we venture to assign a most-probable date of the 10th century AD.

In southern Africa, few high-resolution records are sufficiently well-dated and understood to adequately address paleoclimate questions at sub-millennial time scales (Fig. 4). Exceptions are speleothem $\delta^{18}O$ records from Cango Cave on the temperate southern coast of South Africa (Talma and Vogel, 1992); and from Cold Air Cave in the northeastern part of South Africa's summer rainfall zone (Repinski et al., 1999; Stevenson et al., 1999; Lee-Thorp et al., 2001; Holmgren et al., 2003). These records have long defined regional narratives regarding climate change during the last 2000 years (Tyson and Lindesay, 1992; Tyson et al., 2000a), but their interpretation remains a matter of discussion (Chase et al., 2010; Woodborne et al., 2015). While $\delta^{18}O$ records from (sub-)tropical

speleothems are usually interpreted as primarily reflecting variation in rainfall amount, with more depleted values indicating increased precipitation (Neff, 2001; Wang et al., 2004), the Cango Cave $\delta^{18}O$ record was interpreted by Talma and Vogel (1992) to reflect changes in mean annual air temperature. There is, however, no obvious correlation between these authors' temperature reconstruction from Cango Cave and global or Northern Hemisphere temperature reconstructions (e.g., Moberg et al., 2005; PAGES 2k, 2013). The $\delta^{18}O$ records from Cold Air Cave speleothems are of much higher resolution, but also their climatic significance has not been straightforward. Lee-Thorp et al. (2001) and Holmgren et al. (2003) suggested that both temperature and the nature/source of precipitation effect dominant control on $\delta^{18}O$, with intense thunderstorms contributing more to annual rainfall during cooler, drier periods. Support for this interpretation is clearest in the record from speleothem T7, where more enriched $\delta^{18}O$ values correlate reasonably well with darker greyscale values (enhanced production of organic matter; Lee-Thorp et al., 2001), particularly between 6000 and 3000 cal yr BP. This relationship is less clear, however, in the speleothem section representing the last 2000 years.

New analyses (Truc et al., 2013; Chevalier and Chase, 2015) of the Wonderkrater pollen record (Scott, 1982) showed a strong positive relationship between Holocene precipitation in the wider Cold Air Cave region and southwest Indian Ocean SSTs over millennial timescales (Sonzogni et al., 1998). In turn, at these time scales both records exhibit a first-order negative relationship with the Cold Air Cave $\delta^{18}O$ record. An argument can therefore be made for the amount effect to be a significant control – at least during certain periods – on Cold Air Cave $\delta^{18}O$. In combination, these records imply a positive correlation between continental rainfall and both sea-surface and continental temperatures, consistent with the conceptual model of Tyson and colleagues (Tyson, 1986; Cockroft et al., 1988; Tyson and Lindesay, 1992; Tyson et al., 2000b), which calls for invigorated easterly flow during warmer periods. However, Lee-Thorp et al. (2001) and Sundqvist et al. (2013) have found that, at least during the last century, only a weak relationship exists between Cold Air Cave $\delta^{18}O$ and rainfall amount, prompting the latter authors to conclude that temperature has been the dominant driver of the $\delta^{18}O$ record over the last several hundred years. These findings suggest that under different climate regimes, different drivers may dominate the Cold Air Cave $\delta^{18}O$ record, and a clear, complete interpretation will require further data from independent sources. In the context of the last two millennia, it is interesting to note that a generally inverse correlation exists between the Cold Air Cave and Cango Cave $\delta^{18}O$ records which, if both sites have experienced similar temperature trends, would call for fundamentally different paleotemperature transfer functions.

One other promising source of hydroclimate data are $\delta^{13}C$ records from baobab trees (*Adansonia digitata*). Records obtained from Pafuri in northern-most South Africa indicate that at centennial time scales over the last millennium, a negative relationship exists between Cold Air Cave $\delta^{18}O$ and baobab $\delta^{13}C$ (Woodborne et al., 2015). Using the paleotemperature reconstruction of Sundqvist et al. (2013), these data indicate that during this period variation in Cold Air Cave $\delta^{18}O$ may indeed have been driven primarily -but perhaps not exclusively- by temperature changes, and that warmer conditions generally correlated with increased regional humidity. The Pafuri data also support Holmgren et al.'s (2003) interpretation of the Cold Air Cave $\delta^{13}C$ data. These have been interpreted as primarily reflecting the proportion of C_3 plants (trees, shrubs and cool-season grasses; depleted $\delta^{13}C$) and C_4 plants (warm season grasses; enriched $\delta^{13}C$) in the vegetation (and thus soil carbon)

above the cave. However, rather than the traditional explanation that more arid conditions result in enrichment in $\delta^{13}C$ because of a reduction in tree cover (cf. Castaneda et al., 2007), Holmgren et al. (2003) concluded that at Cold Air Cave such conditions restricted grass growth, leaving a dominance of tree and shrubs that could access deeper groundwater resources. Combined, the Pafuri baobab and Cold Air Cave speleothem records indicate highly variable conditions during the late Holocene in northeastern South Africa, with but a general trend towards more arid conditions over the last 2000 years.

In southern Africa's western summer rainfall zone in Namibia, at the southern distal limit of the African monsoon, records from hyrax middens at Spitzkoppe (Chase et al., 2009) and the speleothems in Dante's Cave (Sletten et al., 2013) indicate relatively stable dry or drying conditions from BCE 1000 to ca. AD 200. At Spitzkoppe, episodes of increased humidity at AD 200 and AD 550 (Chase et al., 2009) may relate to $\delta^{18}O$ and growth-rate indications for increased rainfall at Dante's Cave from AD 200 to 800 (Sletten et al., 2013). Over the time period considered here, it appears that the western portion of the summer rainfall zone experienced perturbations generally out-of-phase to those observed in the east, with a broad negative relationship between the records from Spitzkoppe and Dante's Cave and the speleothem record from Cold Air Cave.

In the winter rainfall zone of South Africa's Western Cape, rock-hyrax midden $\delta^{15}N$ records from Seweweekspoort (Chase et al., 2013) indicate a long-term humidity increase throughout the last two millennia. This long-term trend also seems to be reflected in Cango Cave $\delta^{13}C$ variation (either as a function of an increase in C_3 grasses reduced water-use efficiency under more humid conditions; cf. Chase et al., 2013), and the Verlorenvlei diatom record which indicates increased freshwater input over the last 1400 years (Stager et al., 2012). Although a greater number of highly resolved records would be helpful, it appears that a generally in-phase relationship may exist between the southwestern Cape and the western summer rainfall zone, with both exhibiting signals in opposition to those observed in the eastern summer rainfall zone. This is consistent with the findings of Chevalier and Chase (Chevalier and Chase, 2015), who identified a north-south dipole within the eastern summer rainfall zone during recent millennia.

4.2 The Medieval Climate Anomaly (AD 950 - 1250)

Around the transition between the first and second millennium AD, high northern-latitude regions experienced mostly warm conditions (Jones and Mann, 2004; Moberg et al., 2005; Mann et al., 2008). Hemisphere-wide and global syntheses suggest that this Medieval Warm Period (MWP) or Medieval Climate Anomaly (MCA: Jones et al, 2001; Briffa & Matthews, 2005) was generally warmer than the subsequent Little Ice Age. However, the nature and timing of the MCA temperature anomaly is now recognised as being spatially complex, and distinct at the scale of the different continents (PAGES 2k Consortium, 2013). The few existing temperature reconstructions from Africa with adequate resolution in the last 2000 years suggest a generally warm MCA, but do not allow comprehensive assessment of the continent's temperature variability during this period (Nicholson et al., 2013; PAGES 2k Consortium, 2013). Evidence describing the nature of Africa's hydroclimate during the MCA is more extensive, but some geographical gaps do remain.

Numerous historical texts cover the MCA period in the western Sahel region of North Africa (Nicholson, 1979). Between the 9th and 13th century AD, several towns in Mauritania are said to

have flourished on caravan trade. Their locations, and that of the routes upon which they were founded, would seem to suggest that the region was wetter than today. This is consistent with the agricultural practices of the Gangara people who occupied the sandy plains of Assaba and the Tagant in Mauritania from the 8th to the 15th century AD, and practiced wet cultivation in areas where present-day aridity makes this impossible. Around the 11th century AD, the water level in wells of the caravan city of Awdaghast (Tedgaoust) was some 8 m higher than today. A synthesis of many other archival sources suggests that the MCA was wetter than today all across the Sahel (Nicholson, 1979). Evidence from Senegal and Niger suggests that sand dunes were fixed by vegetation about the same time, with conditions sufficiently stable that tombs were built on top of them near Rao, Senegal. These humid conditions may have extended as far as the limit of African monsoon penetration in northern Chad. The Tibesti mountain massif appears to have become depopulated in the 10th through 13th centuries, indicating that conditions were wet enough to sustain its population in the surrounding plains. The history of Lake Chad over the past 900 years (Maley, 1973) has been revised and updated several times. Compilation of the sedimentological and palynological data (Maley, 1981), anchored in three radiocarbon dates (Maley, 1993) and tuned with available documentary proxy data (Maley, 1989), indicate that Lake Chad stood high from before AD 1100 to 1400 and again in the 17th century, separated by low to intermediate levels during the 15th and 16th centuries. Slightly wetter conditions in this region at around this time (AD 1000 to 1200) are also apparent in Sr/Ca and $\delta^{18}O$ data from carbonates in Lake Kajemarum (northeastern Nigeria; Street-Perrott et al., 2000). Additional evidence that relatively humid conditions extended to the easternmost Sahel include the presence of elephants and giraffes near Dongola in Sudan during the 12th century (present annual rainfall there is ~20 mm), and extensive pilgrim traffic across the Red Sea during the 13th century from a port (probably Port Sudan) which was later abandoned for lack of drinking water.

In the more humid regions south of the Sahel, the MCA appears to have been a period of relative aridity. Dry conditions from c. AD 900 to 1150 are evident in lake level and stable isotope data from Lake Bosumtwi (Shanahan et al., 2009) and in peak dust flux in marine sediment core GeoB9501 from offshore Senegal (Mulitza et al., 2010). To the east, in Cameroon, Lake Bambili also records a rapid shift from forest to a more open landscape at around AD 900 (Lézine, 2013), consistent with the evidence for drier conditions during the MCA in humid tropical West Africa. However, the Bambili pollen data indicate that the forest does not recover until ca AD 1500, suggesting that dry conditions lasted much longer than in records to the west (Lézine, 2013). Additional support for an extended dry interval originating during the MCA comes from Lake Ossa, where an increase in the proportion of alkaliphilous diatoms (interpreted as decreased precipitation) places the most arid conditions of the past 2,700 years between c. AD 950 and 1150 (Nguetsop et al., 2010). Slightly to the north, at Lakes Tizong and Mbalang (Vincens, 2010; Nguetsop et al., 2013), pollen data indicate that open conditions were maintained throughout the last c. 1500 years. However, at Tizong, the onset and termination of the MCA is characterized by two periods of slightly increasing arboreal pollen –possibly suggesting slightly wetter conditions. In the southern Congo, the signal is more complex. Overall, conditions appear to have become wetter overall just before the MCA, between c. AD 700-800. At Lake Kamelété (Ngomanda et al., 2007) and Sinnda (Bertaux et al., 2000), pollen and weathering indicators in records suggest that more humid conditions were maintained during subsequent centuries, with

no change during the MCA. In contrast, the pollen record from nearby Lake Nguene (Ngomanda et al., 2007) suggests a slight shift back to a more open landscape between AD 800 and 1400. And at Lake Kitina, clay weathering indicators have been interpreted as signifying wetter conditions between AD 900-1250 (Bertaux et al., 2000).

Records from East Africa indicate that the region was relatively dry for much of the period between 950 and 1250 AD. The onset of the MCA was marked by a dramatic increase in the frequency of extremely low Nile River floods in Egypt (Hassan, 2007), reflecting reduced rainfall in the source areas on the Ethiopian plateau and at Lake Victoria. Low Nile floods remained common until AD 1350, but were interrupted by an interval of high discharge between AD 1070 and 1180. Historical reports of widespread famine at that time cover the entire Nile catchment, from Egypt (Hassan, 2007) to headwater areas around Lake Victoria (Webster, 1979). A diatom-based lake-level reconstruction from Lake Victoria itself starting around AD 1000 (Stager et al., 2005) suggests relatively dry conditions during the MCA, but it was not the driest period of the last millennium, with severe drought mostly confined to a c.100-year episode centred on 1200 AD. Carbonate levels at Lake Turkana reflect an abrupt decrease in Omo River input at ca. AD 900 (Halfman et al., 1994). Afterward, core 7P suggests variable but relatively low humidity, while core 8P seems to indicate gradually increasing precipitation. However, both cores agree on a strong recovery toward the end of the MCA, with humidity peaking at AD 1200. A section of enriched $\delta^{18}O$ values of authigenic carbonate deposited in Lake Hayq suggest that in northern Ethiopia, the negative water balance which had already started around AD 800 ended ca. AD 1200 (Lamb et al., 2007), i.e. about the same time as in Lake Turkana. The stratigraphy of salt minerals in the sediments of Lake Bogoria dates the end of this long dry period in northern Kenya to around AD 1150 (Chapter 4). The level of Lake Naivasha was also low during most of the interval AD 1000-1250 (Verschuren et al., 2000), however was interrupted by a short-lived transgression locally dated to around 1150 AD. On the western shoulder of the East African plateau, Lake Edward experienced a distinct drying trend over the course of the MCA, with most pronounced drying around 1050 AD and after 1150 AD, and ending around 1200 AD (Russell and Johnson, 2007). This medieval drought is also recorded at four maar crater lakes in western Uganda (Van Zinderen Bakker and Coetzee, 1972; Russell et al., 2007; Mills et al., 2014) though mostly with less detail. While not distinctly recorded in the stromatolite record (Cohen et al., 1997), the MCA at Lake Tanganyika seems to have been a period of declining humidity culminating in peak drought dated to AD 1150 (Alin and Cohen, 2003; Stager et al., 2009). In southernmost East Africa, a large lake level fall is reported for Lake Malawi between AD 1150 and 1250 (Owen et al., 1990). In easternmost equatorial East Africa, the Lake Challa BIT-index record suggests that an abrupt aridification between 1150 and 1200 AD resulted in peak MCA drought, which predominated until 1300 AD (Buckles et al. 2016). The combined information from all these sites points to generally drier-than-average conditions during the MCA throughout East Africa, from Ethiopia in the North to Lake Malawi in the South. However, the marked trends within this time window observed at several sites do not allow the MCA to be treated as a single 300-year dry event. In this context, Verschuren and Charman (2008) pointed out that the Naivasha lake-level record during the MCA, indicating continuous shallow-water conditions and hydrologic closure of the basin, may be discontinuous across this interval. This is may be the case for other shallow endorheic lakes as well, precluding precise statements on the exact timing, duration and possible short-term

variability of the MCA in these records. The certifiably continuous records (e.g., Lakes Edward, Victoria, Tanganyika, Challa) all seem to suggest that peak MCA drought prevailed in the second half of the 12th century.

Using speleothem data from northeastern South Africa, Tyson and Lindesay (1992) and Tyson et al. (2000b) inferred that the summer rainfall region south of Lake Malawi may have been wetter and perhaps significantly warmer than today (~+3°C) during the MCA. Subsequent refinements of the age model for Cold Air Cave's speleothem records indicate that the period between ca. AD 800 and 1200 was actually a period of highly variable conditions (speleothem T7 data; Holmgren et al., 1999; Lee-Thorp et al., 2001), or even consistently cooler (speleothem T8 data; Holmgren et al., 2003, applying paleotemperature transfer function of Sundqvist et al., 2013). While Holmgren et al. (2003) conclude that the Cold Air Cave records provide evidence for medieval warming, the MCA *sensu stricto* (AD 950-1250) is a period of strongly depleted $\delta^{18}O$ values in speleothem T8, a situation very similar to the coldest period of the LIA, from ca. AD 1500-1800. Similarities do seem to exist, however, between the Cold Air Cave T7 speleothem and Cango Cave $\delta^{18}O$ records, perhaps suggesting that the more muted response recorded in the T7 speleothem is a more accurate reflection of prevailing conditions than the strong depletion in the T8 speleothem. The $\delta^{13}C$ records from the T7 and T8 speleothems are more coherent, and, following the interpretations of Holmgren et al. (2003), indicate a phase of more variable, but generally mesic conditions, similar to the BCE 1000-AD 900 period.

Estimation of temperature and humidity variations on the basis of a pollen record at the nearby site of Wonderkrater suggest warm, wet conditions from c. AD 900–1200, as indicated by covariance in moist-loving taxa such as Proteaceae, Oleaceae and Combretaceae, and a reduction in drought-tolerant Chenopodiacae-Amaranthaceae (Scott, 1999) compared with the first millennium AD. The temporal resolution of this record is quite low, however, and it is difficult to fully situate these findings in the context of the changes occurring in the last millennia. Variability across the MCA and early LIA are, however, generally consistent with the $\delta^{13}C$ records from Cold Air Cave and the Pafuri baobab (Woodborne et al., 2015), with a peak in humidity beginning at c. AD 980 and an inferred return to drier conditions towards AD 1250, which ended with a return to moist conditions around AD 1350. General support for these findings is also found in pollen records from across the lower Limpopo Valley, where trees become more dominant between AD 800 and 1400, presumably in response to higher rainfall (Ekblom et al., 2012).

On the western margin of southern Africa, at Spitzkoppe, depleted $\delta^{15}N$ in rock-hyrax middens indicate greater water availability during the MCA (Chase et al., 2009). This record also shows substantial variability, with a period of generally increased humidity between AD 900 and 1250 interrupted by a period of significantly drier conditions around AD 1200. This pattern correlates with records of sea-surface temperature (SST) and upwelling from the adjacent southeast Atlantic ocean at marine core site ODP 1084B, where variation in the abundance of the foraminifer *Neogloboquadrina pachyderma* (left coiling) (Farmer et al., 2005) infer a reduction of upwelling intensity during the periods of increased humidity as registered at Spitzkoppe. From the same region, pollen records from hyrax middens along the Kuiseb River valley show increases in frost-sensitive *Salvadora* during the MCA, with peaks around AD 1100 and 1250 suggesting warmer conditions (Scott, 1996). The similarities between these Namibian records suggest that warmer, more humid

conditions prevailed during the MCA in the western summer rainfall zone. As a counterpoint, evidence from Verlorenvlei in southernmost South Africa, where precipitation is currently linked most strongly to the westerly storm track, indicates that conditions were relatively dry throughout the period AD 550–1300 (Stager et al., 2012).

4.3 The Little Ice Age (AD 1300 – 1750)

Analyses of glacier and paleoclimate records have justified the distinction of an "early" LIA phase, characterised by glacier advances in the Alps from around AD 1300 onward, and a "main" LIA phase (c. AD 1550 – 1850) when mean annual Northern Hemisphere temperature fell significantly below the AD 1961–1990 mean (Matthews and Briffa, 2005). Recent paleoclimate data syntheses (Jones and Mann, 2004; Moberg et al., 2005; PAGES 2k Consortium, 2013) indicate that the Northern Hemisphere as a whole had already experienced distinct cooling from the end of the MCA around 1250 AD, but also that manifestation of LIA cooling was certainly not uniform between continents.

Temporal patterns of precipitation during the LIA vary across Africa. Numerous lines of evidence suggest that the Sahel and nearby regions were much wetter than today, particularly during the main LIA phase (Nicholson, 1980). Lake Chad, for example, of which the drainage basin straddles both Sahel and equatorial rainfall regions, stood some 4 m above its modern mean from about AD 1600 to sometime in the 18th century (Maley, 1976). Chronicles of West African empires suggest that drought was rare throughout most of the 1500s through early 1700s. There are also numerous references to large floods of the Niger, active waterways replacing dry wadis in northern Chad, and a vegetation cover much more verdant than today. Archaeological finds, some dated, and rare meteorological reports, provide further evidence of these wetter conditions. Wetter conditions appear to have prevailed on the temperate side of the Sahara, as evidenced by a low frequency of droughts and by some meteorological reports. Farther south, at Lakes Tizong and Mbalang in northern Cameroon, a small increase in arboreal pollen may indicate wetter conditions during the LIA, though the landscape continued to be dominated by the open grasslands established at c. AD 500 (Nguetsop et al., 2013; Vincens, 2010). At Kajemarum Oasis, the LIA signal is also small. Both the Sr/Ca and the d18O data indicate that the climate was wetter than during the most extreme phase of drying between c. AD 500 and 1000 and a second period of aridity following the MCA (AD 1250- 1450). However, overall the proxy data spanning the LIA from Kajemarum Oasis is variable, with conditions becoming wetter during the initial and later parts of the LIA with a period of drier conditions during AD 1600-1700. Chronological control is insufficient to fully evaluate the regional synchrony of these shifts (Holmes et al., 1999), but the LIA does not stand out as an exceptionally wet period at this site. In contrast to the evidence for wetter conditions in northern subtropical West Africa, there is considerable evidence for a drier climate in the humid West-African tropics during the main phase of the LIA. At Lake Bosumtwi, Ghana, lacustrine $\delta^{18}O$ data show a post MCA return to wet conditions that continued into the early 15th century, but this was abruptly followed by a period of pronounced drought lasting from c. AD 1450 to 1750 (Shanahan et al., 2009). Judging from the Lake Bosumtwi record, dry conditions peaked during the 16th century. Diatom-inferred water depth of Lake Ossa decreased between AD 1300 and 1700, culminating in the lowest levels of the past 2 millennia (Nguetsop et al., 2010). Further to the south, pollen data from Lakes Nguene and Kamelete also indicate more arid conditions between AD 1550-1700 and AD 1500-1750, respectively (Ngomanda et al., 2007), broadly synchronous with the main-phase LIA drought at Lake Bosumtwi. Documentary evidence appears to

support the timing of maximum drought in these records as well. A unique time series of documentary data on drought and disease in coastal Angola spanning AD 1560 to the 1870s based on Portuguese colonial archives (Dias, 1981; Miller, 1982), suggests that the most calamitous conditions occurred during the 1580s (Verschuren, 2004). This is synchronous, within dating precision, with the peak LIA aridity recorded at Lake Bosumtwi. Together, these data suggest that in western equatorial Africa the period from c. AD 1450 to 1750 appears to have been the driest of the late Holocene, i.e. at least as dry as MCA drought.

In East Africa, peak MCA drought ended with a return to a moister hydroclimate c. AD 1200-1250, broadly coeval with the onset of the early-LIA phase in Europe and other northern Hemisphere regions (Matthews and Briffa, 2005; Moberg et al., 2005; PAGES 2k Consortium, 2013). Early paleolimnological studies on lakes Turkana (Butzer, 1971), Abhé (Gasse, 1977) and Ugandan crater lake Katwe (Van Zinderen Bakker and Coetzee, 1972) had already suggested high lake levels during the LIA, but chronology was insufficient to constrain their exact timing. Nile flood levels, recorded in Cairo but depending mainly on rainfall over the Blue Nile catchment in the Ethiopian highlands, increased from 1325 to 1470, after which historical records are interrupted (Nicholson, 1980; Fraedrich et al., 1997; Kondrashov et al., 2005). In the central Kenya Rift Valley, abrupt wetland formation at Loboi Swamp and Kesubo Marsh is dated to AD 1250 (Ashley et al., 2004; Driese et al., 2004). A growing number of high-resolution, well-dated lake-sediment records distributed over the region suggest that, after this common initial stage of post-MCA lake transgression, notable spatial differences developed in the amplitude and timing of LIA hydroclimate variability. In easternmost East Africa, specifically the region situated eastward of the CAB year-round, relatively humid conditions continued through the main-LIA phase (Verschuren, 2004), as exemplified by the records of Lake Naivasha (Verschuren et al., 2000; Verschuren, 2001) and Lake Challa (Verschuren et al., 2009; Wolff et al., 2011). At Lake Naivasha, this 500-year period of relatively moist climate was nevertheless interrupted by two multi-decadal episodes of prominent lake-level decline in the late-14^{th} and late-16^{th} centuries, reflecting intermittent drought events prominent enough to be recorded also in regional vegetation (Lamb et al., 2003) and ethnographical history (Webster, 1979; Verschuren et al., 2000). The high-resolution δD record from Sacred Lake attests to peak pluvial conditions between c. 1700 and 1870 AD, although chronological control of this record for the past centuries is probably not adequate enough to treat this timing with confidence (Konecky et al., 2014). At Lake Challa near Mt. Kilimanjaro, the gradual post-MCA shift to wetter conditions overprinted quite large short-term variability in the BIT index proxy used (Buckles et al., 2016). A clear peak in LIA humidity was reached between c. 1570 and 1670 AD, preceding peak levels at Lake Naivasha by c. 50-100 years. In western regions of equatorial East Africa, influenced to a significant extent by the Atlantic Ocean, lake records from western Uganda (Russell and Johnson, 2007; Russell et al., 2007; Mills et al., 2014) and Lake Tanganyika (Cohen et al., 1997; Alin and Cohen, 2003) display an early humidity maximum lasting from about AD 1200 to 1500, followed by establishment of sustained dry conditions during most of the main-phase LIA. The high-resolution %Mg record from Lake Edward suggests that regional aridity at that time was comparable to that of climax MCA drought (Russell and Johnson, 2007). At this site, LIA drought seems to have set in already by 1450 AD. A similar pattern is documented by the 700-year biogenic silica (BSi) record of Lake Malawi (Johnson et al., 2001), where humidity seems to have peaked at AD 1500, after which aridification set

in, culminating at first at AD 1700, followed by an additional, very severe drought pulse at AD 1800. An earlier study, using a variety of sources such as diatom assemblages, mapping of desiccation horizons, oral traditions and archaeological finds, had also reported major lake level falls within the period AD 1500-1850 (Owen et al., 1990). A growing number of East African lake records seem to present an intermediate temporal pattern between these 'eastern' and 'western' histories, in which climate during the main-phase LIA was drier than during the early-phase LIA, but still clearly wetter than during peak MCA drought or the 20th-century average. One example is the carbonate $\delta^{18}O$ record from Lake Hayq in northern Ethiopia (Lamb et al., 2007), and results from Lake Bogoria also seem to suggest as much (Chapters 3, 4). The most prominent example is Lake Victoria, which according to a lake-level reconstruction based on the ratio between open-water and near-shore diatoms (Stager et al., 2005) seems to have reached its highest level of the LIA between AD 1400 and 1600, followed by a more modest highstand during the main-phase LIA.

In southern Africa, Tyson and Lindsay (1992) and Tyson et al. (2000b) found the LIA to be a robust feature in a range of paleoenvironmental records, and concluded that during this period relatively cool (~-1°C) and dry conditions prevailed over most of the subcontinent. Again, these syntheses rely heavily on data from the Cango Cave and Cold Air Cave speleothems, with the LIA being identified as the period of low $\delta^{18}O$-inferred temperature at Cango Cave from c. AD 1100 – 1900, and relatively depleted $\delta^{18}O$ values at Cold Air Cave from ca. AD 1500 – 1800. The Cango Cave $\delta^{18}O$ record is often cited to constrain the timing and trends of climate change in the region over the last 2000 years (Tyson and Lindesay, 1992), but while the authors of the original record (Talma and Vogel, 1992) found no conflict with other data available at the time, their results do not clearly show a pattern coherent with the timing of the MCA or LIA. This may be a function of the site's position, which is influenced by both tropical and temperate systems, and distant from regions recognised to be most sensitive to Northern Hemisphere signals (see Chase et al., 2011; Schefuß et al., 2011; Chase et al., 2015b; Chevalier and Chase, 2015). Additionally, or alternatively, inconsistencies with trends observed elsewhere may be a product of these records' chronology, which may require revision (cf. Chase et al., 2013), and/or their low resolution. Cognisant of these caveats, similarities do seem to exist with the Cold Air Cave T7 speleothem $\delta^{18}O$ record, perhaps indicating a relatively warm early-LIA from ca. AD 1400-1600 followed by more pronounced cooling between ca. AD 1650 and 1850.

Links between the summer rainfall zones of northeastern South Africa and Namibia have been proposed (Chase et al., 2010), but within the context of the MCA and LIA, signals of moisture availability between these sub-regions seem to be anti-phased. Accepting a degree of error in age models as well as site/proxy specific variations, the $\delta^{18}O$ and growth-rate records from Dante's Cave (Sletten et al., 2013), the Spitzkoppe rock hyrax middens (Chase et al., 2009) indicate the early LIA (c. AD 1250 – 1500) was characterised by variable/generally drier conditions relative to the MCA, followed by a rapid transition to more humid conditions across the coldest period of the LIA from ca. AD 1600 – 1850. In the eastern summer rainfall zone, climate reconstructions derived from the Wonderkrater pollen sequence indicate cooler, drier conditions c. AD 1400 – 1800 (Scott, 1982; Thackeray, 1999; Truc et al., 2013), but the resolution and chronological control of this sequence is too low to elucidate the precise nature of environmental change during this period. Better resolved $\delta^{13}C$ records from Pafuri baobabs (Woodborne et al., 2015) and Cold Air Cave speleothems (Lee-

Thorp et al., 2001; Holmgren et al., 2003) indicate relatively humid conditions during the early LIA, from ca. AD 1400-1600, followed by marked aridification from ca. AD 1600-1800.

Evidence provided by shell middens and marine cores from the west coast of southern Africa suggest that SSTs in the region were somewhat lower than today during the LIA. However, the low resolution of these records makes identification of the LIA as a discrete period difficult. At Elands Bay, a SST depression is seen to have existed from ca. AD 1300 to at least AD 1580, but as pre-LIA temperatures between AD 0 and 1300 are constrained by only a single data point, the context for this apparent anomaly is unclear (Cohen et al., 1992). Farmer et al. (2005) obtained a more complete record of SSTs and upwelling activity along the west coast of Namibia from marine core ODP 1084b near Luderitz. In it, more intense upwelling appears to have occurred from ca. AD 1050 to 1500, corresponding broadly with a period of reduced SSTs AD 950 – 1600. While neither can be said to represent a distinct manifestation of the LIA, the terrestrial records from Namibia mentioned above register similar fluctuations, particularly a marked shift ca. AD 1500, suggesting either a causal link or a shared response between coastal upwelling and regional climates.

Regional reviews for southern Africa have proposed an inverse relationship in hydroclimate trends between its summer and winter rainfall zones (Tyson and Lindesay, 1992; Tyson et al., 2000a; Chase and Meadows, 2007). Diatom data from Verlorenvlei in the southwestern Cape, i.e. in the heart of the winter rainfall zone, do indicate increasing precipitation following the MCA, potentially linked to equatorward shifts of the westerly storm tracks (Stager et al., 2012). Stable isotope records from the southern Cape at Seweweekspoort indicate a period of generally wetter conditions during the LIA, but not significantly different from the MCA, and more clearly part of a general long-term increase in humidity (Chase et al., 2013).

4.4 The end of the LIA (AD 1750-1850)

During the last century of the LIA (AD 1750 to 1850), paleoenvironmental records from lakes, speleothems and other natural archives start to be supplemented by documentary evidence (e.g. Nicholson, 1981; Vogel, 1989; Nicholson, 2000; Nash and Endfield, 2002; Kelso and Vogel, 2007; Nash and Endfield, 2008; Nash and Grab, 2010; Norrgård, 2015; Nash et al., 2016), tree-ring records (e.g. Dunwiddie and LaMarche, 1980; Therrell et al., 2006; Woodborne et al., 2015), reconstructions from ships' logbooks (Hannaford et al., 2015) and early rain-gauge data from a handful of countries (Nicholson et al., 2012a; Nicholson et al., 2012b).

The most detailed historical evidence for the late 18th century comes from West Africa. Here, documents suggest that the Sahel, especially around the Niger Bend close to Timbuktu, and inland areas of the Guinea coast, experienced successive droughts from the late 1730s to the mid-1750s (Nicholson, 1980; Nicholson, 1996; Nicholson et al., 2012a; Norrgård, 2015). Annually-resolved records from 1750 onwards indicate that these regions then experienced decadal-scale alternating wetter (1757-65, 1781-88) and drier (1765-80, 1789-98) periods (Norrgård, 2015). Conditions at the Guinea coast appear to have been, at times, in antiphase with those of the Sahel, with wetter conditions extending from 1750-77 and 1788-98 and drier from 1777-87 (Norrgård, 2015). Records from the late 18th century are also available for southwest Africa. Around Luanda on the Atlantic coast, the 1780s and 1790s appear to have been among the driest decades since 1560 AD, second only to the 1580s (Miller, 1982).

Historical records are relatively sparse for the early 19th century. The first decade appears to have been dry over much of the continent, although there are some discrepancies between documentary and other proxy data where these are available (Hannaford and Nash, 2016). For example, while the documentary record of Nicholson et al. (2012a) suggests protracted drought across southern Africa between 1800 and 1811, tree-ring series for Zimbabwe (Therrell et al., 2006) and meteorological observations carried out on European trading ships passing by South Africa (Hannaford et al., 2015) for the same period suggest above-average rain alternating with drought.

The most notable event identified from historical sources was a near-continent wide episode of below-average rainfall that prevailed throughout much of the 1820s and 1830s (Nicholson et al., 2013). This appears to have been the culmination of a drying trend that began in the late 18th century, possibly during the mid-1780s (Nicholson, 1996) or slightly later in coastal West Africa (Norrgard, 2015). Ships' logbook-based reconstructions for KwaZulu-Natal (Hannaford et al., 2015), and documentary records for the Kalahari (Nash and Endfield, 2002), Namaqualand (Kelso and Vogel, 2007) and the Eastern Cape (Vogel, 1989), all suggest reduced austral rain-season (November through March) precipitation over southern Africa during these decades. Elsewhere, drought conditions were evident across the entire Sahel, all the way westward to the Cape Verde Islands, where some 40% of the population reportedly perished in 1830 alone (Brooks, 2006). Severe drought struck Ethiopia in the years AD 1828-1829 (Wolde-Georgis, 1997), while a disastrous famine during the 1830s in East Africa (Hartwig, 1979) resulted in massive population migrations. Burton (1860) suggested that famine and drought prevailed in the Pangani Valley of Tanzania for roughly two decades in the 1820s and 1830s. Krapf (1860) described a similar situation in Mombasa, Kenya. Water levels of Lake Tanganyika and Lake Rukwa, as deduced from historical and geographical information, were low during the late 18th and early 19th century until the 1840s (Nicholson, 1999). Assuming that the drying trend in East Africa commenced around AD 1785, Nicholson and Yin (2001) used a water-balance model calibrated with 20th-century gauge data to estimate that rainfall in the Lake Victoria catchment between AD 1785 and 1835 was roughly 13% below the 20th-century mean.

In agreement with these historical data, the majority of well-resolved paleoclimate records for East Africa show that the main-phase LIA climate regime ended in an episode of aridity dated to the late 1700s and early 1800s. In the Lake Victoria region it appears to have been the driest period of the last millennium (Stager et al., 2005), i.e. drier than the MCA. In the Lake Malawi sediment record, a short-lived peak in BSi indicates severe aridity centred on AD 1800 (Johnson et al., 2001). At Lake Challa near Mt. Kilimanjaro, the BIT index record indicates that the period AD 1780–1820 was the most arid since the MCA (Buckles et al., 2016). Lake Naivasha in Kenya's central Rift Valley dropped to its lowest level since the MCA, resulting in complete desiccation of its main basin (Verschuren, 2001). Severe aridity between AD 1750 and 1830 has also been inferred for the Lake Baringo area, on the basis of pollen, fungal spores and charcoal counts by Kiage and Liu (2009). Bessems et al. (2008) had earlier reported that the desiccation of Lake Baringo was synchronous with that of two shallow crater lakes in western Uganda, showing that this widespread drought temporarily overwrote the east-west contrasts across the CAB observed during the LIA.

(Verschuren, 1999a) constrained the end of the early 19th century drought in East Africa by renewed lake filling to 1815±8 AD using high-resolution ^{210}Pb-dating on freeze-cored sediments from Lake Sonachi, a small crater lake close to Lake Naivasha. This age is indistinguishable from the date of AD

1822-1826 assigned to a prominent peak in the Ba/Ca ratio of a coral from Malindi Reef on the Kenyan coast, which is inferred to reflect increased soil runoff within the Sabaki River catchment caused by drought-breaking flood events (Fleitmann et al., 2007). Although a widespread phenomenon, the amplitude of lake transgression across East Africa in the 1820s-1830s remained relatively modest. Many lakes both in western Uganda and the Kenya Rift Valley were shallower than today and either swampy or more saline (Verschuren, 1999a; Verschuren, 1999b; Bessems et al., 2008).

The combined evidence suggests that average mid-19th century climate conditions remained relatively dry for East Africa, and that the 19th century was drier, on average, than the 20th century. In contrast, a multiproxy reconstruction for the southern African summer rainfall zone indicates that the 19th century was significantly wetter than the 20th (Neukom et al., 2014; Nash et al., 2016).

4.5 The Early Modern Period (AD 1850 – AD 1950)

Evidence for spatial hydroclimate variability across Africa during the early modern period comes from a combination of documentary evidence and rain-gauge data. Rain-gauge stations became plentiful in Algeria from the 1860s onwards and in South Africa from the 1880s, and widely available across the continent from the early 20th century (Nicholson et al., 2012a). In North Africa, conditions in coastal Algeria became notably drier around the 1860s but very wet conditions prevailed in the 1890s (Nicholson et al., 2012a). The Sahel became markedly wetter around 1850 and remained so through to the end of this period, with the exception of drought in the 1910s. Maximum rainfall appears to have occurred in the 1880s in the Sahel and regions to the north, although a handful of very wet years occurred in the 1870s. Rainfall conditions along the Guinea coast showed little change from early in the 19th century; the most notable occurrences were prolonged dry intervals in the 1860s and 1870s.

East Africa became wetter commencing in the 1830s following extreme early-19th century drought (see above), but regional rainfall was near rather than above average in the 1850s and 1860s (Nicholson et al., 2012a). At the same time, abnormally dry conditions prevailed in equatorial regions. Throughout East Africa, a variety of evidence points to a severe drought event during the second half of the 19th century. In the Kenya Rift Valley, very low water levels and/or elevated salinity is dated to between AD 1870 and the early 1890s from multi-proxy sedimentary evidence and early historical reports at Lake Naivasha and its satellite lakes Oloidien and Sonachi (Verschuren, 1999a-b; Verschuren et al., 1999a-b). Just to the north, lakes Nakuru and Elementeita stood completely dry (de Cort et al., 2013). In Ethiopia, major late-19th century drought is associated with the one of the most severe famines of the last few centuries (Pankhurst, 1966), and is also recorded in the sediments of Lake Abiyata (Legesse et al., 2002). This “Great Ethiopian Famine” of AD 1888-1892 is said to have cost the lives of one third of Ethiopia’s population. In northern Tanzania, as much as 40 to 75% of pastoralist Maasai may have succumbed (Iliffe, 1987). Lake Tanganyika’s level also dropped suddenly during this period (Nicholson, 1999). Fragmentary historical information on the level of Lake Naivasha since the 1880s show a major trangression from 1880 onwards, reaching the historically highest recorded level between 1890 and 1900 (Ase et al., 1986). After the turn of the century, lake levels gradually dropped until the mid-1950s. A hydrological study at Lake Turkana explored numeric relations between Western Indian and Eastern Atlantic SSTs and lake level change for the period AD

1992-2013 (Bloszies and Forman, 2015). Based on this calibration, the historical SST record was used to reconstruct Turkana lake level back to AD 1857, successfully capturing the main moisture patterns known from the discontinuous 20th century observational record while comprehensively dissecting the role of western and eastern moisture sources over time. A decreasing contribution of Atlantic-derived moisture to East African precipitation throughout the 20th century is suggested, consistent with earlier work (Williams et al., 2012).

In southern Africa, the end of the early 19th century arid interval was spatially variable. Documentary and rain-gauge data suggest that very dry years prevailed in south-central regions until the 1890s (Nicholson et al., 2012a). South of c. 15°S, however, multiproxy reconstructions for the summer rainfall zone reveal the early 1860s to be the driest period of the 19th century, and the 1870s, 1880s and early-mid 1890s the wettest decades of the last 200 years (Neukom et al., 2014; Nash et al., 2016). In the winter rainfall zone of southwest South Africa, wetter conditions prevailed from the 1870s through to the late 1910s (Vogel, 1989; Nicholson et al., 2012a; Neukom et al., 2014), with comparatively dry conditions occurring until around 1950 (Nicholson et al., 2012a; Neukom et al., 2014).

A handful of extreme years occurred during the early modern period. For example, tremendous rains fell in East Africa in 1877, in conjunction with the protracted El Niño event of 1877-78 (Aceituno et al., 2009). This El Niño was preceded by unusually heavy rains in central southern Africa in early 1877 (Nash and Endfield, 2008). Widespread very heavy rains and flooding were also recorded in 1890 and early 1891 across eastern South Africa, eastern Botswana and Lesotho prior to the very strong El Niño of 1891 (Nash and Endfield, 2002, 2008; Nash and Grab, 2010). In the southern African winter rainfall zone, the 5-year period of 1888-1892 was the wettest of the 19th century (Neukom et al., 2014), while Ethiopia was struck by severe drought during this period (Pankhurst, 1966). Extremely heavy rainfall also occurred throughout southwest Africa in 1934, with rainfall generally at least 50% above average throughout Namibia and much of northern South Africa (Nicholson et al., 1988).

A number of the longer records discussed earlier also include this early modern period. Lake Bosumtwi (Shanahan et al., 2009), Lake Edward (Russell et al., 2007), Lake Naivasha (Verschuren et al., 2000) and Spitzkoppe (Chase et al., 2009) all show a mid-19th-century period of modest wetness (or relative aridity) followed by much wetter conditions from the 1880s until the 1920s or 1930s, and a general drying trend from then until the 1950s. Obviously, uncertain dating of those records lacking historical counterparts limits our ability to make even decadal-scale correlations, but pattern similarities between them are highly suggestive of pan-African coherence.

4.6 The period of recent warming (AD 1950 – AD 2010)

The most recent era has been characterised by several continent-wide episodes of anomalous rainfall, each lasting a decade or longer (Nicholson, 2001). Rainfall during the 1950s was well above average throughout the subtropics of both hemispheres, but the equatorial latitudes were comparatively dry. The inverse of this pattern prevailed during the 1960s, with exceptional rainfall in 1961 (Conway, 2002) leading to peak river discharge and peak levels for Lake Albert (Sutcliffe and Parks, 1999), Lake Victoria (Sene and Plinston, 1994), Lake Naivasha (Ase et al., 1986) and Lake Tanganyika (Nicholson, 1999) in 1963-1964. This equatorial humid anomaly extended to the southern Sahel, where rainfall remained above normal until the later 1960s. The 1970s were dry throughout

most of the continent, but particularly so in the Sahel. In contrast, a series of wet years prevailed in parts of southern Africa during the mid-late 1970s (Nicholson, 2001). The 1980s was a decade of continent-wide aridity (Nicholson, 2001), with 1983 the driest of the last 200 years across the summer rainfall zone of southern Africa (Neukom et al., 2014). Exceptions were parts of the northern and southern mid-latitude extremes and isolated sectors of East Africa, particularly the highlands. Arid conditions continued throughout most of the 1990s, except in much of East Africa and in the winter rainfall zone of South Africa (Nicholson, 2001).

During the period 1950-present, the most extreme conditions occurred in the Sahel, which suffered three decades of drought spanning 1968-1997 (Nicholson, 2001). At least partial recovery occurred early in the 21st century. In other parts of Africa, some very extreme years occurred between 1950 and the present time. The mid-1970s included some of the wettest years on record for parts of southern Africa, particularly 1974 and 1976.

Hulme et al. (2001) evaluated a subset of annual rainfall records for the African continent (1901 to 1995), and found that, throughout the continent, the trend over the course of the 20th century was less than 10% of the annual mean, except over the highlands around Sierra Leone and Cameroon and in a few areas of southern equatorial Africa. However, clear trends emerge since the 1960s, with rainfall generally increasing in the equatorial region and decreasing in the subtropics of both hemispheres. Between the period 1960-1989 and 2000-2009, mean March-June and July-September rainfall in the western Sahel decreased by some 20-40 mm per decade (Funk et al., 2012). Mean annual rainfall increased marginally over the same time period in the central Sahel, with a particularly strong increase during both seasons over Ethiopia and western Kenya. Climate modelling shows a link between high SSTs in the western Indian Ocean and enhanced precipitation over East Africa during the short-rain (OND) season (Ummenhofer et al., 2009). Consequently, Shongwe et al. (2011) project that excessive OND rainfall will drive an overall increase in mean precipitation as a consequence of anthropogenic global warming. In contrast, Williams and Funk (2011) report decreasing long-rain (MAM) precipitation over eastern Kenya and the eastern flank of the Ethiopian highlands during the period 1979-2009, for which they identify a remarkably strong warming of the Indian Ocean and consequent suppression of convection over eastern equatorial Africa as the main drivers. This drying trend during the main growing season is observed all along the western rim of the Indian Ocean, and could be problematic given the importance of rain-fed agriculture in often food-insecure countries with strong population growth (Funk et al., 2008). These contrasting trends in seasonal rainfall demonstrate the necessity of an improved understanding of East African climate dynamics.

During the last 10-15 years, a number of extreme events have occurred. While the Sahel has partially recovered from prolonged drought in the 1970s and 1980s, rainfall has recently been highly variable, and in general it remained below the 1920-2003 average. In the far eastern Sahel and East Africa, drought appears to have become more frequent and more intense. During the years 2008-2011, rainfall was 30-75% below average over the Horn of Africa, Kenya and most of the Sudan. Between July 2010 and June 2011 the situation was even more severe, with rainfall being at least 50-75% below average in nearly half of the drought-stricken region (Nicholson, 2014). Southern Africa was affected by severe drought in 2007 and 2011, but in some regions (Namibia and Botswana), a considerable rainfall increase and green-up occurred in the intervening years (Stockhall, 2010).

Following the 2008-2011 drought in East Africa, Kenya has seen a spectacular transgression of its Rift Valley lakes after 2011. By September 2013, lakes Naivasha, Nakuru, Bogoria and Baringo had risen to levels not experienced since (at least) the early 1900s, with surface-area expansions of between 30 and 70% causing the flooding of surrounding settlements, agricultural land and wildlife sanctuaries (Onywere et al., 2013).

5 DISCUSSION

Several obstacles, including patchy geographical coverage, low data resolution and high chronological uncertainty of available records complicate the construction of a complete picture of African hydroclimate history for the past 2000 years. When dealing with natural archives of environmental change, any climatic interpretation should take into account climate-to-proxy control, the translation of climatic developments to proxy signals that are stored in the archive. This is often system-specific and not always unambiguous. In much of Africa, lakes are the dominant source of paleoclimate information. Typically, they illustrate the sometimes complex relationship between rainfall and lake level (the basis of many long-term hydroclimate proxies), depending on rainfall seasonality and catchment hydrology. Ideally, such water-balance relationships should be taken into account when interpreting reconstructed past lake-level fluctuations in terms of precipitation variability (Nicholson, 1999). Over the course of the 20th century, human impact has become a major additional factor influencing lake systems throughout the continent. Practices such as water extraction for agriculture and artificial evaporation for salt mining now greatly influence the water levels of certain African lakes (e.g. Ayenew, 2002; Becht and Harper, 2002; Mekonnen et al., 2012), and caution should be exercised when using recent relationships between precipitation and lake level to calibrate past lake-level reconstructions.

5.1 Drivers of past hydroclimate variability

The broad data synthesis presented in this paper allows the recognition of some general, broad-scale patterns. Overall, Africa's moisture balance history contains marked differences within and between regions, combined with large-scale climate changes that are (nearly) uniform across the continent. Obvious candidates to explain decadal- to century-scale interregional precipitation differences are fluctuations in the position of the ITCZ and its variable extension away from the equator during northern or southern hemisphere summer (Schneider et al., 2014). Moisture balance patterns during the first millennium AD inferred from tropical and subtropical West Africa support this suggestion. As discussed above, records from the northern portion of equatorial West Africa, spanning a north-south transect from Nigeria to Cameroon, indicate wetter conditions overall during the first half of the first millennium AD than during the second. In some records, this is manifested as an abrupt aridification centred around AD 500, while in others the changes are more gradual. This pattern shows up in both pollen and hydrological records, making it more likely that it is related to changes in climate as opposed to land use. The strength of the signal also appears to decrease towards the equator, though this may be in part a reflection of proxy sensitivity. Available data suggest that this northern hemisphere drying was accompanied by a shift to more humid conditions in the southern tropical latitudes, as evident from the lake records of Gabon and the Congo, and further south at Dante's Cave, Namibia. These opposing north-south precipitation changes are consistent with a

southward shift in the ITCZ, which would have reduced the length of the rainy season in the north while increasing it in the south.

On longer timescales, a connection between North Atlantic Ocean dynamics and the tropical Atlantic monsoon has been established (Street-Perrott, 1990), with large injections of fresh water into the northern North Atlantic leading to reduced thermohaline circulation and a southward displacement of the ITCZ. Evidence for an ITCZ shift associated with northern high-latitude cooling has also been brought forward for the LIA (Haug et al., 2001; Brown and Johnson, 2005). Under this scenario, southward ITCZ migration and reduced meridional heat transport in the Atlantic Ocean are predicted to cause strong, positive SST anomalies in the equatorial and southern tropical Atlantic Ocean (Vellinga and Wood, 2002), which would weaken the Atlantic monsoon system. This mechanism has been invoked to explain declining rainfall at tropical sites under an Atlantic Ocean regime during the LIA, as far east as western portions of the East African plateau (exemplified by the records of Lake Edward and nearby crater lakes; Russell and Johnson, 2007; Russell et al., 2007). General circulation modelling indicates that northern high-latitude cooling and a weaker thermohaline circulation is coupled to a more El Niño-like SST gradient in the Pacific Ocean (Zhang and Delworth, 2005). This is confirmed by coral records from the Pacific Ocean covering the LIA (Cobb et al., 2003). Henke et al. (2015) further suggest, through a study integrating a global array of proxy records, that precipitation patterns were significantly more ENSO-like during the LIA than during the MCA. This would explain the observed main-phase LIA highstands at Lake Naivasha and Lake Challa, sites where the Indian Ocean monsoon dominates annual precipitation and which generally receive more short rainy-season precipitation during El Niño years (Goddard and Graham, 1999).

The dichotomy of a drier tropical LIA in West Africa contrasting with a wetter easternmost East Africa has been described previously (Russell and Johnson, 2007; Russell et al., 2007), most recently in a study by Tierney and deMenocal (2013). Focusing on the seven available records with sufficient time control, this investigation robustly demonstrated that sites closer to the Indian Ocean and Horn of Africa have varied mostly in antiphase with interior Albertine Rift Valley sites since the early LIA, driven mainly by variations in SST gradient across the Indian Ocean.

The CAB also plays an important role in LIA climate, with some studies inferring a weakened convergence (Tierney et al., 2011b) and possible westward migration (Russell and Johnson, 2007) of the boundary during the LIA. The hydrology of lake-basins between western and easternmost East Africa can be expected to be under the influence of both Atlantic and Indian Ocean regimes, creating an intermediate pattern. Evidence suggests that the influence of the Indian Ocean at sites including Lake Victoria (Stager et al., 2005), Lake Bogoria (Chapters 3, 4) and Lake Hayq (Lamb et al., 2007) was counteracted by the weaker Atlantic monsoon, damping the effects of maximum ENSO-related precipitation during the later stages of the LIA.

The scenario of a westward migration of the CAB during the LIA might also explain the patterns observed for a set of sites in southern Africa. The records from Dante's Cave ($\delta^{18}O$), Spitzkoppe ($\delta^{15}N$) and Verlorenvlei (diatoms) in southwest-Africa, for example, all evolve from a humidity minimum at the start of the LIA to a maximum during the early 18th century, i.e. following the eastern East Africa LIA regime. Some of these sites are located close to or west of the contemporary CAB during the time of the year in which they receive the majority of precipitation. Their consistency with the LIA rainfall

patterns of eastern East Africa may suggest a weaker Atlantic-sourced African monsoon during the main-phase LIA which resulted in an overall westward shift in the mean longitudinal position of the CAB, allowing Indian Ocean dominance to be established over the western part of southern Africa. At the same time, drying of sites in eastern South Africa (e.g. Wonderkrater, Pafuri, Cold Air Cave) over the course of the LIA is in agreement with a scenario of generally more El Niño-like conditions, since these sites are well-known to be drought-prone during El Niño episodes (Lindesay et al., 1986; Camberlin et al., 2001). Future studies should attempt to shed light on this scenario, as no solid evidence is available at the moment to test this hypothesis.

By employing principal component analysis on an extensive set of historical precipitation data covering the 19th and 20th centuries, Nicholson (2014) identified a limited number of continental-scale patterns that have dominated spatial rainfall variability on the inter-annual time scale. The study demonstrates that the most common modes are (1) anomalies of the same sign over most of the continent, (2) contrasting anomalies between the low latitudes and the subtropics, and (3) an east-west opposition in the equatorial region and southern Africa. The stability of these patterns over the past 200 years strongly suggests that they constitute inherent attributes of rainfall variability over Africa. Within these modes, the shift between opposing poles can occur over small spatial scales, which has important implications for the interpretation of paleoclimate archives that are situated at or close to these transition areas. In principle, the paleoclimate record should allow to consider whether the relative dominance of these main types of hydroclimate variability, appearing stable throughout the past 200 years, changed over longer time periods. For instance, the widespread drought of the late-18th to early-19th century is an example of a prolonged continent-wide, in-phase climate anomaly. In contrast, the LIA epoch strongly reminds of the third mode, i.e. an equatorial east-west out-of-phase pattern that was also found to explain a significant part of the interannual variability in the historical period. Furthermore, the preceding MCA reminds of the second mode stated above, with drought throughout the equatorial regions contrasted by wetter conditions in the Sahel and in southern Africa. This sequence of shifting interregional moisture balance relationships suggests that the mutual dominance of these common modes of continental rainfall variability may change over time. As no apparent link to large-scale phenomena (SST and atmospheric factors) was found by the author of the original study, their balance remains poorly understood. Looking further into this would be an example of how the study of historical records and longer, natural archives could greatly complement each other.

5.2 Directions for future research

The preceding discussion has highlighted a number of geographical and temporal gaps in our understanding of the evolution of African hydroclimates over the last 2000 years, together with some potential future research questions. The limited number of high-quality records going further back in time impedes testing of whether the observed hydroclimate patterns of the LIA were unique. More and longer archives are needed to robustly integrate low-latitude African hydroclimate variability into global paleoclimate patterns. For an adequate characterization of climate evolution on the time scales that are most important during the past two millennia, a data resolution of at least several data points per century will be required. Decades of research in Africa have taught us that high-potential records are not readily available on the continent, so the actual availability, rather than the pursuit of an ‘ideal’ geographical coverage, of records will always have the highest impact on which

archives will be exploited. A revisit of previously explored sites using newly developed proxies could also be part of improving the archival network. Future efforts should aim to constrain the interactions between the main African convergence zones (ITCZ and CAB) and oceanic modes of variability and their responses to global climate dynamics. These main actors do not suffice to explain all observed hydroclimate patterns of the past 2000 years. For example, the scenario of a decreased Atlantic monsoon activity and southward shift of the ITCZ inferred for the LIA are in stark contrast to the wetter-than-present conditions of the Sahel at that time (Nicholson and Webster, 2007). Such differences further cannot be explained by more El Niño-like conditions, given the negative correlation of summer precipitation in the Sudano-Sahelian belt to ENSO identified by some studies (e.g. Camberlin et al., 2001). Apparently, complex smaller-scale mechanisms can significantly interact with large-scale atmospheric and oceanic drivers of precipitation, counteracting them in some regions.

Future efforts of the paleoclimatology community should concentrate on improving the geographical coverage of high-resolution, (semi-)quantitative reconstructions of moisture balance records, to capture not only inter-regional differences but also sub-regional patterns. Much is already known from contemporary climatology about the role of SSTs as drivers of rainfall across the continent (e.g. Goddard and Graham, 1999; Reason and Jagadheesha, 2005), including during El Niño and La Niña phases (e.g. Nicholson and Kim, 1997; Nicholson and Selato, 2000). The extension of the SST record should lead to a more complete reconstruction of African rainfall over the past 2000 years. Historical climatologists could usefully work to address gaps in the Africa-wide rainfall reconstruction compiled by Nicholson et al. (2012a); these are most notable in equatorial and more arid areas (Nash and Adamson, 2014). Clearly, progress will be dependent upon the availability of historical sources, but it should be possible to achieve similar temporal resolution for the 19th century in East Africa and coastal West Africa to that already available for southern Africa. Major collections of French, German, English, Portuguese and Arabic language documents remain largely unexplored for their climate reconstruction potential. The analysis of Arabic-language manuscripts in various cities across the Sahel, for example, would permit the reconstruction of long-term rainfall variability along the southern margin of the Sahara, and bridge the gap between lake sediment and instrumental records (Nash and Adamson, 2014). Importantly, however, any improved knowledge of past climate change should be translated into an understanding of current climate patterns and expectations for the future.

REFERENCES

Aceituno P, Prieto MR, Solari M, Martínez A, Poveda G, Falvey M. (2009) The 1877–1878 El Niño episode: associated impacts in South America. Climatic Change 92:389-416.

Alin SR, Cohen AS. (2003) Lake-level history of Lake Tanganyika, East Africa, for the past 2500 years based on ostracode-inferred water-depth reconstruction. Palaeogeography, Palaeoclimatology, Palaeoecology 199:31-49.

Ase LE, Sernbo K, Syren P. (1986) Studies of Lake Naivasha, Kenya and its drainage area. Institute of Physical Geography, Stockholm University.

Ashley GM, Mworia JM, Muasya AM, Owen RB, Driese SG, Hover VC, Renaut RW, Goman MF, Mathai S, Blatt SH. (2004) Sedimentation and recent history of a freshwater wetland in a semi-arid environment: Loboi Swamp, Kenya, East Africa. Sedimentology 51:1301-1321.

Ayenew T. (2002) Recent changes in the level of Lake Abiyata, central main Ethiopian Rift. Hydrological Sciences Journal 47:493-503.

Bayon G, Dennielou, B., Etoubleau, J., Ponzevera, E., Toucanne, S., Bermell, S. (2012) Intensifying Weathering and Land Use in Iron Age Central Africa. Science 335:1219-1222.

Becht R, Harper DM. (2002) Towards an understanding of human impact upon the hydrology of Lake Naivasha, Kenya. Hydrobiologia 488:1-11.

Bertaux J, Schwartz D, Vincens A, Sifeddine A, Elenga H, Mansour M, Mariotti A, Fournier M, Martin L, Wirrmann D, Servant M. (2000) Enregistrement de la phase sèche d'Afrique Centrale vers 3000 ans BP par la spectrométrie IR dans les lacs Sinnda et Kitina (Sud-Congo). In: Servant M, Servant-Vildary S (eds), Dynamique à long terme des écosystèmes forestiers intertropicaux. IRD/UNESCO/MAB/CNRS, Paris, France, pp. 43-49.

Bessems I, Verschuren D, Russell JM, Hus J, Mees F, Cumming BF. (2008) Palaeolinmological evidence for widespread late 18th century drought across equatorial East Africa. Palaeogeography Palaeoclimatology Palaeoecology 259.

Bloszies C, Forman SL. (2015) Potential relation between equatorial sea surface temperatures and historic water level variability for Lake Turkana, Kenya. Journal of Hydrology 520:489-501.

Braconnot P, Joussaume S, de Noblet N, Ramstein G. (2000) Mid-Holocene and Last Glacial Maximum African monsoon changes as simulated within the Paleoclimate Modelling Intercomparison Project. Global and Planetary Change 26:51-66.

Brooks GE. (2006) Cabo Verde: Gulag of the South Atlantic: Racism, fishing prohibitions, and famines. History in Africa 33:101-135.

Brown ET, Johnson TC. (2005) Coherence between tropical East African and South American records of the Little Ice Age. Geochem Geophys Geosyst 6:Q12005.

Buckles LK, Verschuren D, Weijers JWH, Cocquyt C, Blaauw M, Sinninghe Damsté JS. (2016) Interannual and (multi)-decadal variability in the sedimentary BIT index of Lake Challa, East Africa, over the past 2200 years: assessment of the precipitation proxy. Climate of the Past 12:1243-1262.

Burton RF. (1860) The Lake Regions of Central Africa, A Picture of Exploration. Longman, Green, Longman and Roberts, London.

Butzer KW. (1971) Recent history of an Ethiopian delt: the Omo River and the level of Lake Rudolf. Departmentt of Geography Research Paper. University of Chicago.

Camberlin P, Janicot S, Poccard I. (2001) Seasonality and atmospheric dynamics of the teleconnection between African rainfall and tropical sea-surface temperature: Atlantic vs. ENSO. International Journal of Climatology 21:973-1005.

Camberlin P, Okoola RE. (2003) The onset and cessation of the "long rains" in eastern Africa and their interannual variability. Theoretical and Applied Climatology 75:43-54.

Castaneda IS, Werne JP, Johnson TC. (2007) Wet and arid phases in the southeast African tropics since the Last Glacial Maximum. Geology 35:823-826.

Chase BM, Meadows ME. (2007) Late Quaternary dynamics of southern Africa's winter rainfall zone. Earth-Science Reviews 84:103-138.

Chase BM, Meadows ME, Scott L, Thomas DSG, Marais E, Sealy J, Reimer PJ. (2009) A record of rapid Holocene climate change preserved in hyrax middens from southwestern Africa. Geology 37:703-706.

Chase BM, Meadows ME, Carr AS, Reimer PJ. (2010) Evidence for progressive Holocene aridification in southern Africa recorded in Namibian hyrax middens: implications for African Monsoon dynamics and the "African Humid Period''. Quaternary Research 74:36-45.

Chase BM, Quick LJ, Meadows ME, Scott L, Thomas DSG, Reimer PJ. (2011) Late glacial interhemispheric climate dynamics revealed in South African hyrax middens. Geology 39:19-22.

Chase BM, Scott L, Meadows ME, Gil-Romera G, Boom A, Carr AS, Reimer PJ, Truc L, Valsecchi V, Quick LJ. (2012) Rock hyrax middens: a palaeoenvironmental archive for southern African drylands. Quaternary Science Reviews 56:107-125.

Chase BM, Boom A, Carr AS, Meadows ME, Reimer PJ. (2013) Holocene climate change in southernmost South Africa: rock hyrax middens record shifts in the southern westerlies. Quaternary Science Reviews 82:199-205.

Chase BM, Boom A, Carr AS, Carre M, Chevalier M, Meadows ME, Pedro JB, Stager JC, Reimer PJ. (2015a) Evolving southwest African response to abrupt deglacial North Atlantic climate change events. Quaternary Science Reviews 121:132-136.

Chase BM, Lim S, Chevalier M, Boom A, Carr AS, Meadows ME, Reimer PJ. (2015b) Influence of tropical easterlies in southern Africa's winter rainfall zone during the Holocene. Quaternary Science Reviews 107:138-148.

Chevalier M, Chase BM. (2015) Southeast African records reveal a coherent shift from high- to low-latitude forcing mechanisms along the east African margin across last glacial-interglacial transition. Quaternary Science Reviews 125:117-130.

Claussen M, Kubatzki C, Brovkin V, Ganopolski A, Hoelzmann P, Pachur HJ. (1999) Simulation of an abrupt change in Saharan vegetation in the mid-Holocene. Geophysical Research Letters 26:2037-2040.

Cobb KM, Charles CD, Cheng H, Edwards RL. (2003) El Nino/Southern Oscillation and tropical Pacific climate during the last millennium. Nature 424:271-276.

Cockcroft MJ, Wilkinson MJ, Tyson PD. (1987) The application of a present-day climatic model to the late Quaternary in southern Africa. Climatic Change 10:161-181.

Cockroft MJ, Wilkinson MJ, Tyson PD. (1988) A palaeoclimatic model for the late Quaternary in southern Africa. Palaeoecology of Africa 19:279-282.

Cohen AL, Parkington JE, Brundrit GB, van der Merwe NJ. (1992) A Holocene marine climate record in mollusc shells from the Southwest African coast. Quaternary Research 38:379-385.

Cohen AS, Talbot MR, Awramik SM, Dettman DL, Abell P. (1997) Lake level and paleoenvironmental history of Lake Tanganyika, Africa, as inferred from late Holocene and modern stromatolites. Geological Society of America Bulletin 109.

Collins JA, Schefuß E, Heslop D, Mulitza S, Prange M, Zabel M, Tjallingii R, Dokken TM, Huang E, Mackensen A, Schulz M, Tian J, Zarriess M, Wefer G. (2011) Interhemispheric symmetry of the tropical African rainbelt over the past 23,000 years. Nature Geoscience 4:42-45.

Conway D. (2002) Extreme rainfall events and lake level changes in East Africa: recent events and historical precedents. In: Odada E, Olago D (eds), The East African Great Lakes: limnology, palaeolimnology and biodiversity. Springer, The Netherlands, pp. 63-92.

Cook ER, Esper J, D'Arrigo RD. (2004) Extra-tropical Northern Hemisphere land temperature variability over the past 1000 years. Quaternary Science Reviews 23:2063-2074.

Cremaschi M, Pelfini M, Santilli M. (2006) Cupressus dupreziana: a dendroclimatic record for the middle-late Holocene in the central Sahara. The Holocene 16:293-303.

De Cort G, Bessems I, Keppens E, Mees F, Cumming B, Verschuren D. (2013) Late-Holocene and recent hydroclimatic variability in the central Kenya Rift Valley: The sediment record of hypersaline lakes Bogoria, Nakuru and Elementeita. Palaeogeography Palaeoclimatology Palaeoecology 388:69-80.

Dias J. (1981) Famine and disease in the history of Angola c. 1830-1930. Journal of African History 22:349-378.

Driese SG, Ashley GM, Li ZH, Hover VC, Owen RB. (2004) Possible Late Holocene equatorial palaeoclimate record based upon soils spanning the Medieval Warm Period and Little Ice Age, Loboi Plain, Kenya. Palaeogeography Palaeoclimatology Palaeoecology 213:231-250.

Dunbar RB, Cole JE. (1999) Annual records of tropical systems (ARTS). PAGES Workshop Report.

Dunwiddie PW, LaMarche VC. (1980) A climatically responsive tree-ring record from Widdringtonia cedarbergensis, Cape Province, South Africa. Nature 286:796-797.

Ekblom A, Gillson L, Risberg J, Holmgren K, Chidoub Z. (2012) Rainfall variability and vegetation dynamics of the lower Limpopo Valley, Southern Africa, 500 AD to present. Palaeogeography, Palaeoclimatology, Palaeoecology 363–364:69-78.

Farmer EC, deMenocal PB, Marchitto TM. (2005) Holocene and deglacial ocean temperature variability in the Benguela upwelling region: implications for low-latitude atmospheric circulation. Paleoceanography 20:doi:10.1029/2004PA001049.

Fleitmann D, Dunbar RB, McCulloch M, Mudelsee M, Vuille M, McClanahan TR, Cole JE, Eggins S. (2007) East African soil erosion recorded in a 300 year old coral colony from Kenya. Geophysical Research Letters.

Foerster V, Junginger A, Langkamp O, Gebru T, Asrat A, Umer M, Lamb HF, Wennrich V, Rethemeyer J, Nowaczyk N, Trauth MH, Schaebitz F. (2012) Climatic change recorded in the sediments of the Chew Bahir basin, southern Ethiopia, during the last 45,000 years. Quaternary International 274:25-37.

Fraedrich K, Jiang JM, Gerstengarbe FW, Werner PC. (1997) Multiscale detection of abrupt climate changes: application to River Nile flood levels. International Journal of Climatology 17:1301-1315.

Funk C, Dettinger MD, Michaelsen JC, Verdin JP, Brown ME, Barlow M, Hoell A. (2008) Warming of the Indian Ocean threatens eastern and southern African food security but could be mitigated by agricultural development. Proceedings of the National Academy of Sciences of the United States of America 105:11081-11086.

Funk C, Michaelsen J, Marshall M. (2012) Mapping recent decadal climate variations in precipitation and temperature across eastern Africa and the Sahel. In: Wardlow B, Anderson M, Verdin J (eds), Remote Sensing of Drought: Innovative Monitoring Approaches, Cambridge, pp. 331–358.

Gasse F. (1977) Evolution of Lake Abhe (Ethiopia and Tfai), from 70,000 Bp. Nature 265:42-45.

Gasse F. (2000) Hydrological changes in the African tropics since the Last Glacial Maximum. Quaternary Science Reviews 19:189-211.

Gasse F, Van Campo E. (1994) Abrupt post-glacial climate events in West Asia and North Africa monsoon domains. Earth and Planetary Science Letters 126:435-456.

Giannini A, Saravanan R, Chang P. (2003) Oceanic forcing of Sahel rainfall on interannual to interdecadal time scales. Science 302:1027-1030.

Goddard L, Graham NE. (1999) Importance of the Indian Ocean for simulating rainfall anomalies over eastern and southern Africa. J Geophys Res 104:19099-19116.

Halfman JD, Johnson TC, Finney BP. (1994) New AMS dates, stratigraphic correlations and decadal climatic cycles for the past 4-ka at Lake Turkana, Kenya. Palaeogeography Palaeoclimatology Palaeoecology 111:83-98.

Hannaford MJ, Jones JM, Bigg GR. (2015) Early-nineteenth-century southern African precipitation reconstructions from ships' logbooks. The Holocene 25:379-390.

Hannaford MJ, Nash DJ. (2016) Climate, history, society over the last millennium in southeast Africa. WIREs Climate Change.

Hartwig GW. (1979) Demographic considerations in East Africa during the late nineteenth century. International Journal of African Historical Studies 4:653-672.

Hassan FA. (2007) Extreme Nile floods and famines in Medieval Egypt (AD 930-1500) and their climatic implications. Quaternary International 173-174:101-112.

Hastenrath S, Nicklis A, Greischar L. (1993) Atmospheric-hydrospheric mechanisms of climate anomalies in the western equatorial Indian Ocean. Journal of Geophysical Research-Oceans 98:20219-20235.

Haug GH, Hughen KA, Sigman DM, Peterson LC, Röhl U. (2001) Southward migration of the Intertropical Convergence Zone through the Holocene. Science 293:1304-1308.

Henke LMK, Lambert FH, Charman DJ. (2015) Was the Little Ice Age more or less El Niño-like than the Mediaeval Climate Anomaly? Evidence from hydrological and temperature proxy data. Climate of the Past Discussions 11:5549-5604.

Hoelzmann P, Keding B, Berke H, Kropelin S, Kruse HJ. (2001) Environmental change and archaeology: lake evolution and human occupation in the Eastern Sahara during the Holocene. Palaeogeography Palaeoclimatology Palaeoecology 169:193-217.

Holmes JA, Allen MJ, Street-Perrott FA, Ivanovich M, Perrott RA, Waller MP. (1999) Late Holocene palaeolimnology of Bal Lake, Northern Nigeria, a multidisciplinary study. Palaeogeography Palaeoclimatology Palaeoecology 148:169-185.

Holmgren K, Karlen W, Lauritzen SE, Lee-Thorp JA, Partridge TC, Piketh S, Repinski P, Stevenson C, Svanered O, Tyson PD. (1999) A 3000-year high-resolution stalagmite-based record of palaeoclimate for northeastern South Africa. Holocene 9:295-309.

Holmgren K, Lee-Thorp JA, Cooper GRJ, Lundblad K, Partridge TC, Scott L, Sithaldeen R, Talma AS, Tyson PD. (2003) Persistent millennial-scale climatic variability over the past 25,000 years in Southern Africa. Quaternary Science Reviews 22:2311-2326.

Hulme M, Doherty R, Ngara T, New M, Lister D. (2001) African climate change:1900 - 2100. Climate Research 17:145-168.

Iliffe J. (1979) A modern history of Tanganyika. Cambridge University Press.

Johnson TC, Barry SL, Chan Y, Wilkinson P. (2001) Decadal record of climate variability spanning the past 700 yr in the Southern Tropics of East Africa. Geology 29:83-86.

Jones PD, Osborn TJ, Briffa KR. (2001) The evolution of climate over the last millennium. Science 292:662-667.

Jones PD, Mann ME. (2004) Climate over past millennia. Reviews of Geophysics 42.

Joussaume S, Taylor KE, Braconnot P, Mitchell JFB, Kutzbach JE, Harrison SP, Prentice IC, Broccoli AJ, Abe-Ouchi A, Bartlein PJ, Bonfils C, Dong B, Guiot J, Herterich K, Hewitt CD, Jolly D, Kim JW, Kislov A, Kitoh A, Loutre MF, Masson V, McAvaney B, McFarlane N, de Noblet N, Peltier WR, Peterschmitt JY, Pollard D, Rind D, Royer JF, Schlesinger ME, Syktus J, Thompson S, Valdes P, Vettoretti G, Webb RS, Wyputta U. (1999) Monsoon changes for 6000 years ago: results of 18 simulations from the Paleoclimate Modeling Intercomparison Project (PMIP). Geophysical Research Letters 26:859-862.

Kelso C, Vogel CH. (2007) The climate of Namaqualand in the nineteenth century. Climatic Change 83:257-380.

Kiage LM, Liu K-B. (2009) Palynological evidence of climate change and land degradation in the Lake Baringo area, Kenya, East Africa, since AD 1650. Palaeogeography Palaeoclimatology Palaeoecology 279.

Kondrashov D, Feliks Y, Ghil M. (2005) Oscillatory modes of extended Nile River records (AD 622-1922). Geophysical Research Letters 32.

Konecky B, Russell J, Huang Y, Vuille M, Cohen L, Street-Perrott FA. (2014) Impact of monsoons, temperature, and CO2 on the rainfall and ecosystems of Mt. Kenya during the Common Era. Palaeogeography Palaeoclimatology Palaeoecology 396:17-25.

Krapf JL. (1860) Travels, Researches and Missionary Labours, During an Eighteen Years' Residence in Eastern Africa. Trübner and Co., London.

Kröpelin S, Verschuren D, Lezine AM, Eggermont H, Cocquyt C, Francus P, Cazet JP, Fagot M, Rumes B, Russell JM, Darius F, Conley DJ, Schuster M, von Suchodoletz H, Engstrom DR. (2008) Climate-driven ecosystem succession in the Sahara: the past 6000 years. Science 320:765-768.

Kutzbach JE. (1981) Monsoon climate of the early Holocene: climate experiment with the Earth's orbital parameters for 9000 years ago. Science 214:59-61.

Kutzbach JE, Otto-Bliesner B. (1982) The sensitivity of the African-Asian monsoon climate to orbital parameter changes for 9000 years BP in a low-resolution general circulation model. Journal of Atmospheric Science 39:1177-1188.

Kutzbach JE, Liu Z. (1997) Response of the African Monsoon to orbital forcing and ocean feedbacks in the middle Holocene. Science 278:440-443.

Lamb HF, Darbyshire L, Verschuren D. (2003) Vegetation response to rainfall variation and human impact in central Kenya during the past 1100 years. Holocene 13:285-292.

Lamb HF, Leng MJ, Telford RJ, Ayenew T, Umer M. (2007) Oxygen and carbon isotope, composition of authigenic carbonate from an Ethiopian lake: a climate record of the last 2000 years. The Holocene 17.

Lee-Thorp JA, Hohngren K, Lauritzen S-E, Linge H, Moberg A, Partridge TC, Stevenson C, Tyson PD. (2001) Rapid climate shifts in the southern African interior throughout the mid- to late Holocene. Geophysical Research Letters 28:4507-4510.

Legesse D, Gasse F, Radakovitch O, Vallet-Coulomb C, Bonnefille R, Verschuren D, Gibert E, Barker P. (2002) Environmental changes in a tropical lake (Lake Abiyata, Ethiopia) during recent centuries. Palaeogeography, Palaeoclimatology, Palaeoecology 187:233-258.

Levin NE, Zipser EJ, Cerling TE. (2009) Isotopic composition of waters from Ethiopia and Kenya: Insights into moisture sources for eastern Africa. Journal of Geophysical Research-Atmospheres 114.

Lindesay JA, Harrison MSJ, Haffner MP. (1986) The Southern Oscillation and South African rainfall. South African Journal of Science 82:196-197.

Liu Z, Harrison SP, Otto-Bliesner B. (2004) Global monsoons in the mid-Holocene and oceanic feedback. Climate Dynamics 22:157-182.

Lorrey A. (2014) Australasian climate over the last 2,000 years: The PAGES Aus2k Synthesis. Journal of Climate Special Collections.

Losada T, Rodriguez-Fonseca B, Janicot S, Gervois S, Chauvin F, Ruti P. (2010) A multi-model approach to the Atlantic Equatorial mode: impact on the West African monsoon. Climate Dynamics 35:29-43.

Lézine A-M, Hély C, Grenier C, Braconnot P, Krinner G. (2011) Sahara and Sahel vulnerability to climate changes, lessons from paleohydrological data. Quaternary Science Reviews 30:3001-3012.

Lézine A-M, Assi-Kaudjhis, C. Roche, E., Vincens, A., Achoundong, G. (2013) Towards an understanding of West African montane forest response to climate change. Journal of Biogeography 40:183–196.

Machado MJ, Perez-Gonzalez A, Benito G. (1998) Paleoenvironmental changes during the last 4000 yr in the Tigray, northern Ethiopia. Quaternary Research 49:312-321.

Maley J. (1973) Les variations climatiques dans le bassin du Tchad durant le dernier Millenaire, essai d'interpretation climatique de l'Holocene. C Acad Sci Paris 276:1673-1675.

Maley J. (1976) Mécanisme des changements climatiques aux basses latitudes. Paleogeography, Paleoclimatology, Palaeoecology 14:193-227.

Maley J. (1981) Etudes palynologiques dans le basin du Tchad et paleoclimatologie de l'Afrique nord-tropicale de 30.000 ans l'epoque actuelle. Trav Doc ORSTOM 129:1-586.

Maley J. (1989) L'importance de la tradition orale et des donnees historiques pour la reconstitution paleoclimatique du dernier millenaire sur l'Afrique nord-tropicale. Sud Sahara, Sahel Nord, Centre Culturel Francais d'Abijan, pp. 53-57.

Maley J. (1993) Chronologie calendaire des principales fluctuations du lake Tchad au cours du dernier millenaire I. In: Barreteau D, Graffenreid CV (eds), Datation et Chronologie dans le Bassin du Lac Tchad. ORSTOM, Paris, pp. 161-163.

Maley J, Giresse P, Doumenge C, Favier C. (2012) Comment on “Intensifying Weathering and Land Use in Iron Age Central Africa”. Science 337.

Mann ME, Zhang Z, Hughes MK, Bradley RS, Miller SK, Rutherford S, Ni F. (2008) Proxy-based reconstructions of hemispheric and global surface temperature variations over the past two millennia. Proceedings of the National Academy of Sciences of the United States of America 105.

Mapande AT, Reason CJC. (2005) Links between rainfall variability on intraseasonal and interannual scales over western Tanzania and regional circulation and SST patterns. Meteorology and Atmospheric Physics 89:215-234.

Marshall MH, Lamb HF, Davies SJ, Leng MJ, Kubsa Z, Umer M, Bryant C. (2009) Climatic change in northern Ethiopia during the past 17,000 years: a diatom and stable isotope record from Lake Ashenge. Palaeogeography, Palaeoclimatology, Palaeoecology 279:114-127.

Masson-Delmotte V, Schulz M, Abe-Ouchi A, Beer J, Ganopolski A, González Rouco JF, Jansen E, Lambeck K, Luterbacher J, Naish T, Osborn T, Otto-Bliesner B, Quinn T, Ramesh R, Rojas M, Shao X, Timmermann A. (2013) Information from Paleoclimate Archives. In: Stocker TF, Qin D, Plattner

GK, Tignor M, Allen SK, Boschung J, Nauels A, Xia Y, Bex V, Midgley PM (eds), Climate Change 2013: The Physical Science Basis Contribution of Working Group I to the Fifth Assessment Report of the Intergovernmental Panel on Climate Change. Cambridge University Press, Cambridge, pp. 383-464.

Matthews JA, Briffa KR. (2005) The 'Little Ice Age': re-evaluation of an evolving concept. Geografiska Annaler: Series A, Physical Geography 87:17-36.

Meadows ME, Chase BM, Seliane M. (2010) Holocene palaeoenvironments of the Cederberg and Swartruggens mountains, Western Cape, South Africa: pollen and stable isotope evidence from hyrax dung middens. Journal of Arid Environments 74:786-793.

Mekonnen MM, Hoekstra AY, Becht R. (2012) Mitigating the Water Footprint of Export Cut Flowers from the Lake Naivasha Basin, Kenya. Water Resources Management 26:3725-3742.

Miller J. (1982) The Significance of Drought, Disease and Famine in the Agriculturally Marginal Zones of West-Central Africa. Journal of African History 23:17-61.

Mills K, Ryves DB, Anderson NJ, Bryant CL, Tyler JJ. (2014) Expressions of climate perturbations in western Ugandan crater lake sediment records during the last 1000 years. Climate of the Past 10:1581-1601.

Moberg A, Sonechkin DM, Holmgren K, Datsenko NM, Karlen W. (2005) Highly variable Northern Hemisphere temperatures reconstructed from low- and high-resolution proxy data. Nature 433:613-617.

Mulitza S, Heslop D, Pittauerova D, Fischer HW, Meyer I, Stuut JB, Zabel M, Mollenhauer G, Collins JA, Kuhnert H, Schulz M. (2010) Increase in African dust flux at the onset of commercial agriculture in the Sahel region. Nature 466:226-228.

Nash DJ, Endfield GH. (2002) A 19th century climate chronology for the Kalahari region of central southern Africa derived from missionary correspondence. International Journal of Climatology 22:821-841.

Nash DJ, Endfield GH. (2008) "Splendid rains have fallen": links between El Nino and rainfall variability in the Kalahari, 1840-1900. Climatic Change 86:257-290.

Nash DJ, Grab SW. (2010) "A sky of brass and burning winds": documentary evidence of rainfall variability in the Kingdom of Lesotho, Southern Africa, 1824–1900. Climatic Change 101:617-653.

Nash DJ, Adamson GCD. (2014) Recent advances in the historical climatology of the tropics and subtropics. Bulletin of the American Meteorological Society 95:131-146.

Nash DJ, Pribyl K, Klein J, Neukom R, Endfield GH, Adamson GCD, Kniveton DR. (2016) Seasonal rainfall variability in southeast Africa during the nineteenth century reconstructed from documentary sources. Climatic Change 134:605-619.

Neff U. (2001) Strong coherence between solar variability and the monsoon in Oman between 9 and 6 kyr ago. Nature 411:290-293.

Neukom R, Luterbacher J, Villalba R, Kuttel M, Frank D, Jones PD, Grosjean M, Esper J, Lopez L, Wanner H. (2010) Multi-centennial summer and winter precipitation variability in southern South America. Geophysical Research Letters 37.

Neukom R, Gergis J. (2012) Southern Hemisphere high-resolution palaeoclimate records of the last 2000 years. Holocene 22:501-524.

Neukom R, Nash DJ, Endfield GH, Grab SW, Grove CA, Kelso C, Vogel CH, Zinke J. (2014) Multi-proxy summer and winter precipitation reconstruction for southern Africa over the last 200 years. Climate Dynamics 42:2713-2716.

Neumann K, Eggert MKH, Oslisly R, Clist B, Denham T, de Maret P, Ozainne S, Hildebrand E, Bostoen K, Salzmann U, Schwartz D, Eichhorn B, Tchiengué B, Höhn A. (2012) Comment on "Intensifying Weathering and Land Use in Iron Age Central Africa". Science 337:1040.

Ngomanda A, Jolly D, Bentaleb I, Chepstow-Lusty A, Makaya M, Maley J, Fontugne M, Oslisly R, Rabenkogo N. (2007) Lowland rainforest response to hydrological changes during the last 1500 years in Gabon, Western Equatorial Africa. Quaternary Research 67:411-425.

Nguetsop VF, Bentaleb I, Favier C, Martin C, Bietrix S, Giresse P, Servant-Vildary S, Servant M. (2011) Past environmental and climatic changes during the last 7200 cal yr BP in Adamawa plateau (Northern-Cameroun) based on fossil diatoms and sedimentary carbon isotopic records from Lake Mbalang. Climate of the Past 7:1371-1393.

Nguetsop VF, Servant-Vildary S, Servant M, Roux M. (2010) Long and short-time scale climatic variability in the last 5500 years in Africa according to modern and fossil diatoms from Lake Ossa (Western Cameroon). Global and Planetary Change 72:356-367.

Nguetsop VF, Bentaleb I, Favier C, Bietrix S, Martin C, Servant-Vildary S, Servant M. (2013) A late Holocene palaeoenvironmental record from Lake Tizong, northern Cameroon using diatom and carbon stable isotope analyses. Quaternary Science Reviews 72:49-62.

Nicholson SE. (1979) The methodology of historical climate reconstruction and its application to Africa. Journal of African History 20:31-49.

Nicholson SE. (1980) Saharan climates in historic times. In: Williams MAJFH (ed), The Sahara and the Nile. Balkema, Rotterdam, pp. 173-200.

Nicholson SE. (1981) The Historical Climatology of Africa. In: Wigley TML, Ingram MJ, Farmer G (eds), Climate and History. Cambridge University Press, Cambridge, pp. 249-270.

Nicholson SE. (1996) Environmental Change within the Historical Period. In: Goudie ASAWMaOA (ed), The Physical Geography of Africa. Oxford University Press, Oxford, pp. 60-75.

Nicholson SE. (1999) Historical and modern fluctuations of Lakes Tanganyika and Rukwa and their relationship to rainfall variability. Climatic Change 41.

Nicholson SE. (2000) The nature of rainfall variability over Africa on time scales of decades to millenia. Global and Planetary Change 26:137-158.

Nicholson SE. (2001) Climatic and environmental change in Africa during the last two centuries. Climate Research 17:123-144.

Nicholson SE. (2008) The intensity, location and structure of the tropical rainbelt over west Africa as factors in interannual variability. International Journal of Climatology 28:1775-1785.

Nicholson SE. (2009) On the factors modulating the intensity of the tropical rainbelt over West Africa. International Journal of Climatology 29:673-689.

Nicholson SE. (2011) Dryland Climatology. Cambridge University Press, Cambridge.

Nicholson SE. (2014) Spatial teleconnections in African rainfall: A comparison of 19th and 20th century patterns. Holocene 24:1840-1848.

Nicholson SE, Kim J, Hoopingarner J. (1988) Atlas of African Rainfall and its Interannual Variability. Department of Meteorology, Florida State University, Tallahassee, Florida.

Nicholson SE, Kim E. (1997) The relationship of the El Nino Southern Oscillation to African rainfall. International Journal of Climatology 17:117-135.

Nicholson SE, Selato JC. (2000) The influence of La Nina on African rainfall. International Journal of Climatology 20:1761-1776.

Nicholson SE, Yin XG. (2001) Rainfall conditions in equatorial East Africa during the nineteenth century as inferred from the record of Lake Victoria. Climatic Change 48:387-398.

Nicholson SE, Webster PJ. (2007) A physical basis for the interannual variability of rainfall in the Sahel. Quarterly Journal of the Royal Meteorological Society 133:2065-2084.

Nicholson SE, Dezfuli AK, Klotter D. (2012a) A two-century precipitation dataset for the continent of Africa. Bulletin of the American Meteorological Society 93:1219-1231.

Nicholson SE, Klotter D, Dezfuli AK. (2012b) Spatial reconstruction of semi-quantitative precipitation fields over Africa during the nineteenth century from documentary evidence and gauge data. Quaternary Research 78:13-23.

Nicholson SE, Nash DJ, Chase BM, Grab SW, Shanahan TM, Verschuren D, Asrat A, Lézine A-M, Umer M. (2013) Temperature variability over Africa during the last 2000 years. The Holocene 23:1085-1094.

Norrgård S. (2015) Practising historical climatology in West Africa: a climatic periodisation 1750-1800. Climatic Change 129:131-143.

Ogallo LJ, Janowiak JE, Halpert MS. (1988) Teleconnection between seasonal rainfall over East Africa and global sea-surface temperature anomalies. Journal of the Meteorological Society of Japan 66:807-822.

Okoola RE. (1999) A diagnostic study of the eastern Africa monsoon circulation during the northern hemisphere spring season. International Journal of Climatology 19:143-168.

Onywere SM, Shisanya CA, Obando JA, Ndubi AO, Masiga D, Irura Z, Mariita N, Maragia HO. (2013) Geospatial extent of 2011-2013 flooding from the Eastern African Rift Valley lakes in Kenya and its implication on the ecosystem. The soda lakes of Kenya: their current conservation status and management, Naivasha, Kenya.

Owen RB, Crossley R, Johnson TC, Tweddle D, Kornfield I, Davison S, Eccles DH, Engstrom DE. (1990) Major low-levels of Lake Malawi and their implications for speciation rates in cichlid fishes. Proceedings of the Royal Society Series B-Biological Sciences 240:519-553.

Pankhurst R. (1966) The great Ethiopian famine of 1888-1892: A new assessment. Journal of the history of medicine and allied sciences 21:95-124.

Past Global Changes (PAGES) 2k Consortium (2013) Continental-scale temperature variability during the past two millennia. Nature Geoscience 6:339-346.

Pohl B, Camberlin P. (2011) Intraseasonal and interannual zonal circulations over the Equatorial Indian Ocean. Theoretical and Applied Climatology 104:175-191.

Preston-Whyte RA, Tyson PD. (1993) The Atmosphere and Weather of Southern Africa. Oxford University Press, Cape Town.

Reason CJC, Mulenga H. (1999) Relationships between South African rainfall and SST anomalies in the southwest Indian Ocean. International Journal of Climatology 19:1651-1673.

Reason CJC, Jagadheesha D. (2005) Relationships between South Atlantic SST variability and atmospheric circulation over the South African region during austral winter. Journal of Climate:3339-3355.

Renssen H, Brovkin V, Fichefet T, Goosse H. (2006) Simulation of the Holocene climate evolution in Northern Africa: the termination of the African Humid Period. Quaternary International Impact of rapid environmental changes on humans and ecosystems 150:95-102.

Repinski P, Holmgren K, Lauritzen SE, Lee-Thorp JA. (1999) A late Holocene climate record from a stalagmite, Cold Air Cave, Northern Province, South Africa. Palaeogeography, Palaeoclimatology, Palaeoecology 150:269-277.

Russell JM, Johnson TC. (2005) A high resolution geochemical record from Lake Edward, Uganda-Congo, and the timing and causes of tropical African drought during the late Holocene. Quaternary Science Reviews 24:1375-1389.

Russell JM, Johnson TC. (2007) Little Ice Age drought in equatorial Africa: intertropical Convergence Zone migrations and El Nino-Southern Oscillation variability. Geology 35:21-24.

Russell JM, Verschuren D, Eggermont H. (2007) Spatial complexity of 'Little Ice Age' climate in East Africa: sedimentary records from two crater lake basins in western Uganda. Holocene 17:183-193.

Saji NH, Goswami BN, Vinayachandran PN, Yamagata T. (1999) A dipole mode in the tropical Indian Ocean. Nature 401:360-363.

Schefuß E, Kuhlmann H, Mollenhauer G, Prange M, Patzold J. (2011) Forcing of wet phases in southeast Africa over the past 17,000 years. Nature 480:509-512.

Schneider T, Bischoff T, Haug GH. (2014) Migrations and dynamics of the intertropical convergence zone. Nature 513:45-53.

Scott L. (1982) A late Quaternary pollen record from the Transvaal bushveld, South Africa. Quaternary Research 17:339-370.

Scott L. (1996) Palynology of hyrax middens: 2000 years of palaeoenvironmental history in Namibia. Quaternary International 33:73-79.

Scott L. (1999) Vegetation history and climate in the Savanna biome South Africa since 190,000 ka: a comparison of pollen data from the Tswaing Crater (the Pretoria Saltpan) and Wonderkrater. Quaternary International 57-8:215-223.

Sene KJ, Plinston DT. (1994) A review and update of the hydrology of Lake Victoria in East Africa. Hydrological Sciences Journal 39:47-63.

Shanahan TM, Overpeck JT, Anchukaitis KJ, Beck JW, Cole JE, Dettman DL, Peck J, Scholz CA, J.W. K. (2009) Atlantic forcing of persistent drought in West Africa. Science 324:377-380.

Shanahan TM, McKay NP, Hughen KA, Overpeck JT, Otto-Bliesner B, Heil CW, King J, Scholz CA, Peck J. (2015) The time-transgressive termination of the African Humid Period. Nature Geoscience 8:140-144.

Shongwe ME, van Oldenborgh GJ, van den Hurk B, van Aalst M. (2011) Projected Changes in Mean and Extreme Precipitation in Africa under Global Warming. Part II: East Africa. Journal of Climate 24:3718-3733.

Sletten HR, Railsback LB, Liang F, Brook GA, Marais E, Hardt BF, Cheng H, Edwards RL. (2013) A petrographic and geochemical record of climate change over the last 4600 years from a northern Namibia stalagmite, with evidence of abruptly wetter climate at the beginning of southern Africa's Iron Age. Palaeogeography, Palaeoclimatology, Palaeoecology 376:149-162.

Sonzogni C, Bard E, Rostek F. (1998) Tropical sea-surface temperatures during the last glacial period: a view based on alkenones in Indian Ocean sediments. Quaternary Science Reviews 17:1185-1201.

Stager JC, Ryves D, Cumming BF, Meeker LD, Beer J. (2005) Solar variability and the levels of Lake Victoria, East Africa, during the last millenium. Journal of Paleolimnology 33:243-251.

Stager JC, Cocquyt C, Bonnefille R, Weyhenmeyer C, Bowerman N. (2009) A late Holocene paleoclimatic history of Lake Tanganyika, East Africa. Quaternary Research 72:47-56.

Stager JC, Mayewski PA, White J, Chase BM, Neumann FH, Meadows ME, King CD, Dixon DA. (2012) Precipitation variability in the winter rainfall zone of South Africa during the last 1400 yr linked to the austral westerlies. Clim Past 8:877-887.

Stevenson C, Lee-Thorp JA, Holmgren K. (1999) A 3000-year isotopic record from a stalagmite in Cold Air Cave, Makapansgat Valley, Northern Province. South African Journal of Science 95:46-48.

Stockhall S. (2010) A wetter Botswana? Peolwane:22-24.

Street-Perrott FA, Perrott RA. (1990) Abrupt climate fluctuations in the tropics: the influence of Atlantic Ocean circulation. Nature 343:607-612.

Street-Perrott FA, Homes JA, Waller MP, Allen MJ, Barber NGH, Fothergill PA, Harkness DD, Ivanovich M, Kroon D, Perrott RA. (2000) Drought and dust deposition in the West African Sahel: a 5500-year record from Kajemarum Oasis, northeastern Nigeria. The Holocene 10:293-302.

Sundqvist HS, Holmgren K, Fohlmeister J, Zhang Q, Bar-Matthews M, Spötl C, Körnich H. (2013) Evidence of a large cooling between 1690 and 1740 AD in southern Africa. Scientific Reports 3.

Sutcliffe JV, Parks YP. (1999) The East African lakes below Lake Victoria. The hydrology of the Nile. International Association of Hydrological Sciences Special Publication No. 5, pp. 37-56.

Talma AS, Vogel JC. (1992) Late Quaternary paleotemperatures derived from a speleothem from Cango Caves, Cape Province, South Africa. Quaternary Research 37:203-213.

Thackeray JF. (1999) Calibration of temperature indices from a late Quaternary terrestrial sequence at Wonderkrater, South Africa. Quaternary International 57-8:225-227.

Therrell MD, Stahle DW, Ries LP, Shugart HH. (2006) Tree-ring reconstructed rainfall variability in Zimbabwe. Climate Dynamics 26:677-685.

Tierney JE, Lewis SC, Cook BI, LeGrande AN, Schmidt GA. (2011a) Model, proxy and isotopic perspectives on the East African Humid Period. Earth and Planetary Science Letters 307:103-112.

Tierney JE, Russell JM, Sinninghe Damsté JS, Huang Y, Verschuren D. (2011b) Late Quaternary behavior of the East African monsoon and the importance of the Congo Air Boundary. Quaternary Science Reviews 30:798-807.

Tierney JE, deMenocal PB. (2013) Abrupt shifts in Horn of Africa hydroclimate since the Last Glacial Maximum. Science 342:843-846.

Trabucco A and Zomer RJ. (2009) Global aridity index (Global-Aridity) and global potential evapo-transpiration (Global-PET) geospatial database. CGIAR Consortium for Spatial Information, published online, available from the CGIAR-CSI GeoPortal at http://www.csi.cgiar.org.

Truc L, Chevalier M, Favier C, Cheddadi R, Meadows ME, Scott L, Carr AS, Smith GF, Chase BM. (2013) Quantification of climate change for the last 20,000 years from Wonderkrater, South Africa: Implications for the long-term dynamics of the Intertropical Convergence Zone. Palaeogeography Palaeoclimatology Palaeoecology 386:575-587.

Tyson PD. (1986) Climatic Change and Variability in Southern Africa. Oxford University Press, Cape Town.

Tyson PD, Lindesay JA. (1992) The climate of the last 2000 years in southern Africa. The Holocene 2:271-278.

Tyson PD, Preston-Whyte RA. (2000a) The Weather and Climate of Southern Africa. Oxford University Press, Cape Town.

Tyson PD, Karlen W, Holmgren K, Heiss GA. (2000b) The Little Ice Age and medieval warming in South Africa. South African Journal of Science 96:121-126.

Ummenhofer CC, Sen Gupta A, England MH, Reason CJC. (2009) Contributions of Indian Ocean sea surface temperatures to enhanced East African rainfall. Journal of Climate 22:993-1013.

Van Zinderen Bakker EM. (1976) The evolution of late Quaternary paleoclimates of Southern Africa. Palaeoecology of Africa 9:160-202.

Van Zinderen Bakker EM, Coetzee JA. (1972) A reappraisal of late Quaternary climatic evidence from tropical Africa. Palaeoecology of Africa 7:151-182.

Vellinga M, Wood RA. (2002) Global climatic impacts of a collapse of the Atlantic thermohaline circulation. Climatic Change 54:251-267.

Verschuren D. (1999a) Sedimentation controls on the preservation and time resolution of climate-proxy records from shallow fluctuating lakes. Quaternary Science Reviews 18:821-837.

Verschuren D. (1999b) Influence of depth and mixing regime on sedimentation in a small, fluctuating tropical soda lake. Limnology and Oceanography 44.

Verschuren D. (2001) Reconstructing fluctuations of a shallow East African lake during the past 1800 yrs from sediment stratigraphy in a submerged crater basin. Journal of Paleolimnology 25.

Verschuren D. (2003) Lake-based climate reconstruction in Africa: progress and challenges. Hydrobiologia 500:315-330.

Verschuren D. (2004) Decadal to century-scale climate variability in tropical Africa during the past 2000 years. In: Battarbee RW, Gasse F, Stickley C (eds), Past climate variability through Europe and Africa. Kluwer, Dordrecht, pp. 139-158.

Verschuren D, Cocquyt C, Tibby J, Roberts CN, Leavitt PR. (1999a) Long-term dynamics of algal and invertebrate communities in a small, fluctuating tropical soda lake. Limnology and Oceanography 44:1216-1231.

Verschuren D, Tibby J, Leavitt PR, Roberts CN. (1999b) The environmental history of a climate-sensitive lake in the former 'White Highlands' of central Kenya. Ambio 28:494-501.

Verschuren D, Laird KR, Cumming BF. (2000) Rainfall and drought in equatorial Africa during the past 1100 years. Nature 403:410-444.

Verschuren D, Charman D. (2008) Latitudinal linkages in late-Holocene moisture-balance variation. In: Battarbee RW, Binney HA (eds), Natural climate variability and global warming. Wiley-Blackwell, Chichester, UK.

Verschuren D, Damste JSS, Moernaut J, Kristen I, Blaauw M, Fagot M, Haug GH, Members CP. (2009) Half-precessional dynamics of monsoon rainfall near the East African Equator. Nature 462.

Verschuren D, Russell JM. (2009) Paleolimnology of African lakes: beyond the exploration phase. PAGES News 17:112-114.

Vincens A, Buchet, G., Servant, M. and ECOFIT Mbalang collaborators. (2010) Vegetation response to the "African Humid Period" termination in Central Cameroon (7° N) – new pollen insight from Lake Mbalang. Climate of the Past 6:281-294.

Vincens A, Schwartz D, Elenga H, Reynaud-Farrera I, Alexandre A, Bertaux J, Mariotti A, Martin L, Meunier J-D, Nguetsop F, Servant M, Servant-Vildary S, Wirrmann D. (1999) Forest response to climate changes in Atlantic Equatorial Africa during the last 4000 years BP and inheritance on the modern landscapes. Journal of Biogeography 26:879–885.

Vogel CH. (1989) A documentary-derived climatic chronology for South Africa, 1820–1900. Climatic Change 14:291-307.

Wang X, Auler AS, Edwards RL, Cheng H, Cristalli PS, Smart PL, Richards DA, Shen C-C. (2004) Wet periods in northeastern Brazil over the past 210 kyr linked to distant climate anomalies. 432:740-743.

Webster JB. (1979) Chronology, Migration and Drought in Interlacustrine Africa. Longman & Dalhousie University Press, London, UK.

Williams AP, Funk C. (2011) A westward extension of the warm pool leads to a westward extension of the Walker circulation, drying eastern Africa. Climate Dynamics 37:2417-2435.

Williams AP, Funk C, Michaelsen J, Rauscher SA, Robertson I, Wils THG, Koprowski M, Eshetu Z, Loader NJ. (2012) Recent summer precipitation trends in the Greater Horn of Africa and the emerging role of Indian Ocean sea surface temperature. Climate Dynamics 39:2307-2328.

Wolde-Georgis T. (1997) El Niño and Drought Early Warning in Ethiopia. Internet Journal of African Studies 2.

Wolff C, Haug GH, Timmermann A, Damste JSS, Brauer A, Sigman DM, Cane MA, Verschuren D. (2011) Reduced Interannual Rainfall Variability in East Africa During the Last Ice Age. Science 333:743-747.

Woodborne S, Hall G, Robertson I, Patrut A, Rouault M, Loader NJ, Hofmeyr M. (2015) A 1000-year carbon isotope rainfall proxy record from South African baobab trees (Adansonia digitata L.). PLoS ONE 10:e0124202.

Yang Y, Xie S-P, Wu L, Kosaka Y, Lau N-C, Vecchi GA. (2015) Seasonality and Predictability of the Indian Ocean Dipole Mode: ENSO Forcing and Internal Variability. Journal of Climate 28:8021-8036.

Zhang R, Delworth TL. (2005) Simulated tropical response to a substantial weakening of the Atlantic thermohaline circulation. Journal of Climate 18:1853-1860.

3 LATE-HOLOCENE AND RECENT HYDROCLIMATIC VARIABILITY IN THE CENTRAL KENYA RIFT VALLEY: THE SEDIMENT RECORD OF HYPERSALINE LAKES BOGORIA, NAKURU AND ELEMENTEITA

De Cort, Gijs[1,2]; Bessems, Ilse[1]; Keppens, Edward[3]; Mees, Florias[2]; Cumming, Brian[4]; Verschuren, Dirk[1]

[1]*Limnology Unit, Department of Biology, Ghent University. Ledeganckstraat 35, B-9000, Gent, Belgium.*
[2]*Department of Earth Sciences, Royal Museum for Central Africa. Leuvensesteensweg 13, B-3080 Tervuren, Belgium.*
[3]*Isotope Geology and Evolution of the Paleoenvironments Research Unit, Department of Geology, Free University of Brussels (VUB). Pleinlaan 2, B-1050, Brussel, Belgium.*
[4]*Paleoecological Environmental Assessment and Research Laboratory, Department of Biology, Queen's University. 116 Barrie Street, Kingston, Ontario K7L 3N6, Canada.*

This chapter was published in *Palaeogeography, Palaeoclimatology, Palaeoecology (2013) 388:69-80.*

The sedimentology, salt mineralogy and stable oxygen- and carbon-isotope signatures of a mid-lake sediment sequence from hypersaline Lake Bogoria in Kenya reveals marked climate-driven changes in water-column mixing regime and salinity over the past 1700 years. Combined with sedimentological data on short sediment sequences from nearby lakes Nakuru and Elementeita, this results in a preliminary reconstruction of hydroclimatic variability in the central Kenya Rift Valley since ca. AD 300. Stratigraphic analyses of bulk sediment composition, texture and magnetic susceptibility of all three cores; and smear slide, XRD and stable-isotope analyses on carbonate minerals in the Bogoria sequence allowed to define a succession of sedimentary units, corresponding to distinct phases in lake history. In the lowermost unit, four characteristic trona layers [$Na_3(HCO_3)(CO_3).2H_2O$] are attributed to predominantly dry conditions during the second half of the first millennium AD and the period equivalent to the Medieval Climate Anomaly, until the first half of the 12th century AD. Lake Bogoria was probably polymictic at that time, its surface level standing significantly lower than today. The second unit displays uniform deposition of nahcolite [$NaH(CO_3)$], indicative of a strongly stratified lake where a layer of less saline surface water (near-)permanently covers a hypersaline water mass with high pCO_2. We propose that this depositional phase reflects the rising lake level related to the transition from dry to more humid climate conditions at the onset of the Little Ice Age, as previously documented for other parts of equatorial East Africa. The third, uppermost Bogoria unit contains only sporadic depositions of magadiite ($Na_2Si_{14}O_{29}.11H_2O$) and various sodium carbonate minerals. This, together with low magnetic susceptibility, is interpreted to indicate humid Little Ice Age conditions, with highest lake level and reduced salinity around the late-15th to early-16th century AD. From the late-18th to early-19th century and again in the 1870's, the region experienced two episodes of drought more severe than any recorded in historical time. Tentative evidence for these events in the Bogoria record is not well constrained in time, but dated desiccation surfaces in the Nakuru and Elementeita records confirm their widespread nature across eastern equatorial Africa.

INTRODUCTION

Lake and swamp deposits are the most important continental archives of climate-proxy data in equatorial East Africa, and in favourable circumstances of accumulation and preservation can allow climate reconstructions at decadal or even inter-annual time scales. As regards climate variability within the last millennium, currently available proxy records (Verschuren and Charman, 2008) show that the region experienced generally drier conditions during the time window equivalent to the

Medieval Climate Anomaly (MCA, ca. 900-1300 AD), i.e. when temperate regions of the Northern Hemisphere experienced a significantly warmer temperature regime than today (e.g., Moberg et al., 2005). Whether equatorial East Africa was also warmer at that time is uncertain; the nearest unambiguous temperature reconstruction, from Lake Tanganyika in southern equatorial Africa, suggests a period of warm conditions between 1100 and 1400 AD, i.e. somewhat later than the traditional MCA chronozone. During the Little Ice Age (LIA, ca. 1300-1850 AD), when temperatures in the Northern Hemisphere were often lower than at present, climatic conditions in tropical East Africa seem to have been regionally varied. Proxy records from Lake Naivasha (Verschuren et al., 2000a), Lake Victoria (Stager et al., 2005) and Lake Challa (Wolff et al., 2011) document relatively wet conditions in easternmost equatorial Africa during both the early and main phases of the LIA (~1300-1500 and ~1500-1750 AD). In contrast, proxy records from Lake Edward (Russell and Johnson, 2007), crater lakes in western Uganda (Russell et al., 2007; Ryves et al., 2011) and Lake Tanganyika (Alin and Cohen, 2003; Stager et al., 2009) suggest that more central portions of equatorial Africa experienced prolonged drought during the main phase of the LIA, resulting in a strong zonal (broadly east-to-west) gradient in historical climate trends across East Africa. This gradient finds its likely cause in the different relative contributions of tropical Atlantic and Indian Ocean moisture sources east and west of the Congo Air Boundary (Verschuren and Charman, 2008; Tierney et al., 2011), i.e. the zone of surface flow convergence which resides over the East African plateau during Northern Hemisphere spring and summer (Nicholson, 1996). This spatially structured forcing of regional climate regimes, and further moisture-balance gradients due to the plateau's dissected topography, complicates identification of a unique anthropogenic signature in current climate trends (Williams and Funk, 2011) and handicaps the long-term climate prediction which developing economies need to strategically prepare for future climate change (Christensen et al., 2007; Hassan, 2010). Specifically, for performance testing of next-generation regional climate models it remains problematic that the number of well-dated and high-resolution climate-proxy records available from East Africa is still an order of magnitude less than the number of such records from Europe or North America. This difference does not reflect lack of attention from palaeoclimatologists and palaeolimnologists, but rather the general scarcity of East African lake sites which survived the most severe late-Holocene drought episodes without desiccation, and thus present reasonable probability to have accumulated an uninterrupted climate-proxy archive (Verschuren, 2003).

As part of a broad effort to identify and exploit East African lake sites for high-resolution climate reconstruction, this study mainly concerns the multi-proxy analysis of a late-Holocene sediment sequence from hypersaline Lake Bogoria, one of a chain of tectonic lakes in Kenya's Eastern Rift Valley between Lake Magadi in the south and Lake Turkana in the north. Following a long tradition of salt-lake palaeolimnology (e.g., Mees et al., 1991; Valero-Garcés et al., 2000; Last, 2001; Morellón et al., 2009), we interpret variations in the texture, bulk composition, mineralogy, and magnetic susceptibility of successive sedimentary facies as being driven by fluctuations in lake level, water-column mixing regime and brine chemistry that reflect the influence of a changing local climate on the lake's water balance. We also report data on the stable oxygen and carbon isotopic composition of selected sodium carbonate minerals which help to reveal the mechanism of mineral deposition and so derive additional information on lake history. Further, we supplement the Lake Bogoria climate-proxy record with bulk sedimentological data on two short sediment cores from lakes Nakuru and Elementeita farther south in the Kenya Rift Valley. As expected, penetration of coring tubes into the bottom of these two exceedingly shallow soda lakes was stopped by stiff clays representing a

(sub-)recent desiccation surface. Dating this surface nevertheless produced valuable information on the relative severity of historical drought episodes in the central Kenya Rift Valley.

MATERIALS AND METHODS

Study sites

Lake Bogoria (0° 11’ to 0° 20’N, 36° 04’ to 36° 07’ E; 989 m above sea level (asl), Fig. 1) occupies the southern end of a half-graben depression at the base of the Marmanet-Laikipia Escarpment, which forms the eastern flank of the Kenya Rift Valley just north of the equator (Tiercelin et al., 1981). Lake Bogoria is ca. 17 km long with a maximum width of ca. 3.5 km, and divided in three sub-basins of which the central basin is the largest and deepest (9.25 m water depth in January 2003). The lake water is alkaline (surface pH = 10.1) and hypersaline. A moderately expressed but distinct chemocline (from 72.7 mS/cm at the surface to 75.4 mS/cm at the bottom) was observed in January 2003 during the seasonal period of water-column stratification. At that time, noticeable amounts of dissolved oxygen were limited to the uppermost 1 m. In August 2001, when presence of dissolved oxygen down to 4 m depth revealed the recent occurrence of deep seasonal mixing, a remnant chemocline (from 68.3 mS/cm to 69.3 mS/cm) still occurred between 4 and 5 m depth. This combined evidence suggests that the modern-day Lake Bogoria is oligomictic sensu Hutchinson (1957): its water column probably does not mix completely every year, but is not permanently stratified (meromictic) either. Prolonged stratification is promoted by fresh (low-density) rain- and spring water undergoing surface heating as it spreads across the lake surface, hampering its complete mixing with the hypersaline water below.

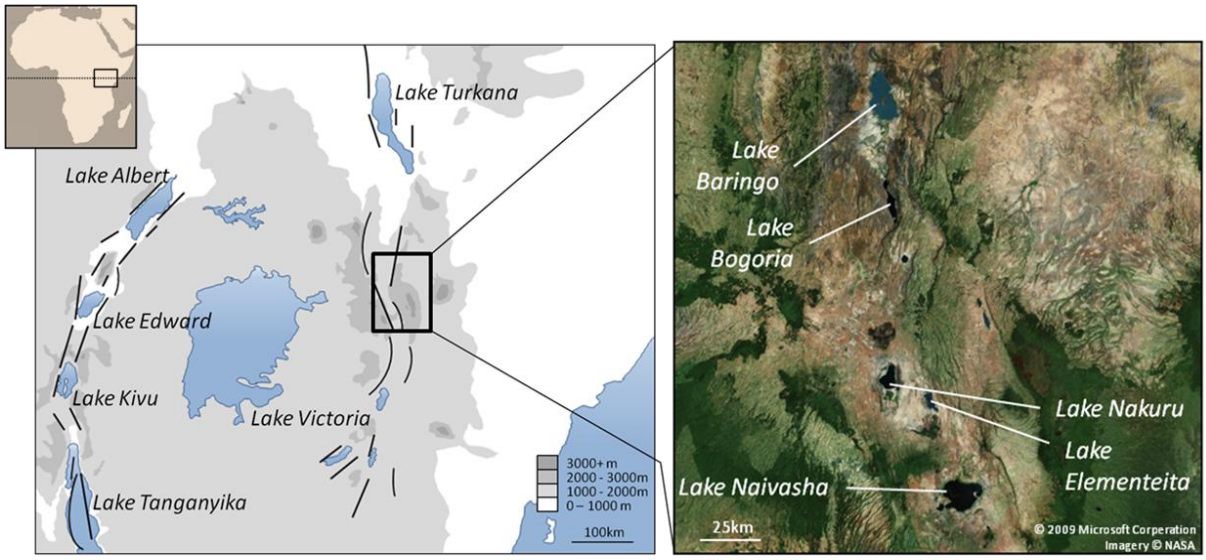

Fig. 1 Location of study sites in the eastern (Gregory) branch of the East African Rift System.

The ionic composition of Lake Bogoria is dominated by Na^+ and CO_3^{2-}, and its isotopic composition is +6‰ $\delta^{18}O_{SMOW}$ and +4‰ $\delta^{13}C_{PDB}$ (Tiercelin et al., 1987). The catchment of Lake Bogoria encompasses ca. 930 km^2 and is composed entirely of Miocene to Pleistocene volcanic deposits (Tiercelin et al., 1987). A strong local climatic moisture deficit and numerous hydrothermal springs, both along the shoreline and below current water level, further contribute to the characteristic hydrochemistry of Lake Bogoria. Annual potential evaporation exceeds 2500 mm, while local precipitation varies from 500 to 1000 mm/year with substantial inter-annual variation (Lavigne and Ashley, 2001). Mainly connected to the twice-yearly passing of the Intertropical Convergence Zone, monsoonal rainfall shows a strong seasonal pattern of two rainy seasons (March-May and September-November). From May to August, frequent late afternoon cloudbursts also produce significant levels of precipitation, while the period from December to February is dry (Lavigne and Ashley, 2001). The lake's sensitivity to hydroclimatic fluctuation is illustrated by its rise to a mid-lake water depth of at least 12.5 m in the summer of 2012, linked to the pronounced positive Indian Ocean Dipole anomaly which prevailed at that time.

Even if water-column mixing in Lake Bogoria occasionally does reach the bottom, occurrence of benthic life is excluded by low solubility of oxygen in warm (27° C in January 2003) and hypersaline water, combined with the typically short-lived nature of such mixing events in tropical lakes (Talling and Lemoalle, 1998). This ensures that sediment accumulation in the profundal zone of the central basin enjoys relatively stable conditions, at least presently. These same conditions are distinctly unfavourable for lake biota, resulting in aquatic life being mainly restricted to cyanobacteria, diatoms, rotifers and copepods which sustain large numbers of flamingos. The lake lies entirely within a 107 km^2 national reserve, limiting direct human impact on the lake and the surrounding landscape. Although the main contributing river, the Waseges, flows through areas now used for crop agriculture before entering the lake's northern basin, there is no indication that anthropogenic soil erosion enhances or modifies sediment delivery to our mid-lake core site in the central basin.

Lakes Nakuru (1770 m asl) and Elementeita (1786 m asl) occupy the floor of the Nakuru-Elementeita basin, ca. 60 km south of Lake Bogoria. This endorheic basin has a 2390 km^2 catchment area (Dühnforth et al., 2006). The western border is formed by east-dipping normal faults of the Mau Escarpment, whereas to the east, the basin is bounded by the Bahati-Kinangop Plateau. To the south, the Eburru volcano forms the divide between the Nakuru-Elementeita and Naivasha basins. Despite the mountainous headwater regions, only minor ephemeral rivers reach lakes Nakuru and Elementeita (Washbourn-Kamau, 1971). Today, lakes Nakuru and Elementeita cover areas of approximately 26 and 40 km^2, respectively, with substantial inter-annual variation. They are both very shallow, with a mean water depth of 1-2 m, and highly alkaline with pH values close to or above 10 (Ballot et al., 2004; Vareschi, 1982). Both lakes are also most often hypersaline, but recorded historical variation in conductivity values is large (9000-160,000 µS/cm for Nakuru; 12,000-40,000 for Elementeita (Vareschi, 1982; Hughes and Hughes, 1992).

Coring

Sediment cores BOG01-1P (0-127 cm) and BOG03-1P (113-234 cm sub-bottom depth) were collected at the deepest point of the central basin of Lake Bogoria in August 2001 and January 2003, using a rod-operated single-drive piston corer which also recovers the sediment-water interface intact (Wright, 1980). Core BOG01-1P was extruded in the field in 1-cm increments using a fixed-interval

sectioning device (Verschuren, 1993) and transferred to Whirl-Pak® bags for transport. The uppermost 30 cm of soft surface sediments were extruded in 5-cm increments, because violent degassing upon the release of hydrostatic pressure disturbed core stratigraphy; this evidence for substantial biogenic gas accumulation in unconsolidated organic surface muds supports our inference from the water-column parameters that present-day Lake Bogoria rarely mixes completely, notwithstanding its relative shallowness. Core BOG03-1P, which consists entirely of older and more consolidated muds, was transported in its polycarbonate tube. After arrival in Ghent, the cores were kept in the dark at 4°C. Sediment cores ELE01-1H (0-47 cm) and NAK01-1H (0-45 cm) were collected in August 2001 from central locations on the flat basin floor of lakes Elementeita (0.55 m water depth) and Nakuru (0.75 m), by hand-pushing a polycarbonate tube into the lake floor and capping its top before retrieval. Both were extruded in 1-cm increments and transferred to Whirl-Pak® bags for transport.

Sedimentology, mineralogy and stable isotope geochemistry

Core BOG03-1P was split lengthwise into two halves, photographed and described following procedures outlined by Schnurrenberger et al. (2003). Description of sediments stored in Whirl-Pak® bags (BG01-1P, NAK01-1H, ELE01-1H) was supplemented by field notes on the presence of fine lamination. Water, organic matter and carbonate content were determined at 1- or 2-cm intervals by the Loss-On-Ignition (LOI) method, which measures the weight loss after drying 1 ml of sediment overnight at 105 °C, burning for 4 hours at 550 °C and ashing for 2 hours at 1000 °C (Bengtsson and Enell, 1986). Saline interstitial water had to be removed before drying to obtain trustworthy bulk-composition data. After recording the wet weight, samples were rinsed with distilled water until pore-water conductivity had decreased to <1 mS/cm. Since sodium carbonate minerals dissolve in water at room temperature, rinsing also removed synsedimentary precipitates that are an integral part of the Bogoria deposits. The difference between LOI data obtained on untreated and rinsed sediment is thus indicative for the local abundance of synsedimentary salt minerals. After rinsing, the inorganic sediment component consists almost entirely of clastic minerals; most smear-slide analyses showed no or very scarce presence of diatoms, as expected in this hypersaline environment. Weight-specific magnetic susceptibility (χ, in 10^{-6} m^3/kg) was measured with a Kappabridge KLY-3 instrument, using 7.7 cm^3 plastic boxes filled with sediment of contiguous 1- or 2-cm core intervals. These data were used to cross-correlate the two cores from Lake Bogoria and to construct a composite master sequence with a total length of 234 cm, identified as BOG01/03. Magnetic susceptibility is mainly an indicator for the relative abundance of ferromagnetic minerals (Dearing, 1999). A total of 60 smear slides were made for microscopic visual characterization of sediment components, although this was complicated by crystallization of salt minerals during drying. Salt minerals were identified by XRD analysis for 18 selected core intervals using Bruker D8 equipment (CuK_α radiation, 15-60°2θ).

Stable oxygen- and carbon-isotope analyses were carried out on pure salt crystals of nahcolite [$NaH(CO_3)$] and trona [$Na_3(HCO_3)(CO_3).2H_2O$]. Ca. 1-2 cm long, nearly pure nahcolite crystals were extracted from five levels between 148 and 132 cm depth, while carefully avoiding rare traces of matrix sediment. Pure trona was sampled at six levels between 204.5 and 168 cm depth, where it occurs as small (up to 0.5 cm long), white crystals with little sediment contamination. The samples were reacted with 100% orthophosphoric acid at 25°C for 36 to 40 h to liberate CO_2 from the more solvable carbonate phase, which was quantitatively isolated after cryogenic trapping in a vacuum extraction line. Isotope analyses were carried out with a Finnigan MAT Delta-E dual-inlet mass

spectrometer. Overall analytical uncertainties (2 SD), including those due to sample heterogeneity are based on duplicate analyses and are better than 0.5‰ for $\delta^{13}C$ and 1.0‰ for $\delta^{18}O$, except when indicated with error bars in Fig. 4. All $\delta^{13}C$ and $\delta^{18}O$ values are reported relative to the PDB standard (Graig, 1957), and typically represent the mean of two samples from the same depth level.

Dating

The chronology of late 19th- and 20th-century sedimentation was determined by analyses of ^{210}Pb, ^{214}Bi and ^{137}Cs by gamma spectrometry at Queen's University (Kingston, Canada). Unsupported ^{210}Pb activity was estimated using both the activity of ^{214}Bi and the stability of total ^{210}Pb at depth. Chronology calculation is based on the Constant Rate of Supply (CRS) model (Appleby and Oldfield, 1978; Binford, 1990); parallel measurement of the anthropogenic radionuclide ^{137}Cs provided a marker horizon for the 1964 nuclear-test maximum.

The age of pre-20th century deposits from Lake Bogoria was constrained with five accelerator mass spectrometry (AMS) ^{14}C dates, one on terrestrial plant macrofossils (grass charcoal) and four on bulk organic sediment. The charcoal was extracted under magnification from the >150 µm sediment fraction, carefully cleaned with a brush, repeatedly rinsed in DDI water and freeze-dried before AMS at Poznan Radiocarbon Laboratory. Although grass charcoal and fine plant debris are rather common in most sections of the studied sediment sequence, fragments larger than 150 µm were generally too low in abundance to recover the equivalent of 0.5 mg carbon required for ^{14}C dating from core increments each representing ca. 40-50 year intervals. For radiocarbon dates on bulk organic sediment, a correction had to be made for the ^{14}C 'reservoir' effect, which in this hydrologically closed lake can be derived either from algae which assimilated dissolved carbon (DIC) out of equilibrium with atmospheric CO_2, or from admixture of old terrestrial organic carbon in catchment soils or reworked lake sediments (Blaauw et al., 2011). Likely the most important dating issue in Lake Bogoria is the contamination of the DIC assimilated by phytoplankton (algae and cyanobacteria) with a carbon source of infinite age (i.e., lacking ^{14}C), supplied by inflow from alkaline hot water springs. The modern-day old-carbon age offset for Lake Bogoria was estimated using bulk organic sediment from 40.5 cm core depth. The true calendar age of this interval was estimated by extrapolating the mean dry mass accumulation rate between 1964 (^{137}Cs peak) and 2001 (the sediment surface) to 40.5 cm depth. The inferred true ^{14}C age of the interval was then subtracted from the measured bulk ^{14}C age to obtain the reservoir age offset. Although reservoir effects can vary over time, in this study we must assume it to be constant over the period covered by our core sequence. AMS ^{14}C ages were calibrated using the Northern Hemisphere terrestrial IntCal09.14C calibration curve (Reimer et al., 2009), and an age-depth model with uncertainty envelope was constructed using CLAM software in R (Blaauw, 2010), with linear interpolation between the dated intervals to account for the significant changes in sedimentation rate expected in this system (Verschuren, 2001). Reported ^{14}C-based dates are rounded to the nearest 50 years in the text.

RESULTS

Chronology

Levels of unsupported ^{210}Pb and ^{137}Cs were low in all cores, which can be attributed to the semi-arid regional climate limiting atmospheric deposition. Low and erratic ^{210}Pb activity in the Lake Bogoria sequence prevented trustworthy age calculations. However, ^{137}Cs activity (n = 20) reaches a

pronounced peak of 0.21 dpm/g at 35 cm core depth, which we attribute to the 1964 peak of atomic bomb testing. Extrapolation of the mean dry mass accumulation between 2001 (0 cm) and 1964 (35 cm) suggests that the sediments at 40.5 cm were deposited in 1943 AD, which corresponds to 182 ^{14}C yr BP. Since the ^{14}C age of bulk sediment from this interval is 4160 ± 35 ^{14}C yr BP, we calculated an modern-day old-carbon age offset of 3980 ^{14}C years. Because of the deterministic character of the age data used for this estimation, it lacks an uncertainty range, implying that the reported error ranges of reservoir-corrected ages are slight underestimations. One sample of terrestrial plant macrofossils from 227 cm depth yields a ^{14}C age of 1630 ± 140 BP, corresponding to a 2-sigma calibrated age range of 120-660 cal yr AD and a median age of 390 cal yr AD (Table 1). The age-depth model resulting from linear interpolation between all dated levels is shown in Fig. 2.

Levels of supported ^{210}Pb in the Nakuru and Elementeita cores were estimated at 2.76 and 2.50 dpm/g, respectively (Fig. 3). In NAK01-1H, unsupported ^{210}Pb increases from the base of the sequence to 37 cm depth, stays roughly constant up to 22 cm, and then increases to its highest values (11-14 dpm/g) at the top. In ELE01-1H, unsupported ^{210}Pb is present from 21.5 cm upwards and rises gradually to a maximum of 9-10 dpm/g at the top. In ELE01-1H, the 1964 time marker of peak ^{137}Cs concentration is in relatively good accordance with its ^{210}Pb age based on the CRS model. In NAK01-1H, the ^{210}Pb-derived depth of 1964 AD does not correspond well to the ^{137}Cs peak. However, the onset of ^{137}Cs increase does coincide with the start of nuclear weapons testing in the 1950's, providing satisfactory support for our ^{210}Pb-based chronology.

Composite depth	Laboratory code and number	Conventional radiocarbon age in ^{14}C yr BP	Calibrated age 2σ range in cal yr AD
40.5[b]	Poz-9820	4160 ± 35	1930 (extrapolated from ^{137}Cs age marker)
136-138[b]	Poz-12606	4780 ± 50	1154-1285 (0.923)
			1054-1077 (0.026)
153-155[b]	Poz-12607	4965 ± 35	989-1154 (0.95)
175-177[b]	Poz-12608	5600 ± 40	376-540 (0.884)
			344-374 (0.065)
227-229[c]	Poz-9824	1630 ± 140	124-654 (0.944)
			90-100 (0.006)

Table 1 AMS radiocarbon ages on bulk organic sediment (b) or grass charcoal (c) from composite core BOG01/03 from Lake Bogoria. Calibrated age ranges were determined using CLAM in R (Blaauw, 2010) and are reported together with their relative area under the probability distribution.

Lake Bogoria sediment stratigraphy

The 234-cm sediment sequence from Lake Bogoria has a dark olive-grey to black colour, and variable texture ranging from clay over silt to sand (Fig. 4). Water content rises gradually from 50 % at the base to 95-97 % in the upper 20 cm, with values locally lower in thick salt layers below 132 cm and in a sand lens at 60 cm. The mean organic matter content increases stepwise from a near-constant 4-5 % below 56 cm to ca. 8 % in the upper 42 cm, separated by a short section of silty clay with 10 % organic matter. Carbonate content as estimated by LOI is low throughout the sequence with a mean value of 5.4 %, and values exceeding 8 % in the section between 70 and 100 cm. In reality carbonate content may be lower still, since ashing at 1000°C dewaters the clay minerals. Calcite crystals were noticed only in smear slides from the upper 60 cm.

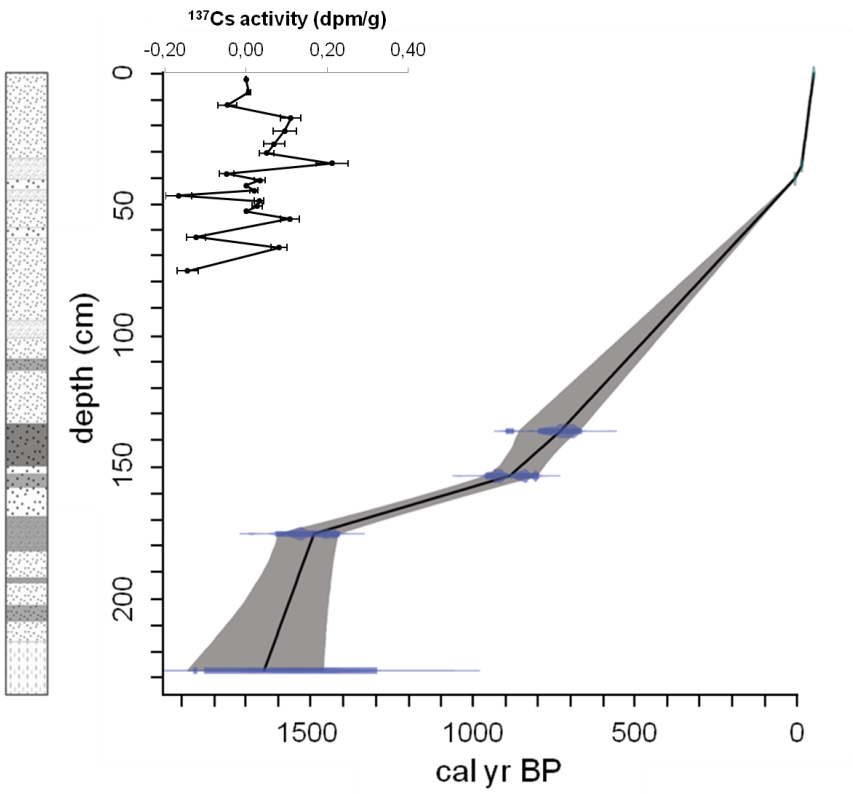

Fig. 2 Simplified lithostratigraphy and age-depth model for the 234-cm long composite sequence BOG01/03 from Lake Bogoria, constructed using CLAM in R (Blaauw, 2010), and based on ^{137}Cs and ^{14}C dating with linear interpolation between sample points. The 'best-age' estimation (black line) is obtained by weighted averaging of the age-probability curves of the calibrated dates, while the grey band depicts the 95% uncertainty envelope around this estimation. The inset plot shows ^{137}Cs activity in the upper portion of core BOG01-1P. See Fig. 4 for a key to the lithostratigraphy.

For samples analyzed after rinsing to remove salts, the inorganic rest fraction is very high with values of ca. 90% throughout the sequence except at 70-100 cm (due to elevated carbonate content) and 0-50 cm (due to high organic matter content). Clastic mineral grains are mainly feldspars, muscovite and biotite, and a minor quantity of hornblende grains. This mostly silt-sized detrital mineral component is ultimately derived from catchment soils, partly reworked in alluvial fan deposits (Tiercelin et al., 1987) and delivered to the lake during periods of high-intensity rainfall. Below 132 cm, weight loss at 1000 °C is much greater in un-rinsed samples, reflecting the high salt content of the sediment. Similar levels of weight loss in the uppermost 25 cm, however, are probably due to dissolved salts in pore-water, which in the soft near-surface sediment (>95% water) make a large contribution to sediment weight after drying. Magnetic susceptibility (χ) varies considerably from ~400 x 10^{-6} m^3/kg in some massive salt layers to ~3000 x 10^{-6} m^3/kg in the upper 60 cm of soft silty muds. As expected, χ is in general inversely correlated with the abundance of diamagnetic salt minerals, which dilute the clastic mineral signal, but in the upper half of the sequence it also appears influenced by variation in composition and concentration of the clastic fraction. When dry mass values exclude salt crystals, χ values below 132 cm are markedly higher (Fig. 4), locally approaching the peak values recorded for the uppermost 60 cm.

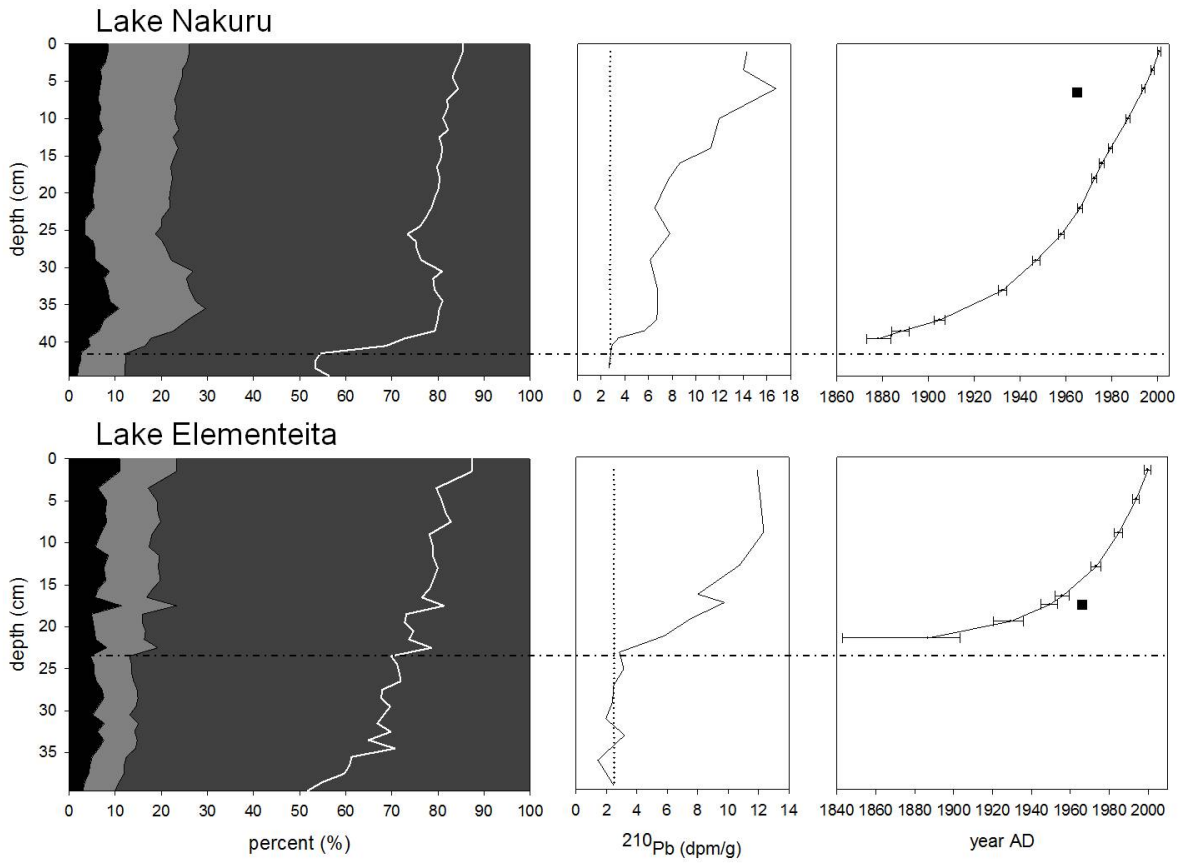

Fig. 3 Bulk sediment composition and water content (left), ^{210}Pb activity (middle) and ^{210}Pb-inferred depth-age relationship (right) for recent offshore sedimentation in Lakes Nakuru and Elementeita. The composition plots show percent organic matter in black, $CaCO_3$ in light grey and the siliciclastic mineral fraction in dark grey with percent water content superimposed as a full white line. The ^{210}Pb plots show total ^{210}Pb activity as a full line, and supported ^{210}Pb as a dotted line. The horizontal dash-dotted line running through all three plots indicates the inferred sub-recent desiccation horizon.

Since massive salt layers are the most obvious and dominant feature in the Bogoria sequence (Fig. 4), we use them to distinguish three major stratigraphic units. The lower section (Unit BOG1: 234-148 cm) consists of dark olive-grey to black sediments with abundant salt minerals. Sediment texture becomes more coarse towards the top of this unit, starting with clay at the bottom (234-214 cm), over silty clay (192-190; 180-167 cm) and silt (214-192; 190-180 cm) to sand (167-148 cm). The clastic mineral content consistently reaches 90 %. No endogenic or detrital calcium carbonate was noticed in the smear slides, and the organic fraction (on average 4.2 %) is dominated by algal matter with rare small fibrous plant remains and grass charcoal. The evaporitic character of the lacustrine environment at that time is most clearly evidenced by the occurrence of four trona beds, as well as by the presence of scattered trona crystals in the intervening intervals. XRD patterns (8 in total) also show the presence of clinoptilolite [$(Ca_3,K_6,Na_6)(Si_{30}Al_6)O_{72}.20H_2O$], associated with feldspar in two samples (196 cm, 166 cm), roughly coinciding with distinct magnetic susceptibility peaks (2360 and 1800 x 10^{-6} m^3/kg), suggesting a temporarily increased supply of clastic minerals. Most XRD patterns also show the presence of minor amounts of thermonatrite [$Na_2(CO_3).H_2O$] and halite (NaCl) crystals, but most likely these minerals formed by drying after sampling, and are not further discussed here.

Unit BOG1 is overlain by a massive layer of dark olive-grey to black sandy silt containing large nahcolite crystals (Unit BOG2: 148-132 cm). Again the clastic mineral content is very high (ca. 90%). No carbonates were noticed in smear slides, and the low organic matter content (4.4% on average) is mainly represented by grass charcoal and fine fibrous plant debris.

The upper half of the sequence (Unit BOG3: 132-0 cm) consists mostly of silty mud, lacking massive salt layers. It is subdivided in four subunits based on colour and the (occasional) presence of diatom frustules and calcite crystals. Subunit BOG3a (132-93 cm) is a dark olive-grey silt with few but clear fibrous plant remains and charcoal fragments, grading to silty clay at the top where this organic debris is lacking. At 111.5 cm a thin layer occurs with clear white trona crystals making up ca. 20% of the sediment matrix. Magadiite aggregates [$Na_2Si_{14}O_{29}.11H_2O$] too were visually recognized at this depth; XRD patterns (six in total for Unit BOG3) indicate their presence at three sampling depths (111.5, 108.5 and 96.5 cm). Their presence coincides with locally elevated values (5.2-11.2%) of $CaCO_3$ content as inferred by LOI, because magadiite decomposes, with quartz formation, between 500 and 700°C (Lagaly et al., 1975*).* No carbonate crystals were observed in smear slides from this section. Subunit BOG3b (93-62 cm) is a uniformly very dark grey-brown silt with a smaller amount of visible coarse organic matter than in the lower subunit, and no salt mineral occurrences other than those that formed after sampling. Subunit BOG3c (62-48 cm) consists of dark olive-brown soft sand and silt without visible plant debris in smear slides, which do include some elongated calcite crystals. At the top of the sediment sequence, Subunit BOG3d (48-0 cm) is composed of soft dark brown or dark yellow brown silty clays, silts and sands with common presence of slightly elongated calcite crystals (ca. 5 % of the smear slide surface). The organic matter content of this subunit is markedly higher (8-10 %) than that of lower sections, and includes significant amounts of fine fibrous plant and charcoal debris. In Subunits BOG3c and BOG3d also needle-shaped diatoms (*Nitzschia* spp.) occur, with a similar distribution as calcite down to 60 cm depth. All calcite observed in the record suggests an endogenic origin since it is present as elongated prismatic crystals of uniform shape and size (usually ca. 5 µm long). However, no calcite was detected by XRD analysis, possibly because of low concentration and overlapping peaks in the diffractograms. Magnetic susceptibility decreases gradually from the base to the top of Subunit BOG3a and increases again in Subunit BOG3b to reach maximum values (ca. 3700 x 10^{-6} m^3/kg) at the BOG3b-BOG3c boundary. In Subunits BOG3c and BOG3d, magnetic susceptibility remains mostly high but shows considerable variability in the soft surface muds.

Mineralogy of non-allogenic phases in Lake Bogoria

Trona occurs as aggregates of small or large lath-shaped crystals throughout Unit BOG1, and as four distinct layers of variable thickness: a pale yellow to greyish white layer (I; Fig. 4) at 200.5-205.5 cm; a thin pale brown to yellow layer (II) at 190-192 cm; a thick, yellow to bright white layer (III) at 167-180 cm with the largest crystals (ca. 0.5 cm); and a pale brown to yellow layer (IV) at 151-156 cm. Trona also occurs in Subunit BOG3a as aggregates of clear white crystals at 111.5 cm depth. XRD patterns for other samples of Unit BOG3 (108.5, 96.5, 74.5, 22.5 and 12.5 cm depth) show scattered trona crystals occurring throughout this interval, although also these occurrences may have formed during drying in storage, as does the thermonatrite and halite detected in Unit BOG1 and BOG3 samples.

Nahcolite occurs only in Unit BOG2, where its presence is noted visually and verified by XRD and smear-slide analysis. It occurs as large (some >20 mm) single and twinned prismatic crystals, white or

transparent with a vitreous luster with only few impurities, embedded in the sediment. We interpret these to have formed by synsedimentary intrasediment growth just below the lake bottom.

The only sodium silicate mineral recorded in the Bogoria sequence is magadiite, detected by XRD analysis in three Subunit BOG3a samples (111.5, 108.5 and 96.5 cm depth). Magadiite occurs as spherical nodules with diffuse edges, suggesting authigenic formation by intra-sediment growth. XRD analysis also revealed the presence of clinoptilolite, a zeolite mineral, in the silts and sands of Unit BOG1 (198 and 165 cm depth). The latter mineral could not be detected in smear slides.

Lake Bogoria stable-isotope geochemistry

Figs. 4 and 5 present the results of carbon and oxygen stable-isotope analyses on the sodium carbonate minerals. Values for the thick nahcolite layer of Unit BOG2 are strongly positive, averaging +9.2 ‰ $\delta^{13}C_{PDB}$ and +12.6 ‰ $\delta^{18}O_{PDB}$. There is no marked trend within this layer in either $\delta^{13}C$ or $\delta^{18}O$, and no co-variance between them (Fig. 5).

The analysed trona crystals are from layers I, II and III in Unit BOG1; trona from layer IV could not be analyzed as a pure phase, because of its small crystal size and presence of abundant sediment inclusions. Both $\delta^{18}O$ and $\delta^{13}C$ are quite uniform across the three lower layers. They are the least positive in layer I (+5.4 ‰ $\delta^{13}C$, +11.5 ‰ $\delta^{18}O$) and except for a $\delta^{13}C$ outlier at 175.5 cm in layer III, most positive in layer II (+6.2 ‰ $\delta^{13}C$, +13.9 ‰ $\delta^{18}O$). Covariance (Fig. 5) between the $\delta^{18}O$ and $\delta^{13}C$ of pure trona crystals is significant and positive ($r = 0.79$, $p = 0.001$, $n = 6$).

Lake Nakuru sediment stratigraphy

Core NAK01-1H consists of uniform very dark grey brown sediments over its entire length, with a clear gradient in water content. The lowermost 4 cm (Unit NAK1: 45-41 cm) consists of dry mud with very low organic matter content (2 %) and also relatively low $CaCO_3$ (10 %). The carbonate content strongly increases in the above-lying unit (NAK2: 41-0 cm) to a relatively constant value of ca. 20 %, while water content and particularly organic matter (4-10 %) vary significantly with maxima in the section 38-30 cm and pronounced minima in water (75 %) and organic matter (4 %) at 24-26 cm. From 24 cm upwards, both gradually increase towards the sediment surface, whereas carbonate content remains constant.

Lake Elementeita sediment stratigraphy

Core ELE01-1H consists of visually uniform olive to olive brown muds throughout. It also has minimum organic matter (3-4 %) and water content (50-60 %) at its base, and higher values above 36 cm, but the transition is less sharp than in NAK01-1H. Water content increases more gradually, reaching a ‘soft-mud’ value of 75 % only at 24 cm. Also at that level, carbonate content increases abruptly from a near-constant 7-8 % to 12-13 %. In contrast, organic-matter content is variable both below and above 24 cm, typically 6-8 % but locally reaching 10 %, also at the surface. Consequently, the transition at 24 cm appears to be a more fundamental stratigraphic boundary justifying distinction between a lower Unit I (23.5-40 cm) and an upper Unit 2 (23.5-0 cm).

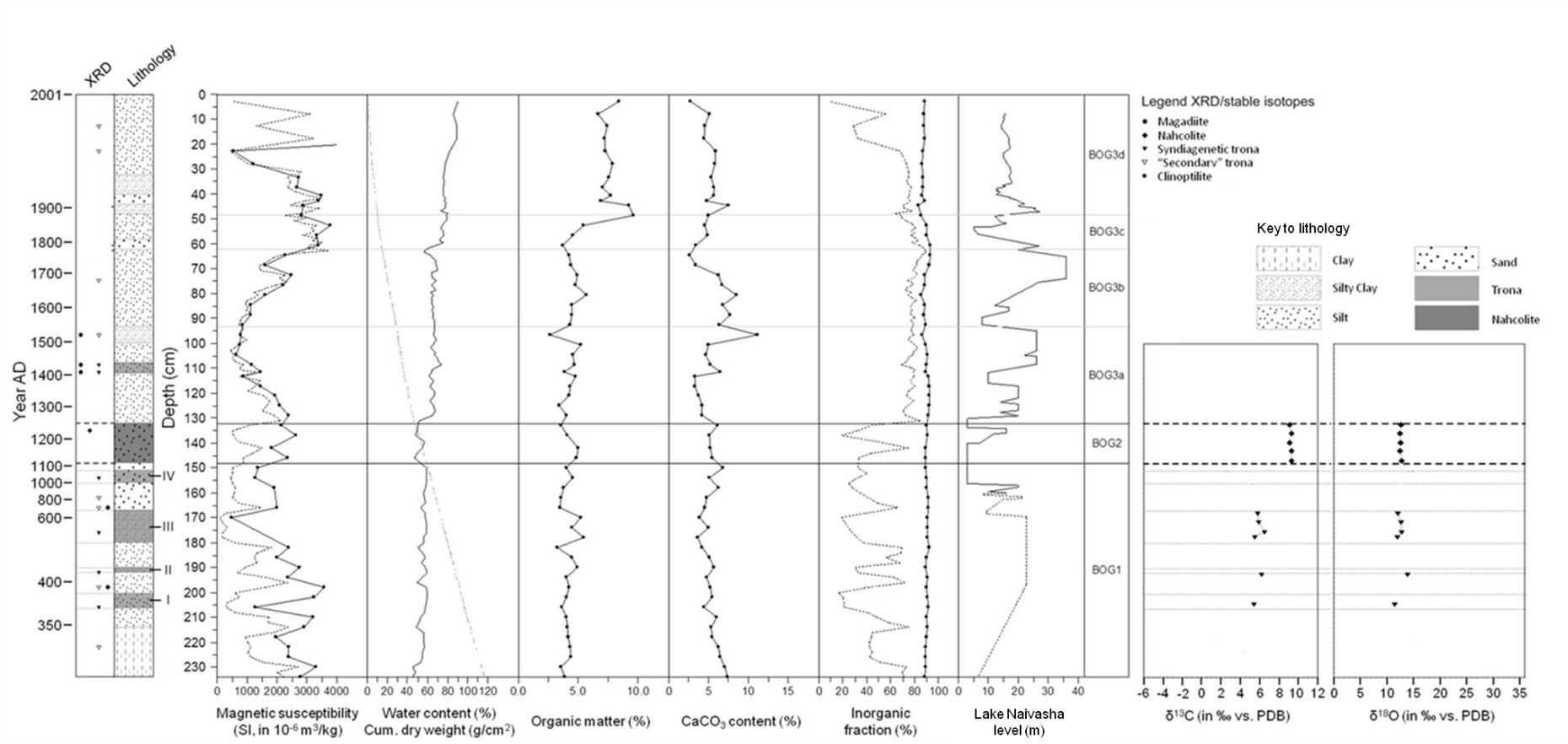

Fig. 4 Lithostratigraphy and composition of composite core BOG01/03 from Lake Bogoria, with distribution (from XRD, left) and carbon- and oxygen-isotopic composition (right plots) of the sodium-carbonate minerals. For magnetic susceptibility and the non-calcite inorganic fraction, the dotted line shows values obtained from untreated mud, and the full line connecting sampling points shows values after removal of salts through rinsing with distilled water. 'Desalted' magnetic susceptibility was calculated using the percentage ratio between the untreated non-calcite inorganic fraction and the 'desalted' inorganic fraction, i.e. the siliciclastic mineral fraction. Naivasha lake-level record modified from Verschuren (2001).

DISCUSSION

Environmental history of Lake Bogoria

Formation of syndiagenetic trona, nahcolite and magadiite requires specific conditions. Consequently, their occurrence and distribution in Lake Bogoria sediments can be used as indicators of flooding events and past changes in lake level and water chemistry, which in turn provides valuable information about the climate regime occurring at that time. When saline alkaline water is concentrated by evaporation, trona and nahcolite precipitate if calcium concentrations are low enough to prevent gaylussite [$Na_2Ca(CO_3)_2.5H_2O$] formation (Renaut et al., 1986). At tropical lake-water temperatures (25°C or higher, as in Lake Bogoria), trona is the stable mineral phase for solutions in equilibrium with the atmosphere (Eugster, 1966; Mees et al., 1991). Nahcolite forms when the partial pressure of dissolved CO_2 is much higher (Renaut et al., 1986). Such high pCO_2 conditions may develop by anaerobic bacterial breakdown of organic matter in an environment with limited or no contact with the atmosphere, such as the lower water column of a meromictic lake. Nahcolite typically precipitates from interstitial brines in anaerobic surface muds containing a considerable amount of organic material, which can also occur in holomictic lakes with poor mixing (Mees et al., 1991).

The trona layers in Unit BOG1 indicate that between ca. 1650 and 850 cal yr BP (ca. 300-1100 AD), Lake Bogoria experienced multiple hypersaline lowstands and a holomictic mixing regime. Any short periods of higher lake level which may have occurred inbetween these do not seem to have resulted in stable stratification of the water column. In these circumstances, strong evaporative concentration led to precipitation of trona. Absence of gaylussite in samples selected for XRD and smear slides points to low calcium concentrations in the water column, presumably because Ca-bearing minerals were formed in mudflat environments around the lake. The highest concentration of sodium carbonates, an almost pure white deposit of large lath-shaped trona crystals, occurs in layer III at 167-180 cm. Their size and shape suggests precipitation from the calm water column of a shallow hypersaline lake phase provisionally dated to between 1500 and 1250 cal yr BP.

The large variation in magnetic susceptibility of Unit BOG1 sediments mainly reflects variable dilution of the clastic mineral signal by diamagnetic salt mineral occurrences. Moderate to high χ values in sections between the four trona layers suggest that relatively dry conditions predominated throughout the period represented by BOG1, which lasted until about 1100 AD. The occurrence of clinoptilolite, together with feldspar, at two levels coinciding with peaks in magnetic susceptibility, suggests a close association with the detrital silt to sand fraction, including feldspar and probably volcanic glass, which occasionally must have reached the basin centre. Clinoptilolite formation by interaction of these compounds with the alkaline lake brines can have taken place either at the coring site or in more marginal areas followed by reworking.

The next phase in Lake Bogoria's history is represented by Unit BOG2, which consists of a single massive accumulation of nahcolite. Precipitation of nahcolite instead of trona requires specific circumstances of anaerobic organic-matter decomposition in a lake with a mixing regime maintaining high bottom-water pCO_2. To generate these conditions we suggest that the water column became permanently stratified when the shallow hypersaline water body filling the Bogoria basin was flooded following an increased freshwater supply. Hereby a considerable volume of low-density water was not immediately mixed into the hypersaline brine but formed a low-salinity layer above a high-

salinity lower water mass. This created strong density stratification and prevented fresh oxygen to be supplied to bottom waters (Mees et al., 1991). Anaerobic decomposition of settling organic matter then allowed synsedimentary nahcolite formation in high-pCO_2 bottom waters. Absence of other sodium carbonates in Unit BOG2 indicates stable conditions, which according to our age-depth model lasted from about 840 to 700 cal yr BP (1100-1250 AD). The exact duration of this stage should be treated with some caution, since sedimentation rate may have been altered significantly during massive nahcolite precipitation. The magnetic susceptibility of bulk material is rather low in this unit (700-1500 x 10^{-6} m^3/kg), due to the high salt content (20 to 65% of sediment dry mass; Fig. 4). In rinsed samples of Unit BOG2, χ values exceed 2000 x 10^{-6} m^3/kg, comparable to those in the lower half of Unit BOG3. The sharp transition between Unit BOG1 and the nahcolite deposit of BOG2, reflecting an abrupt switch to permanent stratification, seems to suggest that freshwater supply to Lake Bogoria increased markedly around the early 12th century.

Conditions favourable for nahcolite formation ended around 1250 AD, probably induced by a weakening of water-column stratification, or by a non-recorded erratic event affecting a lake with large relative hypolimnion volume. Chemocline weakening may have been caused by rising epilimnetic salinity in response to continued evaporation, thus creating the possibility of both water masses to mix. On a yearly basis, the water column was probably most often stratified (as it is today), but on time scales of decades, occasional deep-mixing events may have allowed sufficient release of bottom-water CO_2 to prevent nahcolite formation. Taken in isolation, this evidence appears to suggest a return to a more shallow Lake Bogoria. However, compared to Unit BOG1 the Unit BOG3 sediment has a much lower salt content, suggesting a more dilute, deepwater lake instead. Also, the trend of decreasing χ from >2000 x 10^{-6} m^3/kg at the base of Unit BOG3 to 700-1000 x 10^{-6} m^3/kg at the top of Subunit 3a, together with progressively finer silts culminating in silty clay (Fig. 4), is indicative of sedimentation further offshore. We thus propose that lake level increased almost continuously between ca. 1100 AD (the base of Unit BOG2) and 1550 AD, with an initial ca. 150-year period of meromixis evolving into high-water conditions of less stable water-column stratification as the initial density gradient, created by a sudden supply of fresh water, was gradually eroded. Like today, predominantly fine silt was deposited, except for thin intervals with sand and trona crystals indicating short-lived changes in the local bottom environment that are possibly linked to relatively minor lake-level fluctuation.

The occurrence of magadiite near the top of Subunit BOG3a is compatible with saline alkaline lake conditions, whose high pH allows high dissolved Si concentrations to be reached (Eugster, 1967; Renaut et al, 1986; Mees et al., 1991), typically in settings with abundant reactive silicate minerals within the catchment area. Magadiite forms when the pH is lowered to values at which its solubility is lowest (pH 9; Bricker, 1969), which can happen in response to a large freshwater influx. During Subunit BOG3a sedimentation at Lake Bogoria, this process must have affected the bottom environment, allowing magadiite formation as intra-sediment development of nodules. The distribution of magadiite in the Bogoria sequence therefore supports our inference of relatively dilute conditions with highest water levels between about 1400 and 1550 AD.

Apart from the restricted occurrence of magadiite and the thin interval with dispersed trona crystals at 111-108 cm, indications of lake-level fluctuation in Unit BOG3 are based mainly on textural variations, the occurrence of diatom remains, and magnetic susceptibility data. Especially in Subunits BOG3c and BOG3d, which show a succession of fine- and coarse-grained deposits, sandy sediments

coincide with peak χ values. XRD and smear-slide analyses indicate that these peaks are mainly characterised by high contents of feldspar, mica, quartz, hornblende and rare Fe-bearing minerals. Given that even modest water-level fluctuation can cause significant changes in the surface of Lake Bogoria, it is likely that an elevated presence of terrestrial minerals with coarse grain size correspond to lower lake levels, allowing stream discharge plumes to reach the centre of the lake. This implies that lake level dropped out ca. 150 cal yr BP or around 1800 AD (the top of Subunit BOG3b), where a coincident dip in organic matter and $CaCO_3$ content points to a greater contribution of clastic sedimentation. From the base of BOG3c upward, doubling of organic matter content towards the top of this subunit, together with the occurrence of diatom frustules (however scarce) from 60 cm upward, suggest that more favourable conditions for phytoplankton blooms became established after this late-18th century lowstand, although magnetic susceptibility levels remained high. Between 60 and 30 cm, i.e. from the late-18th or early-19th century until ca. 1970, sediment properties suggest generally low lake levels interspersed with short highstand episodes (deposition of silty clay) at the start of the 20th century and between about 1945 and 1967 AD. The uppermost, uncompacted silt deposit of Subunit BOG3d has a more salty character with presence of trona and halite. Magnetic susceptibility in these uncompacted muds is highly variable, and disturbance during core recovery make the observed proxy data difficult to interpret. Historical records suggest that Lake Bogoria was at least 14 m deep during some episodes between 1890 and 1930 (Tiercelin et al., 1987). We surmise that the thin layer of silty clay at 46 cm depth was deposited during this highstand period. According to a reconstruction based on sporadic observations and aerial photography (Tiercelin et al., 1987), lake level decline from 1930 onward reached a minimum of ca. 7m depth between 1950 and 1960. Thereafter, levels of ca. 9 m were recorded in 1960-1970 and ca. 8 m during the 1970's, followed by a steep increase to ca. 12 m in 1980. During the coring campaigns of 2001 and 2003 a depth of 9.25 m was measured, and levels of at least 12.5 m were observed in 2012. Thus lake depth varied between 7 and at least 12.5 meters over the past 75 years, which can explain the highly variable (but at present, not well-resolved) sediment stratigraphy of Subunit BOG3d.

Stable isotopic signatures of palaeohydrological change

The high $\delta^{18}O$ values (+11.5 to +14 ‰) for all analyzed nahcolite and trona crystals (Fig. 4) are not unexpected in the strongly evaporating conditions of a tropical semi-arid climate (Reitsema, 1980; Mees et al., 1998). The high $\delta^{13}C$ values (up to +6.5 ‰ for trona, +9.3 ‰ for nahcolite) are less easy to ascribe to one specific process. Variations in biological activity such as photosynthesis, anaerobic decomposition of organic matter, and anaerobic methane formation by methanogenic bacteria, but also purely physical processes such as CO_2 degassing during evaporation can all lead to elevated $\delta^{13}C$. In addition, since the inorganic carbon reservoir is much smaller than the oxygen reservoir, it is also more susceptible to changes in isotopic composition.

The $\delta^{18}O$ and $\delta^{13}C$ values of nahcolite in Unit BOG2 do not present any marked trend. Conditions did not change in the course of the period of nahcolite formation, but the length of this stage can be rather short. The $\delta^{18}O$ of the Bogoria nahcolite (+12.6‰) is comparable with values measured for synsedimentary nahcolite from Malha Crater Lake, in the Sahel region of north-western Sudan (Mees et al., 1998). Its $\delta^{13}C$ value of 9.1-9.3 ‰ is on average 1 to 3 ‰ lower than values reported for the Malha deposits. In Malha, nahcolite was inferred to have been deposited in a shallow, holomictic, meso- to hypersaline lake where high pCO_2 was created and maintained within bottom muds rich in organic matter (Mees et al., 1991). For Lake Bogoria, we propose that nahcolite formation may be

related to strong density stratification, creating conditions with high CO_2 partial pressure in the lower part of the water column.

Fractionation factors involved in nahcolite and trona formation are unknown, which complicates comparison of their stable isotope signatures. The strong similarity between the $\delta^{18}O$ of trona and nahcolite from Lake Bogoria is an indication that oxygen fractionation factors are similar for both minerals. For carbon, carbonate balance conditions were too different between episodes of trona and nahcolite formation to allow drawing conclusions about fractionation behaviour. The significantly higher $\delta^{13}C$ values for nahcolite than for trona may be due to a greater contribution of methanogenic bacteria decomposing organic matter in the bottom waters of the stratified lake, producing isotopically light methane and consequently isotopically heavy carbon in the dissolved inorganic carbon reservoir.

A prominent feature of many sets of $\delta^{13}C$ and $\delta^{18}O$ data on lacustrine carbonates from closed lakes is covariance between these two parameters. This has mainly been documented for lacustrine calcium carbonates (Talbot, 1990), but it also exists for sodium carbonates (Mees et al., 1998). In the Lake Bogoria record, the highly significant covariance of $\delta^{18}O$ and $\delta^{13}C$ in three of the four trona beds of Unit BOG1 indicates that oxygen and carbon were subject to the same or coupled controls, namely evaporation of water accompanied by CO_2 degassing. Synsedimentary trona precipitated from brines derived from the same parent water, with differences in the degree of brine evolution between stages of evaporite formation causing differences in the isotopic signature of individual trona layers. The range of $\delta^{18}O$ values within the single nahcolite layer is too small to recognize covariance, but absence of covariance is expected for a mineral forming in conditions of excessive CO_2 production by processes, such as methanogenesis, whose intensity is unrelated to evaporation, the latter being the main control on ^{18}O enrichment (Mees et al., 1998).

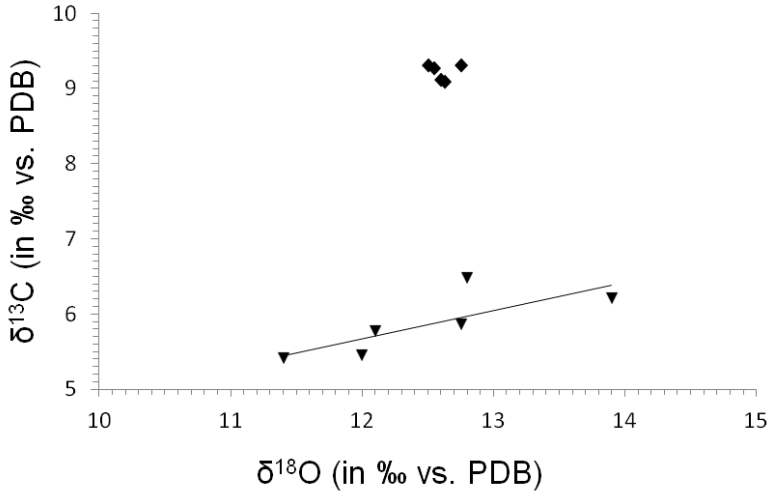

Fig. 5 Covariance between $\delta^{18}O$ and $\delta^{13}C$ for pure trona (reverse triangles) and nahcolite (diamonds) crystals from Lake Bogoria core BOG01/03. See Fig. 4 for the depth distribution of these samples.

Recent palaeohydrology of the Nakuru-Elementeita basin

Water level in the Nakuru-Elementeita basin strongly depends on local rainfall, because the lakes are not fed by major rivers and because surface outflows or significant ground water movement are absent (Dühnforth et al., 2006). Extreme climatic sensitivity of these lakes is illustrated by ancient shorelines at 1940 m asl, indicating that the lake surface was at least 170 m higher than today during the Early Holocene African Humid Period, when Nakuru and Elementeita were joined into one large lake filling a large part of the catchment basin (Nilsson, 1931; Richardson & Dussinger 1986).

Sediment characteristics at the base of the short cores from lakes Nakuru and Elementeita reflect dramatic changes in the hydrological budget of these lakes in the relatively recent past. Low water, organic matter and $CaCO_3$ content (Fig. 3) suggest that the basal core sections represent a desiccation horizon, implying that both Lake Nakuru and Lake Elementeita were nearly or completely dry. Lacustrine sedimentation at the coring sites was interrupted, and previously deposited layers underwent dehydration, oxidation and compaction (Verschuren, 1999a). In the Nakuru core, abruptly changing sediment characteristics above 41 cm suggest refilling of the lake basin, dated by ^{210}Pb to the 1870's AD. Water content exhibits a sudden rise, and organic matter and $CaCO_3$ attain higher mean values, which together with the massive nature of the mud, suggest a relatively shallow but permanent lacustrine environment with microalgae as dominant primary producers. In the Elementeita core a similar transition to more organic muds occurs above 37 cm; however $CaCO_3$ content remains stable at 7-8 % and also water content remains rather low. Based on ^{210}Pb dating, the stratigraphic transition equivalent with the 1870's refilling of Lake Nakuru occurs at 24 cm. The very dry low-organic mud forming the base of the sampled Elementeita sequence must hence represent an earlier phase of lake desiccation.

Drying of Lake Nakuru immediately prior to the final decades of the 19th century is in accordance with reconstructed and historically recorded lake-level data from lakes in the nearby Naivasha basin: Lake Naivasha itself (Åse et al., 1986; Verschuren et al., 2000a), Oloidien (Verschuren et al., 1999, 2000b) and Sonachi (Verschuren, 1999a-b). These hydrologically interconnected lakes were all at a very low level during the 1870's, and rose after the first European settlers arrived in the early 1880's to reach their highest historically recorded levels around the turn of the century. A historically high water level following the 1870's lowstand can be recognized in the Nakuru sediment record as well, in the form of peak organic matter content centred around 35.5 cm core depth. In Lake Elementeita the 1880's return to lacustrine conditions is less clearly recorded by its sediments. Probably, its sedimentological signature has been disturbed during later episodes of low lake level. Indeed, a lake level gauge set up at Lake Nakuru in 1930 recorded that the lake was dry on two separate occasions during the 20th century (1944-1946 and July 1961; Vareschi, 1982). In the Lake Nakuru record these events are visible as the minimum in organic matter at 25 cm depth; at the mid-lake core site they were evidently not extreme enough to cause complete desiccation of exposed surface deposits and obliteration of the signature corresponding to the early-20th century lowstand. However, in the Elementeita sub-basin, these dry phases appear to have caused more significant disturbance, with sediment redistribution and further oxidation of the organic matter deposited previously, resulting in a more erratic variation of organic-matter content in 20th-century sediments. The slightly stiffer muds below 24 cm must represent a succession of phases of (near-) desiccation in the period before the 1870's. We surmise that most of Unit I in Lake Elementeita dates from the early to mid-19th century. Indeed, the base of this unit (and of the cored sequence) may represent the more prolonged and/or

thorough desiccation which must have occurred during the late-18th and earliest 19th centuries, when severe drought was widespread across equatorial East Africa (Bessems et al., 2008) and also the Lake Bogoria record shows evidence of low lake level (the top of Subunit BOG3b, dated to ca. 1780 AD).

Palaeoclimatic implications

The studied sediment record from Lake Bogoria provides evidence for climate change in tropical East Africa during the past 1700 years. The trona layers in the lower half of the sequence are remnants of hypersaline stages during a prolonged, multi-century dry period. These dry conditions seem to have started ca. 1600 cal yr BP (around 350 AD), with a change in sediment texture from clay to silt and increasing magnetic susceptibility suggesting more clastic material reaching the deepest point of the lake, which was then closer to shore. The first trona layers were deposited shortly after, suggesting a further lowering of lake level. The thickness of trona layer III and overlying sandy material suggest that severely dry conditions persisted until the early 12th century AD. If mixed-layer depth was around the same then as it is today, Lake Bogoria was not deeper than 4-5 meters.

East Africa was predominantly dry during the MCA (ca. 900-1300 AD, e.g. Verschuren and Charman, 2008). Our Lake Bogoria record also suggests a prolonged period of dry climatic conditions, at least during the first centuries of the MCA but also during the second half of the first millennium, resulting in a total of almost 800 years during which local climatic conditions were drier than today. Intermittent periods without trona deposition or with lower magnetic susceptibility may correspond to the short wet intervals which interrupted dry conditions at Lake Naivasha immediately before and during the MCA (Verschuren et al., 2000a; Verschuren, 2001). Also at Lake Edward a humid interval preceded MCA drought (Russell and Johnson, 2005).

The more positive local moisture balance indicated by the deposition of nahcolite in Unit BOG2 may reflect the first return of wetter climatic conditions ending the MCA. If that is the case, our present chronology dates this dry to wet transition to ca. 1100 AD. Soils from Loboi Swamp and Kesubo Marsh, wetland areas a few kilometres north of Lake Bogoria, show an abrupt shift of dry scrubland to wetland vegetation corresponding to the transition from the MCA to the LIA (Driese et al., 2004). Other records from eastern equatorial Africa also support this transition to a more humid environment (Verschuren, 2004), such as those from Lake Naivasha, were the first stage of water level rise following the MCA minimum occurred around 1200 AD (Verschuren et al., 2000a). Less is known about how this extra rainfall was distributed over the year. Annually laminated sediments from Lake Challa, on the border between Kenya and Tanzania, suggest that a wetter regional climate, such as inferred for the major part of the LIA, was achieved through enhanced southeastern monsoon rainfall during the long rain season, or a shorter main dry season (Wolff et al., 2011).

The halting of nahcolite deposition and simultaneous transition from sandy to silty sediments at the BOG2/3a boundary indicates a pronounced lake-level rise, sufficient to weaken the lake's stratification and prevent coarse clastics to reach the coring site, dated to ca. 1250 AD. This major lake transgression is also evident from the magnetic susceptibility decreasing throughout BOG3a, suggesting a gradual expansion of the lake's surface area with maximum water depth reached at the end of the BOG3a stage, provisionally dated to the mid-16th century. Deposition of silty clay and precipitation of magadiite during this period provides further support for this scenario. From the second half of the 16th century, magnetic susceptibility gradually increased again and magadiite deposition stopped, indicating that the LIA rainfall maximum was over by that time. Climatic drying

progressed gradually over the next two centuries, interrupted possibly by the brief return of a wetter climate around 1700 AD, to culminate in late 18th-century and 19th-century drought indicated by magnetic susceptibility values peaking above 3500 x 10^{-6} m^3/kg in the more sandy unit BOG3c. Severe drought marking the end of the LIA at the end of the 18th century seems to have been widespread in East Africa. It has so far been recorded from Lake Hayq in Ethiopia (Lamb et al., 2007); Lake Turkana (Halfman et al., 1994; Verschuren, 2004), Lake Baringo (Bessems et al., 2008; Kiage and Liu, 2009), all four lakes in the Naivasha area (Verschuren, 1999b; Verschuren et al., 2000a) and Lake Challa (Wolff et al., 2011) in Kenya; and further Lake Victoria (Stager et al., 2005) and several crater lakes in western Uganda (Bessems et al., 2008). Lake Baringo, situated only a few tens of kilometres north of Lake Bogoria, stood completely dry at this time. This event clearly also affected the hydrology of Lake Bogoria, but as suggested by the present study it seems not to have caused desiccation or even an interruption of sedimentation. High magnetic susceptibility values in units BOG3c and BOG3d suggest that throughout the 19th and 20th centuries, Lake Bogoria was smaller and shallower than at any time during the LIA.

Wet conditions during several centuries following the MCA have been inferred from multiple other lake records in the region (Verschuren and Charman, 2008). Both the Bogoria and Naivasha records point to a climate that was significantly wetter during the early (1300-1500 AD) phase and most of the main (1500-1750 AD) phase of the LIA than at any time during the most recent two centuries. However, based on our current-best chronologies the high lake levels at Bogoria peaked during the late 15th and 16th centuries, about 200 years before Lake Naivasha attained its maximum water depth. Whether this difference is due to spatial variability in climate patterns between northern and central parts of the Kenya Rift Valley is hard to pin down at present. We note that also the first indications of the onset of wet LIA conditions is dated a century earlier in Lake Bogoria (the BOG1/2 boundary, dated to 1100 AD) than in Lake Naivasha (ca. 1200 AD). It is not inconceivable that our estimate for the modern-day old-carbon age offset in Lake Bogoria is about 100 years too old: due to the Suess effect, the ^{14}C age of mid-20th century materials changes much over a relatively short calendar age interval. Also, our constraint on the true duration of massive nahcolite deposition (Unit BOG2) may be defective (Fig. 2). On the other hand, the most arid inferred climate in the recent past (unit BOG3c) is correctly dated to the early 19th century. If the 12th-century meromictic hypersaline lake which promoted nahcolite deposition was little more than a brine pool covered by a flood-produced freshwater lens, then perhaps the BOG2/3a boundary (dated to ca. 1250 AD) represents the true end of local MCA drought, which would be synchronous with the Naivasha area further south.

The flat basin morphometry, lack of river inflow, and strongly negative local hydrological budget of lakes Nakuru and Elementeita makes them prone to desiccation and sediment disturbance, and unfit as candidates for high-resolution hydroclimate reconstruction. Nevertheless, by identifying and dating the most recent desiccation horizon in each lake, we were able to demonstrate that the low lake level of Lake Naivasha recorded in the 1870's by the earliest European explorers also affected the Nakuru-Elementeita basin. The rather low water content of Unit I sediments in Lake Elementeita, again underlain by a desiccation horizon, are consistent with the evidence from Bogoria (BOG3c) for a predominantly dry climate throughout the 19th century. Reconstructions for Crescent Island Crater and lakes Oloidien and Sonachi, the three satellite lakes of Lake Naivasha with an intact sediment record for this period, also suggest lake levels as low or lower than today during much of the 19th century (Verschuren, 1999b; Verschuren et al., 1999, 2000a), with at least two arid episodes leading

to drawdowns more severe than the historical lowstand of the mid-20th century, when Lake Nakuru and probably also Lake Elementeita stood dry (Vareschi, 1982). Historical records of lake-level fluctuation in Lake Bogoria (Tiercelin et al., 1987), Lake Naivasha (Åse et al., 1986) and Lake Nakuru (Vareschi, 1982) show similar patterns, indicating that the factors controlling their hydrological budget at the decadal time scale operate on a geographically broad scale. Minor differences between these records, e.g. the sudden drop of Lake Nakuru in the early 1930's versus the more gradual decline observed for Naivasha and Bogoria through the 1930's and 1940's, can be attributed to the low groundwater buffering capacity of the present-day Lake Nakuru.

Prospects for realizing Lake Bogoria's full potential as climate-proxy record

Dating issues have plagued earlier palaeoenvironmental studies on Lake Bogoria (Tiercelin et al., 1981, 1987; Vincens et al., 1986), and as discussed above this study is no exception. Considering the magnitude of the modern old-carbon age offset (a 'reservoir' effect of nearly 4000 years) relative to the length of the studied sequence (1700 years), the inferred timing of events in the history of Lake Bogoria may be affected by as-yet unconstrained variation through time in the contribution of old dissolved carbon to the DIC assimilated by phytoplankton. Dated bulk organic matter may also contain a variable contribution of fine debris from (assumed contemporary) terrestrial plants, which would proportionally reduce the extent of the required reservoir correction. One or both of these issues, if significant, may well explain the non-linearity in the current reconstructed age-depth relationship (Fig. 2), hence affecting the inferred timing of events deduced from the climate-proxy record of Lake Bogoria. However, the non-linearity in the age-depth relationship can also be fully explained by variation through time in the rate of mid-lake sediment accumulation, and/or by comparably rapid ('event') deposition of the massive trona and nahcolite layers that alternated with accumulation of siliciclastic material and organic debris. In relatively shallow, climate-sensitive lakes, patterns of sediment distribution and focusing associated with changing lake depth can cause average mid-lake sediment accumulation to vary by a factor of up to five on a time scale of decades (Verschuren, 1999a, 2001). Given East Africa's regional scarcity of continuous climate-proxy archives spanning several millennia, being deterred by the geochronological challenges posed by the Lake Bogoria record is no option. Instead, further studies on the high-resolution climate-proxy signals contained in its sediments, using a new suite of sediment cores, must include a focused strategy of multiple, paired dating of bulk sediment and terrestrial plant macrofossils to separate the possible influences of a variable old-carbon age offset and of sedimentation-rate variability.

REFERENCES

Alin SR and Cohen AS. (2003) Lake-level history of Lake Tanganyika, East Africa, for the past 2500 years based on ostracode-inferred water-depth reconstruction. Palaeogeography Palaeoclimatology Palaeoecology 199, 31-49.

Appleby PG and Oldfield F. (1978). The calculation of dates assuming a constant rate of supply of unsupported ^{210}Pb to the sediment. CATENA 5, 1–8.

Åse LE, Sernbo K, Syren P. (1986). Studies of Lake Naivasha, Kenya and its drainage area. Research report. Institute of Physical Geography, Stockholm University.

Ballot A, Krienitz L, Kotut K, Wiegand C, Metcalf JS, Codd GA, Pflugmacher S. (2004). Cyanobacteria and cyanobacterial toxins in three alkaline rift valley lakes of Kenya - Lakes Bogoria, Nakuru and Elmenteita. Journal of Plankton Research 26, 925-935.

Bengtsson L and Enell M. (1986). Chemical analysis. In: Berglund, B.E. (ed.) Handbook of Holocene palaeoecology and palaeohydrology. Wiley and sons, New York, pp. 423-451.

Bessems I, Verschuren D, Russell JM, Hus J, Mees F, Cumming BF. (2008). Palaeolinmological evidence for widespread late 18th century drought across equatorial East Africa. Palaeogeography Palaeoclimatology Palaeoecology 259, 107-120.

Binford MW. (1990) Calculation and uncertainty analysis of ^{210}Pb dates for PIRLA project lake sediment cores. Journal of paleolimnology 3, 253-267.

Blaauw M. (2010). Methods and code for 'classical' age-modelling of radiocarbon sequences. Quaternary Geochronology 5, 512-518.

Blaauw M, van Geel B, Kristen I, Plessen B, Lyaruu A, Engstrom DR, van der Plicht J, Verschuren D. (2011). High-resolution C-14 dating of a 25,000-year lake-sediment record from equatorial East Africa. Quaternary Science Reviews 30, 3043-3059.

Bricker, OP. (1969). Stability constants and Gibbs free energies of formation of magadiite and kenyaite. The American Mineralogist 54, 1026-1033.

Christensen JH, Hewitson B, Busuioc A, Chen A, Gao X, Held I, Jones R, Kolli RK, Kwon W-T, Laprise R, Magaña Rueda V, Mearns L, Menéndez CG, Räisänen J, Rinke A, Sarr A, Whetton P. (2007). Regional Climate Projections. In: Solomon S, Qin D, Manning M, Chen Z, Marquis M, Averyt KB, Tignor M, Miller HL. (eds.) Climate Change 2007: The Physical Science Basis. Contribution of Working Group I to the Fourth Assessment Report of the Intergovernmental Panel on Climate Change. Cambridge University Press, Cambridge, United Kingdom and New York, NY, USA.

Dearing JA. (1999). Holocene environmental change from magnetic proxies in lake sediments. In: Maher BA and Thompson R. (eds.) Quaternary Climates, environments and magnetism, pp. 231-278.

Driese SG, Ashley GM, Li ZH, Hover VC, Owen RB. (2004) Possible Late Holocene equatorial palaeoclimate record based upon soils spanning the Medieval Warm Period and Little Ice Age, Loboi Plain, Kenya. Palaeogeography Palaeoclimatology Palaeoecology 213, 231-250.

Duehnforth M, Bergner AGN, Trauth MH. (2006) Early holocene water budget of the Nakuru-Elmenteita Basin, Central Kenya Rift. Journal of Paleolimnology 36, 281-294.

Eugster HP. (1966) Sodium carbonate-bicarbonate minerals as indicators of pCO_2. Journal of Geophysical Research 71, 3369-3377.

Eugster HP. (1967) Hydrous sodium silicates from Lake Magadi Kenya: precursors of bedded chert. Science 157, 1177-1180.

Graig H. (1957) Isotopic standards for carbon and oxygen and correction factors for mass-spectrometric analysis of carbon dioxide. Geochimica et Cosmochimica Acta 12, 133-149.

Halfman JD, Johnson TC, Finney BP. (1994) New ams dates, stratigraphic correlations and decadal climatic cycles for the past 4-ka at Lake Turkana, Kenya. Palaeogeography Palaeoclimatology Palaeoecology 111, 83-98.

Hassan RM. (2010) Implications of Climate Change for Agricultural Sector Performance in Africa: Policy Challenges and Research Agenda. Journal of African Economies 19, 77-105.

Hughes RH and Hughes JS. (1992) A directory of African wetlands. IUCN, Gland, Switzerland and Cambridge, UK / UNEP, Nairobi, Kenya / WCMC, Cambridge, UK.

Hutchinson GE. (1957) A treatise on limnology. Volume I.Wiley, New York, NY, US.

Kiage LM and Liu K. (2009) Palynological evidence of climate change and land degradation in the Lake Baringo area, Kenya, East Africa, since AD 1650. Palaeogeography Palaeoclimatology Palaeoecology 279, 60-72.

Lagaly G, Beneke K, Weiss A. (1975) Magadiite and h-magadiite 1. Sodium magadiite and some of its derivatives. American Mineralogist 60, 642-649.

Lamb HF, Leng MJ, Telford RJ, Ayenew T, Umer M. (2007) Oxygen and carbon isotope, composition of authigenic carbonate from an Ethiopian lake: a climate record of the last 2000 years. Holocene 17, 517-526.

LaVigne M and Ashley GM. (2001) Climatology and Rainfall Patterns: Lake Bogoria National Reserve (1976–2001). Department of Geological Sciences, Rutgers University, Piscataway, NJ, USA.

Last W. (2001) Mineralogical analysis of lake sediments. In: Last WM and Smol JP (eds.) Tracking environmental change using lake sediments, volume 2, physical and geochemical methods, pp. 143-187.

Mees F, Reyes E, Keppens E. (1998) Stable isotope chemistry of gaylussite and nahcolite from the deposits of the crater lake at Malha, northern Sudan. Chemical Geology 146, 87-98.

Mees F, Verschuren D, Nijs R, Dumont HJ. (1991) Holocene evolution of the crater lake at Malha, Northwest Sudan. Journal of Paleolimnology 5: 227-253.

Moberg A, Sonechkin DM, Holmgren K, Datsenko NM, Karlen W. (2005) Highly variable Northern Hemisphere temperatures reconstructed from low- and high-resolution proxy data. Nature 433, 613-617.

Morellon M, Valero-Garces B, Vegas-Vilarrubia T, Gonzalez-Samperiz P, Romero O, Delgado-Huertas A, Mata P, Moreno A, Rico M, Pablo Corella J. (2009. Lateglacial and Holocene palaeohydrology in the western Mediterranean region: the Lake Estanya record (NE Spain). Quaternary Science Reviews 28, 2582-2599.

Nicholson SE. (1996) A review of climate dynamics and climate variability in eastern Africa. In: Johnson TC, Odada E (eds.) The Limnology, Climatology and Paleoclimatology of the East African Lakes. Gordon & Breach, New York, USA, pp. 25–56.

Nilsson E. (1931) Traces of ancient change of climate in East Africa. Geografiska Annaler 17, 1–21.

Reimer PJ, Baillie MGL, Bard E, Bayliss A, Beck JW, Blackwell PG, Ramsey CB, Buck CE, Burr GS, Edwards RL, Friedrich M, Grootes PM, Guilderson TP, Hajdas I, Heaton TJ, Hogg AG, Hughen KA, Kaiser KF, Kromer B, McCormac FG, Manning SW, Reimer RW, Richards DA, Southon JR, Talamo S, Turney CSM, van der Plicht J, Weyhenmeye CE. (2009). Intcal09 and marine09 radiocarbon age calibration curves, 0-50,000 years cal bp. Radiocarbon 51, 1111-1150.

Reitsema RH. (1980) Dolomite and nahcolite formation in organic rich sediments - isotopically heavy carbonates. Geochimica et Cosmochimica Acta 44, 2045-2049.

Renaut RW, Tiercelin JJ, Owen RB (1986). Mineral precipitation and diagenesis in the sediments of the Lake Bogoria basin, Kenya Rift Valley. In: Frostock, L.E. and Renaut, R.W. (eds.) Sedimentation in the African rifts. Geological Society Special Publication 25, 159-175.

Richardson JL and Dussinger RA. (1986) Paleolimnology of mid-elevation lakes in the Kenya Rift Valley. Hydrobiologia 143: 167–174.

Russell JM and Johnson TC. (2005) A high-resolution geochemical record from Lake Edward, Uganda Congo and the timing and causes of tropical African drought during the late Holocene. Quaternary Science Reviews 24, 1375-1389.

Russell JM and Johnson TC. (2007) Little Ice Age drought in equatorial Africa: Intertropical Convergence Zone migrations and El Nino-Southern Oscillation variability. Geology 35, 21-24.

Russell JM, Verschuren D, Eggermont H. (2007) Spatial complexity of 'Little Ice Age' climate in East Africa: sedimentary records from two crater lake basins in western Uganda. Holocene 17, 183-193.

Ryves DB, Mills K, Bennike O, Brodersen KP, Lamb AL, Leng MJ, Russell JM, Ssemmanda I. (2011). Environmental change over the last millennium recorded in two contrasting crater lakes in western Uganda, eastern Africa (Lakes Kasenda and Wandakara). Quaternary Science Reviews 30, 555-569.

Schnurrenberger D, Russell J, Kelts K. (2003). Classification of lacustrine sediments based on sedimentary components. Journal of Paleolimnology 29, 141-154.

Stager JC, Cocquyt C, Bonnefille R, Weyhenmeyer C, Bowerman N. (2009) A late Holocene paleoclimatic history of Lake Tanganyika, East Africa. Quaternary Research 72, 47-56.

Stager JC, Ryves D, Cumming BF, Meeker LD, Beer J. (2005). Solar variability and the levels of Lake Victoria, East Africa, during the last millenium. Journal of Paleolimnology 33, 243-251.

Talbot MR. (1990) A review of the paleohydrological interpretation of carbon and oxygen isotopic-ratios in primary lacustrine carbonates. Chemical Geology 80, 261-279.

Talling JF and Lemoalle J. (1998) Ecological dynamics of tropical inland waters. Cambridge University Press, Cambridge, UK.

Tiercelin JJ, Renaut RW, Delibrias G, Le Fournier J, Bieda S. (1981) Late Pleistocene and Holocene lake level fluctuations in the lake Bogoria basin, northern Kenya Rift Valley. In: Coetzee JA, Van Zinderen Bakker Sr. EM. (eds.) Palaeoecology of Africa and the surrounding islands, Volume 13.

Tiercelin JJ, Vincens A, Barton CE, Carbonel P, Casanova J, Delibrias G, Gasse F, Grosdidier E, Herbin J-P, Huc AY, Jardiné S, Le Fournier J, Mélières F, Owen RB, Pagé P, Palacios C, Paquet H, Péniguel G, Peypouquet J-P, Raynaud J-F, Renaut RW, de Renéville P, Richert J-P, Riff R, Robert P, Seyve C, Vandenbroucke M, Vidal G. (1987) Le demi-graben de Baringo-Bogoria, Rift Gregory, Kenya. 30000 ans d'histoire hydrologique et sédimentaire. Bulletin des Centres de Recherche Exploration - Production Elf Aquitaine 11(2), 249-540.

Tierney JE, Russell JM, Damste JSS, Huang YS, Verschuren D. (2011) Late Quaternary behavior of the East African monsoon and the importance of the Congo Air Boundary. Quaternary Science Reviews 30, 798-807.

Valero-Garces BL, Navas A, Machin J, Stevenson T, Davis B. (2000) Responses of a saline lake ecosystem in a semiarid region to irrigation and climate variability - The history of Salada Chiprana, central Ebro basin, Spain. Ambio 29, 344-350.

Vareschi E. (1982) The ecology of lake nakuru (kenya), III: abiotic factors and primary production. Oecologia 55:81-101.

Verschuren D. (1993) A lightweight extruder for accurate sectioning of soft-bottom lake sediment cores in the field. Limnology and Oceanography 38, 1796-1802.

Verschuren D. (1999a) Sedimentation controls on the preservation and time resolution of climate-proxy records from shallow fluctuating lakes. Quaternary Science Reviews 18, 821-837.

Verschuren D. (1999b) Influence of depth and mixing regime on sedimentation in a small, fluctuating tropical soda lake. Limnology and Oceanography 44(4), 1103-1113.

Verschuren D. (2001) Reconstructing fluctuations of a shallow East African lake during the past 1800 yrs from sediment stratigraphy in a submerged crater basin. Journal of Paleolimnology 25, 297-311.

Verschuren D. (2003) Lake-based climate reconstruction in Africa: progress and challenges. Hydrobiologia 500, 315-330.

Verschuren D. (2004) Decadal to century-scale climate variability in tropical Africa during the past 2000 years. In: Battarbee RW, Gasse F, Stickley C. (eds.) Past climate variability through Europe and Africa, Kluwer, Dordrecht, The Netherlands, pp. 139-158.

Verschuren D. and Charman D. (2008) Latitudinal linkages in late-Holocene moisture-balance variation. In Battarbee RW and Binney HA (eds.) Natural climate variability and global warming. Wiley-Blackwell, Chichester, UK, pp. 189-231.

Verschuren D, Tibby J, Leavitt PR, Roberts CN. (1999) The environmental history of a climate-sensitive lake in the former 'White Highlands' of central Kenya. Ambio 28, 494-501.

Verschuren D, Laird KR, Cumming BF. (2000a) Rainfall and drought in equatorial east Africa during the past 1,100 years. Nature 403, 410-414.

Verschuren S, Tibby J, Sabbe K, Robberts N. (2000b) Effects of depth, salinity, and substrate on the invertebrate community of a fluctuating tropical lake. Ecology 81(1), 164-182.

Vincens A, Casanova J, Tiercelin JJ. (1986) Palaeolimnology of Lake Bogoria (Kenya) during the 4500 BP high lacustrine phase. In: Sedimentation in the African Rifts. Geological Society Special Publications 25: 323-330.

Washbourn-Kamau, CK. (1971) Late quaternary lakes in Nakuru-Elmenteita basin, kenya. Geographical Journal 137, 522-535.

Williams AP and Funk C. (2011) A westward extension of the warm pool leads to a westward extension of the Walker circulation, drying eastern Africa. Climate Dynamics 37, 2417-2435.

Wolff C, Haug GH, Timmermann A, Damste JSS, Brauer A, Sigman DM, Cane MA, Verschuren D. 2011) Reduced Interannual Rainfall Variability in East Africa During the Last Ice Age. Science 333, 743-747.

Wright HE. (1980) Coring of soft lake sediments. Boreas 9, 107-114.

4 MULTI-BASIN DEPOSITIONAL FRAMEWORK FOR HIGH-RESOLUTION MOISTURE-BALANCE RECONSTRUCTION AT LAKE BOGORIA (CENTRAL RIFT VALLEY, KENYA)

De Cort, Gijs[1,2]; Mees, Florias[2]; Ryken, Els[1]; Christian Wolff[3]; Creutz, Mike[1]; Haug, Gerald[4]; Peter Appleby[5]; Renaut, Robin[6]; Verschuren, Dirk[1]

[1]*Limnology Unit, Department of Biology, Ghent University. K.L. Ledeganckstraat 35, 9000 Ghent, Belgium.*
[2]*Department of Earth Sciences, Royal Museum for Central Africa. Leuvensesteenweg 13, 3080 Tervuren, Belgium.*
[3]*Institute of Earth and Environmental Science, University of Potsdam. Karl-Liebknecht-Strasse 24-25, 14476 Potsdam-Golm, Germany*
[4]*Geological Institute, Department of Earth Sciences, ETH Zürich. Sonneggstrasse 5, 8092 Zürich, Switzerland.*
[5]*Department of Mathematical Sciences, University of Liverpool. Roxby Building, Myrtle Street, Liverpool L69 7ZT, UK.*
[6]*Department of Geological Sciences, University of Saskatchewan. Saskatoon, SK, Canada S7N 5E2.*

This chapter is in preparation for submission to *Sedimentology*. The author list and sequence may still change. Parts of the present discussion may be excised for use in a separate publication focusing on the high-resolution climate-proxy record.

Following a first exploration of hydrological change at Lake Bogoria (see Chapter 3), this chapter presents a new and well-substantiated moisture-balance record from this hypersaline, alkaline lake. Based on high-resolution proxy data for deposits from the small but relatively deep southern basin combined with sedimentological data at four other core sites throughout the lake, it provides clear evidence of strong hydroclimate variability over the past ca. 1,300 years, surpassing the 20th-century range known from historical documentation. By closing a geographical gap in the available network of high-resolution moisture-balance records from equatorial East Africa, this new record contributes significantly to our understanding of the main dynamics and drivers of decade- to century-scale hydroclimate variability in East Africa during the past millennium. This new Bogoria sediment record also provides clear evidence for a severe increase in soil erosion and terrestrial sediment supply in recent decades, which is alarming given the uniqueness and protected status of this geothermal spring-fed lake environment.

INTRODUCTION

The Fifth Assessment Report (AR5) of the Intergovernmental Panel on Climate Change (IPCC) stresses the importance of high-quality paleoclimate data (Masson-Delmotte et al., 2013). For East Africa specifically, studies point out that a better understanding of natural climatic variability is crucial to improve model-simulated forecasts of future climate change (Rowell et al., 2015). However, well-dated climate-proxy records spanning at least the past 1000 years with sufficient time control and resolution to meaningfully contribute to our understanding of regional climate dynamics exist from only a handful of locations in East Africa (Verschuren, 2004). Although this sparse network of reconstructions has already revealed non-uniform sub-regional patterns in moisture-balance variation over the past millennium (Russell & Johnson, 2007; Russell et al., 2007; Verschuren & Charman, 2008; Tierney et al., 2013; Chapter 2), there is a clear need for better geographical coverage to constrain the full natural dynamics of rainfall and drought on the temporal scales most relevant to human activity. In this context, we here further explore the potential of the Lake Bogoria sediment record as a continuous and high-resolution archive for past hydroclimate change in the

central Rift Valley of Kenya, an area where boreal-summer dry-season moisture supplied by westerly flow represents a substantial part of total annual rainfall, and thus potentially affected by past zonal shifts in the mean position of the Congo Air Boundary. The results of multi-proxy but mostly low-resolution sedimentological and geochemical analyses obtained on cores collected in 2001 and 2003 (Chapter 3) already demonstrated that past climatic moisture-balance variations have induced severe changes in the hydrological and sedimentological characteristics of this lake over the past millennium. Unlike most other lakes in Kenya's central Rift Valley, Lake Bogoria did not dry out during the late-18th and early 19th-century episode of pronounced and widespread aridity (Verschuren, 2001; Bessems et al., 2008), distinguishing it as one of the very few Kenyan lakes where continuous paleoclimate reconstruction going back multiple centuries is possible. However, the analyses presented in Chapter 3 were handicapped by poor recovery of the soft and gas-charged uppermost sediments, and by problematic age control owing to a very large old-carbon effect on the sediment's bulk organic matter. In this chapter, we present and integrate sedimentological, geochemical, mineralogical and chronological data on five composite sediment cores, each of them including a perfectly intact sediment-water interface, recovered from central locations in the three basins of Lake Bogoria and from the crest of the sills separating them. The interpretation of sediment proxies is further aided by data on seasonal sedimentation dynamics obtained from sediment traps. This validated multi-proxy and multi-basin approach allows for robust interpretation of the high-resolution hydroclimate signals contained within the sediments of Lake Bogoria, and identifies the sedimentary archive of its southern basin as the optimal site for obtaining a continuous, high-resolution reconstruction of past regional hydroclimate variability.

STUDY SITE

Lake Bogoria (17 km long, 4 km wide) occupies the southern end of a half-graben depression in the central Kenya Rift Valley, ca. 25 km north of the equator (Fig. 1). Rainfall in equatorial East Africa is mainly connected to the twice-yearly passage of the Intertropical Convergence Zone (ITCZ), producing 'long rains' in March-May (MAM) and the 'short rains' in October-December (OND). From June to August (JJA), frequent late afternoon cloudbursts also produce significant amounts of precipitation at Lake Bogoria, whereas the period from December to February (DJF) is dry (Fig. 1, LaVigne and Ashley, 2001). As an endorheic lake in a tropical semi-arid climate regime, its strongly concentrated alkaline waters are usually hypersaline with Na^+, CO_3^{2-}, HCO^{3-} and Cl^- as major ions. The lake's hydrochemistry is further influenced by numerous hot springs above and below the present-day water surface (Fig. 1; Tiercelin et al., 1987), which presently contribute an estimated 30% to the lake's total water budget (Robin Renaut, pers. comm.). Strong chemical stratification, with less saline surface waters overlying a more saline and dense layer of bottom water, results in meromixis with a permanently anoxic hypolimnion. Situated at ca. 996 m above sea level (a.s.l.) in 2014, the lake's overflow level is set at 999 m a.s.l. by the elevation of the Marigat-Loboi plain immediately to the northwest, across which Lake Bogoria used to flow into the Lake Baringo catchment during several episodes in the early and mid-Holocene (Vincens et al., 1986). Along its north-south oriented longitudinal axis, Lake Bogoria is divided in three depositional basins of varying area and depth (Fig. 2, Hickley et al., 2003). The shallow northern basin (12.1 m in 2014) is separated from the large and deeper central basin (16 m in 2014) via a narrow passage over a relatively high sill (the north-central sill: 10.6 m in 2014). A similarly narrow but lower sill (central-south sill: 13.3 m in 2014) leads to the southern basin (15.1 m in 2014), the smallest in surface area but nearly as deep as the central basin. The largest inflowing river system, the Sandai-Waseges, drains two-thirds of the Lake Bogoria

catchment (ca. 700 km^2, Tiercelin et al., 1987) and enters the lake from the north, creating a broad flood plain at the lake's north shore. The river is classified as ephemeral, but can approach perennial character during exceptionally wet years (Renaut et al., 1986). Surface inflow into the central and southern basins is less extensive and only in the form of small seasonal streams.

METHODS

Field operations

In August 2012, short pilot cores were collected from the southern basin, alternatively using a rod-operated single-drive piston corer (Wright, 1980), a modified freeze corer (Verschuren, 2000), and a UWITEC© gravity corer. Only the piston corer successfully recovered the sediment-water interface intact, after several trials to correctly determine the water depth at which to secure the piston cable. The UWITEC gravity corer consistently over-penetrated the exceedingly soft surface sediments, even when it was gently lowered by its own weight. The freeze corer also sank too deep, and an attempt to prevent over-penetration by securing its deployment line to the coring platform made sample collection subject to heave. In July 2014, composite sediment cores were collected at five core sites: the deepest points of the northern, central and southern basins, and the crest of the sills separating them (Fig. 2, Table 1). Depth at the coring sites was initially estimated by means of a handheld echo-sounding device, which had considerable trouble dealing with the well-developed chemocline that was revealed to be perennial by seasonal measurements of conductivity (supplemented with temperature, dissolved oxygen and pH) at 0.5- to 1-m intervals throughout the water column using a Hydrolab® multiprobe device (Fig. 3). At each site the sediment-water interface was recovered using a UWITEC gravity corer; in the event of initial over-penetration, we partly offset its fall weight by means of a submersed float. Extreme care was taken to avoid violent degassing of the soft upper mud (*in situ* water content >95%) during release of hydrostatic pressure, as this would have destroyed the sediment's fine lamination. Afterwards, duplicates of the upper sediments were collected by piston coring, which also allowed the determination of exact water depth by observing the position of the sediment-water interface in the cores (which have a known drive depth).

Core site	*Coordinates*	*Water depth (m), July 2014*	*Sediment sequence*	*Length of sediment sequence (cm)*
North Basin	00°19'11.3" N, 36°04'49.6" E	12.1	BOGN14	222
North-Central Sill	00°18'13.6"N, 36°05'02.3" E	10.6	BOGNC14	143
Central Basin	00°13'23.0" N, 36°06'28.7" E	16	BOGC14	176
Central-South Sill	00°12'18.3" N, 36°07'11.2" E	13.3	BOGCS14	121
South Basin	00°11'31.7" N, 36°06'58.6" E	15.1	BOGS14	299

Table 1 Specifics of the five sediment sequences collected from Lake Bogoria in July 2014.

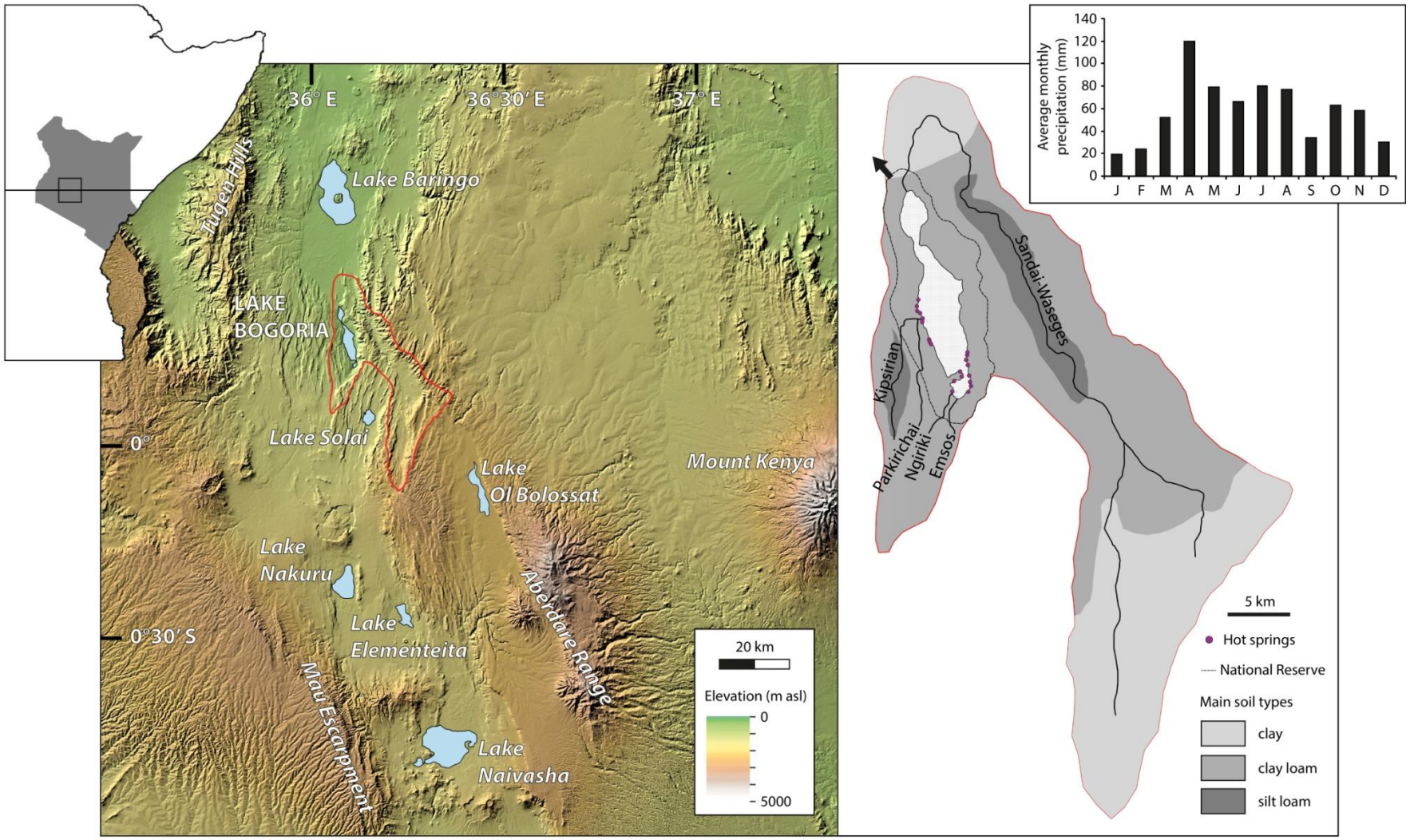

Fig. 1 Left: Location of Lake Bogoria within the Kenya Rift Valley, with the catchment indicated by a red line. Right: Lake Bogoria's catchment, with location of National Reserve boundary, hot springs (Renaut et al., 1986), most important seasonal rivers and soil types (Mugo, 2007). The arrow indicates the overflow point towards Lake Baringo at 999 m a.s.l. Inset: Average monthly rainfall over the period 1977-2001 (LaVigne and Ashley, 2001).

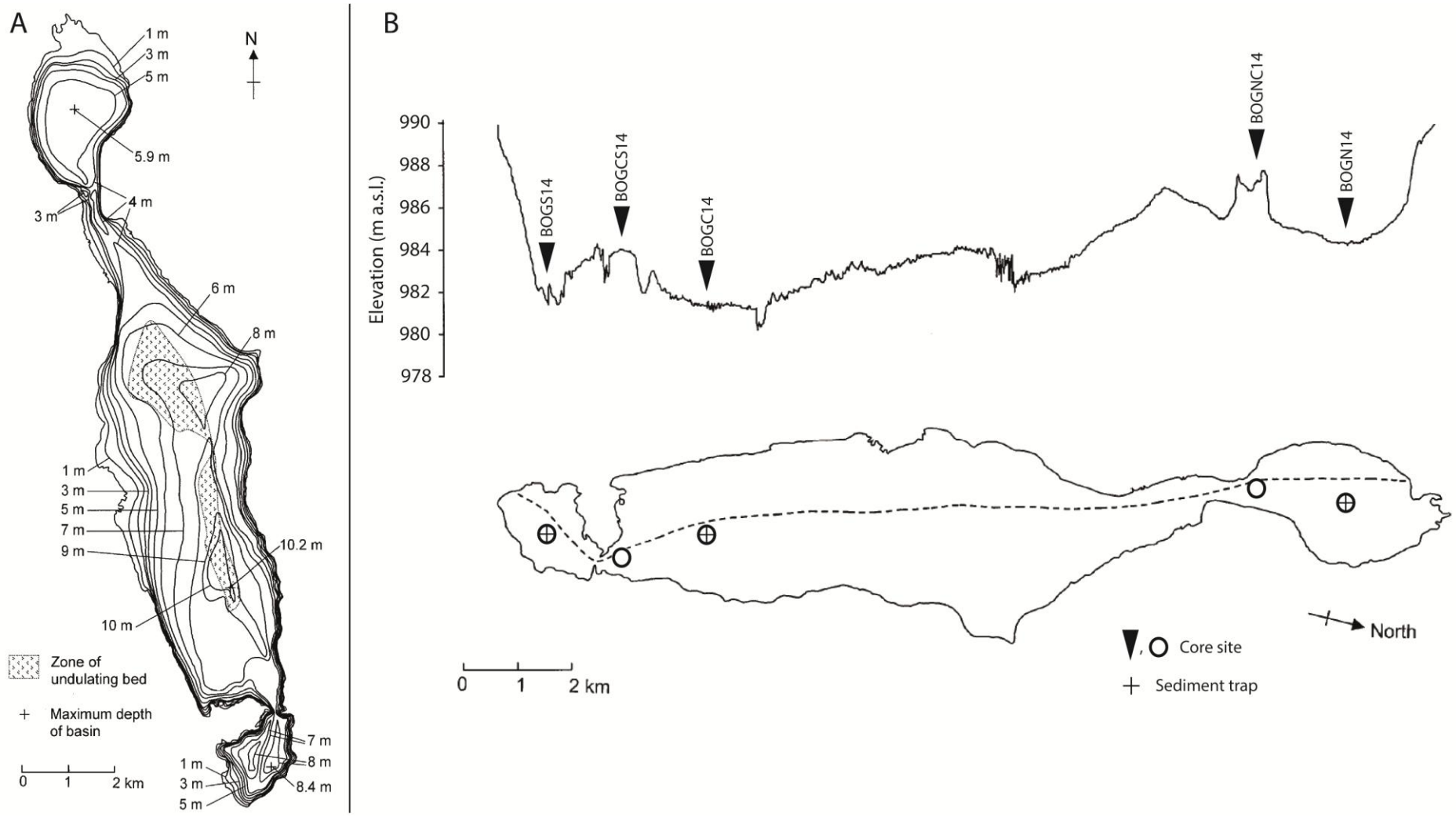

Fig. 2 A: Bathymetric map of Lake Bogoria from a survey in August 2002, when lake level was at ca. 990 m a.s.l. B: Depth of Lake Bogoria along a north-south transect, with indication of the location of the five core sites and three sediment trap sites (see Tables 1, 2). Adapted from Hickley et al. (2003).

On the lake, the gravity cores were stabilized by keeping them upright and adding water up to the tube rim before capping. Onshore the superfluous water was discarded, and the upper part of the cores was drained by drilling a vertical series of small holes below the sediment-water interface. Simultaneously the cores were allowed to evaporate water from their surface for up to ca. 48 hours. This process resulted in the upper core surface to lower by 2-3 cm, and for the mud to become sufficiently stable for transport without mixing. Nevertheless, capped and taped cores were continuously monitored for water loss, the occurrence of which implies the formation of air pockets inside the tubes and, thus, the possibility of sediment moving. In that case, the cores were opened in upright position, pressed down into the tube, and any voids on top filled with wet foam. As a result of this procedure, cores were often several cm shorter upon arrival in the laboratory than as immediately *ex situ*, and had lower water content than *in situ*. However, the preservation of visible fine lamination up to the sediment-water interface confirmed the intact, undisturbed nature of even the most recently deposited watery sediments. The deeper sediment column at all five sites was recovered with a single-drive piston corer, adjusting the tension on the piston to allow a sub-surface drive start. These core sections were capped immediately, but similarly monitored continuously for water loss between their collection and their arrival in the laboratory.

	Deployment	***Sampling 1***	***Sampling 2***	***Sampling 3***	***Sampling 4***	***Sampling 5***
North	9/07/2014	3/10/2014	8/12/2014	5/03/2015	6/06/2015	30/07/2015
Central	13/07/2014	2/10/2014	8/12/2014	5/03/2015	6/06/2015	29/07/2015
South	14/07/2014	2/10/2014	8/12/2014	5/03/2015	6/06/2015	28/07/2015

Table 2 Deployment of sediment traps at Lake Bogoria.

To document the seasonal sedimentation dynamics in Lake Bogoria, duplicate sediment traps were installed below the chemocline, suspended from floating buoys at the coring sites of the north, central and south basins. After deployment in early July 2014 (i.e., mid-way through the main dry season, JJAS), they were emptied five times during the following year (Table 2), namely at the end of each successive wet and dry season recognized in the region of Lake Bogoria, and finally slightly over one year after their initial deployment. Unfortunately, tampering with this set-up by unknown individuals compromised some of the retrieved samples.

Laboratory analyses

The recovered sediment cores were transported to Ghent University, where they were split lengthwise into two identical halves. Core halves were photographed using a digital line-scan camera, and gamma density, volume-specific magnetic susceptibility (κ) and wave-length specific colour reflectance were measured at 2-mm intervals, using a ^{137}Cs-source with gamma-ray detector system, a Bartington point sensor MS2E and a Konica Minolta CM-2600d spectrophotometer mounted on a Multi-Sensor Core Logger installation (Geotek Ltd, Daventry, Northants, UK). Non-destructive x-ray fluorescence (XRF) analysis was conducted on the archive core half using the AVAATECH X-Ray Fluorescence Core Scanner at ETH-Zürich, in contiguous intervals of either 2 or 5

mm. Elemental counts were converted to percentages of total counts, to account for differential equipment settings (energy level of X-ray source, count time) and specimen effects such as water content and core surface geometry (Röhl and Abrams, 2000). Titanium is usually not incorporated in minerals formed by in-lake processes, and is hence used as a proxy for catchment-derived clastic mineral input (Davies et al., 2015). Chlorine has been used as a proxy for salt-water content in marine sediments (Tjallingii et al., 2007). In Lake Bogoria, this element is present in the saline pore water and possibly in salts (i.e. halite) precipitated during the final stages of Na-CO3-HCO3-Cl brine evolution upon extreme evaporative concentration (Eugster and Jones, 1979). When corrected for water content, it can thus be used as a proxy for salinity. The elemental ratio of Mn/Fe has often been used as a proxy for redox conditions (e.g. Haberzettl et al., 2007; Melles et al., 2012), as the solubility of Mn is more readily affected than that of Fe under reducing conditions (Boyle, 2001; Davies et al. 2015). Specific wet and dry weight as well as porosity and water, organic matter, carbonate and siliciclastic content were determined by the loss-on-ignition (LOI) method (Dean, 1974; Bengtsson and Enell, 1986) at contiguous 1-cm intervals, except for the rapidly deposited sediments of the northern basin and north-central sill, where a contiguous 2- or 4-cm resolution was applied. In Lake Bogoria's hydrochemical setting, carbonate content will largely be determined by salt content of pore water or in-situ presence of sodium carbonate minerals. This also means that water content as derived from LOI is systematically underestimated, not only because of partial dehydration of sediment cores for stabilization purposes (see above), but also as dissolved salts (which make up a significant share of the water volume in the sediment) are not removed by heating at 105°C. Specific dry weight (corrected for salt content) was used to calculate mass-specific magnetic susceptibility (χ). The grain-size distribution of the terrigenous clastic fraction was measured at contiguous 1-cm to non-contiguous 4-cm intervals throughout the three mid-basin composite sequences using a Malvern 3000 Laser Diffraction Particle Analyzer (Malvern Instruments Ltd., Worcestershire, UK), after pre-treatment of the sediment samples to sequentially remove carbonates (using HCl), organic matter (using H_2O_2) and biogenic silica (using KOH; Vaasma, 2008). In the sediment sequences of the three mid-basin sites, macro-charcoal particles (sieved using 100-µm mesh size), reflecting past fires in the vegetation surrounding Lake Bogoria, were counted at contiguous 0.5-cm to non-contiguous 2-cm intervals under a binocular microscope. At selected depths guided by lithostratigraphy, the mineralogical composition of bulk sediment and salt occurrence was determined using x-ray diffraction (XRD; Bruker D8 Discover system). These samples were air-dried and ground by mortar and pestle to a fine powder before measurement. A number of bulk samples were rinsed with deionised water through diffusion over a 12-14 kD molecularporous membrane to remove sodium carbonates, with the intention of obtaining clay mineral data for oriented slides, for unsaturated dried suspensions, before and after glycol treatment. However, only limited information could be obtained for the clay fraction, because of the abundance of feldspar. To investigate the nature of the finely laminated upper facies, selected intervals where sampled for the preparation of thin sections. To prevent both shrinkage and sample desintegration through salt crystallization from interstitial solutions, the samples were pre-treated by immersion in acetone until all water was removed. Because initial tests showed strong swelling of unconstrained material, the samples were tightly packed in perforated tin foil. This was followed by impregnation with a cold-setting polyester resin under low vacuum. Subsequently, thin sections were prepared and analysed under plane- and cross-polarized light using a petrographic microscope.

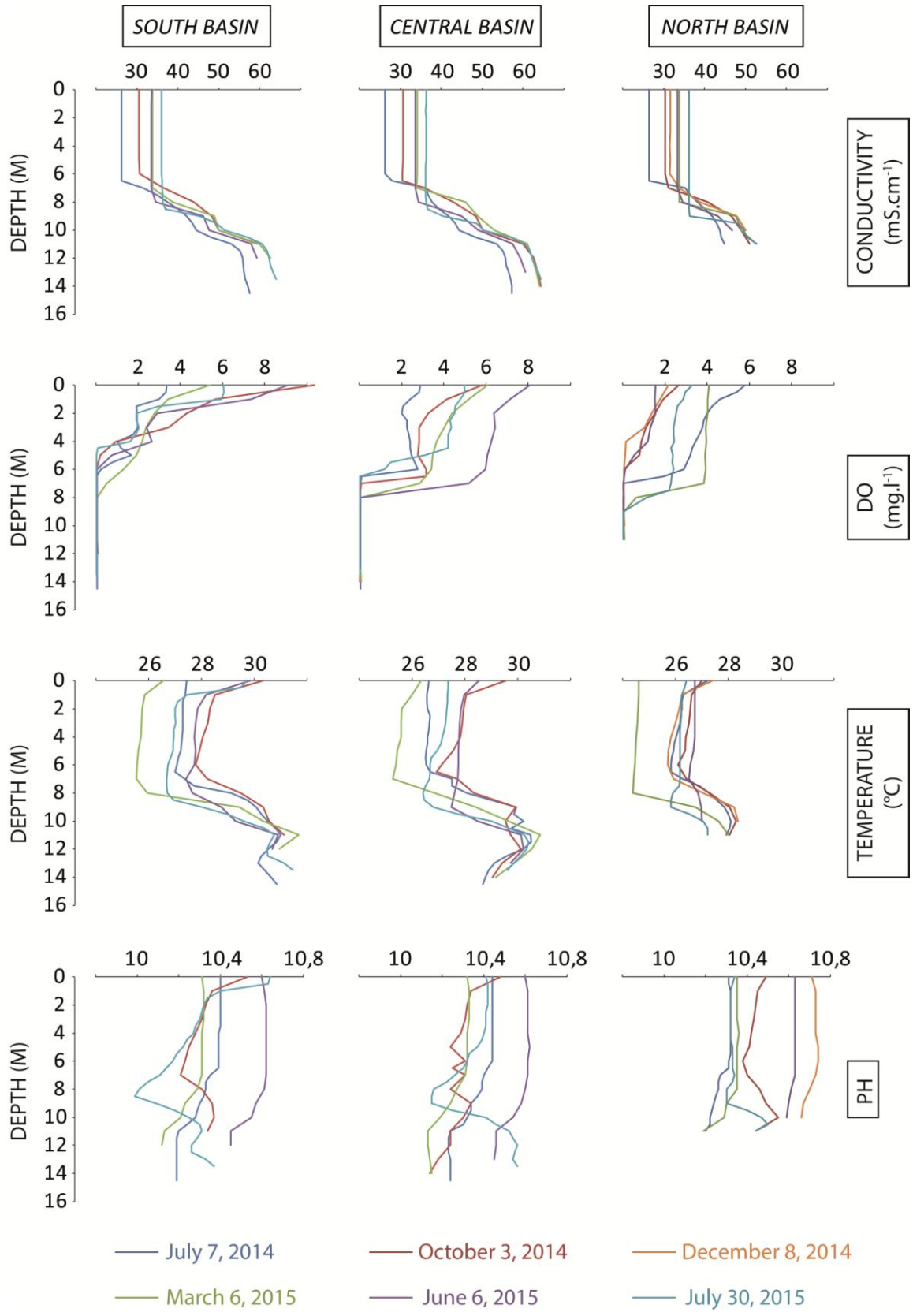

Fig. 3 Seasonal water-column readings of Lake Bogoria, collected between July 2014 and July 2015, demonstrate year-round stable stratification.

Inter-basin core cross-correlation

To correlate temporal patterns of sedimentation across the three mid-basin locations and the two sills, a comprehensive set of tie points was assembled using detailed inspection of the core images (most useful in the uppermost unit of finely laminated sediments) and the available array of high-resolution sedimentological and geochemical data. This comprehensive tie-point procedure allowed direct transfer of all available chronological information between the five core sites, enabling a chronologically robust inter-basin comparison of sedimentation dynamics through time.

Sediment-trap samples

The sediment-trap samples were rinsed through three cycles of diluting with distilled water, settling and decanting to remove the high amounts of dissolved ions in the superfluous water. Afterwards, the samples were freeze-dried and their grain-size distribution analyzed using the method described above. Additionally, samples were analyzed for mass-specific magnetic susceptibility and % TC, TOC and TN at the Helmholtz Centre Potsdam GFZ (Germany). For analysis of the total carbon (TC) and total organic carbon (TOC) content, samples were placed in Ag capsules, treated with 20% HCl at 75°C, and subsequently processed in a Carlo Erba NC 2500 elemental analyzer. The results were referenced against lab-internal soil standards. Total nitrogen (TN) content measurements were carried out with the same analytical facility (Sn capsules, no acid treatment).

Chronology

To date the uppermost sediments, 17 freeze-dried samples from the top 40 cm of the sediment sequence from Lake Bogoria's central basin (BOGC14) were analysed for ^{210}Pb and ^{226}Ra by direct gamma assay in the Environmental Radioactivity Laboratory at Liverpool University. Additionally, the depth profile of ^{137}Cs was measured to constrain the 1963 fallout maximum of above-ground nuclear bomb testing. To compensate for the low levels of deposition of these radio-nuclides in this low-rainfall area, which had hindered previous dating exercises (see Chapter 3), large sample sizes (1.5 to 2 g dry sediment) were combined with long counting times (up to > 4 days for samples close to equilibrium). Pb-210 dates were calculated using the constant-rate-of-supply (CRS) dating model (Appleby *et al*., 1978), using the 1963 ^{137}Cs time marker as reference point (Appleby, 2001). Age estimates for the deeper sediments were obtained by radiocarbon dating. Given the extremely large old-carbon effect on bulk-sediment ages from Lake Bogoria (ca. 4,000 years; Chapter 3), the deliberate choice was made to consider ^{14}C dates obtained on terrestrial plant materials only. Availability of a complete macro-charcoal inventory permitted targeted extraction, and as the distribution of such plant macrofossils in the sediment cores was highly uneven, our selection of levels for ^{14}C dating was guided more by the distribution of sediment intervals with abundant charcoal than by lithostratigraphic boundaries.

A total of ten radiocarbon dates on organic material recovered from the different core sites have been obtained thus far. All dated core intervals, both ^{210}Pb- and ^{14}C-derived, could be individually transferred to the corresponding sediment depths at the other core sites using proxy-derived tie points as far as allowed by differential sediment recovery. The southern basin is chosen here for age-depth modelling, since this site has the highest potential for continuous, high-resolution paleoenvironmental reconstruction (see below). An initial age-depth model was made incorporating the (^{137}Cs-anchored) ^{210}Pb-chronology and all available terrestrial ^{14}C dates, using the CLAM software

in R (Blaauw, 2010) with a smooth spline function (smoothing factor 0.75) and 10,000 model iterations. Radiometric dates resulting in clear age reversals were omitted from the final age model.

RESULTS

Lithostratigraphy and sediment characteristics

Combination of visual facies stratigraphy and proxy data on sediment texture and composition (Fig. 3, 4, Table 3) allow delineating a sequence of five sedimentary units (Table 4). To the extent that they are covered by the respective sediment profiles, these lithostratigraphic units are shared by the sediment sequences of all five core sites, and together describe the evolution of Lake Bogoria through time.

The lowermost unit (Unit I) was retrieved only from the south and central basins. In the central basin, Unit I (176-125 cm) is dominated by three massive layers, between 3 and 14 cm thick, of near-pure crystalline trona [$Na_3(HCO_3)(CO_3)\cdot 2H_2O$] containing trace amounts of the other evaporative salt minerals thermonatrite [$Na_2(CO_3)\cdot H_2O$] and halite [NaCl]. *In-situ* presence of the latter is ambiguous, since it possibly is detected by XRD because of precipitation from saline pore water during sample drying. These massive trona layers are intercalated by sediments containing the sodium silicate mineral magadiite [$Na_2Si_{14}O_{29}\cdot 11H_2O$] and the zeolite clinoptilolite [$(Ca_3,K_6,Na_6)(Si_{30}Al_6)O_{72}\cdot 20H_2O$]. In the southern basin, Unit I (299-255 cm) consists of uninterrupted deposits of banded, black to grey-brown mud without massive salt layers. Upon splitting the core, macroscopically visible salt crystals started forming through evaporation, indicating highly saline pore waters in this unit. XRD revealed the abundant presence of trona, as well as thermonatrite, halite, magadiite (unambiguously discriminated from smectite after treatment of the XRD samples with glycol) and the zeolite erionite [$(Ca_5,K_{10},Na_{10})(Si_{26}Al_{10}O_{72})\cdot 30H_2O$]. Whereas in the central basin the presence of massive salt deposits impedes continuous analysis of bulk sediment composition, uninterrupted sedimentation in the southern basin allows high-resolution proxy data time series throughout this unit. Levels of organic matter (OM), carbonate and charcoal are high throughout Unit I, whereas χ values are fluctuating. Throughout Unit I, Ti and Ca are very low, and are correlated strongly positively to each other in the southern basin. In contrast, Cl levels are highest of the entire sequence. Mn/Fe displays low levels in the lower half of the unit and increases gradually towards the top.

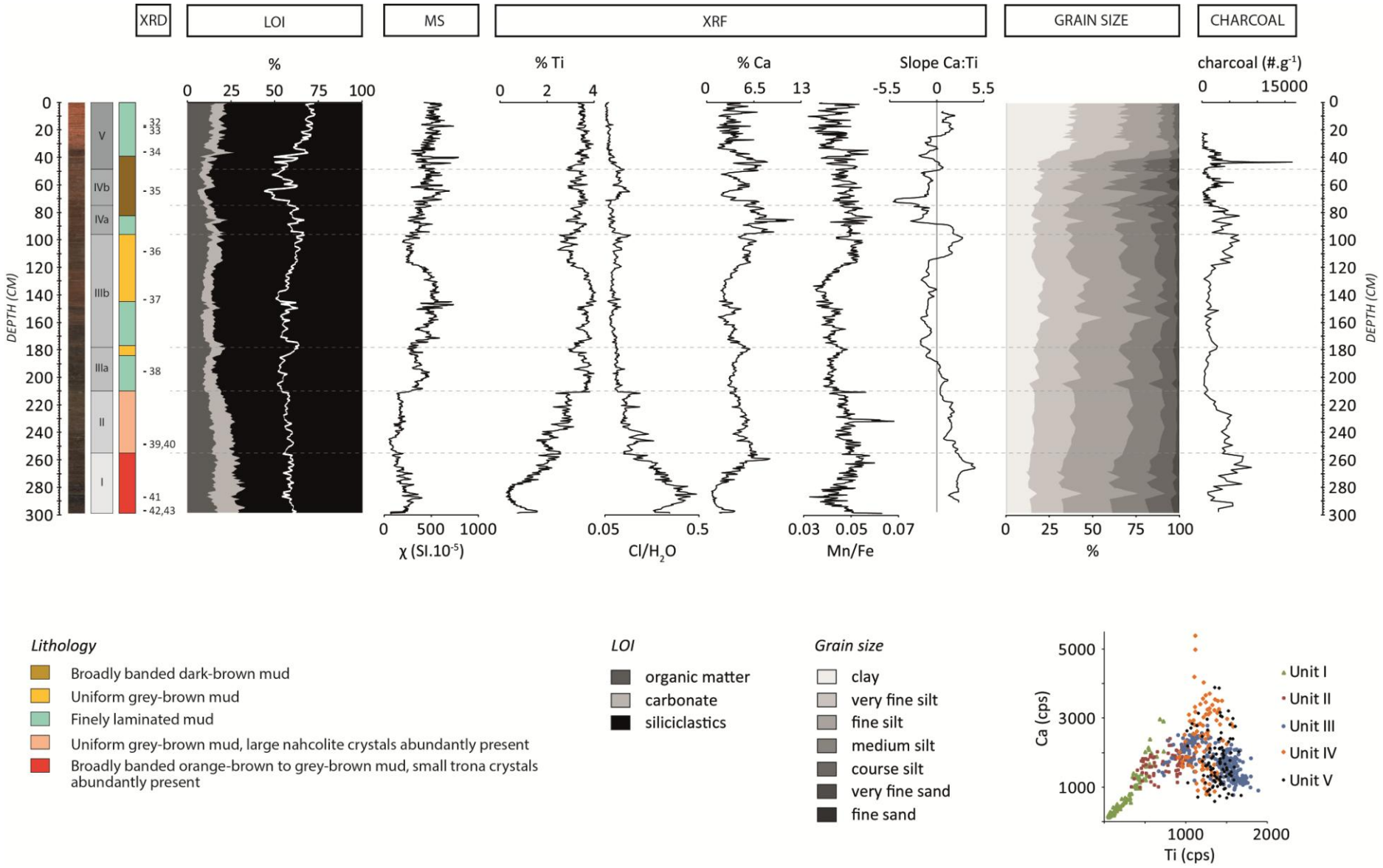

Fig. 4a Core image, lithology and proxy data for BOGS14, i.e. the sediment sequence recovered from Lake Bogoria's south basin. Numbers representing XRD data refer to Table 3. The white line in the LOI graph depicts water content after deliberate partial dewatering of the cores in preparation for transport, and an additional reduction from the dissolved solutes in pore water precipitating during oven drying. Slope of the Ca:Ti correlation was calculated over a 15-cm running window. Variability in the Ca:Ti correlation is also illustrated in a scatter plot depicting data for the different units separately.

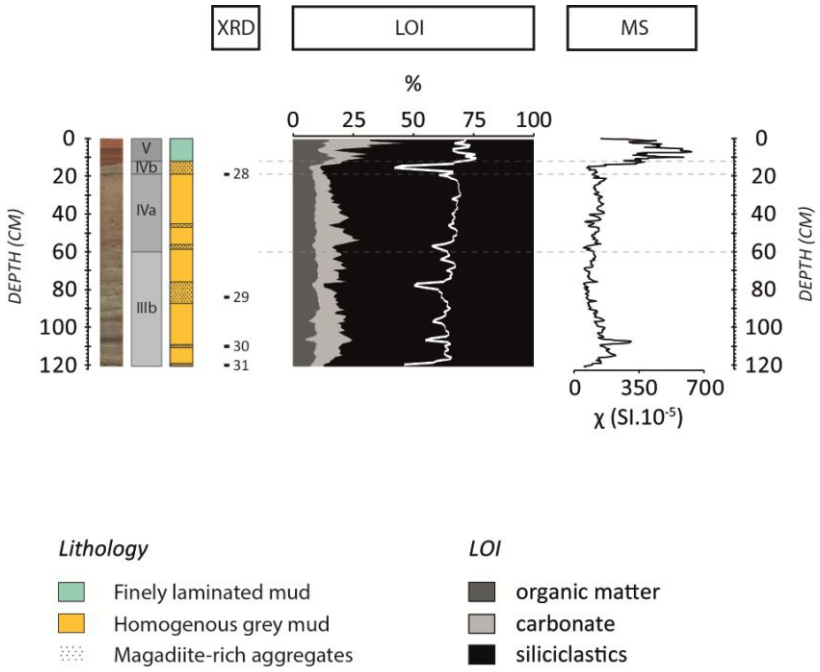

Fig. 4b Core image, lithology and proxy data for BOGCS14, i.e. the sediment sequence recovered from the sill separating Lake Bogoria's south and central basin. Numbers representing XRD data refer to Table 3. The white line in the LOI graph depicts water content after deliberate partial dewatering of the cores in preparation for transport, and an additional reduction from the dissolved solutes in pore water precipitating during oven drying.

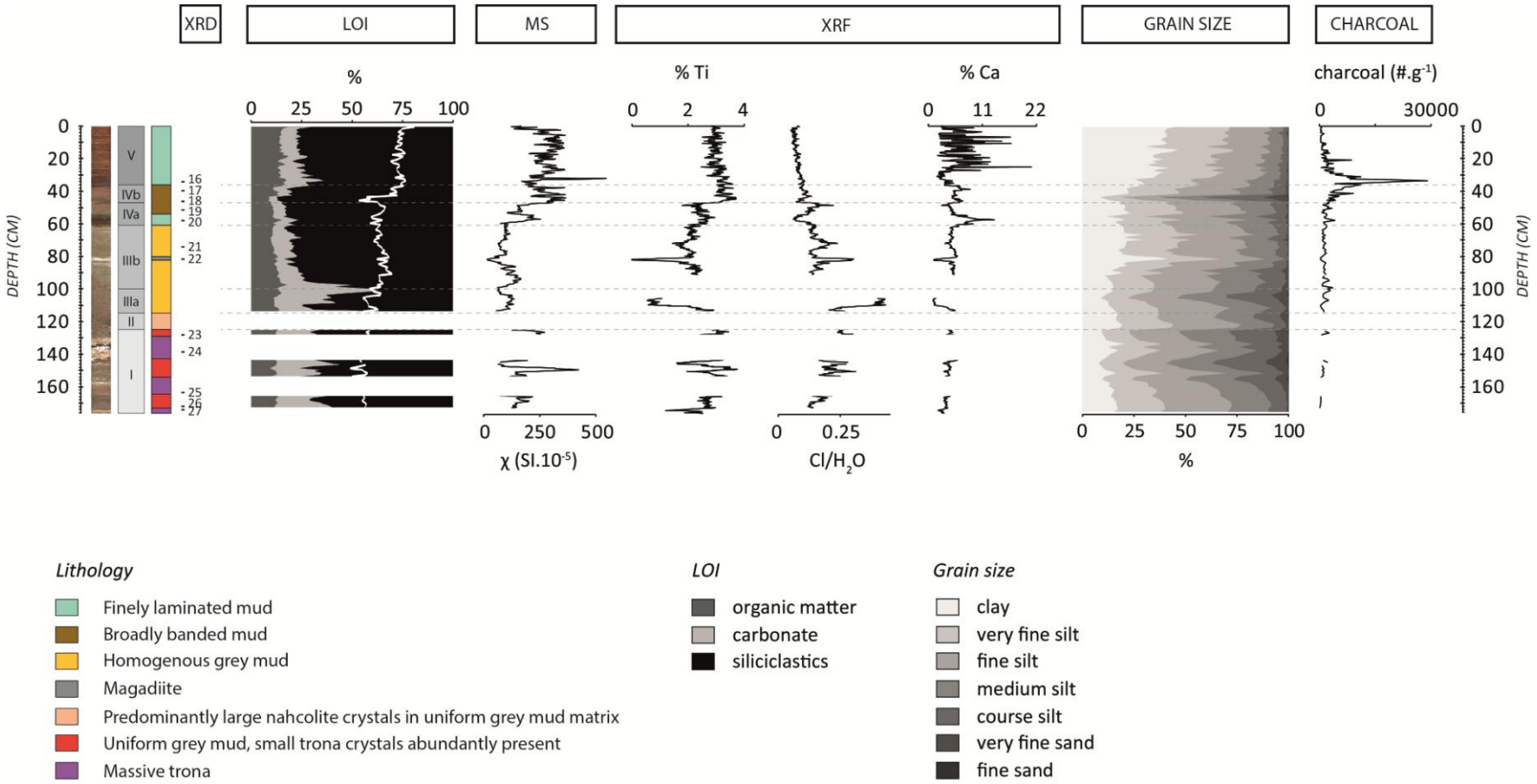

Fig. 4c Core image, lithology and proxy data for BOGC14, i.e. the sediment sequence recovered from Lake Bogoria's central basin. Numbers representing XRD data refer to Table 3. The white line in the LOI graph depicts water content after deliberate partial dewatering of the cores in preparation for transport, and an additional reduction from the dissolved solutes in pore water precipitating during oven drying.

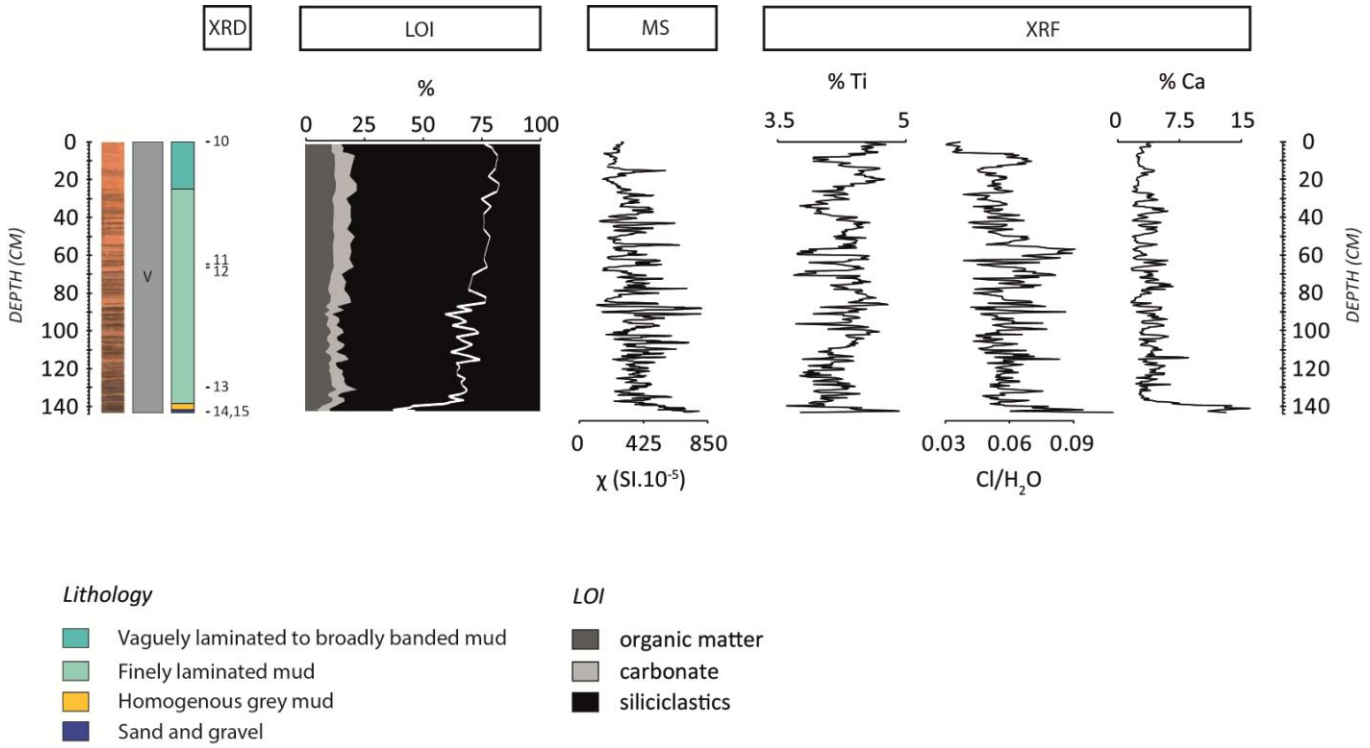

Fig. 4d Core image, lithology and proxy data for BOGNC14, i.e. the sediment sequence recovered from the sill separating Lake Bogoria's central and north basin. Numbers representing XRD data refer to Table 3. The white line in the LOI graph depicts water content after deliberate partial dewatering of the cores in preparation for transport, and an additional reduction from the dissolved solutes in pore water precipitating during oven drying.

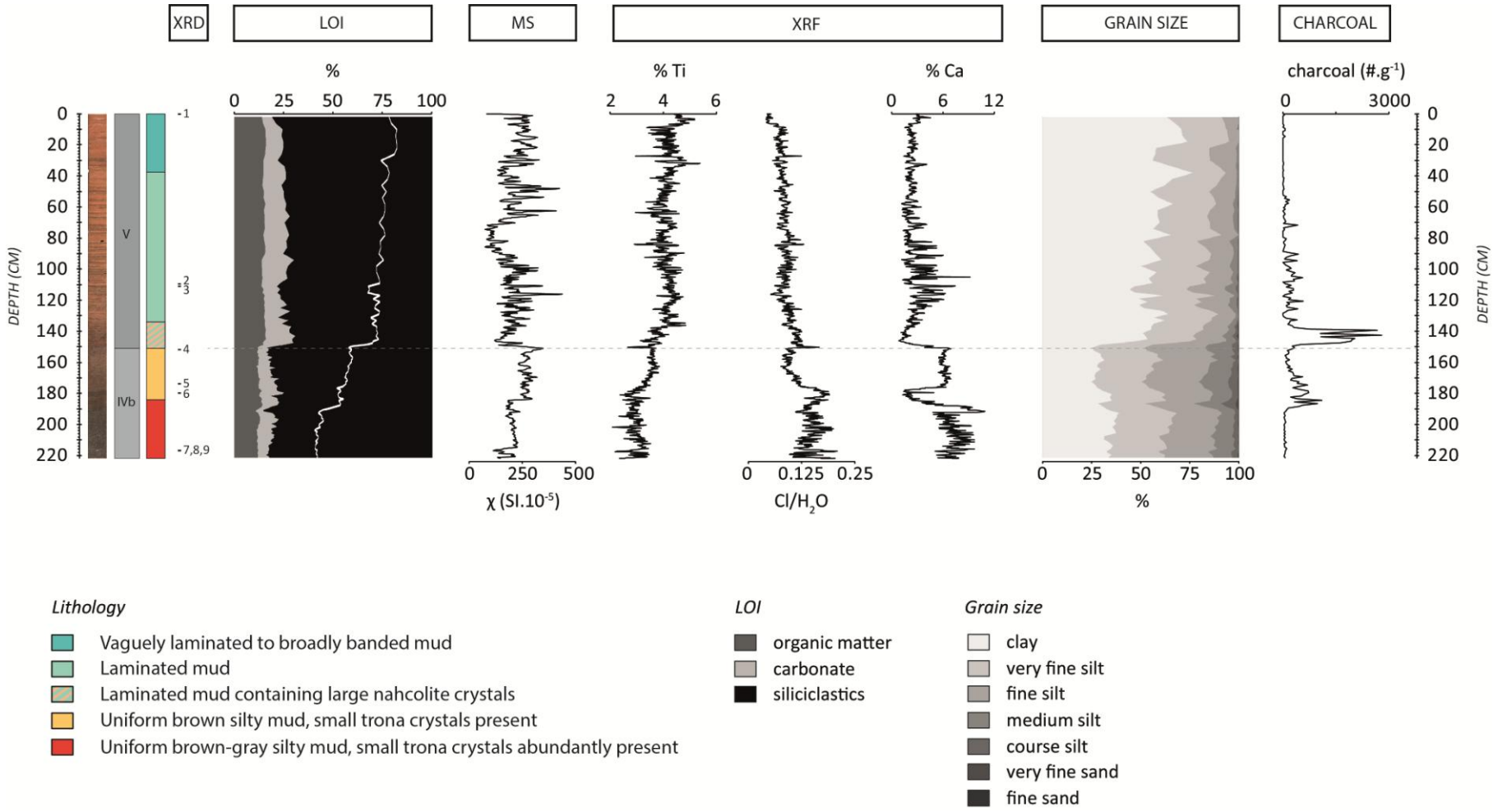

Fig. 4e Core image, lithology and proxy data for BOGN14, i.e. the sediment sequence recovered from Lake Bogoria's north basin. Numbers representing XRD data refer to Table 3. The white line in the LOI graph depicts water content after deliberate partial dewatering of the cores in preparation for transport, and an additional reduction from the dissolved solutes in pore water precipitating during oven drying.

Unit II was also recovered only in the central (115-125 cm) and southern (210-255 cm) basins. In both basins, this unit is characterized by the presence of large (up to several cm) and clear crystals of nahcolite [NaH(CO3)] in a matrix of homogenous grey-brown, silty, mud yielding low χ values. Nahcolite crystals are especially abundant in the lower part of this unit, and form a near-massive layer in the sequence of the central basin. The nature of these nahcolite occurrences (in the form of large, clear, randomly oriented crystals) suggests formation at or just below the sediment-water interface. XRD also recognizes presence of magadiite and clinoptilolite as authigenic silicates in the mud matrix of this unit. The nahcolite deposits of the central basin are too massive to allow reliable analysis of bulk-sediment composition over a large part of this unit, but in the southern basin charcoal and OM content are high, decreasing towards the top. Levels of Ti in Unit II in the southern basin is somewhat higher than in Unit I but still low overall, while Ca and Ti exhibit the same strong positive correlation as observed for Unit I. Levels of Cl are lower than in Unit I, but still relatively high as compared to upper sediment unit. Mn/Fe is relatively high, slightly declining towards the top of the unit.

In Unit III, the sediments of the central and southern basins attest to less saline conditions, with the disappearance of macroscopically visible sodium carbonate minerals and a decrease of bulk carbonate concentration as determined by LOI. In the southern basin, the sediments are brown to dark-brown and display a vaguely laminated to broadly banded pattern, while in the central basin this unit is uniformly grey-brown. Overall, values of χ and Ti are higher than before, while OM, carbonate and Cl are lower. The transition from Unit II to Unit III also marks a shift from strongly positive to negative correlation between Ti and Ca in the southern basin. Also in the southern basin, XRD (at 195 cm composite depth) reveals no sign of sodium silicate or zeolite formation, and the proportion of clay is relatively high throughout Unit III, whereas charcoal abundance is mostly low. Mn/Fe gradually decreases to minimum levels at ca. 135 cm. A short interval of decreasing χ and Ti, mirrored by markedly higher levels of OM, carbonate and Ca, allows dividing Unit III into sub-units III-A and III-B. Whereas the former is only retrieved from the central and southern basins, the base of subunit III-B corresponds to the base of the sediment sequence obtained from the central-south sill. There, it consists of hard, spherical aggregates rich in magadiite impenetrable by the push-rod operated coring device. A second section of low clastic proxies and high OM (150 cm) within subunit III-B of the southern basin corresponds to a magadiite-rich layer in the central (82 cm) and central-south (90 cm) sequences. High abundance of magadiite at this depth in the central basin causes a positive but artefactual anomaly in the % clay values detected by grain-size analysis. This can be attributed to the expected crystal size and morphology of this phyllosilicate-related mineral (Renaut, 2003), in combination with its resistance to the applied sediment pretreatment methods. Towards the top of subunit III-B, levels of clay and clastic input in the southern basin decrease, corresponding to an increase in OM, and charcoal content and distinct peaks in Cl. In this upper part of unit III-B, Mn/Fe shifts to high levels and the correlation between Ti and Ca turns positive in the southern basin, while magadiite and clinoptilolite are deposited in the central basin, reflected again in an artefactually high clay content.

			CLAY			SODIUM SILICATES AND ZEOLITES					SODIUM CARBONATES						
	Sequence	Depth (cm)	*Smectite*	*Mica*	*Kaolinite*	*Magadiite*	*Analcime*	*Erionite*	*Clinoptilolite*	*Calcite*	*Nahcolite*	*Trona*	*Thermonatrite*	*Halite*	*Feldspar*	*Am*	Pretreatment
1	BOGN14	0	x	x	x	-	-	-	-						xxx	(x)	*
2	BOGN14	110	(x)	x	x	-	x	-	-						xxx	(x)	*
3	BOGN14	111	(x)	x	x	-	-	-	-						xxx	(x)	*
4	BOGN14	152	-	x	x	-	x	-	-						xxx	(x)	*
5	BOGN14	174				-	xxx	-	-	-	-	xx	(x)	(x)	xx	-	
6	BOGN14	180	-	x	x	-	x	-	-						xxx	-	*
7	BOGN14	217	-	x	x	-	x	x	-						xxx	-	*
8	BOGN14	217				-	x	-	-	-	-	xxx	(x)	(x)	-	-	
9	BOGN14	217				-	xxx	(x)	-	-	-	x	-	-	xx	-	
10	BOGNC14	0	x	x	x	-	(x)	-	-						xxx	x	*
11	BOGNC14	65	(x)	x	x	-	-	-	-						xxx	(x)	*
12	BOGNC14	67	x	x	x	-	(x)	-	-						xxx	(x)	*
13	BOGNC14	130	(x)	x	x	-	(x)	-	-						xxx	x	*
14	BOGNC14	143	-	(x)	x	-	-	-	-						xxx	(x)	*
15	BOGNC14	143				-	(x)	-	-	xx	-	-	-	-	xxx	-	
16	BOGC14	34	-	x	x	-	(x)	-	-						xxx	-	*
17	BOGC14	40	-	(x)	x	-	-	-	-						xxx	(x)	*
18	BOGC14	46	-	-	(x)	-	x	-	-						xxx	(x)	*
19	BOGC14	51	x	(x)	x	-	x	-	-						xxx	(x)	*
20	BOGC14	58	-	(x)	(x)	-	-	-	-						xxx	(x)	*
21	BOGC14	74				xxx	-	-	-	-	-	xx	-	x	x	-	
22	BOGC14	82	-	x	x	xx	-	-	x						xxx	-	*
23	BOGC14	128	-	x	(x)	(x)	-	-	x						xxx	-	*
24	BOGC14	139	-	x	(x)	x	-	-	xx						xxx	-	*
25	BOGC14	163				-	-	-	-	-	-	xxx	(x)	(x)	-	-	
26	BOGC14	172	-	(x)	(x)	x	-	-	x						xxx	-	*
27	BOGC14	174				(x)	-	-	-	-	-	xxx	(x)	(x)	-	-	
28	BOGCS14	19	-	x	-	x	-	-	-						xxx	-	*
29	BOGCS14	84				xxx	-	-	-	-	-	x	-	x	x	-	
30	BOGCS14	110				xxx	-	-	-	-	-	x	-	x	x	-	
31	BOGCS14	120	-	x	-	xxx	-	-	-						xxx	-	*
32	BOGS14	17	-	x	x	-	(x)	-	-						xxx	x	*
33	BOGS14	18	-	x	x	-	-	-	-						xxx	x	*
34	BOGS14	36	-	x	x	-	-	-	-						xxx	-	*
35	BOGS14	64	-	-	x	-	-	-	-						xxx	-	*
36	BOGS14	108	-	-	x	-	-	-	-						xxx	-	*
37	BOGS14	143	-	-	x	-	-	-	-						xxx	-	*
38	BOGS14	196	-	-	x	-	-	-	-						xxx	-	*
39	BOGS14	249	-	-	x	x	-	-	x						xxx	-	*
40	BOGS14	249				(x)	-	-	-	-	xxx	-	-	-	-	-	
41	BOGS14	287				x	-	-	-	-	-	x	xx	x	xxx	-	
42	BOGS14	297	-	x	-	x	-	x	-						xxx	-	*
43	BOGS14	297				x	-	x	-	-	-	xxx	(x)	x	xx	-	

Table 3 Results of XRD analyses on 43 samples obtained from the five sediment sequences. Sample numbers refer to the numbers used in fig. 4. Asterisks denote samples that underwent pretreatment by rinsing with deionized water to remove sodium carbonates.

	BOGS14	BOGCS14	BOGC14	BOGNC14	BOGN14
	cm	*cm*	*cm*	*cm*	*cm*
V	0-48.8	0-12	0-36	0-143	0-151
IV-B	48.8-75	12-19	36-47	n.r.	151-222
IV-A	75-96.8	19-60.2	47-60.7	n.r.	n.r.
III-B	96.8-178	60.2-121	60.7-100	n.r.	n.r.
III-A	178-210	n.r.	100-115	n.r.	n.r.
II	210-255	n.r.	115-125	n.r.	n.r.
I	255-299	n.r.	125-176	n.r.	n.r.

n.r.: not recovered

Table 4 Depth boundaries of corresponding sediment units in the five sequences collected from Lake Bogoria.

Unit IV is characterized by marked variability in sediment composition as reflected by proxy values and can be divided into subunit IV-A and IV-B. Subunit IV-A starts with a shift to low OM and Cl levels and higher values of χ and Ti, while a temporary presence of fine lamination is recorded in the central and southern basins. No authigenic evaporative minerals are detected at this point. Higher up in this subunit, fine lamination disappears again. Instead, the sediments of the central basin consist of uniform grey mud containing the zeolite mineral analcime [$Na(AlSi_2O_6)\cdot H_2O$], while sediment in the southern basin displays a vaguely banded pattern. The sediments of the central-south sill are relatively uniform throughout subunit IV-A, with the exception of a layer of magadiite-containing nodules at 46 cm. The transition to subunit IV-B is marked by a shift to higher χ and Ti levels (highly abrupt in the central basin), which also marks the base of the recovered northern basin sediment sequence. In the central and southern basins, subunit IV-B is made up of broadly banded sediments, while on the sill separating the central and southern basins, this subunit consists of a layer of hard magadiite-rich aggregates. In the northern basin, IV-B is made up of dark-brown sediments containing abundant trona crystals (and, in the upper part of the unit, moulds of similar crystals), supplemented with analcime and erionite, with high levels of siliciclastics and Cl. OM, Cl and charcoal display peaks in the middle of this subunit in the three lake basins, and while covariance between Ca and Ti in the southern basin is mostly positive throughout Unit IV, low R^2 values mirror the short-term variability observed in other proxies.

The start of Unit V marks the onset of sedimentation on the sill separating the north and central basins, following a lowstand of unknown duration which left a sand and gravel horizon at the base of the north-central sill sequence. In all five sequences, this unit is characterized by finely laminated sediments and a sharp rise to remarkably high levels of clay compared to the lower sediment units. In the lowermost 15 cm of Unit V in the northern basin, large nahcolite crystals are present. Overall, OM content and Ti values are high at all core sites, while Ca and Ti display a weak and variable correlation in the southern basin. Associated with the finely laminated nature of the sediments, the compositional proxies show marked short-term variability. Microscopic investigation of thin sections, combined with bulk-sediment proxy data obtained at high resolution from selected intervals, revealed the overall inorganic nature of these laminations. Light brown clay-rich layers are alternated by dark brown laminae richer in feldspar-dominated silt and detrital calcium carbonate (Fig. 5). Accordingly, levels of χ and Ca are highest in these dark laminae, whereas organic matter

content is higher in the light brown laminae. In most cases, silty layers have relatively clear lower boundaries and show a gradual upward increase in clay content, commonly making the transition from silt-dominated to clay-dominated layers diffuse (Fig. 5).

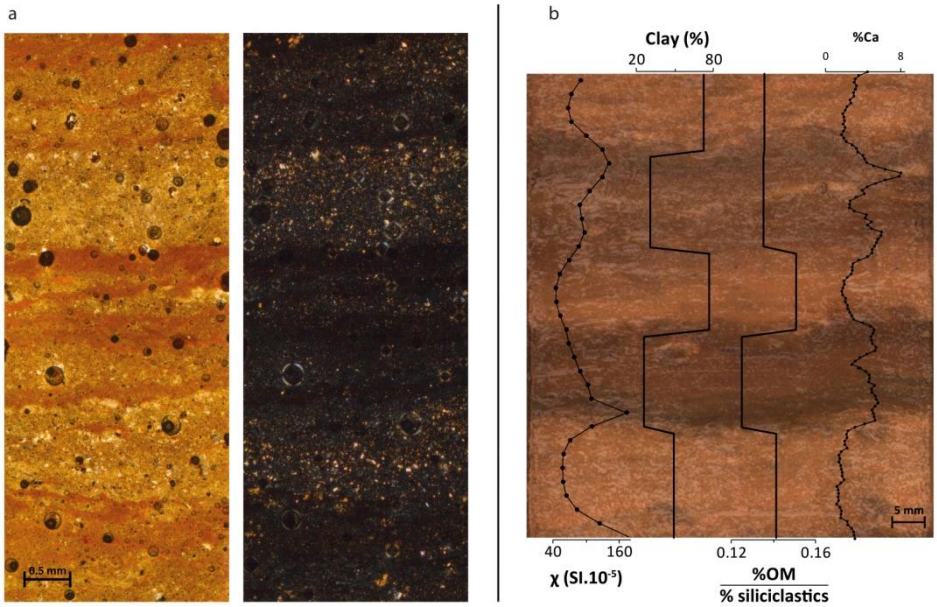

Fig. 5 Characteristics of the fine laminations of Unit I. a: Thin section containing fine lamination of Unit V in the sediment sequence of the southern basin (BOGS14), as seen under plane- and cross-polarized light. Despite a relatively large amount of air bubbles introduced during preparation, the gradual transition from silt to clay can clearly be discerned in each silt-clay couplet. b: Selected proxy data collected on a Unit V section of the north-central sill sediment sequence (BOGNC14). Notice the difference in lamination thickness between the two sequences.

Chronology and rate of sedimentation in Lake Bogoria

The comprehensive set of chronological tie points linking corresponding sedimentation events in the five sediment sequences combines visual characteristics (e.g. presence of fine lamination or macroscopically visible salt crystals), charcoal counts (a terrestrial proxy and therefore unaffected by differential biogeochemical processes at the various coring points), proxies for catchment-derived clastics (χ, XRF elemental composition) and variation in OM content (Fig. 6a-b). The full set of tie points (Table 5) enables a precise comparison of sedimentary processes acting in the different parts of the lake at any given time. Only in the sediment sequence of the sill separating the central and south basins (BOGCS14), which mostly lacks the variations in sediment composition observed in the other sequences, not all tie points could be recognized. Possibly, this sequence has known irregular or temporarily interrupted sedimentation during lowstands (see below).

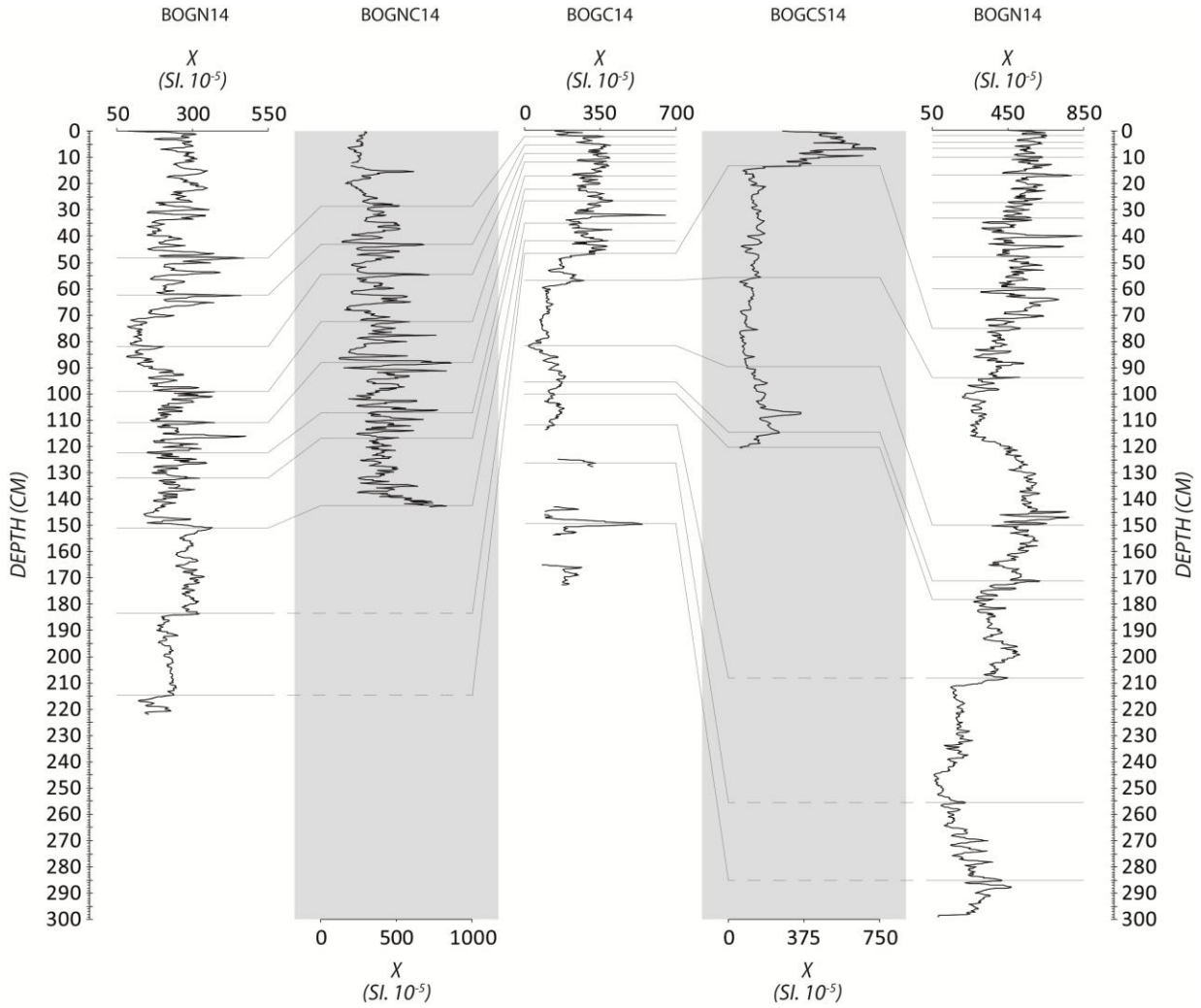

Fig. 6a Illustration of the most important tie points between the five core sequences based on magnetic susceptibility.

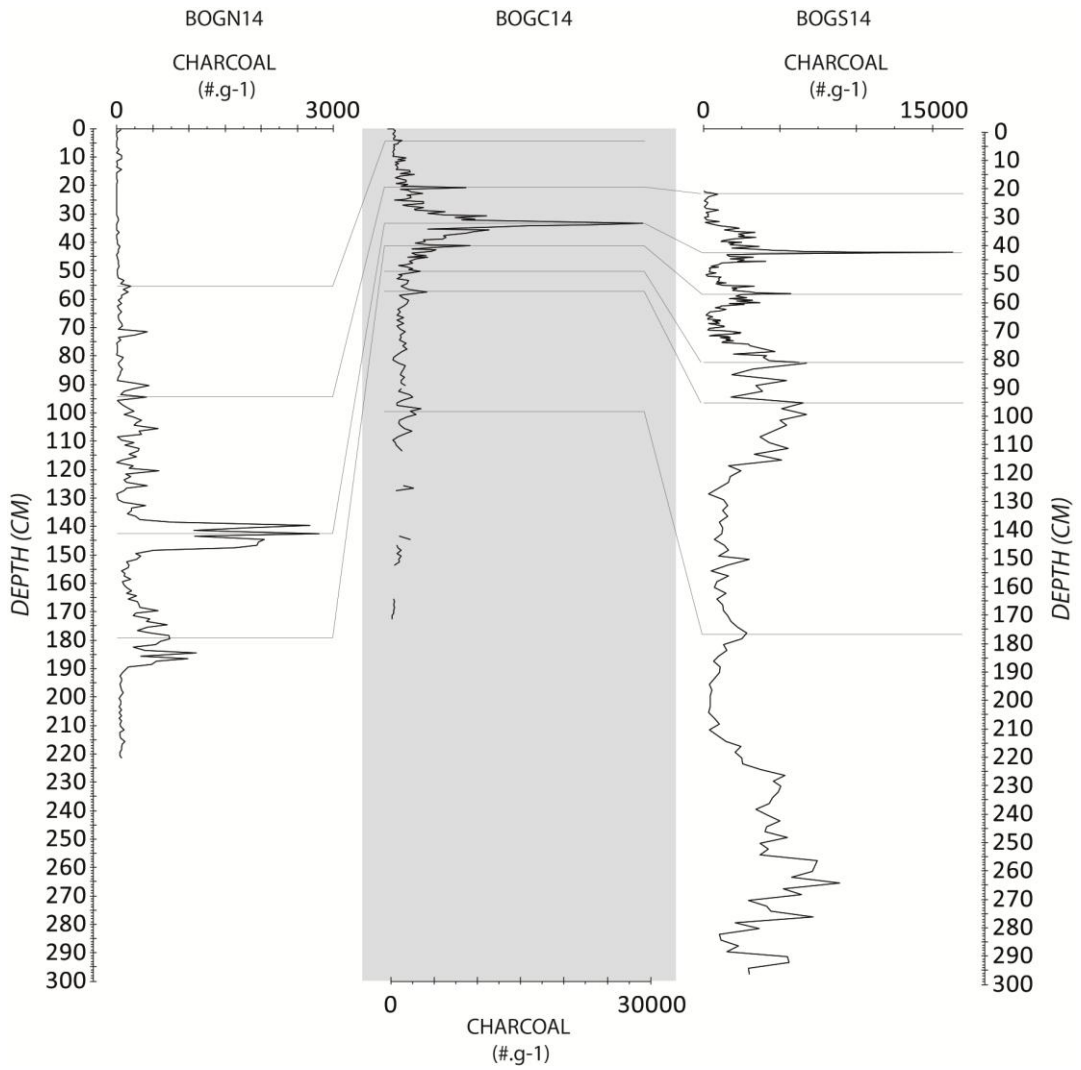

Fig. 6b Illustration of the most important tie points between the three basin core sequences based on charcoal content.

Tie point *number*		BOGS14 *cm*	BOGCS14 *cm*	BOGC14 *cm*	BOGNC14 *cm*	BOGN14 *cm*
1		0	0	0	0	0
2		0.9		0.9	15.4	29.8
3	*	1		1	15.6	30
4		1.6		2	23.3	42
5		1.9		2.5	28.4	48.2
6	*	2.3		3	33.2	51
7		2.7		4	45.6	53.8
8		4		5	35.6	57.6
9		4.7		5.7	43.2	62.4
10	*	4.9		6	44.6	64.2
11		5.7		7	48	70
12	*	6.3		8	51	73.4
13		6.9		8.9	54.6	82
14		7		9	54.8	82.6
15	*	8		10	62.4	90
16		9		11	68.4	95
17		10.3		11.9	72.4	99.2
18		10.4		12	72.6	99.5
19	*	11.6		13	75	101
20	*	13		14	78	103
21		13.9		15	79.2	104.6
22	*	14.9		16	81	106.4
23		16.4		17	86.4	110
24		17.3		17.5	88.2	110.8
25	*	18.4		18	90.2	112.2
26	*	21.1		19	92.4	114.2
27		22.7		20	96.4	116
28	*	24.3		21	100.8	117.8
29		27.5		23	107.4	122.4
30		33.3		26.9	116.8	132
31	**	37.5		30.5	125	137.5
32		43.6		33.25	131	142.5
33	**	48.8	12	36	142.6	151
34		51.3		37.9	n.r.	157.8
35		53.1		39	n.r.	163.6
36		55.5		40	n.r.	174.5
37	**	58		41	n.r.	178.5
38		60.5		42.1	n.r.	183.6
39		61.5		43	n.r.	186.5
40		64.5		44	n.r.	191.5
41		66.8		44.8	n.r.	201
42	**	68.6		45.4	n.r.	204.4
43		72		45.9	n.r.	211.5
44		75	19	47	n.r.	215
45		78		49	n.r.	n.r.
46	**	82.5		50.25	n.r.	n.r.
47		88.5		54.9	n.r.	n.r.
48		94.1	54	57.1	n.r.	n.r.
49		96.8	58	60.7	n.r.	n.r.
50	**	104		65.5	n.r.	n.r.
51		107		67	n.r.	n.r.
52	**	115.5		70	n.r.	n.r.
53		119		72	n.r.	n.r.
54		128.5		74.5	n.r.	n.r.
55		136.5		77.5	n.r.	n.r.
56		150	89.7	82	n.r.	n.r.
57		171.3	115	95.7	n.r.	n.r.
58	**	175	118	98	n.r.	n.r.
59		178	121	100	n.r.	n.r.
60		208	n.r.	112	n.r.	n.r.
61		257.5	n.r.	126.5	n.r.	n.r.
62	**	266	n.r.		n.r.	n.r.
63		277.5	n.r.	144.5	n.r.	n.r.
64		285.1	n.r.	149.7	n.r.	n.r.
65	**	292.5	n.r.	160	n.r.	n.r.

*: directly 210Pb-dated
**: directly 14C-dated
n.r.: not recovered

Table 5 Set of tie points reflecting corresponding depths in the five sediment sequences. Due to relatively low sediment accumulation rates in the top part and low proxy variability in the lower part, not all corresponding levels could be identified in the central-south sill sediment sequence. Tie point 62 corresponds to the uppermost massive trona layer in the central basin, which precludes a precise central-basin depth determination.

Total ^{210}Pb activity appears to reach equilibrium with the supporting ^{226}Ra at a depth of around 30 cm in the sediment sequence of the central basin, while concentrations of the fallout radionuclide ^{137}Cs has a relatively well-defined peak at 15.5 cm that most probably records the 1963 fallout maximum from the above-ground testing of nuclear weapons (Table 6). The ^{137}Cs peak is much better resolved than in the cores obtained in 2001-2003 (Chapter 3), confirming that in those cores, the profile was largely destroyed by disturbance of the upper sediments. Post-1963 ages are relatively unequivocal, but 19th-century and early-20th century ages have relatively large uncertainties because of low ^{210}Pb activity in samples close to equilibrium. We therefore limit chronological inferences from ^{210}Pb data to sediments deposited since 1925, a timing which is assigned to the 23-24 cm depth interval with a 1SD uncertainty of ±12 years. Multiple chronological tie points evident in the fine lamination of Unit V allowed unambiguous transfer of the ^{210}Pb-derived ages to the corresponding depth intervals in the southern basin. All chronological information obtained from the five core sites (radiocarbon dating results are summarized in Table 7) was similarly transferred to the corresponding depth intervals in the southern basin. Since no evidence for complete desiccation could be discerned in sediment sequence BOGS14, we argue that this site has known uninterrupted sedimentation during the entire time frame spanned by the core, being the only site in the lake that has not undergone (near-)complete desiccation at some point during the study period. There has also been no deposition of massive evaporative facies which obscure short-term variability in paleo-environmental proxies recorded in the sediment matrix, or could have resulted in anomalously large variations in sedimentation rate.

Depth	**^{210}Pb**						**^{137}Cs**		**Chronology**	
	Total		Unsupported		Supported					
cm	*Bq kg^{-1}*	*±*	*Bq kg^{-1}*	*±*	*Bq kg^{-1}*	*±*	*Bq kg^{-1}*	*±*	*AD*	*±*
0	-	-	-	-	-	-	-	-	2014.7	0
0.5	320.8	17.2	278.4	17.6	42.4	3.5	0	0	2013	1
2.5	410.3	32.3	374.3	32.7	36	5.6	0	0	2007	2
5.5	225.6	16.9	185.7	17.2	39.9	3.1	0	0	1995	2
7.5	138.5	14.1	107	14.4	31.5	2.9	0	0	1989	3
9.5	164.5	13	125.3	13.4	39.2	3	1.4	1.8	1984	3
12.5	161.1	18.4	122.2	18.8	38.9	3.6	5.9	2.5	1973	5
13.5	146.9	11.4	111.7	11.7	35.2	2.6	2.7	1.4	1968	6
15.5	62.8	7.7	32.9	7.9	29.9	1.8	8.2	1	1963	6
17.5	67.6	7.2	37.7	7.4	30	1.7	6.2	1.3	1956	7
18.5	70.7	10	36.3	10.3	34.4	2.7	2.2	1.6	1951	7
20.5	54.2	7.4	17.6	7.7	36.6	2	1	1.1	1944	8
23.5	61.4	8.7	33.3	8.9	28	1.7	0	0	1925	12
26.5	49.2	10.3	7.4	10.7	41.9	2.7	0	0	-	-
29.5	47.4	12.2	12.6	12.4	34.8	2.5	0	0	-	-
32.5	35.4	10.3	-2.8	10.6	38.2	2.5	2.7	1.7	-	-
35.5	28.9	9.8	-1.5	10	30.4	2.2	0	0	-	-
38.5	38.7	6.8	8.8	7	29.8	1.7	0.5	1.3	-	-

Table 6 ^{210}Pb dating results for the sediment sequence of Lake Bogoria's central basin.

	Sample code	Site of collection	Depth in BOGS14	Material	14C age	Cal age range	Probability
			cm		*14C yr BP*	*Cal yr BP*	*2σ*
*	UBA-26052	BOGS14	37.9-38.3	charred wood	296 ± 30	458-348	0.677
						336-294	0.272
*	Poz-79686	BOGNC14	48-48.5	small charcoal fragments	410 ± 30	358-331	0.120
						518-430	0.830
*	Poz-79718	BOGS14	57.5-59.2	small charcoal fragments	470 ± 30	540-495	0.950
	UBA-26053	BOGS14	68.5-68.7	*Tribulus* sp. seed	247 ± 32	13- -4	0.062
						188-148	0.236
						211-206	0.005
						324-269	0.512
						360	0.001
						428-376	0.134
	Poz-79680	BOGS14	80-82	small charcoal fragments	415 ± 30	355-332	0.096
						519-434	0.854
	Poz-79683	BOGC14	103-105	small charcoal fragments	440 ± 30	346-343	0.009
						532-462	0.941
	Poz-79681	BOGS14	114-117	small charcoal fragments	660 ± 35	606-556	0.477
						674-625	0.473
*	Poz-79685	BOGCS14	174-176	small charcoal fragments	1325 ± 30	1209-1183	0.198
						1299-1231	0.752
	Poz-79774	BOGS14	265-267	small charcoal fragments	915 ± 35	752-747	0.014
						920-760	0.936
	Poz-79682	BOGS14	293-295	small charcoal fragments	1315 ± 30	1210-1182	0.249
						1295-1227	0.701

Table 7 ^{14}C dating results obtained from different core sites, transferred to corresponding depths in the sediment sequence of Lake Bogoria's southern basin. Asterisks indicate radiocarbon dates that resulted in age reversals and were not incorporated in the age model.

The final age-depth model (Fig. 7) obtained at the present stage of this study dates the base of the southern basin sediment sequence to between 1,280 and 1,050 cal yr BP. Four radiocarbon ages caused age reversals and were omitted from the final age model (Table 7). Since care was taken to avoid lake-derived organic matter in the samples prepared for ^{14}C dating, the most likely cause for age over-estimation is the presence of old terrestrial material in the samples. At least for the samples obtained from the two sill sites, this seems a plausible explanation. The samples were extracted from the bottom of these sediment sequences, right above a desiccation horizon in the north-central sill sequence and a layer of magadiite-rich aggregates (signifying, if not desiccation, at least substantially low lake levels with the shoreline very close to the core site). This means that these samples represent the re-establishment of sedimentation at the sills at a given time in the past. Rising water levels possibly remobilized previously deposited sediments, increasing the probability that older, reworked material was delivered to the core site. Throughout most of the sequence, calendar-age probability windows are relatively wide, in part because the ^{14}C dates at 68.5 and 80 cm depth correspond with multiple calendar-age windows as a result of a plateau in the radiocarbon calibration curve. The present lack of reliable dating in a large part of the lower half of the sequence also increases model uncertainty. Our present age-depth model nevertheless appears to suggest marked changes through time in sediment accumulation rate in the southern basin, with highest apparent rates between ca. 800 and 650 cal yr BP.

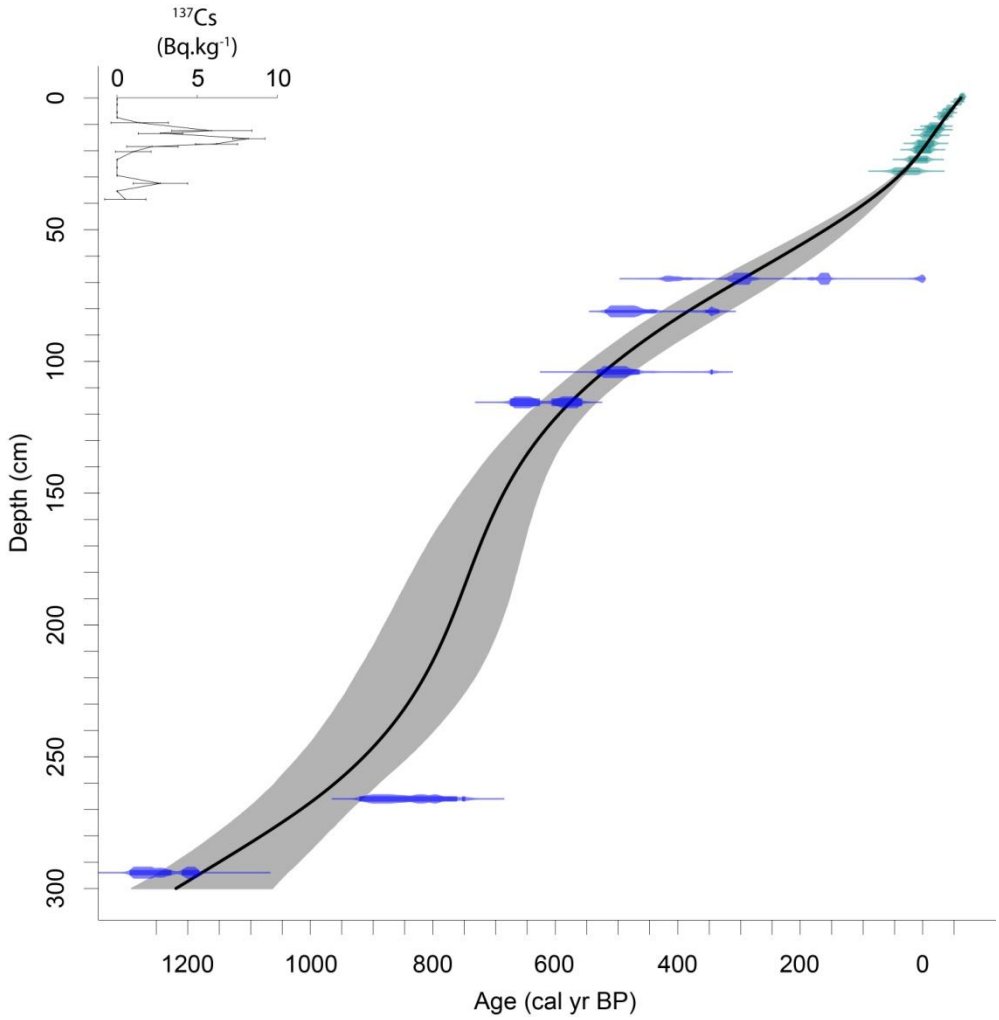

Fig. 7 Age-depth model of BOGS14, i.e. the sediment sequence obtained from Lake Bogoria's southern basin. ^{210}Pb-derived ages are depicted in green, individual calibrated radiocarbon probability ranges in blue. The black line shows the best estimate age based on weighted averaging of the model ensemble, with corresponding 95% confidence range in grey. ^{137}Cs activity is also shown.

Based on the final age model for the south-basin sequence, a best age estimate could be assigned to each tie point, which allowed the south-basin chronology to be transferred to the other four sequences. In combination with data on specific dry weight corrected for salt content derived from LOI, this allowed the calculation of sediment accumulation rates (SARs, in $g.cm^{-2}.yr^{-1}$) over identical time intervals in all three basins (Fig. 8). In the central basin, SAR was not calculated for units I and II because of the dominance of massive salt mineral deposits. At this stage, we do not know whether these massive trona layers are event deposits, originating from extremely severe but short-lived pulses of drought, rather than that they were gradually laid down during prolonged periods of strong evaporative concentration. For most of the sequence, central-basin SARs are consistently lower than south-basin SARs, but exhibit same or even slightly higher levels after ca. AD 1970. From the base of the north-basin sequence (dated to ca. 350 cal yr BP) to ca. 150 cal yr BP, SARs in the north basin are substantially higher than in the central and southern basins. After ca. 150 cal yr BP, north-basin SAR falls to levels comparable to the south basin, to increase sharply again in the early 1970's to levels of 15 to 20 times higher than those of the central and south basins.

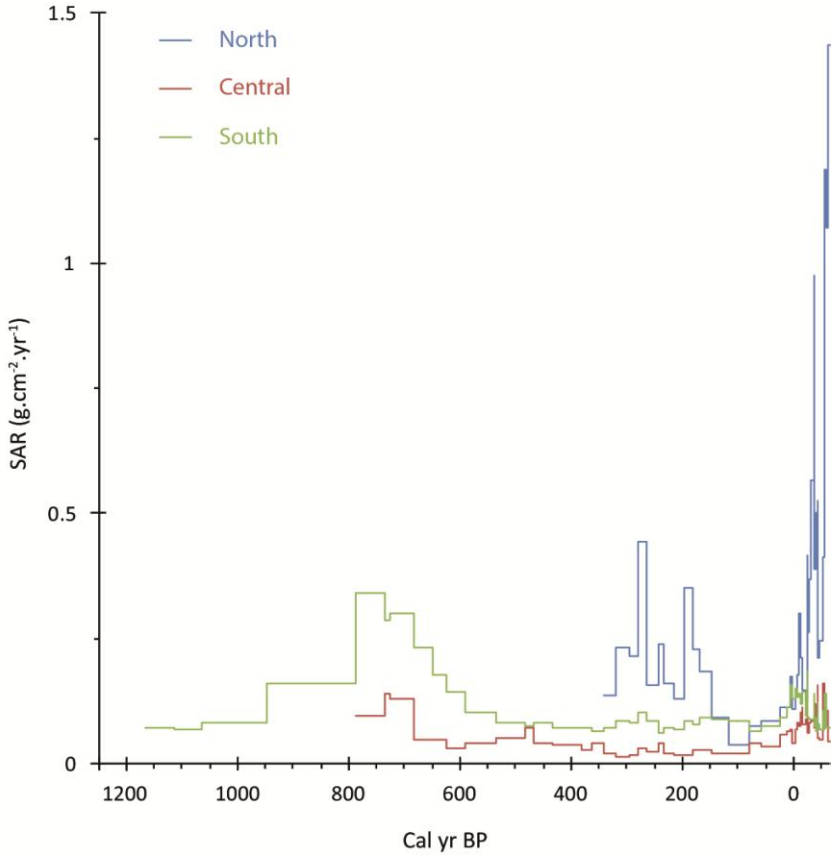

Fig. 8 Sedimentation rate through time in the three basins as calculated from cumulative dry weight (corrected for salt content) between corresponding chronological tie points.

Sediment traps

Compositional data from the sediment-trap samples bear a clear seasonal pattern (Table 8, Fig. 9). Values of χ peak during the MAM rain season in all three basins, suggesting significant delivery of catchment-derived clastic material to the lake at that time. %TOC and %TN are lowest during both the short and long rain seasons. High C/N values suggest that terrestrial organics become enriched relative to algal material at these times, due to increased riverine and overground flow. Total sediment flux was high during the rain seasons, especially during MAM in all three basins. However, the highest SAR occurred during June-July 2015 in the northern basin, without analogue in the central and southern basins. These results confirm the Sandai-Waseges river system to be the dominant source of clastic sediments in the modern-day Lake Bogoria. It runs through areas of clay-rich soils in the southeastern and northern part of the lake, where superficial geology is dominated by old alluvial and lacustrine deposits (Fig. 1). In agreement with this scenario, clay content of the sediment-trap material decreases from north to south, whereas %TOC increases, reflecting a higher contribution of in-lake productivity to sedimentation away from Sandai-Waseges river inflow. A similar pattern is observed in the sediment cores, where clay content of present-day deposits in the northern basin is at least twice as high as those in the corresponding units in the central and southern basin sequences. Grain-size data of the sediment-trap samples also indicate that the relative proportion of clay in rain-season deposits is higher than in dry-season sediments in all three basins.

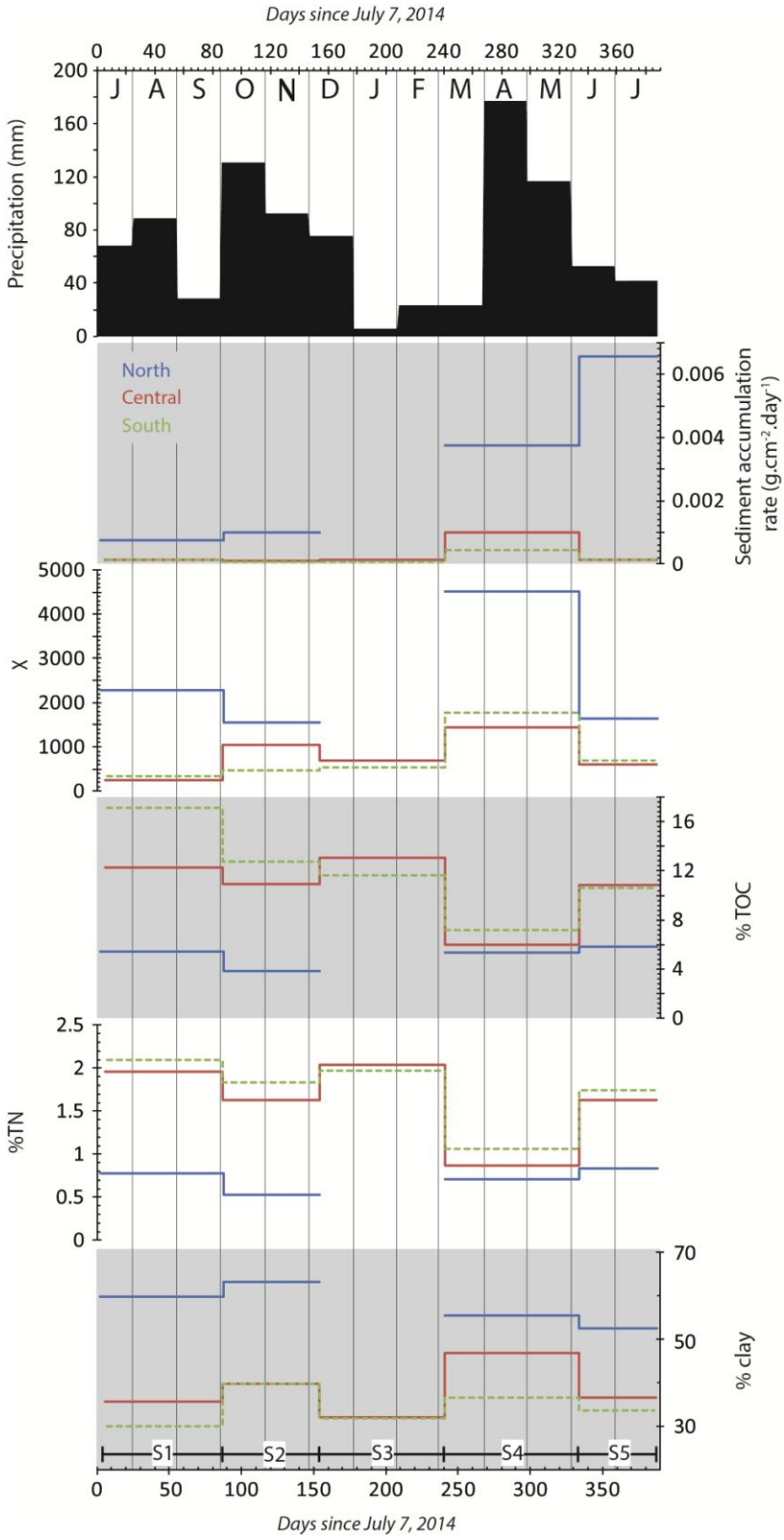

Fig. 9 Results obtained on the sediment trap samples collected between early July 2014 and late July 2015, with the uppermost panel depicting NOAA's CPC Merged Analysis of Precipitation (CMAP) monthly satellite-based precipitation estimates (Xie and Arkin, 1997) over the grid cell containing Lake Bogoria's catchment during the study period. S1-5: sediment trap deployment periods, see Table 2.

	Start of sampled period	End of sampled period	Sediment flux	clay	χ	TOC %	TN %	C/N
			$g.cm^{-2}.day^{-1}$	%	SI	%	%	
North	2014-07-09	2014-10-03	0.0008	59.76	2288	5.5	0.8	7.0
	2014-10-03	2014-12-08	0.0010	63.20	1558	3.9	0.5	7.3
	2014-12-08	2015-03-05						
	2015-03-05	2015-06-06	0.0037	55.61	4520	5.4	0.7	7.6
	2015-06-06	2015-07-30	0.0066	52.58	1638	5.8	0.8	7.1
Central	2014-07-13	2014-10-02	0.0001	35.77	258	12.3	1.96	6.3
	2014-10-02	2014-12-08	0.0001	39.80	1045	11.0	1.6	6.7
	2014-12-08	2015-03-05	0.0001	32.02	685	13.1	2.0	6.4
	2015-03-05	2015-06-06	0.0010	46.79	1450	6.0	0.9	6.9
	2015-06-06	2015-07-29	0.0001	36.66	597	10.9	1.6	6.7
South	2014-07-14	2014-10-02	0.0001	30.17	342	17.1	2.1	8.2
	2014-10-02	2014-12-08	0.0001	39.93	471	12.8	1.84	6.9
	2014-12-08	2015-03-05	0.0001	31.97	527	11.7	2.0	5.9
	2015-03-05	2015-06-06	0.0004	36.74	1770	7.2	1.1	6.7
	2015-06-06	2015-07-28	0.0001	33.82	688	10.6	1.7	6.1

Table 8 Summary of data obtained on the sediment trap samples collected between early July 2014 and late July 2015.

DISCUSSION

Recent sedimentation dynamics and the link to 20th-century moisture balance

The seasonal sediment trap samples collected over the period July 2014 - July 2015 provide insight into the modern-day sedimentation dynamics of Lake Bogoria. Increased delivery of predominantly clastic material to all three basins during wet periods, especially the long rains of MAM, demonstrates the temporarily increased activity of ephemeral rivers, with the Sandai-Waseges being responsible for a strong north-south gradient in the relative proportion of clay. During dry seasons, algal-derived organic matter becomes enriched in the sediment traps, while the inorganic fraction at this time is poorer in clay and richer in fine silt. The latter suggests that the dominant sediment provenance shifts from the Sandai-Waseges to the slopes and flood plains directly surrounding the lake, possibly also with a greater role for aeolian transport. Certain patterns indicate a more complex control on sedimentation, such as the massive delivery of sediment to the northern basin during the dry period of June-July 2015. One possible explanation is the existence of a certain time lag between the rain season precipitation peak and maximum river discharge, which could explain the post-MAM maximum in sediment delivery. However, a similar June-July 2015 SAR peak is not observed for the central and southern basins.

High-resolution proxy data from the cores, supplemented by microscopic investigation of thin sections suggest that both the light and dark laminae alternating throughout Unit V contain predominantly terrigenous components. This would suggest that both types of layers have their origin in increased streamflow, with most larger-grained silts and large clastic carbonate particles settling before the clay fraction can breach the thermocline. Whether these laminations have a yearly or seasonal rhythm, in which case each dark-light couplet would be linked to one wet season,

cannot be decided based on macroscopic features that are documented by high-resolution images. Instead, layer counting should be conducted on a continuous set of overlapping thin sections.

Further indications for hydroclimate-to-sediment control are inferred by comparing the proxy data obtained for the uppermost sediments to information on historical meteorology. The US National Oceanic and Atmospheric Administration (NOAA) Precipitation Reconstruction over Land (PREC/L) combines and interpolates high-quality rain-gauge data to produce a grid of cells containing monthly precipitation data for the period of 1948-present (Chen et al., 2002). Since the dataset exhibits strong short-term fluctuations in annual precipitation, the most optimal sediment record to register this variability is the northern basin sequence, where high sediment accumulation rates allow for maximum temporal resolution. A clear correlation can be made between events of high rainfall and elevated χ levels over the period 1965-present (which has the most robust ^{210}Pb-derived chronology, transferred from the central basin, Fig. 10), confirming precipitation and strong river flow as the main delivery system of detrital material to the lake. This correlation confirms precipitation-driven river flow as the main delivery system of detrital material to the lake.

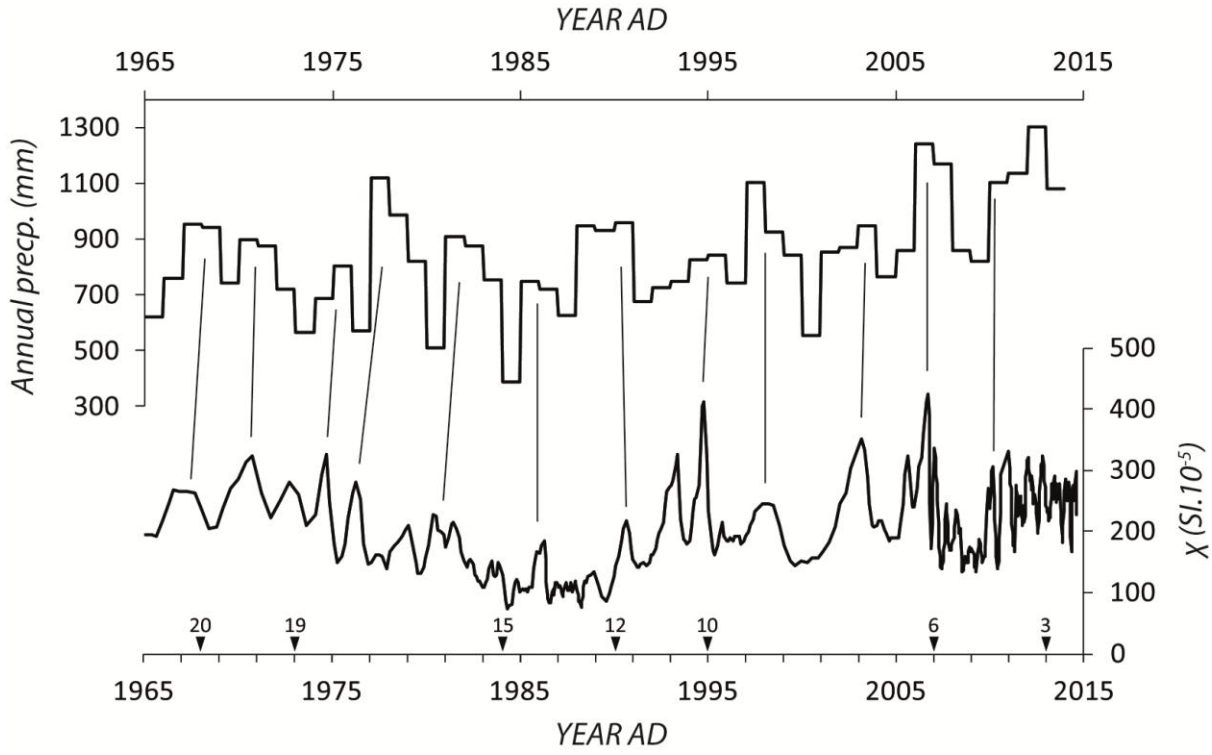

Fig. 10 The χ pattern of the well-dated upper sediments of Lake Bogoria's northern basin corresponds well to interannual rainfall variability in NOAA's Precipitation Reconstruction over Land (PREC/L) for the grid cell containing Lake Bogoria's catchment (Chen et al., 2002). This dataset uses interpolation between nearby gauge stations to produce monthly rainfall estimates, which in this figure have been summed to produce yearly rainfall amounts. Directly ^{210}Pb-dated chronological tie points are indicated, with numbers referring to Table 5.

An additional historical source of hydrological information is found in the late-19th and 20th century lake-level records of lakes Bogoria and Naivasha. Although for a large part poorly constrained by sporadic observational data (this is especially the case for Lake Bogoria), these records suggest

similar recent hydrological histories for these two Kenya Rift Valley lakes ca. 100 km apart. In Lake Bogoria, water level is buffered to a certain extent against strong year-to-year fluctuations by geothermal inflow. Therefore, the high-resolution sediment record of the northern basin, dominated by fast deposition triggered by heavy rainfall (Fig. 10), is less suited for comparison to longer-term lake-level change. In contrast, the southern basin provides the longest continuous sediment sequence of this study. Its distal location makes it less impacted by massive deposits originating from the Sandai-Waseges, making a distinct response to longer-term, climate-driven lake-level change more likely. Indeed, the collected southern basin sediment proxy data shows marked similarities to historical lake levels in the Kenya Rift Valley. An early-20th century highstand of both Lake Naivasha and Lake Bogoria, with water levels of the latter only 1-2 m below the spill point towards Lake Baringo (Tiercelin et al., 1987), is recorded by low levels of %OM, mirrored by high levels of Ti (Fig. 11). For the ensuing period, these proxies continue to capture the gradual drop to minimum levels during the 1950s and the following recovery into the 1960s and 1970s, validating their use as proxies for longer-term lake level change.

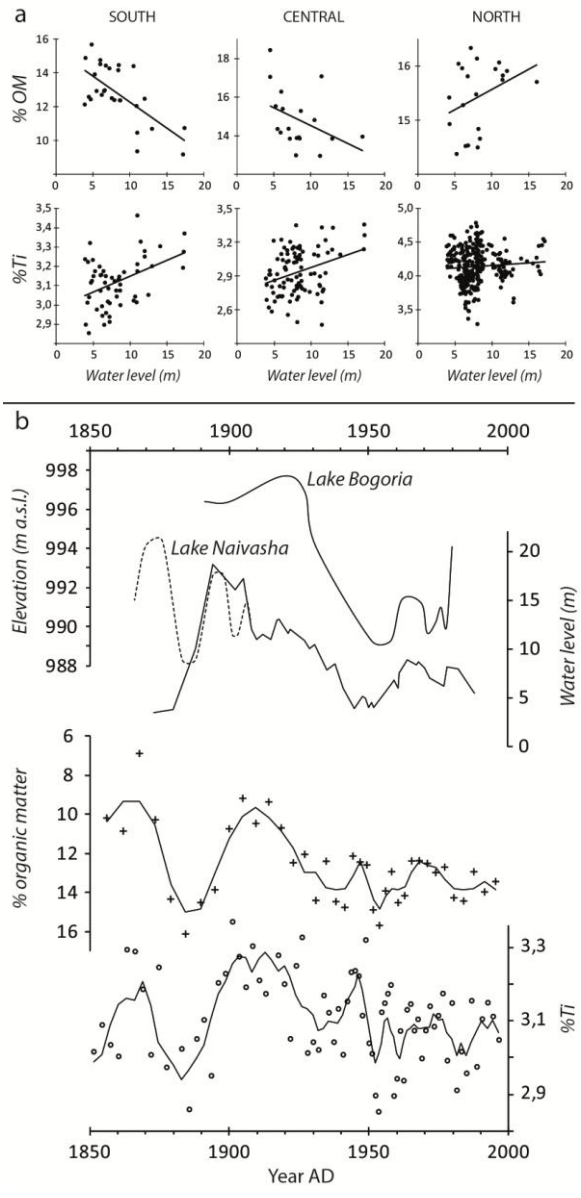

Fig. 11 (previous page) a: Correlation between historical water level of Lake Naivasha (as an approximation for lake level at Lake Bogoria) and Lake Bogoria sediment proxies % organic matter and %Ti over the 20th century, for the three basins. b: 20th-century water level at Lakes Naivasha (full line: Verschuren et al., 2000; dashed line: Nicholson, 1988) and Lake Bogoria (poorly constrained; Tiercelin et al., 1987), compared to % organic matter and %Ti levels from Lake Bogoria's southern basin.

The relationship between salinity and aquatic productivity in saline alkaline lakes is complex, with algal biomass changes in response to hydrochemical variability dependent on several factors such as species composition, salinity range and mixing regime (e.g. Vareschi, 1982; Melack, 1988). A simple, consistent relationship between hydrochemistry and algal biomass on seasonal or longer time scales has not been established for the saline, alkaline lakes of the Kenyan Rift Valley (Schagerl and Oduor, 2008), in part due to inadequate *in-situ* measurement frequencies. However, using remote sensing through satellite imagery covering the period 2000-2012, a weak but significant negative correlation was established between cyanobacterial biomass and water level at Lake Bogoria (Tebbs, 2014). It is proposed that high solute concentrations of surface waters make them more favourable to algal growth, with nitrogen and phosphorus in soluble form at high pH. Deeper wind mixing and chemocline erosion at lower lake levels may also contribute to the recycling of deep-water nutrients and maintenance of high nutrient levels in the upper water column, further promoting cyanobacterial blooming. Jirsa et al. (2013) have alternatively advertised the possible role of evaporative concentration in increased DOC levels in the surface waters of lakes Bogoria and Nakuru during droughts.

In the steep-sided southern basin of Lake Bogoria (Fig. 2), lake level has exhibited a relatively straightforward control on sedimentation over the past century. Due to higher average levels of river flow during moist periods, more terrestrial mineral material gets transported to the center of the southern basin, resulting in relatively high levels of Ti. Inversely, increased aquatic productivity in more saline, nutrient-rich surface waters and decreased dilution of organic matter by clastic material allow for the deposition of organic-rich sediments during drier episodes. Strikingly, the correlations between lake level (with the better-documented Lake Naivasha record as a proxy for Lake Bogoria water level) and sediment OM content and Ti observed in the southern basin weaken towards the north of the lake (Fig. 11). In the northern basin, the flat pan-shaped bathymetry enables a significant southern extension of the Sandai-Waseges river mouth upon relatively modest lake level decline (Fig. 2). This means that in the northern part of the lake, relatively large riverine deposits of terrigenous material during strong rains in overall drier periods have complicated the lake level to OM and Ti relationship observed in the southern basin (Fig. 11). With the central basin in an intermediary position, it seems to exhibit a similar but less well resolved lake level to proxy relationship than the southern basin.

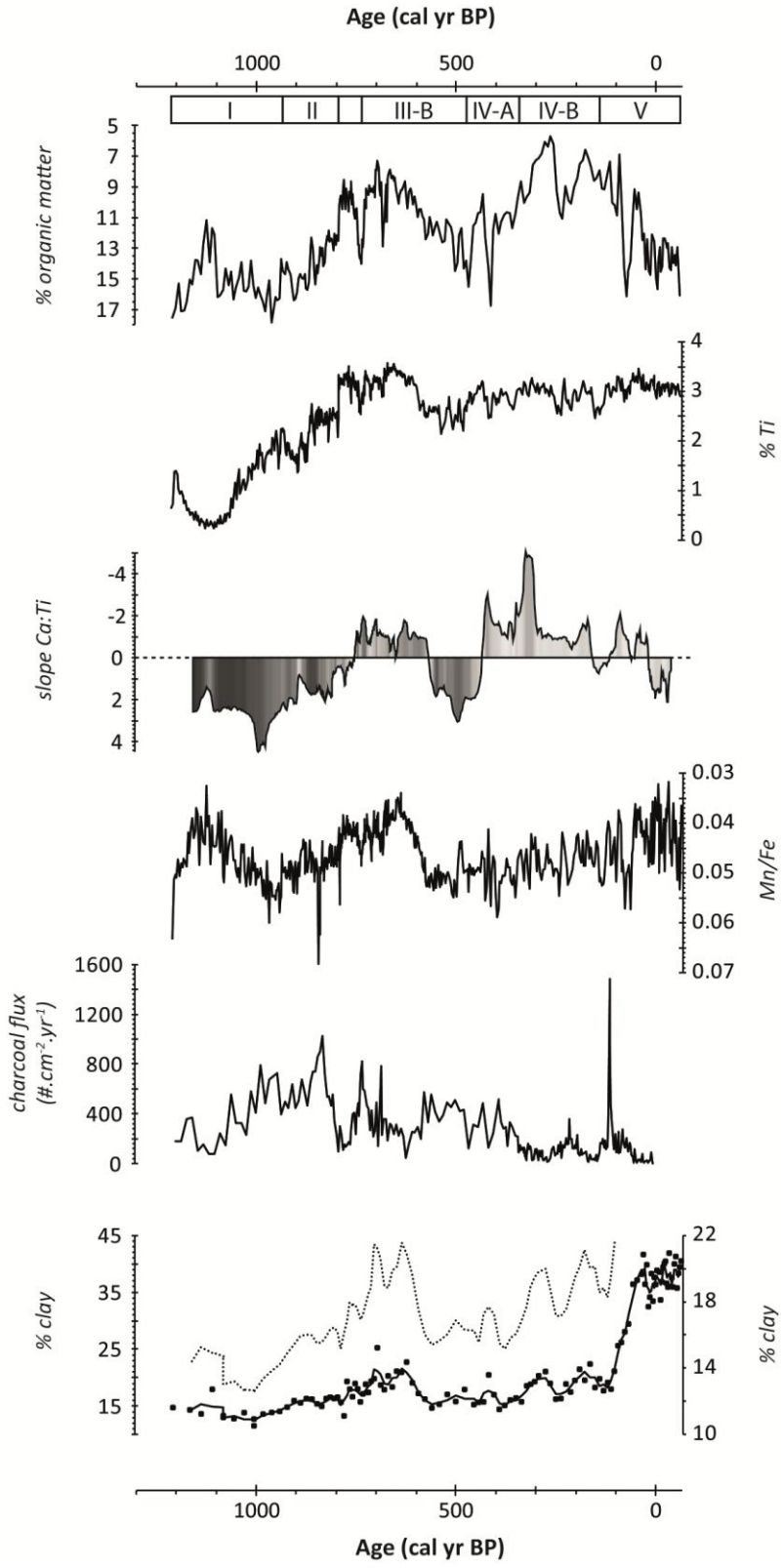

Fig. 12 Hydrologically sensitive proxies of Lake Bogoria's southern basin sediment sequence through time. Slope of the correlation between Ca and Ti was calculated over 15-cm running windows of XRF data, with shading under the curve reflecting strength of the correlation (darker colors indicating higher R^2 values). Clay levels are depicted as individual data points and a three-point running average (full line), with the latter presented also to a smaller scale (dashed line) to clarify pre-anthropogenic patterns.

Longer-term past moisture-balance change at Lake Bogoria

Its continuity and demonstrated, straightforward link between sediment geochemical composition and 20th-century lake level establish Lake Bogoria's southern basin as the preferred sediment sequence for high-resolution proxy-based moisture-balance reconstruction. Patterns of change through time in the most important hydrologically sensitive proxies collected from the southern basin sequence are presented in Fig. 12. In addition, the cores retrieved from the other four drill sites contribute quantitative information on hydrological change. The collected set of sediment sequences indicate severe hydrological variability beyond the range that is documented by historical records covering the past century. The oldest retrieved deposits, constituting Unit I in the cores representing the central and southern basins, indicate a much more negative water balance than today during the period ca. 1,200-950 cal yr BP. The presence of massive trona layers suggests that the central basin underwent extreme evaporative concentration on multiple prolonged stages, while the separating mud layers indicate that intermittent wetter periods periodically re-established sediment supply to the deepest parts of the basin. Trona precipitates from highly saline and alkaline brines in equilibrium with the atmosphere with respect to CO_2 (Eugster, 1971). Additionally, also thermonatrite and halite (although the latter not unambiguously demonstrated) are present in these massive Unit I deposits of the central basin. Characterizing the final stage of evaporative evolution in Na-HCO_3-CO_3-Cl brines (Eugster, 1971), these minerals suggest near-complete desiccation of Lake Bogoria's central basin, at least sporadically. The high temperatures required for thermonatrite formation were probably provided by exposure to intense solar irradiation, which today allows this mineral to precipitate on the sun-baked delta plains at the northern side of the lake (Renaut, 1986). Alternatively, thermonatrite could also have formed subaqueously in a very shallow and exposed brine pool, in which temperatures were possibly additionally raised by geothermal activity. During much of the period represented by Unit I, the central basin was probably comparable to modern-day Lake Magadi (southern Kenya Rift Valley), a sporadically flooded salt pan where ongoing trona precipitation resulted in deposits of many meters in thickness, and which has become a model system for describing brine evolution and present-day trona formation. (Eugster, 1980). At the same time, the southern basin was also reduced to a shallow brine pool, but a smaller surface-to-volume ratio and better sheltering from strong winds, in combination with its seasonal runoff-fed streams, probably protected it from complete desiccation. Alternatively, higher amounts of geothermal spring water being discharged into the southern basin than into the central basin could also explain the maintenance of a perennial water column in the former. Continuous sedimentation was maintained there, but very high organic and Cl content in combination with the presence of authigenic sodium carbonate and silicate minerals attest to extreme evaporative concentration and saline conditions. In the central basin, a number of events with increased clastic supply support the idea that trona deposits were formed during distinct periods of extreme drought alternating with somewhat wetter episodes. Similar to modern-day Lake Magadi, sporadical flooding probably dissolved the upper part of the previously deposited trona crust, restricting its upward growth (Eugster, 1971). The strong positive correlation between Ca and Ti values suggest that Ca is either part of the clastic fraction or that Ca contained in inflow waters was immediately precipitated when reaching the highly alkaline lake.

Abundant presence of nahcolite characterizes Unit II, which covers a next phase in the history of Lake Bogoria dated to ca. 950-800 cal yr BP. This evaporitic sodium carbonate mineral requires pCO_2 levels of at least several times higher than present-day atmospheric levels to precipitate (Eugster,

1966). Its occurrence in ancient deposits of the Green River Formation (western USA) have therefore been used to infer elevated atmospheric CO_2 levels during the early Eocene warm period (Lowenstein and Demicco, 2006*;* Jagniecki et al., 2015), while high rates of microbial respiration have been held responsible for historical nahcolite formation at Lake Bogoria (Renaut, 1986). However, a recent study demonstrated massive release of CO_2 from deep faults in the Magadi Basin and identified continental rifting along the entire EARS as a major contributing process to atmospheric CO_2 levels (Lee et al., 2016). Given Lake Bogoria's tectonic origin and its setting in an area of active faulting (Le Turdu et al., 1999), geothermal CO_2 was possibly an important driver of the nahcolite formation during the period corresponding to Unit II. Water levels were higher as compared to the Unit I stage, ensuring permanent inundation of the central and southern subbasins. This perennial water column had to be of a depth that enabled a sizeable build-up of pCO_2, facilitated by the inundation of the geothermal springs that currently discharge into the deepest part of these basins. However, an upper limit for water depth during this phase can be deduced, being the height of the central-south sill above the lake bottom of the central and southern basins at that time. This upper lake-level limit is plausible, because water levels at or close to the elevation of the sill separating the central and southern basins already were too dilute to form nahcolite (see below). During the phase embodied by Unit II, Lake Bogoria's central and southern basins may have been similar to modern-day Nasikie Engida, a 1.5-meter deep hypersaline, alkaline lake northwest of Lake Magadi, with active nahcolite precipitation and dependent for ca. 90% of its recharge on perennial geothermal springs (see Chapter 5). In the southern basin, %Ti levels suggest a slight increase in pluvial delivery of terrestrial clastics to the core site as compared to the preceding epsiode, though overall conditions were still arid. Organic matter content suggests low lake levels that gradually rose, consistent with the gradually decreasing prevalence of nahcolite towards the end of the period. A consistently positive Ca:Ti correlation in 15-cm running windows of XRF data suggests a dominant clastic origin of calcite, with conditions that remained unfavourable (i.e. too saline) for dissolved Ca storage in the water column. In accordance with this interpretation, a shift to positive correlations between Ca and terrestrial clastic elements has been described for Lake Yoa (Chad) when entering its Late-Holocene hypersaline phase, following a prolonged period of negative correlation when its waters were more dilute (Francus et al., 2013).

Following this episode, the start of Unit III clearly testifies to a shift to wetter conditions shortly after ca. 800 cal yr BP, as lake water became too dilute to support nahcolite precipitation. Organic matter content and Cl decrease, while %Ti sharply increases indicating a greater contribution of the rivers entering the southern basin. The southern basin shows no indication of authigenic zeolite formation at this time, indicating a less saline-alkaline environment. Water levels must have risen above the elevation of the central-south sill, connecting the two basins for the first time since at least the time corresponding to the base of the record (ca. 1,200 cal yr BP). At ca. 750 cal yr BP, the correlation between Ca and Ti becomes negative for the first time. This inverse correlation indicates that at this time, surface waters were dilute enough to preclude rapid calcium carbonate precipitation, and more so during periods of increased runoff. This would allow authigenic calcite formation at times when detrital influx temporarily decreased. Such a dilution would require high lake levels, possibly, up to the spill point towards Lake Baringo at 999 m a.s.l. In accordance with this scenario, elevated clay content between ca. 800 and 625 cal yr BP suggests lake levels were high enough to connect all three basins and establish a link to the northern Sandai-Waseges river, the major source of clay in the area. Increased sedimentation rates and low organic matter values at this time are indicators of

invigorated stream activity, supplying the southern basin with terrestrial material. Mn/Fe displays low levels between 800 and 625 cal yr BP with a minimum at ca. 650 cal yr BP, indicating a deep and permanently stratified water column at this time. Proxy information (%OM, %Ti, χ, Mn/Fe) from the southern basin provides evidence for two short-lived episodes of drier conditions and reduced water levels at ca. 750-720 cal yr BP and 690-670 cal yr BP. There is no evidence for nahcolite precipitation at these intervals, so water levels probably remained well above Unit-II levels. However, the base of the sediment sequence of the central-south sill is made up of mud aggregates rich in magadiite which hardened irreversibly upon exposure to air (Renaut 2003). This implies that during the first of these short dry spells, which corresponds to the timing of the base of the central-south sill sequence, lake level was close to or at the level of this sill. Alternatively, this magadiite aggregate layer could also have been transported to the south-central sill core site from nearby shallower regions upon lake level lowering. The second of these short intervals did not lower lake level to the same extent. However, evaporative concentration of the large amounts of dissolved silica that had been able to build up in the water column during the preceding decades of predominantly wet conditions, triggered extensive magadiite precipitation in the central subbasin and on the central-south sill.

Following peak humidity at ca. 650 cal yr BP, the proxy record suggests a return to drier conditions during the period covered by the upper part of Unit III (ca. 600-480 cal yr BP). This is supported in the southern basin by a.o. a decrease in runoff (χ, Ti) and increased levels of organic matter, Mn/Fe and Cl. A return to a more negative moisture balance and evaporative concentration of the water column is suggested by a switch to strongly significant positive Ca:Ti correlation, while the central subbasin contained a brine saline enough to allow magadiite and clinoptilolite precipitation. Magadiite was also precipitated at the central-south sill at this point, with relatively limited aggregate formation at the timing of maximum drought suggesting water levels close to or temporarily at the sill elevation (or, alternatively, transport of material from nearby newly-exposed areas). Increased levels of Mn/Fe suggest that the water column was shallow enough to allow regular mixing. Together with clay levels falling back to values of Units I and II, these are all indications that the southern part of the lake was cut off again from the northern basin and Sandai-Waseges flow.

The start of Unit IV marks the end of the drought recorded by the upper part of Unit III, with increased supply of terrigenous clastic material to the southern basin coring site. Decreasing levels of organic matter and a shift to negative Ca:Ti correlation suggest more dilute waters and higher lake levels. This scenario is also supported by the temporary deposition of finely laminated sediments in the central and south basins, indicating a deep, permanently stratified water column between ca. 480 and 440 cal yr BP, with wind mixing or salt-tolerant benthic fauna unable to disturb the deposited sediments. Levels of Mn/Fe are also somewhat lower during this interval than during the preceding lowstand, but do not reach the minimum levels of the ca. 650 cal yr BP high stand. Also, no authigenic sodium silicate minerals were formed in the central basin at this time, further supporting temporarily dilute conditions.

The array of evidence suggests that this wet episode heralded the start of a prolonged period of short-term variability that lasted until ca. 150 cal yr BP. From the early 16th century onwards, water levels were low enough, at least occasionally, to allow authigenic analcime precipitation in the central basin. Importantly, this episode also comprised extreme evaporative concentration of the north basin, with conditions in this basin reminiscent of Unit-1 conditions in the southern basin (i.e.

trona precipitation in a shallow hypersaline brine pool). The resistance of these salt-rich deposits prevented the collection of sediments pre-dating ca. 1610 from the northern basin. Moisture balance remained variable afterwards, with the main feature being a shift to predominantly drier conditions between ca. 250 and 150 cal yr BP. While organic matter content in deposits of the southern basin is relatively low, especially between ca. 350 and 250 cal yr BP, other evidence suggests that Lake Bogoria was not at maximum levels between 350 and 150 cal yr BP. Relatively high Cl content indicates increased salinity, and weak levels of Ca:Ti correlation suggest short-term hydrochemical variability. Also, during the 350-150 cal yr BP period, SAR of the northern basin was consistently about twice as high as those of the southern basin, and more than five times as high as in the central basin (Fig. 8). This implies that lake level during this period was never high enough to connect the northern to the more southerly basins, restricting deposition of the Sandai-Waseges sediment load to the northern basin while cutting it off from the more distal parts of the lake, creating the observed interbasin offsets in SAR. The northern basin sediments contain evidence of much more saline conditions than present from the base of the sequence at ca. 340 until 150 cal yr BP. The end of this period corresponds to a layer of magadiite-rich mud aggregates in the central-south sill sequence, similar to the layer that makes up the base of that sequence. Whether lake level fell down to the level of this sill is uncertain, but in any case, it was lowered to a level that allowed transport of material from nearby slopes that had fallen dry. When lake-level rise finally inundated the north-central sill shortly after 150 cal yr BP (corresponding to the base of the north-central sill sediment sequence) and re-established the connection between the northern basin and the more southern parts of the lake, north:south and north:central SAR ratios swiftly drop to values around 1 and 2 respectively, reflecting a relatively more even distribution of Sandai-Waseges sediment load over the whole surface area of the lake.

Since ca. 150 cal yr BP, water level at Lake Bogoria has consistently been higher than 987 m a.s.l. (i.e. the present elevation of the north-central sill minus the thickness of the sediment that has been deposited since), never breaking the connection between the three basins. This is evident from the uninterrupted deposition of finely laminated mud at all five core sites. While organic matter content, Ti and Mn/Fe suggest a short-lived episode of drought and lake level decline during the second half of the 19th century, this event was too short-lived to lower water level below the isolation point of the northern basin. During the 20th century, levels of Mn/Fe drop to low levels not attained since the late-13th to early-14th century. Together with levels of χ and Ti that are high overall when compared to the entire record, this suggests generally stable conditions of high lake level and thus relatively moist conditions during recent times. On the other hand, Ca:Ti correlation does not show any clear patterns over the past two centuries, with a variable sign and low R^2 values. It seems likely that other elements beside lake level exert influence on this proxy, and deeper study of hydrochemistry-linked processes should allow a better understanding of the response to carbonate precipitation to water level change.

Lake Bogoria in the context of regional moisture balance history

Overall, this new moisture-balance record obtained from Lake Bogoria displays marked similarities to the well-established 1200-year hydroclimate record of Lake Edward in westernmost East Africa, at the Uganda-DR Congo border (Fig. 13; Russell and Johnson, 2007). The most arid conditions of the entire new Lake Bogoria record, dated to ca. 1,250-950 cal yr BP, overlap with a prolonged dry phase at Lake Edward during most of the second half of the first millennium AD. A short episode of moist

conditions at Lake Edward around ca. AD 1000 could also have affected Lake Bogoria, raising water levels enough to end massive trona deposition in the central basin and allow nahcolite precipitation. Afterwards, rainfall at Lake Edward declined again to minimum levels in the second half of the 12th century AD, reflecting Medieval Climate Anomaly (MCA) drought. Aridity seems to have been the general rule throughout East Africa at this time, as described in detail in Chapter 2. Similarly, Lake Bogoria's levels remained relatively low during this episode, until a sharp increase in water level and stream flow at ca. 800 cal yr BP ended conditions favourable for nahcolite precipitation. Similar to Lake Edward, Lake Bogoria attained peak humidity levels relatively soon afterwards, at around 650 cal yr BP. Earlier research has dated sudden wetland formation at Loboi Swamp, bordering Lake Bogoria to the north, to 680±40 cal yr BP (i.e. AD 1230-1310; Driese et al., 2004), corresponding well to the wet conditions inferred from the lake proxy record. After the early- to mid-14th century humidity optimum, the similarity between Lake Bogoria and Lake Edward partly breaks down. While the latter demonstrates a gradual and quasi-uninterrupted decline in moisture balance, Lake Bogoria's evolution throughout the following centuries seems more variable. Chapter 2 comprehensively deals with the spatial variability observed throughout East Africa during the Little Ice Age, the time window of AD 1250-1750 when the northern hemisphere experienced temperatures significantly cooler than today. It seems that during this period, Lake Bogoria's hydroclimatic regime was influenced by the evolution of both western and eastern moisture sources. Following the early-LIA rainfall optimum, an evolution to late-LIA aridity as observed at Lake Edward (which receives a substantial amount of precipitation from the Atlantic Ocean), is counteracted by a simultaneous rise in moisture transport from the Indian Ocean, which is shown to peak towards the end of the LIA (Tierney et al., 2013). Therefore, Lake Bogoria seems to have held the middle between Lake Edward and sites from eastern East Africa such as Lake Naivasha (Fig. 13; Verschuren et al., 2000) and Lake Challa (Buckles et al., 2016). A number of droughts at Lake Bogoria can also be linked to events at these other sites. For example, the short-lived drought that severely concentrated the northern basin of Lake Bogoria, matching the base of the northern basin sediment sequence at ca. 340 cal yr BP, possibly corresponds to the late-16th to early-17th century Nyarubanga drought known from historical traditions and the lake-level record of Lake Naivasha (Webster, 1979; Verschuren et al., 2000). The lake level rise that reconnected the northern basin to the more southerly parts of the lake is dated to a best estimate of 150 ± 35 cal yr BP, which is within uncertainty range of the inferred ending of the late-18th to early-19th century drought that manifested itself throughout almost the whole continent (see Chapter 2). At Lake Sonachi, a small crater lake close to Lake Naivasha, the onset of lacustrine sedimentation following drought-related desiccation is dated to AD 1815±8 (Verschuren, 1999), while a coral record from the Kenyan coast provides evidence for increased soil runoff within the Sabaki River catchment caused by drought-breaking pluvial events at AD 1822-1826 (Fleitmann et al., 2007). Lake Baringo was completely dry during this event, as well as a number of small crater lakes in Uganda (Bessems et al., 2008). The results obtained from this new set of sediment cores demonstrate that levels of Lake Bogoria were also significantly lower at this time, with the northern basin separated as an individual small, shallow water body from the more southerly parts of the lake. It has to be pointed out that, once this separation into separate northern and southern lakes is in place, the levels of both water bodies did not have to be at the same elevation. For example, during the late-18th to early 19th-century dry event, the presence of magadiite aggregates suggests a decline of the southern part of the lake to levels at or close to the central-south sill. Though this sill was only at a slightly higher elevation than the deepest part of the northern basin in the early 19th century, the data clearly indicates a sustained

lacustrine phase in the latter during this time. This does not have to be a contradiction, since the northern and southern parts of the lake fall under differential hydrological recharge regimes after separation. Once cut-off from the Sandai-Waseges, the southern lake could, and probably did, decline much faster than the northern lake which continued to receive inflow from the largest river in the catchment.

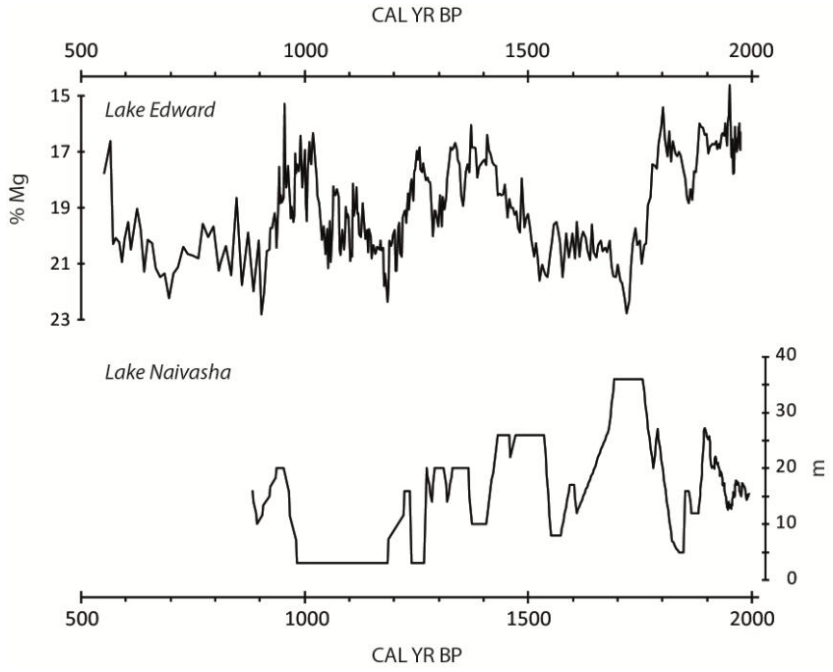

Fig. 13 Lake Edward %Mg in calcite (Russell and Johnson, 2007) and Lake Naivasha water level (Verschuren et al., 2000).

Over the past two centuries, lake level at Lake Bogoria has uninterruptedly been high when compared to its entire 1,300-year history. This is similar to other East African lakes, such as Lake Edward (Russell and Johnson, 2007), Lake Tanganyika (Cohen et al., 2005) and Lake Malawi (Brown and Johnson, 2005). However, the longer history of these lakes, including Lake Bogoria, suggests that severe, decadal-scale drought greatly exceeding the 20th-century range of variability should be expected to occur again sometime in the future. Even though some (but not all) models project an increase in precipitation over East Africa (Shongwe et al., 2011), long-term water and agriculture management plans should incorporate the knowledge on this inherent variability of water resources if future problematic scenarios are to be avoided.

Evidence for recent human impact in the Lake Bogoria catchment

The most prominent feature of Unit V is a remarkable rise in clay content of which the start is dated to ca. 110 cal yr BP, multiplying the contribution of clays to the total inorganic fraction by a factor of 2 to 3. Right before this sedimentological change, charcoal supply reaches the highest levels of the entire record in a short but distinct peak clearly observable in all three basins, with amounts remaining high during the steep increase in clay. The most plausible explanation is the onset of significant human impact on the landscape in the catchment of the Sandai-Waseges river. Clearing of natural vegetation must have destabilized the clay soils of these areas. This severely increased soil

runoff further established the dominance of the Sandai-Waseges over other seasonal rivers as the main source of terrigenous material to all three basins. This first signal of pronounced human impact definitely proves pre-colonial human presence in the Bogoria catchment, but it seems to postdate developments in the nearby Lake Baringo catchment, where it has been proposed that indigenous pastoralists and farmers have been actively shaping the landscape for the past 250-300 years (Ashley et al., 2004; Kiage and Liu, 2009). A second change is observed in the early 1970's, when SAR in the northern basin again increases dramatically, corresponding to the deposition of a meter of sediment over the past 30 years. A recent increase in the occurrence of large sediment plumes in the northern part of the lake, observable on satellite imagery, is in accordance with this trend (Tebbs, 2014), as are the recovered sediment-trap samples from the northern basin which contained very large amounts of terrigenous material (Fig. 9). In recent decades, SAR in the central basin became higher than in the southern basin for the first time in the entire record, due to its more proximal location to the Sandai-Waseges and the further reduction in relative share of the other seasonal rivers in supplying sediment to the central and southern basins. Around Lake Baringo, land degradation intensified in the 1960s due to population growth and corresponding expansion of subsistence agriculture, in combination with the abandonment of colonial soil-conservation programmes (Johansson and Svensson, 2002). Soil erosion and subsequent high sedimentation rates have severely transformed the ecological structure of Lake Baringo, with potential risks for future sustenance of local communities (Hickley et al., 2004). It seems that, despite its management within the Kenya National Reserve framework, Lake Bogoria has been subject to similar processes altering its natural sedimentation dynamics. Centers of human settlement and agriculture currently exist at the northern edge of the lake, but are most developed at the origin of the Sandai-Waseges river in the southeastern part of the catchment, outside of the reserve's boundaries, where forests have been cleared for large-scale commercial farms and ranches during the colonial period, that were afterwards subdivided into many small-scale holdings (Mugo, 2007). Besides the obvious rapid infilling of the northern basin, the ongoing increase in terrigenous sediment delivery to the lake may have additional consequences for this unique lacustrine ecosystem. For example, increased turbidity might harm the planktonic community of the lake, which in turn drives the population of lesser flamingos which the national reserve is famous for (Harper et al., 2003).

CONCLUSIONS

This study improves our understanding of hydrological change at Lake Bogoria over the past ca. 1,300 years in the context of the evolution of its sedimentation dynamics. Integration of high-resolution proxy data from the southern basin in combination with documentation of major sedimentological changes observed at four other locations in the lake reveals major hydrochemical and lake-level fluctuations which suggest climate variability far outside the known 20th-century range. The record starts with a period of major aridity, effectively separating the three basins and leaving the deep central basin in a predominantly desiccated state in resemblance to modern-day Lake Magadi. In a following, still severely dry phase, the separated central and southern basins held permanent but shallow water bodies enriched in CO_2 by geothermal injection, probably in a setting similar to modern Nasikie Engida. Later, at ca. 800 cal yr BP, local climate shifted to wetter conditions to reach a humidity optimum around ca. 650 cal yr BP, similar to the early-Little Ice Age optimum in western East Africa. Following mostly variable conditions with a number of severe droughts during the rest of the Little Ice Age, water level during the past two centuries has overall been high and historically documented fluctuations should be regarded as minor when compared to

the longer-term history of the lake. The youngest sediments have recorded the onset of human activity in the catchment, and recent decades have seen a spectacular increase in terrigenous sediment delivery to the lake. With the main cause of this evolution situated outside the boundaries of the natural reserve, additional research should aim for a better documentation of these developments and their ecological implications, so adequate measures can be incorporated in future conservation strategies.

REFERENCES

Appleby P. (2001) Chronostratigraphic techniques in recent sediments. In: Last W, Smol J (eds), Basin analysis, coring and chronological techniques. Kluwer Academic, pp. 171-203.

Appleby P, Oldfield F. (1978) The calculation of 210Pb dates assuming a constant rate of supply of unsupported 210Pb to the sediment. Catena 5:1-8.

Ashley GM, Mworia JM, Muasya AM, Owen RB, Driese SG, Hover VC, Renaut RW, Goman MF, Mathai S, Blatt SH. (2004) Sedimentation and recent history of a freshwater wetland in a semi-arid environment: Loboi Swamp, Kenya, East Africa. Sedimentology 51:1301-1321.

Bengtsson L, Enell M. (1986) Chemical analysis. In: Berglund B (ed), Handbook of Holocene palaeoecology and palaeohydrology. Wiley, New York, US, pp. 485-496.

Bessems I, Verschuren D, Russell JM, Hus J, Mees F, Cumming BF. (2008) Palaeolimnological evidence for widespread late 18th century drought across equatorial East Africa. Palaeogeography Palaeoclimatology Palaeoecology 259.

Blaauw M. (2010) Methods and code for 'classical' age-modelling of radiocarbon sequences. Quaternary Geochronology 5:512-518.

Boyle J. (2001) Inorganic geochemical methods in paleolimnology. In: Last W, Smol J (eds), Tracking environmental change using lake sediments: physical and geochemical methods. Kluwer, Dordrecht, The Netherlands, pp. 83-141.

Brown ET, Johnson TC. (2005) Coherence between tropical East African and South American records of the Little Ice Age. Geochemistry Geophysics Geosystems 6.

Buckles LK, Verschuren D, Weijers JWH, Cocquyt C, Blaauw M, Sinninghe Damsté JS. (2016) Interannual and (multi)-decadal variability in the sedimentary BIT index of Lake Challa, East Africa, over the past 2200 years: assessment of the precipitation proxy. Climate of the Past 12:1243-1262.

Chen MY, Xie PP, Janowiak JE, Arkin PA. (2002) Global land precipitation: A 50-yr monthly analysis based on gauge observations. Journal of Hydrometeorology 3:249-266.

Cohen A, Palacios-Fest M, Msaky E, Alin S, McKee B, O'Reilly C, Dettman D, Nkotagu H, Lezzar K. (2005) Paleolimnological investigations of anthropogenic environmental change in Lake Tanganyika: IX. Summary of paleorecords of environmental change and catchment deforestation at Lake Tanganyika and impacts on the Lake Tanganyika ecosystem. Journal of Paleolimnology 34:125-145.

Colombaroli D, Ssemmanda I, Gelorini V, Verschuren D. (2014) Contrasting long-term records of biomass burning in wet and dry savannas of equatorial East Africa. Global Change Biology 20:2903-2914.

Davies S, Lamb H, Roberts S. (2015) Micro-XRF core scanning in palaeolimnology: recent developments. In: Croudace I, Rothwell R (eds), Micro-XRF studies of sediment cores. Springer, pp. 189-226.

Dean WE. (1974) Determination of carbonate and organic-matter in calcareous sediments and sedimentary-rocks by loss on ignition - comparison with other methods. Journal of Sedimentary Petrology 44:242-248.

Driese SG, Ashley GM, Li ZH, Hover VC, Owen RB. (2004) Possible Late Holocene equatorial palaeoclimate record based upon soils spanning the Medieval Warm Period and Little Ice Age, Loboi Plain, Kenya. Palaeogeography Palaeoclimatology Palaeoecology 213:231-250.

Eugster H. (1971) Origin and deposition of trona. Wyoming University Contribution to Geology 10:49-55.

Eugster H. (1980) Lake Magadi, Kenya, and its precursors. In: Nissenbaum A (ed), Hypersaline brines and evaporitic environments. Elsevier, Amsterdam, The Netherlands, pp. 195-232.

Eugster HP. (1966) Sodium carbonate-bicarbonate minerals as indicators of pCO2. Journal of Geophysical Research 71:3369-3377.

Eugster HP, Jones BF. (1979) Behavior of major solutes during closed-basin brine evolution. American Journal of Science 279:609-631.

Fleitmann D, Dunbar RB, McCulloch M, Mudelsee M, Vuille M, McClanahan TR, Cole JE, Eggins S. (2007) East African soil erosion recorded in a 300 year old coral colony from Kenya. Geophysical Research Letters 34.

Francus P, Von Suchodoletz H, Dietze M, Donner RV, Bouchard F, Roy AJ, Fagot M, Verschuren D, Kropelin S. (2013) Varved sediments of Lake Yoa (Ounianga Kebir, Chad) reveal progressive drying of the Sahara during the last 6100 years. Sedimentology 60:911-934.

Haberzettl T, Corbella H, Fey M, Janssen S, Lucke A, Mayr C, Ohlendorf C, Schdbitz F, Schleser GH, Wille M, Wulf S, Zolitschka B. (2007) Lateglacial and Holocene wet-dry cycles in southern Patagonia: chronology, sedimentology and geochemistry of a lacustrine record from Laguna Potrok Aike, Argentina. Holocene 17:297-310.

Harper D, Childress R, Harper M, Boar R, Hickley P, Mills S, Otieno N, Drane T, Vareschi E, Nasirwa O, Mwatha W, Darlington J, Escute-Gasulla X. (2003) Aquatic biodiversity and saline lakes: Lake Bogoria National Reserve, Kenya. Hydrobiologia 500:259-276.

Hickley P, Boar R, Mavuti K. (2003) Bathymetry of Lake Bogoria, Kenya. Journal of East African Natural History 92:107-117.

Hickley P, Muchiri M, Boar R, Britton R, Adams C, Gichuri N, Harper D. (2004) Habitat degradation and subsequent fishery collapse in Lakes Naivasha and Baringo, Kenya. Ecohydrology & Hydrology 4:503-517.

Jagniecki EA, Lowenstein TK, Jenkins DM, Demicco RV. (2015) Eocene atmospheric CO2 from the nahcolite proxy. Geology 43:1075-1078.

Jirsa F, Gruber M, Stojanovic A, Omondi SO, Mader D, Korner W, Schagerl M. (2013) Major and trace element geochemistry of Lake Bogoria and Lake Nakuru, Kenya, during extreme draught. Chemie Der Erde-Geochemistry 73:275-282.

Johansson J, Svensson J. (2002) Land degradation in the semi-arid catchment of Baringo, Kenya: a minor field study of physical causes with socioeconomic aspect. Department of Geography, Göteborg University, Sweden.

Kiage LM, Liu K-b. (2009) Palynological evidence of climate change and land degradation in the Lake Baringo area, Kenya, East Africa, since AD 1650. Palaeogeography Palaeoclimatology Palaeoecology 279.

LaVigne M, Ashley G. (2001) Climatology and rainfall patterns: Lake Bogoria National Reserve (1976-2001). Department of Geological Sciences, Rutgers University, Piscataway, NJ, USA, p. 48.

Le Turdu C, Tiercelin J, Richert J, Rolet J, Xavier J, Renaut R, Lezzar K, Coussement C. (1999) Influence of preexisting oblique discontinuities on the geometry and evolution of extensional fault patterns: evidence from the Kenya Rift using SPOT imagery. In: Morley C (ed), Geoscience of rift systems - Evolution of East Africa: AAPG studies in Geology, pp. 173-191.

Lee H, Muirhead JD, Fischer TP, Ebinger CJ, Kattenhorn SA, Sharp ZD, Kianji G. (2016) Massive and prolonged deep carbon emissions associated with continental rifting. Nature Geoscience 9:145-149.

Lowenstein TK, Demicco RV. (2006) Elevated eocene atmospheric CO2 and its subsequent decline. Science 313:1928-1928.

Masson-Delmotte V, Schulz M, Abe-Ouchi A, Beer J, Ganopolski A, González Rouco J, Jansen E, Lambeck K, Luterbacher J, Naish T, Osborn T, Otto-Bliesner B, Quinn T, Ramesh R, Rojas M, Shao X, Timmermann A. (2013) Information from paleoclimate archives. In: Stocker T, Qin D, Plattner G, Tignor M, Allen S, Boschung J, Nauels A, Xia Y, Bex V, Midgley P (eds), Climate Change 2013: the physical science basis Contribution of Working Group I to the Fifth Assessment Report of the Intergovernmental Panel on Climate Change, Cambridge, UK New York, USA

Melack JM. (1988) Primary producer dynamics associated with evaporative concentration in a shallow, equatorial soda lake (Lake Elmenteita, Kenya). Hydrobiologia 158:1-14.

Melles M, Brigham-Grette J, Minyuk PS, Nowaczyk NR, Wennrich V, DeConto RM, Anderson PM, Andreev AA, Coletti A, Cook TL, Haltia-Hovi E, Kukkonen M, Lozhkin AV, Rosen P, Tarasov P, Vogel H, Wagner B. (2012) 2.8 Million Years of Arctic Climate Change from Lake El'gygytgyn, NE Russia. Science 337:315-320.

Mugo K. (2007) Lake Bogoria National Reserve: integrated management plan 2007-2012. County Council of Baringo, County Counsil of Koibatek, WWF-EARPO.

Nicholson S. (1988) Historical fluctuations of Lake Victoria and other lakes in the northern Rift Valley of East Africa. Monographiae Biologicae:7-36.

Renaut R. (2003) Magadiite. In: Middleton G (ed), Encyclopedia of sediments and sedimentary rocks. Kluwer Academic.

Renaut R, Tiercelin J, Owen R. (1986) Mineral precipitation and diagenesis in the sediments of the Lake Bogoria basin, Kenya Rift Valley. Geological Society, London, Special Publications 25:159-175.

Rowell DP, Booth BBB, Nicholson SE, Good P. (2015) Reconciling Past and Future Rainfall Trends over East Africa. Journal of Climate 28:9768-9788.

Russell JM, Johnson TC. (2007) Little Ice Age drought in equatorial Africa: Intertropical Convergence Zone migrations and El Nino-Southern Oscillation variability. Geology 35:21-24.

Russell JM, Verschuren D, Eggermont H. (2007) Spatial complexity of 'Little Ice Age' climate in East Africa: sedimentary records from two crater lake basins in western Uganda. Holocene 17:183-193.

Röhl U, Abrams L. (2000) High-resolution, downhole and nondestructive core measurements from Site 999 and 1001 in the Caribbean Sea: application to the Late Paleocene Thermal Maximum. Proceedings of the Ocean Drilling Program Scientific Results 165:191-203.

Schagerl M, Oduor SO. (2008) Phytoplankton community relationship to environmental variables in three Kenyan Rift Valley saline-alkaline lakes. Marine and Freshwater Research 59:125-136.

Shongwe ME, van Oldenborgh GJ, van den Hurk B, van Aalst M. (2011) Projected Changes in Mean and Extreme Precipitation in Africa under Global Warming. Part II: East Africa. Journal of Climate 24:3718-3733.

Tebbs E. (2014) Remote sensing for the study of ecohydrology in East African Rift lakes. PhD thesis. Department of Physics and Astronomy. University of Leicester, Leicester, UK.

Thomson J, Croudace I, Rothwell R. (2006) A geochemical application of the ITRAX scanner to a sediment core containing eastern Mediterranean sapropel units. In: Rothwell R (ed), New techniques in sediment core analysis, pp. 65-77.

Tiercelin J, Vincens A. (1987) Le demi-graben de Baringo-Bogoria, Rift Gregory, Kenya. 30000 ans d'histoire hydrologique et sédimentaire. Bulletin des Centres de Recherches Exploration-Production Elf-Aquitaine 11:249-540.

Tierney JE, Smerdon JE, Anchukaitis KJ, Seager R. (2013) Multidecadal variability in East African hydroclimate controlled by the Indian Ocean. Nature 493:389-392.

Tjallingii R, Rohl U, Kolling M, Bickert T. (2007) Influence of the water content on X-ray fluorescence core-scanning measurements in soft marine sediments. Geochemistry Geophysics Geosystems 8.

Vaasma T. (2008) Grain-size analysis of lacustrine sediments: a comparison of pre-treatment methods. Estonian Journal of Ecology 57:231-243.

van der Werf GR, Randerson JT, Giglio L, Gobron N, Dolman AJ. (2008) Climate controls on the variability of fires in the tropics and subtropics. Global Biogeochemical Cycles 22.

Vareschi E. (1982) The ecology of Lake Nakuru (Kenya) .3. Abiotic factors and primary production. Oecologia 55:81-101.

Verschuren D. (1999) Influence of depth and mixing regime on sedimentation in a small, fluctuating tropical soda lake. Limnology and Oceanography 44.

Verschuren D. (2001) Reconstructing fluctuations of a shallow East African lake during the past 1800 yrs from sediment stratigraphy in a submerged crater basin. Journal of Paleolimnology 25.

Verschuren D. (2004) Decadal to century-scale climate variability in tropical Africa during the past 2000 years. In: Battarbee R, Gasse F, Stickley C (eds), Past climate variability through Europe and Africa. Kluwer, Dordrecht, The Netherlands, pp. 139-158.

Verschuren D, Charman D. (2008) Latitudinal linkages in late-Holocene moisture-balance variation. In: Battarbee R, Binney H (eds), Natural climate variability and global warming. Wiley-Blackwell, Chichester, UK.

Verschuren D, Laird KR, Cumming BF. (2000) Rainfall and drought in equatorial east Africa during the past 1,100 years. Nature 403:410-414.

Vincens A, Casanova J, Tiercelin J. (1986) Palaeolimnology of Lake Bogoria (Kenya) during the 4500 BP high lacustrine phase. In: Frostick L, Renaut R, Reid I, Tiercelin J (eds), Sedimentation in the African rifts. Blackwell Scientific Publications, pp. 323-330.

Webster J. (1979) Chronology, Migration and Drought in Interlacustrine Africa. Longman & Dalhousie University Press, London, UK.

Wright HE. (1980) Cores of soft lake sediments. Boreas 9:107-114.

Xie PP, Arkin PA. (1997) Global precipitation: A 17-year monthly analysis based on gauge observations, satellite estimates, and numerical model outputs. Bulletin of the American Meteorological Society 78:2539-2558.

5 EXPLORING THE SEDIMENT RECORD OF NASIKIE ENGIDA ('LAKE LITTLE MAGADI') AS POTENTIAL ARCHIVE OF PAST HYDROCLIMATE CHANGE IN THE SOUTHERN KENYA RIFT VALLEY

De Cort, Gijs[1,2]; Renaut, Robin[3]; Van Der Meeren, Thijs[1]; Mbuthia, Anthony[4]; Mees, Florias[2]; Verschuren, Dirk[1]

[1]*Limnology Unit, Department of Biology, Ghent University. K.L. Ledeganckstraat 35, 9000 Ghent, Belgium.*
[2]*Department of Earth Sciences, Royal Museum for Central Africa. Leuvensesteenweg 13, 3080 Tervuren, Belgium.*
[3]*Department of Geological Sciences, University of Saskatchewan. Saskatoon, SK, Canada S7N 5E2.*
[4]*Tata Chemicals Magadi, Magadi, Kenya.*

This chapter will be extended for publication in *Journal of Paleolimnology*.

In search for new high-quality lake-sediment records to close geographical gaps in the existing network of high-resolution paleoclimate archives from East Africa, we use a newly acquired sediment sequence from Nasikie Engida ('Lake Little Magadi') to evaluate the potential of this hypersaline lake as an archive for past hydroclimate variability in the southern Kenya Rift Valley. We find that geothermal spring input supplementing low local rainfall has buffered the lake against complete desiccation throughout the time period covered by the 4.62-m sediment sequence, which (pending availability of radiometric dating) may cover a good part of the mid- to late Holocene. Stratigraphic description and a limited set of non-invasive analyses reveal Nasikie Engida as a promising site to produce the first paleoclimate reconstruction for the southernmost Kenya Rift Valley covering at least the late Holocene with high resolution.

INTRODUCTION

Lake sediments make up the largest part of available paleoclimate archives throughout Africa (Verschuren, 2003), especially in East Africa where tectonic activity has resulted in the development of a major rift system hosting a series of sedimentary basins (East African Rift System, EARS; Westcott et al., 1996). Due to the endorheic nature of lake basins in the Eastern (Gregory) branch of the EARS running through Kenya, the water bodies they contain often fluctuate drastically in response to climate change. The combination of low lake-to-catchment surface areas, the contrast between the dry rift valley floor and the wetter surrounding highlands and an often well-developed hydrographic system of ephemeral streams has been recognized as an important factor in East African lake-level variability (Street, 1980). This means that the naturally low precipitation-evaporation (P-E) ratio that characterizes East Africa's mostly semi-arid tropical climate makes them prone to intermittent complete desiccation, even in response to relatively modest hydroclimate fluctuations in the relatively recent past (e.g. Verschuren, 1999; Bessems et al., 2008; De Cort et al., 2013). This severely limits the recovery of continuous records of historical climate variability that would cover more than the last few hundreds of years, and has resulted in the fact that, even after several decades of targeted research, the number of available high-resolution records and their geographical coverage is still insufficient to robustly describe regional climate patterns on timescales most relevant to human societies (Verschuren, 2004; Verschuren and Russell, 2009; see chapter 2). Since East Africa is a region where sites at relatively short distances from each other can be under different hydrological regimes, either because of topographic factors or contrasting moisture sources (Nicholson, 2000), new records going back in time far enough will be needed to delineate the spatial

patterns of moisture balance variability over the past centuries and millennia, of which our current understanding is based on only a handful of sediment archives (see thesis chapter 2). For this reason, we evaluate the potential of the previously unstudied sediment record of Nasikie Engida (also known as 'Little Magadi') in the southern Kenya Rift Valley, for paleoclimate reconstruction. Like Lake Bogoria (chapters 3, 4) this lake has a unique hydrological setting that buffers against desiccation, at least as far as has been documented during recent decades. However, nothing is known about its longer-term moisture-balance history. In this chapter, preliminary results obtained for a new set of sediment cores are used to assess the value of this site as a target for paleoenvironmental reconstruction.

STUDY SITE

Nasikie Engida is a 10-km² shallow endorheic lake in the southern Kenya Rift Valley (Fig. 1). A narrow shoulder (horst) at its southern end separates it from the much larger Lake Magadi, a 100-km², sporadically flooded saline pan containing thick trona ($Na_3(HCO_3)(CO_3).2H_2O$) deposits which have been commercially mined since 1911 during the early British colonial period. Situated beyond the remote northeastern edge of well-studied Lake Magadi (Eugster, 1986), Nasikie Engida has received much less attention from the scientific community. An early-20th century survey covering the southern Kenya Rift Valley mentions a site with peculiar mineralogical features called 'Little Magadi' (Walther, 1922), but both its location relative to Lake Magadi and the description of the site itself imply that this was almost certainly not the lake under study here. At 607 and 600 m above sea level (a.s.l.) respectively, Nasikie Engida and Lake Magadi are situated at the southern base of the Kenya dome, which culminates to maximum elevations of the rift valley floor around Lake Naivasha (1885 m a.s.l.) in the central Kenya Rift Valley. As a result of this setting, both lakes are sinks for groundwater and solutes reaching the Magadi basin through deep geothermal flow (Becht et al., 2006). Nasikie Engida's catchment is relatively small (ca. 40 km²), with a geological substrate consisting entirely of the faulted volcanic trachytes dated to 1.4-0.78 Ma that make up the floor of the wider Magadi Basin (Baker and Mitchell, 1976). Aquatic fauna is virtually absent* from the lake due to the extremely saline conditions, while the phytoplankton community is dominated by prokaryotic assemblages.

Whereas the extremely negative local moisture balance (local evaporation exceeds rainfall by 2400 to 500 mm/yr; Damnati and Taieb, 1995) prevents permanent inundation of Lake Magadi, nearby Nasikie Engida receives enough inflow from geothermal springs to maintain a perennial body of water. It is estimated that this hot-spring recharge accounts for over 90% of Nasikie Engida's annual water budget (R. Renaut, unpublished data). Nasikie Engida's hydrochemistry is determined mainly by this geothermal inflow, followed by evaporative concentration.

**A peculiar exception is the occurrence of an isolated population of Alcolapia grahami, a particular lineage of "dwarf" tilapia (Wilson et al. et al., 2004). This fish species has developed remarkable adaptations to cope with the obvious environmental challenges, and currently survives as small fragmented populations in isolated lagoons of Lake Magadi and in the northern, most dilute part of Nasikie Engida. Genetic research has confirmed the hypothesis that they represent the remnants of a much larger fish population that inhabited paleo-lake Oloronga (Kavembe et al., 2014), a large water body that occupied the Magadi basin at least 800,000 years ago (Eugster, 1980).*

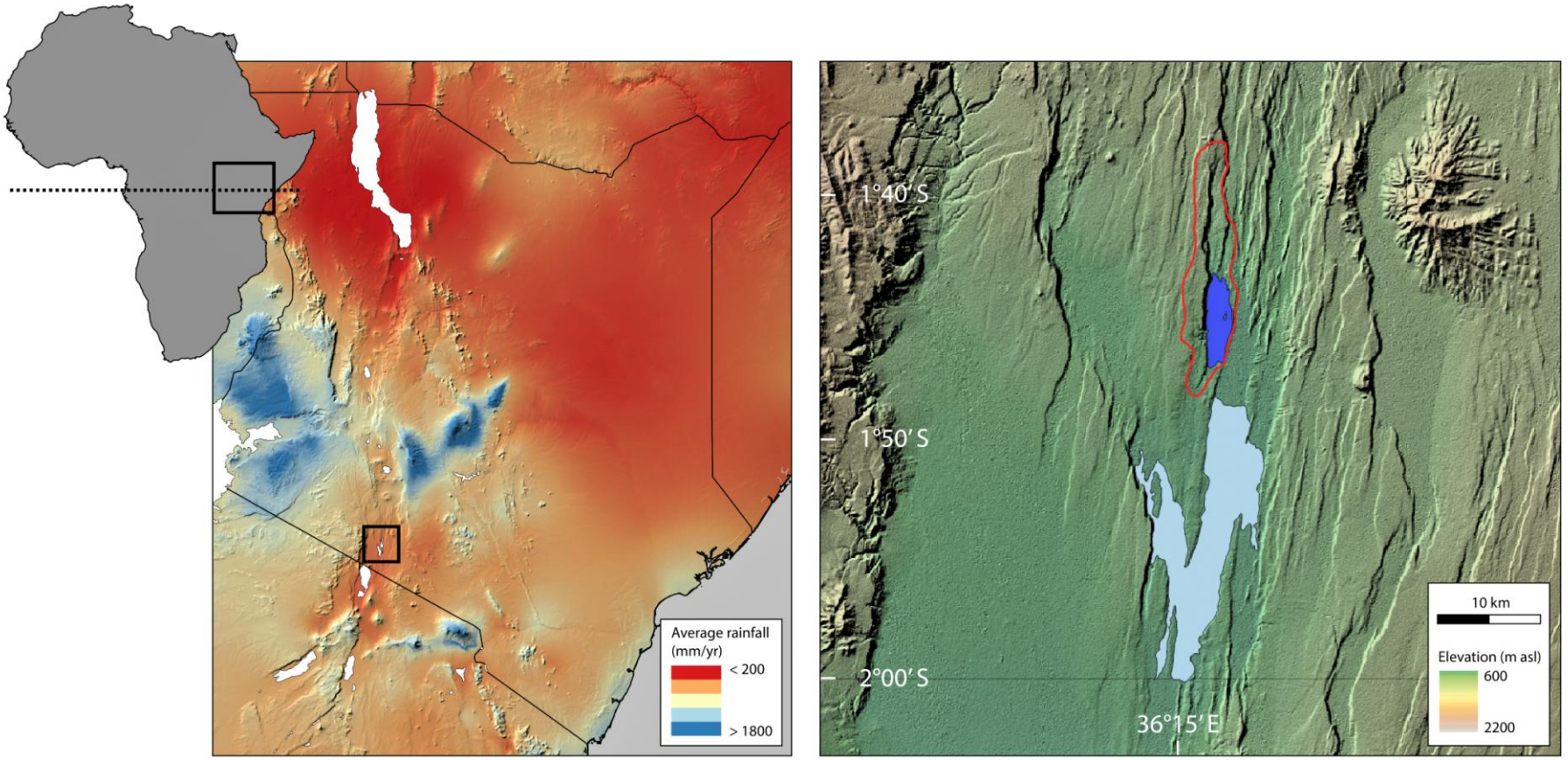

Fig. 1 Setting of the study area. Left: Location of the Magadi Basin within the dry southern Kenya Rift Valley. Right: Nasikie Engida (dark blue) and its catchment (red line), close to the episodically flooded salt pan of Lake Magadi (light blue).

The hot springs are clustered in two groups at the north end of the lake, providing an inflow of alkaline saline waters (ca. 35 $g.l^{-1}$ total dissolved solids, TDS) dominated by Na^+, HCO_3^-, CO_3^{2-} and Cl^-. After emergence, the spring water forms small hot streams which flow toward the lake over saline mudflats, at the mouth of ephemeral streams draining the northern part of the catchment during wet seasons. Evaporative concentration of the water sometimes results in a north-south chemical gradient of the lake water when wind-mixing is limited, to ca. 270 $g.l^{-1}$ TDS at the south end of the lake, where rafts composed of the sodium carbonate mineral nahcolite [$NaH(CO_3)$] may be observed floating on the water surface during the dry season. A large part of the lake floor consists of coarse-crystalline nahcolite deposits. High-volume geothermal recharge buffers Nasikie Engida against significant seasonal lake-level fluctuation, and at least in recent decades has protected the lake against desiccation during prolonged periods of low rainfall to which nearby Lake Magadi was not resistant. However, although better buffered against evaporation than water bodies at the Earth's surface (Crane, 1981), even deep aquifers are ultimately also dependent on recharge by rainfall, and geothermal recharge of lakes can temporarily diminish as a consequence of prolonged drought (Renaut et al., 2013). Nothing is known about the resilience of Nasikie Engida against widespread drought on decadal and longer timescales, such as that of the late-18th and early-19th century (Chapters 2, 3, 4).

METHODS

In August 2015, a continuous sequence of sediment cores was recovered from the deepest point of the lake (01°44'02.7"S, 36°16'39,4"E), including the intact sediment-water interface. The sequence consists of six overlapping core sections, collected using a rod-operated single-drive piston corer (Wright, 1980) for the uppermost 2 m and a square-rod piston corer with higher penetration capacity (Wright, 1967) for the deeper sediments. Exceptional release of gas was noticed beneath the coring platform each time the corer penetrated fresh sediments. The best location for coring was determined after conducting a bathymetric survey to document the main relief of the lake floor. Water depth was traced along one north-south transect and six east-west transects across the lake (Fig. 2), using a Garmin GPSMAP 178 acoustic depth sensor with built-in global positioning system, mounted on an inflatable kayak. Given the limited depth across much of the lake, acoustic measurements were supplemented by manual probing.

The overlapping core sections together represent a 462-cm composite sediment sequence (LMA15). One section was left out of the final compilation because of its severe disruption by violent degassing of the sediment at the moment of extraction. Consequently the presented data contain a gap over the depth interval 197.5-280 cm. Probing with long metal rods suggested the presence of a hard, impenetrable layer some 20 cm below the deepest recovered sediments. Unfortunately, no material of this facies could be collected.

The sediment cores were transported to Ghent, where they were split lengthwise and photographed using a Geotek GEOSCAN digital line-scan camera. Immediately after opening, the cores were scanned at 2-mm intervals for volume-specific magnetic susceptibility (MS), gamma-ray density and wavelength-specific reflectance throughout the visible light spectrum, using respectively a Bartington point sensor MS2E, a ^{137}Cs-source with gamma-ray detector system and a Konica Minolta CM-2600d spectrophotometer mounted on a Geotek Multi-Sensor Core Logger installation. Gamma-ray density was used to convert volume-specific MS to mass-specific MS (χ). The spectrophotometer data

allowed calculating the relative absorption band depth at 660-670 nm ($RABD_{660-670}$). By calculating ratios and normalizing reflectance at distinct wavelengths throughout the visible light spectrum, RABD spectrophotometry has been used to obtain an approximation of the abundance of the universal algal pigment chlorophyll-a and its diagenetic products preserved in sediments (Rein and Sirocko, 2002). The mineralogical composition of bulk sediment and identity of individual salt crystals at selected depths was determined by X-ray diffraction (XRD) analysis (Bruker D8 Discover system). Samples were air-dried and powdered by hand before measurement.

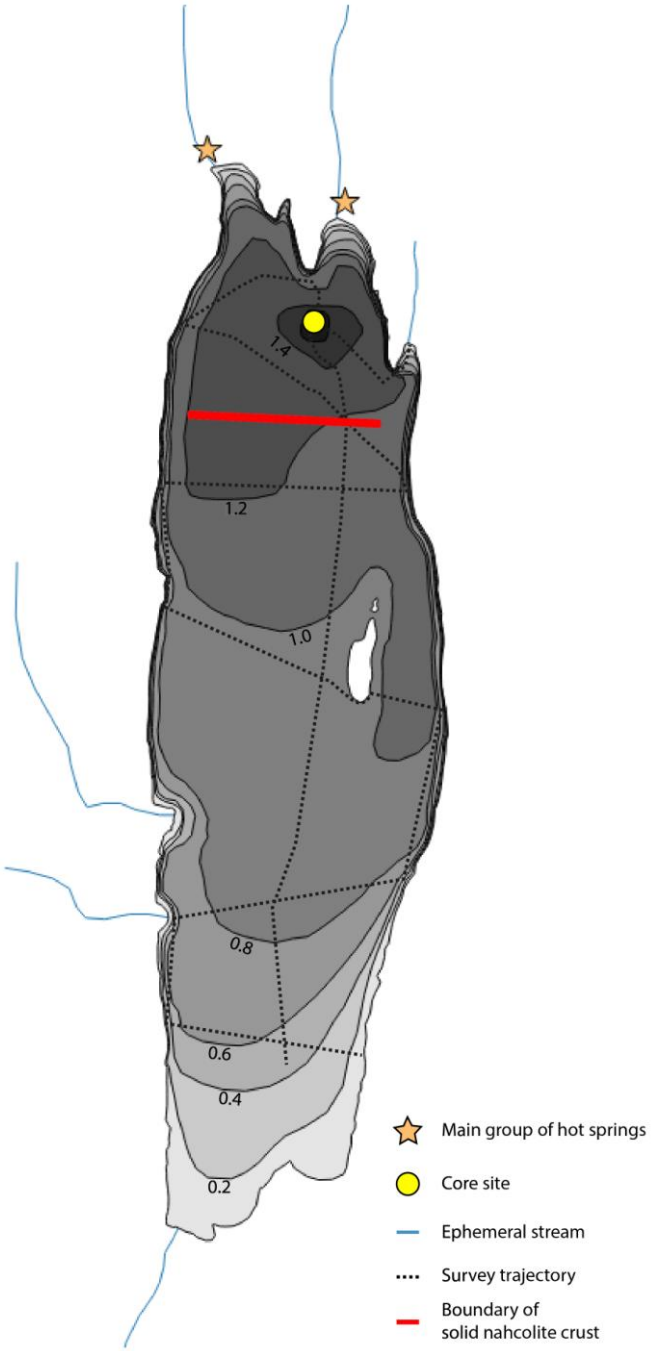

Fig. 2 Bathymetry and hydrography of Nasikie Engida.

RESULTS

The bathymetric survey revealed the lake floor to be gently sloping downward from south to north, with the deepest part (1.6 m) close to the northern shore and the entrance points of the mostly geothermally sourced streams (Fig. 2). A solid, hard nahcolite crust extended from the southern shore to cover ca. 85% of the total surface area of the lake (Fig. 2), excluding the possibility of collecting sediment cores except in the area around the deepest point.

The collected core sequence represents the uppermost ca. 4.6 m of the sediment column of Nasikie Engida (Fig. 3, Table 1). Even though the sedimentary measurements currently available are interrupted by a ca. 82-cm data gap corresponding with the defective core section, the 462-cm composite sediment sequence can be divided in two main units based on major sedimentological characteristics. Unit I (0-374 cm) consists of laminated grey to red-brown mud containing scattered salt crystals intercalated by layers entirely composed of large (mm- to cm-scale) and translucent nahcolite crystals (Fig. 4). Although the sediments between 197.5 and 280 cm depth were not recovered intact, no anomalous features were detected at this level during coring, providing no reason to assume that sediment characteristics in the gap of the sequence were significantly different from upper- and lower-lying Unit I deposits. XRD data identify the clastic mineral fraction as predominantly composed of feldspars. Trace amounts of the zeolite erionite, which probably has an authigenic origin in this evaporative context, are also detected, as well as the sodium silicate magadiite ($Na_2Si_{14}O_{29}{\cdot}11H_2O$). Besides these primary minerals also high amounts of the sodium carbonates trona [$Na_3(HCO_3)(CO_3){\cdot}H_2O$] and halite (NaCl) were detected within the bulk sediment. However, these were probably formed mostly by precipitation from the hypersaline pore waters during sample pretreatment. At the transition to Unit II (3.74-4.62 m), the nature of the sediment changes to finely laminated mud of a predominantly grey colour, rich in feldspar (Fig. 4). Macroscopically visible nahcolite disappears abruptly at the start of this unit, and is also absent at microscopic level as revealed by XRD. Visible lamination disappears briefly between 4.38 and 4.51 m, but resumes below this interval until the base of the sequence. As in Unit I, traces of erionite are present, and the detection of trona and halite is again possibly related to sample drying. However, lower amounts of these sodium carbonates suggest less saline conditions at the time of deposition. Given the current salinity of inflowing geothermal water at Nasikie Engida (see above), the pore water at present can be more saline than the lake was when this mud was deposited.

In the salt-rich Unit I, the 2-mm resolution MS signal is dominated by the alternation between layers of pure nahcolite (low values) and mud (higher values, Fig. 3). In Unit II, MS also shows marked short-term variability reflecting the finely laminated nature of the sediment, superimposed on longer-term trends of greater amplitude and with overall higher values than in Unit I. $RABD_{660\text{-}670}$ similarly fluctuates sharply between successive 2-mm intervals, but overall values are higher in nahcolite-rich Unit I than in Unit II (Fig. 3). Since the nahcolite crystals themselves do not contain chlorophyll or its derivatives, this implies that Unit I muds are more organic than the Unit II muds. For both χ and $RABD_{660\text{-}670}$, high-frequency variation related to the fine lamination is superimposed on low-frequency fluctuations covering core intervals on the order of tens of centimetres. Correlation of these two proxies is weakly negative, and in Unit I obscured by the wide data range caused by a large amount of non-informative measurements on translucent nahcolite layers (Fig. 5).

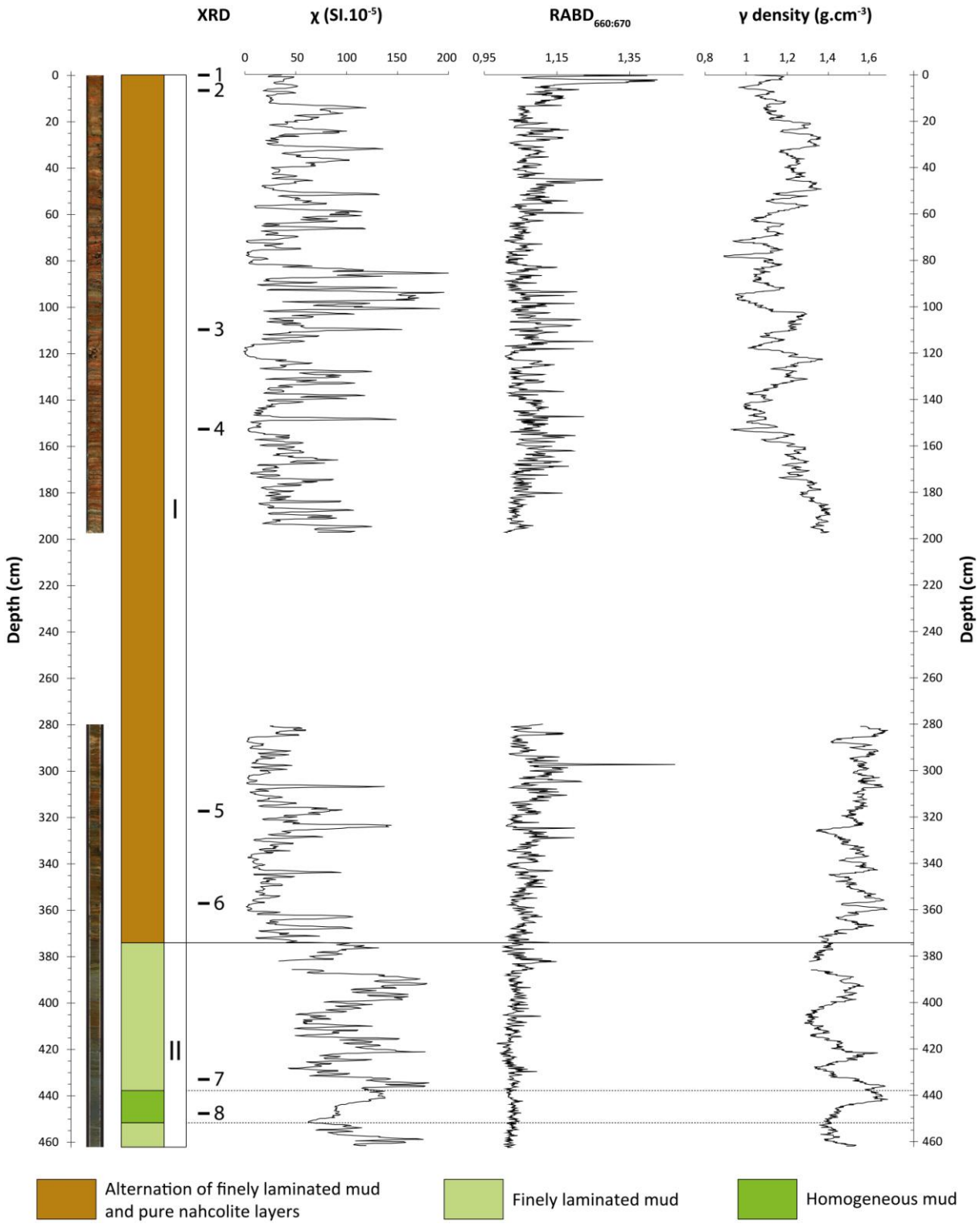

Fig. 3 Core imaging, lithology and results of non-invasive analyses for sediment sequence LMA15. Scanning for gamma-density, mass-specific magnetic susceptibility (χ) and $RABD_{660\text{-}670}$ was done at 2-mm interval. Numbers corresponding to XRD samples refer to Table 1. The stratigraphic hiatus represents a core section which was recovered but could not be saved due to explosive degassing. As far as could be ascertained in the field, its sediment character is comparable to the adjacent sections, therefore justifying continuity of Unit I across this hiatus.

			Sodium Carbonates			*Sodium silicates and zeolites*		*Terrestrial clastics*	
Sample	**Depth (cm)**	**Material**	**Nahcolite**	**Trona**	**Halite**	**Magadiite**	**Erionite**	**Feldspar**	**Amphibole**
1	0	isolated salt crystals	xxx	x	x	-	-	(x)	-
2	6.5	isolated salt crystals	xxx	x	x	-	-	(x)	-
3	109.5	bulk sediment	x	xx	xxx	-	(x)	xx	(x)
4	152.5	isolated salt crystals	xxx	x	x	-	-	(x)	-
5	317.5	bulk sediment	xx	xx	xxx	-	(x)	x	(x)
6	357	isolated salt crystals	xxx	x	x	(x)	-	(x)	-
7	433	bulk sediment	-	x	x	-	(x)	xxx	(x)
8	447.5	bulk sediment	-	x	xx	-	(x)	xxx	(x)

Table 1 XRD results for selected samples throughout LMA15.

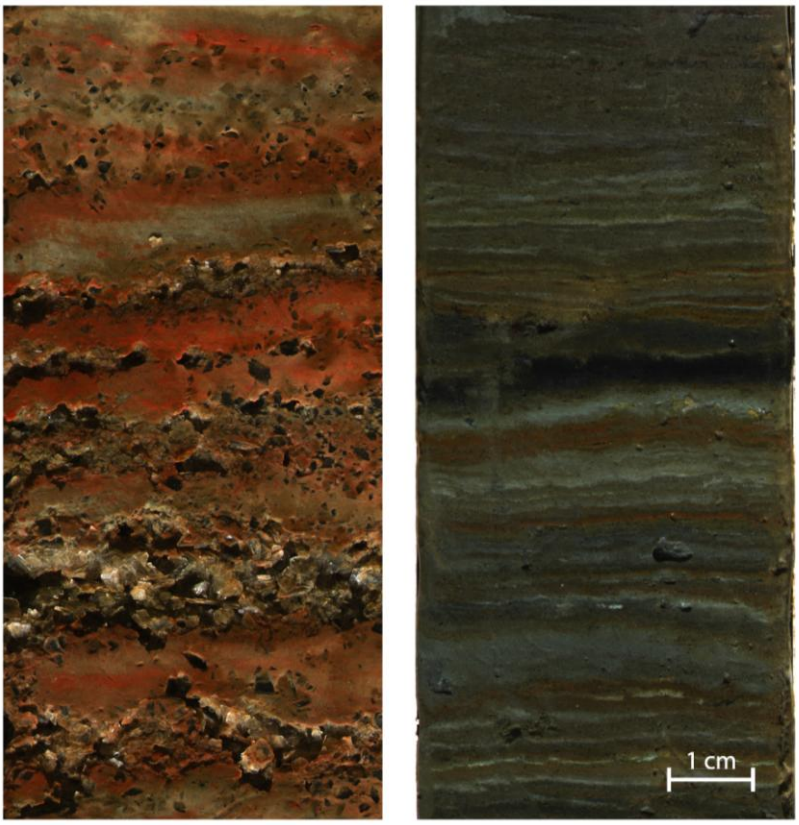

Fig. 4 Detailed images representative of Unit I (left) and Unit II (right) facies.

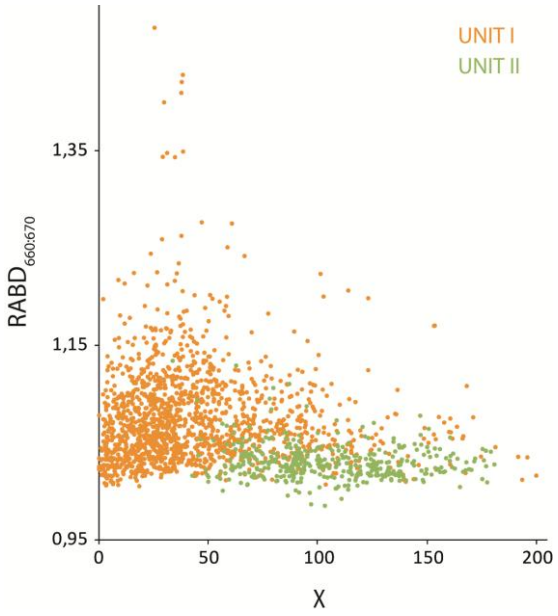

Fig. 5 Regression of $RABD_{660:670}$ to χ.

DISCUSSION

Neither Unit I nor Unit II sediments contain any of the tell-tale signs of complete lake desiccation, such as thick trona deposits as could be expected in this hydrochemical setting (Eugster and Jones, 1979), or stiff and/or cracked low-organic clays or a flooded playa surface (e.g. Verschuren, 1999; Valero-Garcés et al., 2000; Bessems et al., 2008). Obviously, the loss of the 82-cm section impedes ruling out of such a scenario with 100% certainty. However, with the limited available evidence, the assumption of Unit I homogeneity is made until future fieldwork is undertaken. With exception of the 13-cm thick section of unlaminated mud in Unit II (4.51-4.38 m), and parts of Unit I where exceptionally severe syn-sedimentary nahcolite growth has obscured sediment characteristics, all sediments are finely laminated, indicative of a low-energy lake bottom environment sustaining no or limited benthic fauna. Thus, the recovered Nasikie Engida cores represent a sequence of continuous lacustrine deposition in an offshore location, with no temporal hiatuses.

Nahcolite [$NaH(CO_3)$] is an evaporitic sodium carbonate mineral whose formation supposedly requires a CO_2 partial pressure (pCO_2) at least several times higher than present-day levels in the free atmosphere (Eugster, 1966). Because of this requirement, nahcolite was thought not to form at the earth's surface today, and its occurrence in ancient deposits such as the Eocene Green River Formation (western USA) has been used to infer substantially elevated atmospheric CO_2 levels during that time (Lowenstein and Demicco, 2006*;* Jagniecki et al., 2015). The presence of nahcolite covering much of the lake floor at Nasikie Engida seems to be unique, as no other lacustrine sites with active nahcolite formation are currently known. Two mechanisms could be invoked in providing favourable conditions for its precipitation. On the one hand, alkaline saline lakes are among the most productive aquatic systems on Earth, despite their apparently hostile environmental conditions (Grant, 2006). Correspondingly, the shallow water column of Nasikie Engida promotes abundant growth of a phytoplankton community dominated by phototrophic bacteria. Massive blooms produce large quantities of CO_2 by respiration (especially at night, when no CO_2 is used for photosynthesis) and bacterial degradation after die-off. This contribution of biogenic CO_2 possibly makes up a significant share of the total pCO_2 at the sediment-water interface, in part because salinity-related high water density hampers its escape to the air. However, an additional source is likely, since many shallow, hypertrophic sodium carbonate lakes exist that at present do not support nahcolite formation.

Lee et al. (2016) recently demonstrated massive release of CO_2 from deep faults in the Magadi Basin, indicating that continental rifting along the entire EARS is a major contributing process to atmospheric CO_2 levels. This tectonic degassing could be the main mechanism through which high CO_2 levels are maintained in the water column and surface sediments of Nasikie Engida, triggering nahcolite precipitation as soon as evaporitic concentration of the lake water allows it. Nasikie Engida's hydrochemical setting makes it a unique modern analogue for rift valley lakes along geothermally active faults undergoing extreme evaporative concentration, such as Lake Bogoria which precipitated nahcolite within the last millennium (De Cort et al. 2013; chapters 3, 4). Syn-sedimentary formation has also been described for late-Holocene lake deposits in a desert crater lake at Malha in northwestern Sudan (Mees et al., 1991). Clearly, a better understanding of the depositional and hydrochemical processes acting today at Nasikie Engida could allow further constraining past hydrological change at these other sites.

The presence of abundant macroscopic nahcolite crystals throughout the upper 374 cm of the sediment column (Unit I) demonstrates that, during the corresponding period, Nasikie Engida contained a brine of high ionic concentration similar to present-day conditions. Alternation of pure nahcolite layers and (nahcolite-containing) laminated muds suggests periodical dilution of salt crystals by inflowing terrigenous material. This pattern is possibly caused by the alternation of dry and wet periods. While arid episodes promote evaporative concentration and deposition of nahcolite, increased rainfall should deliver more catchment-derived clastics to the deepest part of the lake, given its proximity to the entrance points of the northern streams. In addition, dilution of the shallow water column by rainfall could occasionally induce dissolution of previously formed sodium carbonate minerals, or at least temporarily prevent new deposition. A comparable process is observed at nearby Lake Magadi, where the uppermost trona layers are often partially dissolved during episodes of increased runoff (Eugster, 1970).

The dominant stratigraphic feature of the Nasikie Engida sequence is the absence of nahcolite below 374 cm depth. Conditions supporting nahcolite formation seem to have arisen suddenly at the time corresponding to the sharp boundary between Units I and II. An increase in the supply of geothermal CO_2 to the lake and its sediments could be a cause of this sudden appearance of nahcolite in the sediment record. However, the tectonic processes that supply the lake with CO_2 are typically variable only over much longer time scales. Therefore, it can be argued that a change in the climatic moisture balance was likely an important driver of the transition from mildly saline, clastic-dominated sediments to hypersaline deposits rich in nahcolite. In chapter 1, the notion that the hydrology (and thus hydrochemistry) of lake systems tends to respond non-linearly to gradual rainfall decline was highlighted, especially when stimulated by short-lived pulses of extreme drought. Abrupt increases in carbonate precipitation have been observed in African lakes as a response to the transition from a wet early Holocene to a dry late Holocene (e.g., Street-Perrott et al., 2000; Lamb et al., 2000). Whether conditions for nahcolite formation in Nasikie Engida were created by the crossing of a similar hydrochemical threshold during a gradual decline in rainfall (or P-E ratio) is uncertain given the limited preliminary data available so far.

With the core site close to the northern seasonal-stream mouths, peaks in MS are most probably linked to greater amounts of terrestrial mineral materials being delivered to the lake with increased river flow after high rainfall, which in this dry setting readily flushes unstable dust and soil from the catchment. This mechanism could also explain longer-term patterns, such as the MS fluctuations over several tens of centimetres of mud that are clearest in Unit II, where the signal is not overprinted by the occurrence of large quantities of sodium carbonates. The inverse correlation between $RABD_{660\text{-}670}$ and MS, though weak, could indicate variability in the relative amounts of autochthonous organic matter (i.e., derived from aquatic algae or bacteria) and catchment-derived clastic material. The overall greater abundance of pigments in Unit I possibly points to increased levels of primary productivity during recent hypersaline stages. Alternatively, clastic dilution due to increased sedimentation rates during deposition of Unit II sediments or differential preservation because of changing redox conditions at the sediment-water interface could equally have played a role. The sharp rise in $RABD_{660\text{-}670}$ in the uppermost 5 cm of the core is most probably a diagenetic signal, as pigments in these recent deposits have not yet undergone degradation. The hypersaline bottom waters and sediments of Nasikie Engida do not support macroscopic benthic fauna, which would otherwise erase this pattern by homogenizing the uppermost centimetres of mud through

bioturbation. The fine laminations preserved throughout much of the sequence must have been created by hydroclimate oscillation at very high frequency. Possible mechanisms would be the alternation between wet- and dry-season conditions that is typical for the region, or the succession of relatively sporadic flash floods that are able to mobilize a significant amount of terrigenous material from the catchment. However, deeper investigation into the nature of these laminations is obviously needed before any conclusions can be drawn regarding their origin and significance for paleoclimate reconstruction.

Gathering more proxy data will be crucial to reach a better understanding of the lake's sedimentary dynamics and ecosystem changes within its catchment. Importantly, radiometric dating should at least give an indication of the period spanned by the composite core. A saddle at the southeastern side of the Nasikie Engida catchment forms the lowermost separation point with the Lake Magadi catchment. Several episodes of lake level higher than today have been described for Lake Magadi, most recently during the Pleistocene-Holocene transition following the Younger Dryas event (Roberts et al., 1993), but the exact magnitude remains unresolved (Eugster, 1980; Hillaire-Marcel and Casanova, 1987; Damnati and Taieb, 1995). Indications for formerly more dilute conditions have also been found at Nasikie Engida, in the form of stromatolites occurring along the lake's western side, multiple meters above the present-day shoreline (R. Renaut, pers. comm.). Possibly, Nasikie Engida episodically united with neighbouring Lake Magadi during such high stands. However, if such a merger occurred during the Holocene, nothing is known about the timing of final separation. One possible scenario is that the appearance of nahcolite in the sediments of Nasikie Engida corresponds to abrupt evaporative concentration linked to lake-level decline following its separation from Lake Magadi, which went on to even more extreme conditions afterwards. Similarity to a large number of other African lake-sediment records that demonstrate similar abrupt and permanent hydrological shifts, dated to between ca. 8.5 and 4 kyr BP in most cases, suggests that the Nasikie Engida sediment sequence presented in this chapter spans a good part of the Holocene, into the early- to mid-Holocene African Humid Period (chapter 1). As stated above, radiometric dating will be needed to confirm this. Additionally, resolving the chronology of this record will also illustrate whether the sudden onset of nahcolite precipitation coincided with one of the major drought events at Lake Rutundu, as seems to have been the case for a large number of other East-African paleoclimate records (chapter 1).

Paleohydrological research on neighbouring Lake Magadi is complicated by the burial of older sediments beneath a thick (up to 40 m at some places) bed of recently deposited trona, and studies have therefore mainly focussed on marginally deposited formations and outcrops (e.g. Eugster, 1980; Damnati and Taieb, 1995). In 2014, the International Continental Scientific Drilling Programme (ICDP) project "Hominin Sites and Paleolakes Drilling Project" obtained long cores from the center of Lake Magadi, which will allow climate reconstruction in the region over the past million years or so (Cohen et al., 2016). However, the sediment sequence collected at Nasikie Engida is unique in that it provides evidence for the existence of continuous, undisturbed deposits that probably cover a significant portion of the Holocene in the wider Magadi area. With additional efforts to collect more data, this site has the potential to produce the first paleoclimate reconstruction of the southernmost Kenya Rift Valley covering at least the late Holocene at high resolution.

REFERENCES

Baker BH, Mitchell JG. (1976) Volcanic stratigraphy and geochronology of the Kedong-Olorgesailie area and the evolution of the south Kenya rift valley. Journal of the Geological Society 132:467-484.

Becht R, Mwango F, Muno FA. (2006) Groundwater links between Kenyan Rift Valley lakes. In: Odada E, Olago DO (eds), Proceedings of the 11th World Lakes Conference, Nairobi, Kenya, pp. 7-14.

Bessems I, Verschuren D, Russell JM, Hus J, Mees F, Cumming B. (2008) Palaeolimnological evidence for widespread late 18th century drought across equatorial East Africa. Palaeogeography, Palaeoclimatology, Palaeoecology 259:107-120.

Cohen A, Campisano C, Arrowsmith R, Asrat A, Behrensmeyer AK, Deino A, Feibel C, Hill A, Johnson R, Kingston J, Lamb H, Lowenstein T, Noren A, Olago D, Owen B, Potts R, Reed K, Renaut R, Schäbitz F, Tiercelin J, Trauth M, Wynn J, Ivory S, Brady K, O'Grady R, Rodysill J, Githiri J, Russell J, Foerster V, Dommain R, Rucina S, Deocampo D, Russell J, Billingsley A, Beck C, Dorenbeck G, Dullo L, Feary D, Garello D, Gromig R, Johnson T, Junginger A, Karanja M, Kimburi E, Mbuthia A, McCartney T, McNulty E, Muiruri V, Nambiro E, Negash EW, Njagi D, Wilson JN, Rabideaux N, Raub T, Sier MJ, Smith P, Urban J, Warren M, Yadeta M, Yost C, Zinaye B. (2016) The Hominin Sites and Paleolakes Drilling Project: inferring the environmental context of human evolution from eastern African rift lake deposits. Scientific Drilling 21:1-16.

Crane, K. (1981) Thermal variations in the Gregory Rift of southern Kenya (?). Tectonophysics 74:239-262.

Damnati B, Taieb M. (1995) Solar and ENSO signatures in laminated deposits from Lake Magadi (Kenya) during the Pleistocene/Holocene transition. Journal of African Earth Science 21:373-382.

De Cort G, Bessems I, Keppens E, Mees F, Cumming B, Verschuren D. (2013) Late-Holocene and recent hydroclimatic variability in the central Kenya Rift Valley: The sediment record of hypersaline lakes Bogoria, Nakuru and Elementeita. Palaeogeography Palaeoclimatology Palaeoecology 388:69-80.

Eugster H. (1966) Sodium carbonate-bicarbonate minerals as indicators of pCO_2. Journal of Geophysical Research 71:3369-3377.

Eugster H. (1970) Chemistry and origin of the brines of Lake Magadi, Kenya. Mineralogical Society of America Special Paper 3:213-235.

Eugster H. (1980) Lake Magadi, Kenya, and its precursors. In: Nissenbaum A (ed), Hypersaline brines and evaporitic environments. Elsevier, Amsterdam, The Netherlands, pp. 195-232.

Eugster H. (1986) Lake Magadi, Kenya: a model for rift valley hydrochemistry and sedimentation? Geological Society, London, Special Publications 25:177-189.

Eugster H and Jones BF. (1979) Behavior of major solutes during closed-basin brine evolution. American Journal of Science 279:609-631.

Grant WD. (2006) Alkaline environments and biodiversity. In Gerday C and Glansdorff N. (eds) Encyclopedia of Life Support Systems. EOLSS Publishers, Oxford.

Hillaire-Marcel C, Casanova J. (1987) Isotopic hydrology and paleohydrology of the Magadi (Kenya)-Natron (Tanzania) basin during the late Quaternary. Palaeogeography Palaeoclimatology Palaeoecology 58:155-181.

Jagniecki EA, Lowenstein TK, Jenkins DM, Demicco RV. (2015) Eocene atmospheric CO_2 from the nahcolite proxy. Geology 43:1075-1078.

Kavembe GD, Machado-Schiaffino G, Meyer A. (2014) Pronounced genetic differentiation of small, isolated and fragmented tilapia populations inhabiting the Magadi Soda Lake in Kenya. Hydrobiologia 739:55-71.

Lamb AL, Leng MJ, Lamb HF, Mohammed MU. (2000) A 9000-year oxygen and carbon isotope record of hydrological change in a small Ethiopian crater lake. Holocene 10:167-177.

Lee H, Muirhead JD, Fischer TP, Ebinger CJ, Kattenhorn SA, Sharp ZD, Kianji G. (2016) Massive and prolonged deep carbon emissions associated with continental rifting. Nature Geoscience 9:145-149.

Lowenstein TK, Demicco RV. (2006) Elevated Eocene atmospheric CO_2 and its subsequent decline. Science 313:1928-1928.

Mees F, Verschuren D, Nijs R, Dumont H. 1991. Holocene evolution of the crater lake at Malha, Northwest Sudan. Journal of Paleolimnology 5:227-253.

Nicholson SE. (2000) The nature of rainfall variability over Africa on time scales of decades to millenia. Global and Planetary Change 26:137-158.

Rein B, Sirocko F. (2002) In-situ reflectance spectroscopy - analysing techniques for high-resolution pigment logging in sediment cores. International Journal of Earth Sciences 91:950-954.

Renaut RW, Owen RB, Jones B, Tiercelin JJ, Tarits C, Ego JK, Konhauser KO. (2013) Impact of lake-level changes on the formation of thermogene travertine in continental rifts: Evidence from Lake Bogoria, Kenya Rift Valley. Sedimentology 60:428-468.

Roberts N, Taieb M, Barker P, Damnati B, Icole M, Williamson D. (1993) Timing of the Younger Dryas event in East Africa from lake-level changes. Nature 366:146-148.

Street FA. (1980) The relative importance of climate and local hydrogeological factors in influencing lake-level fluctuations. Palaeoecology of Africa 12:137-158.

Street-Perrott FA, Holmes JA, Waller MP, Allen MJ, Barber NGH, Fothergill PA, Harkness DD, Ivanovich M, Kroon D, Perrott RA. (2000) Drought and dust deposition in the West African Sahel: A 5500-year record from Kajemarum Oasis, northeastern Nigeria. Holocene 10:293-302.

Valero-Garcés BL, Navas A, Machin J, Stevenson T, Davis B. (2000) Responses of a saline lake ecosystem to irrigation and climate variability. Ambio 29(6):344-350.

Verschuren D. (1999) Sedimentation controls on the preservation and time resolution of climate-proxy records from shallow fluctuating lakes. Quaternary Science Reviews 18:821-837.

Verschuren D. (2003) Lake-based climate reconstruction in Africa: progress and challenges. Hydrobiologia 500:315-330.

Verschuren D. (2004) Decadal to century-scale climate variability in tropical Africa during the past 2000 years. In: Battarbee R, Gasse F, Stickley C (eds), Past climate variability through Europe and Africa. Kluwer, Dordrecht, The Netherlands, pp. 139-158.

Verschuren D, Russell JM. (2009) Paleolimnology of African lakes: beyond the exploration phase. PAGES news 17:112-114.

Walther P. (1922) Sodium carbonate minerals of the Mogadi Lakes, British East Africa. American Mineralogist 25:86-88.

Wescott W, Morley C, Karanja, F.M. (1996) Tectonic controls on the development of rift-basin lakes and their sedimentary character: examples from the East African Rift System. In: Johnson TC, Odada EO (eds), The limnology, climatology and paleoclimatology of the East African lakes. Gordon and Breach Publishers, pp. 3-21.

Wilson PJ, Wood CM, Walsh PJ, Bergman AN, Bergman HL, Laurent P, White BN. (2004) Discordance between genetic structure and morphological, ecological, and physiological adaptation in Lake Magadi Tilapia. Physiological and Biochemical Zoology 77:537–555.

Wright HE. (1967) A square-rod piston sampler for lake sediments. Journal of Sedimentary Petrology 37:975-976.

Wright HE. (1980) Cores of soft lake sediments. Boreas 9:107-114.

It is widely recognised that the study of naturally occurring climate fluctuations in the past is crucial for our understanding of the causes of such climate dynamics, in particular for the development of climate-simulation models that are able to accurately generate future scenarios of anthropogenic climate change. This thesis had the general aim of making a contribution to our understanding of natural hydroclimatic change in equatorial East Africa at different time scales during the Holocene, the geological epoch which followed the last ice age and started ca. 11,700 yr BP. The main thread throughout this work was the use of lake sediments as natural archives for climate-driven environmental change. More specifically, information on past climatic variability at different time scales was extracted from sediment cores obtained from three climate-sensitive lakes in Kenya. Most analyses focused on sedimentological and geochemical climate proxies contained in those cores, and analysed with relatively fast techniques such as the determination of bulk sediment composition using loss-on-ignition (LOI); non-destructive high-resolution scanning of magnetic susceptibility (MS), spectroscopic colour reflectance and X-ray fluorescence (XRF); and the determination of biogenic silica content and grain-size distribution of the clastic mineral fraction. These were complemented in some cases by X-ray diffraction (XRD) and stable-isotope geochemistry of mineral phases.

The choice was made not to pursue the investigation of biological proxies in this thesis. Although these classically have proven their utility in East African paleolimnology (e.g. Gasse et al., 1995; Eggermont et al., 2010), there are a number of drawbacks related to the use of biological proxies. Next to the fact that documenting species assemblage changes throughout sediment cores is often very time-intensive and requires considerable training of the investigator (possibly impeding high-resolution studies), there are additional complications specific for this study. The most popular aquatic taxonomic groups used for paleoenvironmental reconstruction are diatoms, ostracods and chironomids (Smol et al. 2001a-b). However, applying these biota in the lakes under study here is not evident. The siliceous tests of diatoms readily dissolve in the strongly alkaline waters of the soda lakes in the rift valley, resulting in incomplete or selective preservation (Tiercelin et al., 1987; Barker et al., 1994). In the dilute freshwater lakes of Mount Kenya, diatoms are a dominant component of the phytoplankton community, and are well preserved in the sediments. However, in Africa diatoms are mostly used for salinity and pH reconstruction, and the calibration data sets for this purpose (Gasse et al. 1983) are largely limited to low-elevation lakes. Much less is known about diatom autecology in the cold and hydrologically open alpine lakes of East Africa (Cocquyt, 2007), limiting their use as paleoecological indicators.

The diagnostic teeth structures and head capsules of chironomid larvae are made up of chitin and as such do not suffer from the same post-depositional degradation issues as diatoms (Verschuren et al., 2004; Verschuren & Eggermont 2006). Using a chironomid-based transfer function and regional calibration dataset for temperature reconstruction (Eggermont et al., 2010) did allow assessment of temperature variation over the past 19,000 years at Lake Rutundu (Beirincx, 2013) and during the last few centuries in a complete elevational gradient on Mt. Kenya (Daniëls, 2016). However, their use as indicators for moisture balance change in these mountain lakes is less straightforward, as the hydrochemical changes there are expected to have been inferior to temperature effects as drivers of

chironomid assemblage composition through time. Previous work on fossil chironomid assemblages in the sediments of Lake Bogoria, from its side, has shown that throughout the period covered by the cores of Chapters 3 and 4, only two salt-tolerant species were able to establish themselves in the lake (of which one was observed in only one sample; Franck, 2007), making studies of community variability through time uninformative. A similar lack of species diversity is at play for ostracods at Lake Bogoria (Tiercelin et al., 1987) and other East African saline alkaline lakes (Rumes, 2010). However, it is important to stress that other, rather novel biological indicators could in future make important contributions to further enhance the potential of the sediment archives studied in this thesis (see below).

The studied sediment sequences (with the exception of Nasikie Engida) were anchored in time by a combination of ^{210}Pb- and ^{137}Cs-dating on late 19th- and 20th-century sediments, and AMS ^{14}C dating on older sediments. In Lake Rutundu and Lake Bogoria, also complete profiles of charcoal abundance were produced, and, in the case of Lake Bogoria, used for cross-correlation between core sites and to identify core intervals with sufficient terrestrial plant material for ^{14}C dating. The latter proved to be crucial in significantly increasing the quality of the chronology of this lake. Although the three lakes under study occupy a range of markedly different hydrological settings, all of them proved to be climate-sensitive, and the multi-proxy approach adopted in this thesis mostly allowed a good understanding of how climate signals were transferred to variations in sedimentary climate proxies.

Over most of the studied period, human impact on the lakes under study can be considered minimal, so any environmental changes inferred from the sediment records in this thesis can safely be assumed as non-anthropogenic, unless stated otherwise. The remote alpine environment of Lake Rutundu (3080 m above sea level) has proved unsuitable for human settlement prior to the erection of a small tourist lodge. The lake and its catchment remain largely pristine up to this day, with the exception of 20th-century introduction of trout for small-scale sports fishing. Much remains to be learned on anthropogenic developments in the lowlands of East Africa. But while many aspects of the spread of early farming and its impact on the natural environment in East Africa are hotly debatedate (Gelorini and Verschuren, 2013), it is generally agreed that in the drier areas of the central Kenya Rift Valley, the agricultural practices and population density required to significantly impact landscapes and lake systems arose not earlier than ca. 300 years ago, when Kikuyu settlers moved into the surrounding highlands (Lamb et al., 2003). Before that, local population mostly consisted of small groups of mobile pastoralists. However, when studying central Kenya Rift Valley lake sediments covering the past ca. two to three centuries, the possibility of anthropogenic impact on sedimentation dynamics should be taken into account on a case-by-case basis, as demonstrated by Lake Baringo (Anderson, 2002; Bessems et al. 2008), Lake Naivasha (Becht and Harper, 2002) and our new Lake Bogoria record discussed in Chapters 3 and 4. The small catchment of Nasikie Engida is currently almost uninhabited, but is used by Maasai herders as livestock grazing grounds. It is hard to assess the exact impact of herding on soil stability and sediment delivery to the lake at this point, but the effect should be minor given the small scale of human activities and the naturally sparse vegetation.

Chapter 1 concerned the study of a continuous, 19,000-year sediment record from Lake Rutundu, a small mid-elevation (3080 m a.s.l.) crater lake on the eastern flank of Mount Kenya, where organic-matter content as determined by LOI proved to be the most informative indicator of climate-driven change in lake moisture balance. Supported by a solid chronological framework, this record clearly

displays the punctuated climate development associated with global deglaciation following the Last Glacial Maximum (LGM), including the Younger Dryas (YD) leading up to the early-Holocene African Humid Period (AHP). Significantly, it reveals a well-resolved sequence of five century-scale droughts that are superimposed on the longer-term Holocene drying trend associated with orbital precession, i.e. the slow evolution of Earth's orbit around the sun. Importantly, these five Holocene drought episodes (centred at 8.2, 6.5, 5.3, 4.2 and 2.9 kyr BP) correspond to events described from northern subtropical and warm-temperate speleothem records throughout southern Eurasia, suggesting that these were the equatorial East African expression of large-scale climate phenomena. Additionally, the timings of these arid episodes strikingly match the seemingly abrupt but temporally variable ending of the AHP that has been inferred from a large number of paleoclimate records throughout the African continent. These results are an important contribution to the elucidation of the question whether the AHP termination was gradual or abrupt, a subject which has been widely debated within the scientific community. This chapter ends by highlighting important implications of the Rutundu record for the interpretation of African paleoenvironmental proxy records, which often reflect non-linear and irreversible hydrological or ecosystem responses, rather than climate change itself. Specifically within the context of this thesis, chapter 1 also forms a good illustration of the backdrop against which the content of the following chapters should be seen. Climate change is a complex process involving multiple drivers operating at different time scales. Developments during the past few millennia should as such always be interpreted with the longer-term Holocene trends in mind. Although this chapter provides evidence on a sequence of large-scale droughts during the Holocene, the possible driving mechanisms behind these events remain largely unknown. Their widespread appearance suggests that global climate reorganizations were involved. Such abrupt climate anomalies are often explained as originating in the North Atlantic, following outburst flooding or ice-sheet surging (Clark et al., 2002; Teller et al., 2002). For example, the most widely accepted hypothesis for the cause of the 8.2 kyr event is a sudden release of fresh water from proglacial Lake Agassiz into the Labrador Sea (Clarke et al., 2004; Alley and Agustsdottir, 2005). Cyclical variability of the Atlantic subpolar gyre and associated atmospheric reorganizations have also been put forward as an important mechanism in triggering important climate fluctuations in Europe and, potentially, further afield (Sorrel et al., 2012). However, tropical causes for abrupt climate change have been proposed as well (e.g. Clement et al., 2001). Unravelling the mechanisms behind the separate Holocene drought pulses remains a major challenge for future paleoclimate research.

Following this first chapter on multi-century climate variability during the Holocene, the focus of the thesis shifts to more recent patterns of climate change. As product of the Past Global Changes programme 'Africa-2k', **Chapter 2** presented a broad review of previously published work on hydroclimate variability over the whole African continent during the past 2,000 years. Although the limited number of high-resolution, well-dated paleoclimate records and their highly uneven geographical coverage formed major limitations, an effort was undertaken to describe general spatial patterns of past climate change, including those which affected Africa during the globally recognized time windows of the Medieval Climate Anomaly (MCA) and Little Ice Age (LIA). Candidate mechanisms that may explain the observed historical trends were proposed and explored. Further unravelling the hydroclimate fluctuations that have played out over Africa's different regions during the last two millennia will be crucial to correctly frame present and future climate developments, and this chapter has provided a valuable reference framework for this endeavour. In the future,

three main factors need to be attended in order to fully exploit the integration of paleoclimate records and climate models. Firstly, model shortcomings need to be addressed. For example, a recent study showed that general circulation model (GCM) simulations from the Paleoclimate Modelling Intercomparison Project (PMIP) and the Coupled Model Intercomparison Project (CMIP) are incompatible with proxy reconstructions and fail to converge on a comparable pattern of precipitation over the past millennium in East Africa (Klein et al., 2016). Secondly, more efforts should be directed to correctly assessing the quality of individual paleoclimate records. Ideally, this should be done through a set of objective criteria that evaluate the most important archive features and allow a well-reasoned decision on in- or exclusion from integrative statistical or modelling studies. The most important features that should be considered are chronology (e.g. How well-constrained in time is the record? Is there an old carbon effect at work?), proxy quality (e.g. Is there any ambiguity in proxy interpretation? Were multiple independent proxies considered?) and overall archive integrity (e.g. Were the sediments deposited in a stable environment? What is the likelihood of cryptic hiatuses?). An example of a way to rate the accuracy of sediment chronologies, is the 'Chron Score', designed by Sundqvist et al. (2014) to systematically and reproducibly evaluate radiocarbon-based age models of sediment cores. Another important, recently developed method is the use of 'Monte Carlo Empirical Orthogonal Function' (MCEOF) analysis to assess time uncertainty in proxy records while identifying coherent spatiotemporal variability between multiple independent time series, also allowing the statistical testing of the synchronicity of major climate events observed in the separate records (Anchukaitis and Tierney, 2012). Whereas chapter 2 of this thesis had the aim of exploring and exhibiting all available work covering the whole continent, it can be used as the basis for a future in-depth quality assessment of individual records. A thorough evaluation process of paleoclimate records following a well-defined methodology would provide objectiveness to the process of deciding which records are most suitable for testing hypotheses using advanced statistical methods or climate modelling. Applying such an approach specifically for records covering the past 2,000 years could be worked out as a next step in the Africa-2k project. Since the largest amount of data has been gathered for East Africa, the need for such an effort seems highest for this region. If a similar exercise were to be conducted for South or West Africa, most previously published records would probably be situated toward the low-quality end of the spectrum. Finally, a good understanding of hydrology-to-proxy relationships in paleoclimate archives should be strived for. Decades of research have resulted in a wide array of paleohydrological proxies being developed and applied. Records that are deemed the most trustworthy and are hence combined into regional or continental syntheses of past climate change, are often based on completely different sources of information and may not all represent a one-to-one representation of local climate. Attention should be given to the comparability of different records, even if these are individually deemed of high quality. Important factors to keep in mind here are differential response times of individual lakes (which may or may not allow reconstruction of climate variability at short time scales), and the specific elements of the hydrological variability that are captured by the proxies under study.

Chapter 3 presented a first exploration of moisture-balance change at the partly spring-fed, hypersaline Lake Bogoria in the central Rift Valley of Kenya over the past ca. 1,600 years, based on a sediment core of the central basin obtained in 2001-2003. Supported by low-resolution data on sediment composition, salt mineralogy and stable isotope signatures, a general sequence of a dry Medieval Climate Anomaly followed by a wet Little Ice Age is proposed, although high chronological uncertainty and poor recovery of the soft and gas-charged uppermost sediments formed major

obstacles for their interpretation. In an effort to correct for this handicap, new and previously unstudied data on short sediment cores of the nearby saline lakes Nakuru and Elementeita were used to provide further evidence for an episode of significant drought following the late 18th century.

Chapter 4 presented a more elaborate study of the sediments of Lake Bogoria. This chapter significantly improved upon the previous work by integrating data obtained from new sediment cores collected at five sites across the lake (one from each of its three basins and two from the submerged sills separating them) to obtain a best-possible interpretation of climate-sensitive proxies. Past experiences in the field allowed a refinement of coring techniques, which resulted in a much better sediment recovery. The coring procedures described in Chapter 4 were able to circumvent the practical difficulties that have traditionally impeded the coring of extremely soft, gassy sediments of tropical lakes, and can be seen as a guideline for future field work. Radiocarbon dating of undisputed terrestrial material (grass charcoal) to avoid large old carbon offsets, in combination with improved ^{210}Pb and ^{137}Cs analyses, raised the level of confidence in the age-depth model proposed for Lake Bogoria. Over the past 1,300 years, the lake has undergone water-balance changes far outside the range of documented 20th-century variability, with fluctuations between near-desiccation to levels close to or at its point of overflow into the catchment of Lake Baringo. Lake Bogoria was effectively split into two or three separate water bodies during multiple occasions throughout the studied time period, most recently about 200 years ago (during a well-documented late-18th to early-19th century drought) when its north basin was cut off from the more southerly parts of the lake. The results indicate that climate history in the Lake Bogoria region resembled a hybrid pattern of those observed in westernmost (represented by Lake Edward; Russell and Johnson, 2007) and easternmost (represented by Lake Naivasha and Lake Challa; Verschuren et al., 2000; Buckles et al., 2016) East Africa, with an early Little Ice Age humidity maximum followed by variable conditions up to the major drought ca. AD 1800. This potentially has implications for the role of the Congo Air Boundary (CAB) as an intra-regional regulator of hydroclimate patterns within East Africa. Although Lake Bogoria and Lake Naivasha are both situated on the Kenya Rift Valley floor, separated by only 100 km, the currently available information suggests that they are both situated on different sides of a climatologically important 'hinge' area. While the similarity of Lake Naivasha to eastern Lake Challa points to an Indian Ocean dominance during the past millennium, the different scenario inferred for Lake Bogoria suggests the importance of Congo Basin moisture penetration into the central Kenya Rift Valley. This implies that the Kenya Rift Valley is a promising area to study past CAB dynamics. It would be interesting to try obtain an independent, long-term reconstruction of rainfall source rather than rainfall amount, as this would expose past in- or exclusions of a certain site from the farthest reaches of the Atlantic Ocean. A promising candidate proxy for this might be the hydrogen-isotopic signature of plant leaf waxes, which in recent years has received a substantial amount of attention. Precipitation coming from the West, intensively recycled over the humid Congo Basin, is isotopically lighter than rainfall sourced over the Indian Ocean. This has led to the suggestion that δD_{wax}, which reflects isotopic composition of local precipitation, may represent moisture source at sites that have received rain from just one dominant source at a time throughout the period of interest (Tierney et al., 2011), although its interpretation as a pure amount indicator is still more prevalent. An ambitious but potentially highly rewarding effort would be to set up an east-west transect of well-chosen lake sites, including the Kenya Rift Valley sites discussed in this thesis. Comparing moisture-balance patterns (ideally containing information of rainfall amount as well as

source area) along such a transect would allow a quantitative reconstruction of CAB migration through time.

Focusing on the historical evolution of sedimentation dynamics in Lake Bogoria, Chapter 4 presents a good basis for a high-resolution moisture-balance reconstruction over the past millennium. However, a further exploitation of the proxy record is needed to work out a robust and detailed paleohydrological scenario. For closed-basin lakes such as Lake Bogoria, sedimentological and geochemical proxies are mostly good indicators of past hydroclimate changes, since moisture-balance fluctuations are often translated in, and amplified through, changes in water level and hydrochemistry. However, other indicators are also available to deduce lake and catchment evolution over time, and could be valuable additions to the already collected data. For example, pollen assemblages can reveal climate-related changes in the terrestrial environment, and together with charcoal data allow to study vegetation dynamics in relation to climate change. And while the alkaline waters of Lake Bogoria and Nasikie Engida is not favourable for diatom preservation or a diverse chironomid community, other biota such as salt-tolerant aquatic insects could provide independent information on past hydrochemical conditions. For example, high abundances of *Micronecta* sp., small aquatic bugs of the Corixidae family, were observed in the upper water column over the entire surface of Lake Bogoria during field work in 2014. These animals can probably only colonize the lake in such large numbers at high lake levels, when epilimnion salinity drops below a critical level (Hammer 1986). As the chitinous body parts of these aquatic bugs preserve relatively well in lake sediments (also under saline, anoxic conditions; Rumes et al., 2005), they are good candidates to discern rapid lake transgressions, and might even allow a semi-quantitative comparison of lake salinity during different humid episodes. Application of recently developed climate-sensitive molecular biomarkers could also be an interesting future approach, but inherently require a good understanding of their mechanisms of origin, deposition and post-depositional behaviour (e.g. Tierney et al., 2010; Buckles et al., 2014).

Analysis of changes in dry-sediment accumulation rate (SAR) provided strong evidence for historical and recent anthropogenic disturbance in the Lake Bogoria catchment in the form of increased soil erosion and supply to the lake, originating from outside the National Reserve boundaries. Lake Bogoria is a valuable wetland site protected under the international RAMSAR framework. The recent increase in sediment delivery is alarming, as it suggests that processes are at work similar to those that are known to have deeply affected nearby Lake Baringo. Further research should urgently investigate possible downstream effects of land-use change in the upper catchment of the lake, guided by the lessons learned at Lake Baringo (Anderson, 2002).

In **Chapter 5**, a new sediment core from Nasikie Engida ('Little Magadi') was used to explore the potential of this hypersaline, alkaline lake in the Rift Valley of southern Kenya as an archive of past hydroclimate change in this so-far poorly documented region. The 4.6-m record shows no indication of desiccation events, suggesting that the lake never dried out during the period spanned by the core despite the arid local climate regime and the lake's endorheic nature and high surface-to-volume ratio. Although the high share of geothermal recharge may complicate the relationship between climate and lake level, it has been pivotal in maintaining a permanent lacustrine environment where a diversity of independent climate indicators could accumulate. Besides its value as paleoclimate archive, this site has provided the first evidence for contemporary, continuous deposition of the sodium carbonate mineral nahcolite in a modern-day lacustrine environment,

making it a suitable analogue for the formation of this mineral in other saline-alkaline lakes in the past, such as Lake Bogoria. The hypothesis that nahcolite precipitation at these Kenya Rift Valley lakes has been facilitated by significant amounts of geothermal CO_2 input adds an important side note to the use of this mineral as an indicator of past atmospheric pCO_2 (Lowenstein and Demicco, 2006). Obviously, all non-atmospheric sources of carbon dioxide need to be eliminated before the occurrence of nahcolite can be invoked to deduce previous high atmospheric concentrations, which requires a good understanding of past sedimentary environments. Further, Nasikie Engida's sediment record clearly testifies of climatic moisture-balance variability at different time scales. The most important feature revealed by this exploratory study is the sudden onset of nahcolite precipitation, suggesting that the lake has undergone major climate-related hydrochemical change over time. Additional analyses on the sediment record of Nasikie Engida will be necessary to further document its sedimentological characteristics. Ideally, hydrochemically sensitive proxies such as the occurrence and stable-isotope signature of sodium carbonates may be combined with independent indicators of moisture balance, to get a full understanding of Nasikie Engida's environmental history.

As a first step, non-invasive scanning techniques such as XRF could swiftly provide high-resolution information on the conditions under which the sediments were deposited. Scanning of the sediments (especially the lower part of the core, devoid of nahcolite) for the presence of any remains of aquatic fauna or flora should provide an idea of the environmental changes that have taken place since the start of the record. The large share of geothermal spring water to the lake's total water budget requires a critical treatment of certain hydrological or geochemical proxies, as lake level change might lag precipitation patterns and certain aspects of water or sediment chemistry (e.g. isotopic composition of lake or sediment pore water) might carry a geothermal overprint. However, this does not have to compromise the entire climate reconstruction potential, as proxies derived from terrestrial sources are unaffected by these caveats.

The exploration of Nasikie Engida demonstrates that there are still untapped lacustrine archives with considerable potential to be found in East Africa, even after decades of research in the region. This effort to expand the spatial network of paleoclimate records should be sustained in the future. In addition, recent advances in dating and proxy analysis techniques could greatly improve the information we currently have from previously studied sites, justifying their re-examination.

When focusing on events and variability that play out over years to decades and centuries, supporting a lake-sediment record with a robust chronological framework is crucial. A good number of reliable dates, well-positioned throughout the sediment sequence, is necessary to cope with the inherent uncertainties associated with age-depth modelling at these time scales. This issue requires great care, especially in settings where it is markedly difficult to obtain reliable samples for radiocarbon dating because of old geothermal carbon inflow and a scarcity of terrestrial plant macrofossils reaching the core site. As applied in Chapter 4, the compilation of the complete charcoal inventory of a core, followed by sampling directed at charcoal-peak intervals, can provide a solution. Additionally, dates from different sites sufficiently close together can be combined, if independent time markers (such as short-lived but pronounced droughts) can be discerned. The results obtained here clearly demonstrate that the fluctuating lakes of the rift valley floor can display major changes in sedimentation rate, further stressing the need for adequate chronological control. This is an area in which the records of Lake Bogoria and Nasikie Engida, the latter currently lacking any age information altogether, should be improved.

To optimally valorise research findings, the paleolimnological community should aim to cooperate with, and build on developments in, other scientific fields. For example, hydrological modelling can allow lake-level changes to be translated into quantitative information on local rainfall variability, a crucial step towards the integration of paleodata with climate-modelling efforts. Combination of the study of natural proxy archives with paleoclimate modelling can strengthen both of these research fields, allowing the development and testing of new hypotheses about climate drivers or exposing poorly understood processes. Furthermore, extending our knowledge on the evolution of the large-scale elements of the climate system, such as the oceans and the atmosphere, would allow a deeper look into the temporal variability of the influence of these components on the African climate system. And the further exploration of (semi-)recent meteorological data, not only from historical sources but also from reanalysis studies, can provide a firm basis to interpret paleoclimate records further back in time. These interdisciplinary approaches have resulted in breakthrough results over the past years, and will undoubtedly prove crucial for solving currently unanswered questions related to African paleoclimatology.

While future scenarios of climate change related to anthropogenic global warming are uncertain regarding precipitation trends over East Africa (Rowell et al., 2015), it would be wise to take the region's natural moisture-balance variability into account when contemplating water-resource management. The study of Lake Bogoria presented in this thesis agrees with most other paleohydrological records from the region (Verschuren, 2004) that severe, decadal-scale drought exceeding the historically documented range is an inherent part of East Africa. For example, until now, most of the evidence for widespread drought of the late-18th and early-19th century came from lake-sediment proxy records (e.g. Bessems et al., 2008). However, a recent study involving historical evidence, such as oral traditions gathered amongst the peoples of the Rift Valley and contemporary observations recorded by travellers, demonstrates just how large the societal consequences were (Anderson, 2016). Dubbed 'The Great Catastrophe', this episode resulted in large-scale upheaval and dispersal of the Kenya Rift Valley communities, with ensuing wars and hierarchical transformations largely setting the stage for history as it unfolded over the following decades. Obviously, if such an event would set in again, the humanitarian and economic costs would be enormous. In the vast semi-arid regions of equatorial East Africa, unsustainable irrigation is used to enable crop cultivation in areas formerly exclusively reserved for animal husbandry. For example, agriculture on the Loboi Plain, between Lake Bogoria and Lake Baringo, is currently supported by direct water extraction from Loboi Swamp, a freshwater wetland originally occupying the southwestern part of the plain. Aerial photographs have revealed a reduction of ca. 60% between 1969 and 2002 (Ashley et al., 2004), and the dramatic drainage and conversion to farmland has continued to the present, as evident during field work in 2014. Even if the future scenario of an average increase in precipitation, currently proposed by GCMs (Shongwe et al., 2011) though not universally supported (Williams and Funk, 2011), would prove veritable, decadal-scale arid events will most likely continue to emerge. Water resource management plans for these naturally water-stressed areas should incorporate the possibility of strong future moisture balance decline, and should strive for a limitation of water consumption practices that are unsustainable even under contemporary hydroclimatic conditions.

REFERENCES

Alley RB, Agustsdottir AM. (2005) The 8k event: cause and consequences of a major Holocene abrupt climate change. Quaternary Science Reviews 24:1123-1149.

Anchukaitis KJ, Tierney JE. (2012) Identifying coherent spatiotemporal modes in time-uncertain proxy paleoclimate records. Climate Dynamics doi: 10.1007/s00382-012-1483-0.

Anderson D. (2002) Eroding the commons: the politics of ecology in Baringo, Kenya. University of Ohio Press, Athens, USA, 336 pp.

Anderson DM. (2016) The beginning of time? Evidence for catastrophic drought in Baringo in the early nineteenth century. Journal of Eastern African Studies 10:45-66.

Ashley GM, Mworia JM, Muasya AM, Owen RB, Driese SG, Hover VC, Renaut RW, Goman MF, Mathai S, Blatt SH. (2004) Sedimentation and recent history of a freshwater wetland in a semi-arid environment: Loboi Swamp, Kenya, East Africa. Sedimentology 51:1301-1321.

Barker P, Fontes JC, Gasse F, Druart JC. (1994) Experimental dissolution of diatom silica in concentrated salt solutions and implications for paleoenvironmental reconstruction. Limnology and Oceanography 39(1):99-110.

Becht R, Harper DM. (2002) Towards an understanding of human impact upon the hydrology of Lake Naivasha, Kenya. Hydrobiologia 488:1-11.

Beirinckx, L. (2013) Chironomid-based temperature reconstruction on Mount Kenya: assessment of past and recent climate change. Unpublished MSc thesis, Ghent University.

Bessems I, Verschuren D, Russell JM, Hus J, Mees F, Cumming BF. (2008) Palaeolimnological evidence for widespread late 18th century drought across equatorial East Africa. Palaeogeography Palaeoclimatology Palaeoecology 259.

Brown ET, Johnson TC. (2005) Coherence between tropical East African and South American records of the Little Ice Age. Geochemistry Geophysics Geosystems 6.

Buckles LK, Weijers JWH, Verschuren D, Damste JSS. (2014) Sources of core and intact branched tetraether membrane lipids in the lacustrine environment: Anatomy of Lake Challa and its catchment, equatorial East Africa. Geochimica Et Cosmochimica Acta 140:106-126.

Buckles LK, Weijers JWH, Verschuren D, Cocquyt C, Sinninghe Damsté JS. (2015) Short-term variability in the sedimentary BIT index of Lake Challa, East Africa over the past 2200 years: validating the precipitation proxy. Climate of the Past Discussions 11:1177-1218.

Clark PU, Pisias NG, Stocker TF, Weaver AJ. (2002) The role of the thermohaline circulation in abrupt climate change. Nature 415:863-869.

Clarke GKC, Leverington DW, Teller JT, Dyke AS. (2004) Paleohydraulics of the last outburst flood from glacial Lake Agassiz and the 8200 BP cold event. Quaternary Science Reviews 23:389-407.

Clement AC, Cane MA, Seager R. (2001) An orbitally driven tropical source for abrupt climate change. Journal of Climate 14:2369-2375.

Cocquyt C. (2007) Diatom diversity in Hausburg tarn, a glacial lake on Mount Kenya, East Africa. Diatom Research 22:255-285.

Cohen A, Palacios-Fest M, Msaky E, Alin S, McKee B, O'Reilly C, Dettman D, Nkotagu H, Lezzar K. (2005) Paleolimnological investigations of anthropogenic environmental change in Lake Tanganyika: IX. Summary of paleorecords of environmental change and catchment deforestation at Lake Tanganyika and impacts on the Lake Tanganyika ecosystem. Journal of Paleolimnology 34:125-145.

Daniëls N. (2016) Sensitivity of Mt. Kenya lakes to climate warming: comparison of historical and modern-day communities of chironomid larvae. Unpublished MSc thesis, Ghent University.

Eggermont H, Heiri O, Russell J, Vuille M, Audenaert L, Verschuren D. (2010) Paleotemperature reconstruction in tropical Africa using fossil Chironomidae (Insecta: Diptera). Journal of Paleolimnology 43:413-435.

Franck K. (2007) Dansmugfauna's in het hypersaliene Bogoria-meer, Kenia, tijdens historische periods van volledig circulerende waterkolom (het droge Middeleeuws Optimum) en van permanente stratifiëring (de vochtige Kleine Ijstijd). Unpublished BSc thesis, Ghent University.

Gasse F and Tekaia F. (1983) Transfer-functions for estimating paleoecological conditions (pH) from East-African diatoms. Hydrobiologia 103:85-90.

Gasse F, Juggins S, Khelifa LB. (1995) Diatom-based transfer-functions for inferring past hydrochemical characteristics of African lakes. Palaeogeography Palaeoclimatology Palaeoecology 117:31-54.

Gelorini V, Verschuren D. (2013) Historical climate-human-ecosystem interaction in East Africa: a review. African Journal of Ecology 51:409-421.

Hammer UT. (1986) Saline lake ecosystems of the world. Springer.

Klein F, Goosse H, Graham NE, Verschuren D. (2016) Comparison of simulated and reconstructed variations in East African hydroclimate over the last millennium. Climate of the Past Discussions, doi:10.5194/cp-2015-194

Lamb H, Darbyshire L, Verschuren D. (2003) Vegetation response to rainfall variation and human impact in central Kenya during the past 1100 years. Holocene 13:285-292.

Lowenstein TK, Demicco RV. (2006) Elevated eocene atmospheric CO2 and its subsequent decline. Science 313:1928-1928.

Rowell DP, Booth BBB, Nicholson SE, Good P. (2015) Reconciling Past and Future Rainfall Trends over East Africa. Journal of Climate 28:9768-9788.

Rumes B, Eggermont H, Verschuren D. (2005) Representation of aquatic invertebrate communities in subfossil death assemblages sampled along a salinity gradient of western Uganda crater lakes. Hydrobiologia 542:297-314.

Rumes B. (2010) Regional diversity, ecology and palaeoecology of aquatic invertebrate communities in East African lakes. Unpublished PhD thesis, Ghent University.

Russell JM, Johnson TC. (2007) Little Ice Age drought in equatorial Africa: Intertropical Convergence Zone migrations and El Nino-Southern Oscillation variability. Geology 35:21-24.

Shongwe ME, van Oldenborgh GJ, van den Hurk B, van Aalst M. (2011) Projected Changes in Mean and Extreme Precipitation in Africa under Global Warming. Part II: East Africa. Journal of Climate 24:3718-3733.

Smol J, Birks H, Last W. (2001a) Tracking environmental change using lake sediments vol. 3: Terrestrial, algal and siliceous indicators. Kluwer Academic Publishers.

Smol J, Birks H, Last W. (2001b) Tracking environmental change using lake sediments vol. 4: Zoological indicators. Kluwer Academic Publishers.

Sorrel P, Debret M, Billeaud I, Jaccard SL, McManus JF, Tessier B. (2012) Persistent non-solar forcing of Holocene storm dynamics in coastal sedimentary archives. Nature Geoscience doi:10.1038/NGEO1619.

Sundqvist HS, Kaufman DS, McKay NP, Balascio NL, Briner JP, Cwynar LC, Sejrup HP, Seppa H, Subetto DA, Andrews JT, Axford Y, Bakke J, Birks HJB, Brooks SJ, de Vernal A, Jennings AE, Ljungqvist FC, Ruhland KM, Saenger C, Smol JP, Viau AE. (2014) Arctic Holocene proxy climate database - new approaches to assessing geochronological accuracy and encoding climate variables. Climate of the Past 10:1605-1631.

Teller JT, Leverington DW, Mann JD. (2002) Freshwater outbursts to the oceans from glacial Lake Agassiz and their role in climate change during the last deglaciation. Quaternary Science Reviews 21:879-887.

Tiercelin J, Vincens A. (1987) Le demi-graben de Baringo-Bogoria, Rift Gregory, Kenya. 30000 ans d'histoire hydrologique et sédimentaire. Bulletin des Centres de Recherches Exploration-Production Elf-Aquitaine 11:249-540.

Tierney JE, Russell JM, Damste JSS, Huang YS, Verschuren D. (2011) Late Quaternary behavior of the East African monsoon and the importance of the Congo Air Boundary. Quaternary Science Reviews 30:798-807.

Tierney JE, Russell JM, Eggermont H, Hopmans EC, Verschuren D, Damste JSS. (2010) Environmental controls on branched tetraether lipid distributions in tropical East African lake sediments. Geochimica Et Cosmochimica Acta 74:4902-4918.

Verschuren D, Laird KR, Cumming BF. (2000) Rainfall and drought in equatorial Africa during the past 1100 years. Nature 403:410-444.

Verschuren D, Cumming B, Laird KR. (2004) Quantitative reconstruction of past salinity variations in African lakes: assessment of chironomid-based inference models (Insecta: Diptera) in space and time. Canadian Journal of Fisheries and Aquatic Sciences 61(6):986-998.

Verschuren D. (2004) Decadal to century-scale climate variability in tropical Africa during the past 2000 years. In: Battarbee R, Gasse F, Stickley C (eds.), Past climate variability through Europe and Africa. Kluwer, Dordrecht, The Netherlands, pp. 139-158.

Verschuren D, Eggermont H. (2006) Quaternary paleoecology of aquatic Diptera in tropical and southern Hemisphere rgions, with special reference to the Chironomidae. Quaternary Science Reviews 25:1926-1947.

Williams AP, Funk C. (2011) A westward extension of the warm pool leads to a westward extension of the Walker circulation, drying eastern Africa. Climate Dynamics 37:2417-2435.

SUMMARY

Unlike most other tropical regions on Earth, East Africa is a relatively dry area prone to strong variation in rainfall. This has important consequences for the large part of the population whose livelihood is directly dependent on local precipitation, as demonstrated most recently by the catastrophic drought in the Horn of Africa during 2009-2011. The importance of a good understanding of the regional hydroclimate systems cannot be overstated, especially in the context of a future with rising population densities and pressure on natural water resources. An important objective therefore is the identification of natural patterns of climate variability. Since no historical sources are available that go back far enough in time, researchers have to fall back on natural climate archives. Lakes, capable of storing signals of climate change in their sediments, are the principle sources of such information in East Africa. However, a compilation and evaluation of previously published research shows that extending our knowledge regarding regional patterns of historical hydroclimate variability, on time scales most relevant to humans and societal structures, is crucial.

In this thesis, three Kenyan lakes were investigated for their potential as paleoclimate archive. Sediment cores from these lakes were submitted to an array of analyses, mainly focused on sedimentological, geochemical and mineralogical indicators (proxies) of past changes in lake level and water chemistry. The obtained results form the basis of a reconstruction of past rainfall variability, on different time scales. Lake Rutundu, a small crater lake on the eastern flank of Mount Kenya, demonstrates how moisture balance has evolved over the past 19,000 years. This sediment archive attests convincingly to the large-scale climate changes that were associated with the transition of the Last Glacial Maximum to the Holocene (the present interglacial period that started 11,700 years ago). Additionally, this lake shows that the regional long-term trend of a wet early Holocene to a drier late Holocene, related to changes in the orbit of the Earth around the Sun, was punctuated by a sequence of five episodes of severe drought. This is an important result, given the unresolved character of, and mechanisms behind, the termination of the early-Holocene 'African Humid Period'.

In the lowlands of Kenya, most lakes were not spared from relatively recent intense droughts, resulting in only a handful of sites that are suited for the collection of intact sediment archives that are more than a few centuries old. Lake Bogoria, a tectonic saline lake in the central Kenya Rift Valley, is one of those rare sites. Sediment cores spanning the past 1,300 years demonstrate the high potential of this lake for a detailed study of moisture balance changes that took place on time scales from a few years to centuries. Supported by an extensive set of analyses on cores from five different locations in the lake, supplemented with sediment traps illustrating present sedimentation patterns, changes in sedimentation dynamics through time are documented. There are good indications that the lake has experienced strong hydrological fluctuations during the studied period, surpassing the 20th-century range known from historical documentation. These results provide the basis for a future exploitation of this archive as one of the new high-resolution hydroclimate reconstructions in East Africa, which will contribute to the unravelling of the complex dynamics of precipitation in the region. Additionally, recent anthropogenic impact on sedimentation is demonstrated for the first time at Lake Bogoria, despite the protection of the lake and its immediate surroundings as a National

Reserve. Increasing levels of soil erosion in the catchment result in high amounts of terrigenous material being delivered to the lake. A follow-up of this result is recommended, considering the unique character and high biodiversity of Lake Bogoria.

Since high-quality archives of hydroclimate variability are rare in East Africa, exploration of potentially new sites is an important part of paleoclimate research in the region. For this reason, an exploratory study of Nasikie Engida was conducted, a shallow and extremely saline lake in the dry southern Kenya Rift Valley. This lake is protected from desiccation by geothermal springs, despite the unfavourable balance between local precipitation and evaporation. This thesis presents a first exploration of the sediments of this lake, with, among others, the documentation of the only known modern lacustrine deposits of the sodium carbonate mineral nahcolite. The results suggest that Nasikie Engida contains an uninterrupted registration of climate-related changes in moisture balance during the past millennia, and open the door to further research of this remarkable system.

SAMENVATTING

Anders dan de meeste andere tropische gebieden op Aarde, is Oost-Afrika een relatief droge regio die van nature gekarakteriseerd wordt door sterke variaties in neerslag. Dit heeft belangrijke gevolgen voor het grote deel van de bevolking dat voor levensonderhoud rechtstreeks afhankelijk is van regenval, zoals recent nog aangetoond door de catastrofale droogtes in de Hoorn van Afrika in 2009-2011. Het belang van een goed begrip van de regionale hydroklimaatsystemen kan niet overschat worden, zeker met het oog op een toekomst met stijgende bevolkingsaantallen en toenemende druk op natuurlijke watervoorraden. Een belangrijk element hierbij is de ontrafeling van patronen van natuurlijke variatie. Omdat er geen historische bronnen beschikbaar zijn die ver genoeg terug gaan in de tijd om ons voldoende bij te brengen over klimaatvariatie op tijdschalen van decaden tot eeuwen, moeten onderzoekers terugvallen op natuurlijke archieven. In Oost-Afrika vormen meren, die signalen van klimaatverandering kunnen opslaan in hun constant accumulerende sedimenten, de belangrijkste bron van dergelijke informatie. Een compilatie en evaluatie van eerder gepubliceerd onderzoek maakt echter duidelijk dat een verbreding van onze kennis omtrent regionale patronen van historische klimaatvariatie, op tijdschalen die het meest relevant zijn voor mensen en maatschappelijke structuren, cruciaal is.

In deze thesis werden drie Keniaanse meren onderzocht op hun bruikbaarheid als hydroklimaatarchief. Sedimentkernen uit deze meren werden onderworpen aan uiteenlopende analyses, voornamelijk gericht op sedimentologische, geochemische en mineralogische indicatoren (‘proxies’) van veranderingen in meerniveau en waterchemie. De bekomen resultaten vormden de basis voor een reconstructie van patronen in neerslagvariatie doorheen de tijd, en dit op verschillende tijdschalen. Lake Rutundu, een klein kratermeer op de oostelijke flank van Mount Kenya, demonstreert hoe waterbalans is geëvolueerd doorheen de laatste 19,000 jaar. Dit sedimentarchief getuigt overtuigend van de verregaande klimaatveranderingen die gepaard gingen met de overgang van het Laatste Glaciale Maximum naar het Holoceen (de huidige interglaciale periode die 11,700 jaar geleden begon). Daarnaast toont dit meer aan dat de regionale langetermijntrend van een nat vroeg-Holoceen naar een droger laat-Holoceen, gerelateerd aan veranderingen in de baan van de aarde rond de zon, doorbroken werd door een reeks van vijf episodes van intense droogte. Dit is een belangrijk inzicht, gegeven de grote onzekerheid die op dit moment nog heerst omtrent de aard van, en de mechanismen achter, de beëindiging van de vroeg-Holocene ‘African Humid Period’.

In het Keniaanse laagland zijn slechts weinig meren gespaard gebleven van relatief recente intense droogtes, waardoor slechts enkele locaties geschikt zijn voor het verzamelen van intacte sedimentarchieven die meer dan een paar eeuwen oud zijn. Lake Bogoria, een tectonisch zoutmeer in de centrale Keniaanse Riftvallei, is één van dergelijke zeldzame sites. Sedimentkernen die de laatste 1,300 jaar beslaan, tonen aan dat dit meer een hoog potentiëel heeft voor een gedetailleerde studie van waterbalansveranderingen die hebben plaatsgevonden op tijdsschalen gaande van enkele jaren tot eeuwen. Aan de hand van een uitgebreide set van analyses op kernen verzameld op vijf verschillende plaatsen in het meer, aangevuld met sedimentvallen die de huidige sedimentatiepatronen illustreren, wordt een beeld geschetst van veranderingen in sedimentatiedynamiek doorheen de tijd. Er zijn sterke indicaties dat het meer tijdens de bestudeerde

periode sterke hydrologische veranderingen heeft ondergaan, die ver buiten het bereik van de gedocumenteerde variatie tijdens de 20e eeuw liggen. Deze resultaten vormen de basis voor een toekomstige uitwerking van dit archief als één van de nieuwe hoog-resolutie hydroklimaatreconstructies in Oost-Afrika, die zal bijdragen tot de ontrafeling van de mechanismen achter de complexe neerslagdynamiek in de regio. Verder werd ook voor de eerste keer aangetoond dat er tijdens de laatste decennia een belangrijke menselijke invloed op sedimentatie is ontstaan, ondanks de status van natuurreservaat die de onmiddellijke omgeving van het meer geniet. Toenemende bodemerosie in het stroomgebied zorgt voor een sterke verhoging in de aanvoer van terrigeen materiaal. Opvolging van deze ontwikkeling is aangewezen, gezien het unieke karakter en hoge biodiversiteitswaarde van het Bogoriameer.

Door de zeldzaamheid van voldoende kwalitatieve hydroklimaatarchieven in equatoriaal Oost-Afrika, is exploratie van potentiëel nieuwe sites een belangrijk onderdeel van het paleoklimatologisch onderzoek in de regio. Daarom werd een verkennende studie van Nasikie Engida ondernomen, een ondiep en extreem geconcentreerd meer in de droge zuidelijke Keniaanse Riftvallei. Ondanks de zeer ongunstige lokale balans tussen verdamping en neerslag, wordt dit meer beschermd tegen uitdroging door toevoer van water uit geothermale bronnen. Deze studie bevat de eerste verkenning van de sedimenten van dit meer, met onder andere de beschrijving van de enige gekende moderne lacustriene afzettingen van het mineraal nahcoliet. De resultaten suggereren dat er tot op de dag van vandaag een ononderbroken registratie van klimaatgerelateerde veranderingen in waterbalans tijdens de laatste millennia heeft plaatsgevonden, en openen de deur naar verder onderzoek van dit unieke systeem.

GIJS DE CORT - Scientific résumé during this PhD

Mobility, conferences and workshops:

- May 27 - Jun 1, 2012: European Science Foundation (ESF) research conference 'Modes of variability in the climate system: past-present-future', Obergurgl, Austria. With poster presentation.
- Aug - Sep, 2012: Four-week field campaign in Kenya, coring six alpine lakes on Mount Kenya and Lake Bogoria.
- Sep 9 - 14, 2012: International NCCR climate summer school 'The water cycle in a changing climate: observations, scenarios, impacts'. Monte Verità, Switzerland. With poster presentation.
- Oct 11 - 12, 2012: Association of Polar Early Career Scientists (APECS) Benelux symposium, Ghent, Belgium. With oral presentation.
- Mar 6, 2013: Belgian Union for Quaternary Research (Belqua) annual scientific workshop, Brussels, Belgium. With oral presentation.
- 2013 - 2015: Three one-week work visits to ETH Zürich Geology Department for X-ray fluorescence (XRF) scanning of lake sediment cores.
- Dec 4 -7, 2013: Kenya Wildlife Services (KWS) 'Soda lakes' workshop, Naivasha, Kenya. With poster presentation.
- Jan 13 -16, 2014: 'Age models, chronologies and databases' science workshop, Queen's University Belfast, Northern Ireland.
- Jun - Jul 2014: Four-week field campaign in Kenya, coring and limnological surveying of Lakes Bogoria and Baringo, and assisting in ICDP deep-drilling project 'Hominin Sites and Paleolakes Drilling Project' at Lake Magadi.
- Dec 16, 2014. Royal Academy for Overseas Science (KAOW-ARSOM) young researchers' symposium, Brussels, Belgium. With poster presentation.
- Apr 12 - 17, 2015. European Geosciences Union (EGU) General Assembly, Vienna, Austria. With oral presentation.
- Jul - Aug, 2015. Two-week field campaign in Kenya, coring and limnological surveying of Lakes Bogoria and Nasikie Engida (Little Magadi).
- Jan 29, 2016. Geologica Belgica conference, Université de Mons, Belgium. With oral presentation.

Publications:

- Loomis SE, Russell JM, Verschuren D, Morrill C, **De Cort G**, Sinninghe Damsté JS, Eggermont H, Street-Perrott FA, Kelly MA. The tropical lapse rate steepened during the Last Glacial Maximum. *Submitted.*
- Hodgson DA, Whitehouse PL, **De Cort G**, Berg S, Verleyen E, Tavernier I, Roberts SJ, Vyverman W, Sabbe K, O'Brien P. (2016) Rapid early Holocene sea-level rise in Prydz Bay, East Antarctica. Global and Planetary Change 139:128-140.
- Barão L, **De Cort G**, Meire P, Verschuren D, Struyf E. (2015) Biogenic Si analysis in volcanically imprinted lacustrine systems: the case of Lake Rutundu (Mt. Kenya). Biogeochemistry 125:243-259.
- **De Cort G**, Bessems I, Keppens E, Mees F, Cumming B, Verschuren D. (2013) Climate variability in the central Kenya Rift Valley over the past 1700 years: the sediment record of hypersaline lakes Bogoria, Nakuru and Elementeita. Palaeogeography, Palaeoclimatology, Palaeoecology 388:69-80.